

DISSERTATION

SOLUTE TRANSPORT IN OVERLAND FLOW DURING RAINFALL

Submitted by

R. Lee Peyton, Jr.

Department of Civil Engineering

In partial fulfillment of the requirements

for the Degree of Doctor of Philosophy

Colorado State University

Fort Collins, Colorado

Spring 1985

COLORADO STATE UNIVERSITY

March 1985

WE HEREBY RECOMMEND THAT THE THESIS PREPARED UNDER OUR SUPERVISION
BY R. Lee Peyton, Jr.
ENTITLED SOLUTE TRANSPORT IN OVERLAND FLOW DURING RAINFALL

BE ACCEPTED AS FULFILLING IN PART REQUIREMENTS FOR THE DEGREE OF
Doctor of Philosophy

Committee on Graduate Work

Ronald Dean Adrian

Roger Smith

H.W. Smith

Robert C. Sigel

A.W. Salm

Adviser

J. Papadakis

Department Head

ABSTRACT OF DISSERTATION

SOLUTE TRANSPORT IN OVERLAND FLOW DURING RAINFALL

A numerical model was developed to simulate the movement of a conservative solute in steady overland flow over a smooth impervious plane under a constant rainfall intensity. This movement was described by shear-flow convection, vertical mixing, and rainfall dilution. Mass was convected in flow layers whose velocities varied according to velocity profile relationships developed in this study. Vertical diffusion occurred between flow layers according to the Fickian equation. Mass was diluted due to increasing depth of flow downstream. This model closely reproduced results of several analytical solutions for solute transport in steady, uniform flow. The model was then calibrated to results from overland flow laboratory experiments using the vertical mixing coefficient, ϵ_y , as a calibration parameter. A regression analysis was used to relate the calibrated ϵ_y values to rainfall and flow variables.

The resulting regression equation showed that ϵ_y increased with increasing rainfall intensity and with decreasing mean flow velocity. ϵ_y varied the greatest at low rainfall intensities and near the top of the overland flow plane. The lower range of the calibrated ϵ_y values compared favorably with the molecular diffusion coefficient for the dye tracer used in the laboratory experiments, while the upper range was similar to theoretical vertical mixing coefficients for steady, uniform, turbulent flow at equivalent discharges. It was concluded

that the velocity of the peak concentration can vary between the mean cross-sectional velocity and the maximum point velocity, depending on the ϵ_y value. It was further concluded that rainfall generally does not produce a continuous state of complete vertical mixing in overland flow.

The study was then taken one step further by using the resulting ϵ_y equation to examine the length of the convective distance beyond which Taylor's one-dimensional dispersion analogy is generally valid. This distance was found to be very short where vertical mixing was great and very long where vertical mixing was small. In addition, the ϵ_y equation was used along with Fischer's theoretical expression for the one-dimensional dispersion coefficient for open-channel flow (based on Taylor's research with pipe flow) to compute dispersion coefficients for overland flow during rainfall. In some cases, negative dispersion coefficients were computed. In further checking the applicability of Fischer's expression, it was concluded that it is not appropriate for all velocity profiles.

R. Lee Peyton, Jr.
Civil Engineering Department
Colorado State University
Fort Collins, Colorado 80523
Spring 1985

ACKNOWLEDGEMENTS

I sincerely appreciate

the support of my advisor, Dr. Thomas G. Sanders;
the support of the Hydrology and Water Resources Program Leader,
Dr. Hsieh W. Shen;
the insightful discussions with Dr. D. Dean Adrian;
and the comments of Dr. Roger E. Smith and Dr. Robert C. Ward.

I am deeply grateful for financial support

from the Colorado State Experimental Station, Grant Number 151241,
for my Research Assistantship during 1980, 1981-82, and
1982-83;
from the Chevron Graduate Fellowship
during 1980-81;
from the Department of Civil Engineering
for part-time teaching during 1983-84 and
for computer funding during 1983 and 1984;
from the C.S.U. Environmental Resources Center
for the Dissertation Award in 1984.

During the course of this study, there were many outside the University
who contributed emotional support that helped to complete this
document--including my parents, Gary, Pat, Andy, Frances, Wiley,
Esther, Wally, Ramona, W.D.B., Marguerite, Laverne, Jack, L.C.,
Hugh, Elaine, Carol, Jonathon, Ripp, Debbie, Diane, Phyllis,
Judy, Teresa, Woody, Bob, Andrea, Marte, Cecil, Andy, June, Kathy,
Tom, Betty, Ethel, Tracy, Lou, Kathy, Christian, Virginia Krystal,
Marilyn, Terri, Larry, Pine,
and Crystal Mountain
and others and others.

And for crucial support for the initiation of this endeavor and for
transforming enlightenment during its course, Oma.

TABLE OF CONTENTS

<u>Chapter</u>		<u>Page</u>
I	INTRODUCTION	1
II	LITERATURE REVIEW	3
	A. Overland Flow Hydraulics	3
	B. Raindrop Impact	6
	C. Overland Flow Pollutant Concentration Models	8
	D. Dispersion in Steady, Uniform Open Channel Flow	9
III	MATHEMATICAL MODEL	17
	A. Introduction	17
	B. Velocities and Depths	19
	C. Dilution	34
	D. Vertical Diffusion	38
	E. Proposed Model	42
	1. Convection	42
	2. Dilution	44
	3. Vertical Diffusion	46
	4. Computer Program	46
	F. Model Testing	46
	1. Cleary and Adrian Solution	46
	2. Yeh and Tsai Solution	50
	3. Elder's Theoretical Turbulent-Flow Dispersion Coefficient	57
	4. Theoretical Laminar-Flow Dispersion Coefficient	60
IV	LABORATORY EXPERIMENTS	67
	A. Introduction	67
	B. Indoor Rainfall-Runoff Simulator	67
	1. Rainfall Modules	67
	2. Water Supply	70
	3. Flow Controls	70
	4. Runoff Collection System	72
	C. Experimental Procedure	74
	1. Facility Operation	74
	2. Data Collection	75
V	RESULTS AND DISCUSSION	79
	A. Introduction	79
	B. Laboratory Measurements	79
	C. Numerical Model Results	98
	1. Data Input	98
	2. Calibration Procedure and Results	98

<u>Chapter</u>		<u>Page</u>
	3. Discussion of Figures 5-1 through 5-15	99
	4. Discussion of Figure 5-16	101
	5. Calibrated ϵ_y Values	103
	6. Sensitivity and Limitations of the Numerical Model	109
	D. Regression of Calibrated ϵ_y Values	111
	E. Convective and Taylor Periods T_y	118
	F. Longitudinal Dispersion Coefficient	126
	G. Approximation Method for Peak Concentrations	133
VI	CONCLUSIONS AND RECOMMENDATIONS	137
	A. Conclusions	137
	B. Recommendations	139
	REFERENCES	141
	APPENDIX A - Computer Printout of Numerical Model	146
	APPENDIX B - Comparison of Numerical Model to Cleary and Adrian Solution	199
	APPENDIX C - Comparison of Numerical Model to Yeh and Tsai Solution	211
	APPENDIX D - Derivation of Longitudinal Dispersion Coefficient Using a Constant Vertical Diffusion Coefficient in Infinitely-Wide, Steady, Uniform, Turbulent Flow	220
	APPENDIX E - Series of Computed Concentration-Time Curves Generated by Numerical Model for Each Experiment	224
	APPENDIX F - Data Used in Numerical Model	240
	APPENDIX G - Stepwise Multiple Linear Regression of ϵ_y	247
	APPENDIX H - Evaluation of Terms 1 and 2 in Eq. 5-22	251
	APPENDIX I - List of Symbols	256

LIST OF TABLES

<u>Table</u>		<u>Page</u>
3-1	Results of Polynomial Regression for Lower Portion of Velocity Profile	23
3-2	Comparison of General Velocity Profile Equations for Lower Profile	27
3-3	Results of Polynomial Regression for Upper Portion of Velocity Profile	30
3-4	Measured Velocities and Depths	32
3-5	Comparison of Mean Velocity Equations for Hypothetical Flows	35
3-6	Comparison of Computed and Measured Velocities	36
3-7	Flow Conditions for Cleary and Adrian Test and Yeh and Tsai Test	49
3-8	Tabular Comparison of Numerical Model to Yeh and Tsai Solution	56
3-9	Data Used in Numerical Model for Theoretical Turbulent-Flow Dispersion Test	61
3-10	Data Used in Numerical Model for Theoretical Laminar-Flow Dispersion Test	64
5-1	Summary of Experiments	80
5-2	Calibrated ϵ_y Values	104
5-3	Computed Values for x_{T_E} and T_E for Laboratory Experiments	122
5-4	Comparison of Dispersion Coefficients Computed from Eqs. 3-36, 3-42, and 5-25	130
5-5	Peak Concentrations from Eqs. 5-29 and 5-33	136

<u>Table</u>	<u>Page</u>
B-1	List of Symbols Used in Equations B-1 and B-2 201
B-2	Comparison of Cleary and Adrian Solution to Numerical Model Using 7 Streamtubes 206
B-3	Comparison of Cleary and Adrian Solution to Numerical Model Using 11 Streamtubes 207
B-4	Comparison of Cleary and Adrian Solution to Numerical Model Using 19 Streamtubes 208
C-1	List of Symbols Used in Equations C-1 through C-7 . . . 215
C-2	Bessel Function Arguments Satisfying Eq. C-9 Obtained by Linear Interpolation of Data Presented by Oliver (1960) 216
G-1	Results of Stepwise Multiple Linear Regression Assuming $\varepsilon_y = f(i, \bar{u}, y_s, R_e)$ 248
G-2	Results of Stepwise Multiple Linear Regression Assuming $\varepsilon_y = f(i, \bar{u}, y_s, R_e)$ Using Only Data with Depth-to-Drop Diameter Ratios Greater than 1.0 249
G-3	Results of Stepwise Multiple Linear Regression Assuming $\varepsilon_y = f(i, \bar{u}, R_e)$ 250

LIST OF FIGURES

<u>Figure</u>		<u>Page</u>
3-1	Plot of Transformed Velocity Profile Data (Data Collected by Yoon, 1970)	21
3-2	Plot of \tilde{y} Versus u^*	29
3-3	Change in Volume of a Parcel of Fluid of Fixed Length Moving Through Flow Layer in Nonuniform Flow . .	37
3-4	Simplified Schematic of Proposed Model for Solute Transport in Overland Flow with Rainfall	43
3-5	The Convection Step	45
3-6	Concentration Distribution of Cleary and Adrian (Neglecting Longitudinal Diffusion)	47
3-7	Middepth Injection Used for Cleary and Adrian Test . . .	47
3-8	Comparison of Numerical Model (Using 11 Flow Layers) to Cleary and Adrian Solution	51
3-9	Graphical Comparison of Numerical Model to Yeh and Tsai Solution	55
3-10	Comparison of Concentration Distributions of Numerical Model ($\Delta X/\Delta T = 1.0 \bar{u}$) and Yeh and Tsai Solution at 8 Feet Downstream from Injection	58
3-11	Variance of Vertically-Averaged Concentration Along x Axis Versus Time Since Injection for Turbulent Flow Dispersion Test	62
3-12	Variance of Vertically-Averaged Concentration Along x Axis Versus Time Since Injection for Laminar Flow Dispersion Test	65
4-1	Rainfall Module	68
4-2	Capillary Tube Spacing	69
4-3	Flow Control System (from Buchberger, 1979)	71

<u>Figure</u>		<u>Page</u>
4-4	Overflow Collection Box	73
4-5	Wooden Frame Containing Injection Pipe	76
5-1	Comparison of Measured and Computed Concentration Curves for $S_o = 0.001$ and $i = 2$ (Experiment No. 1a) . .	81
5-2	Comparison of Measured and Computed Concentration Curves for $S_o = 0.001$ and $i = 2$ (Experiment No. 1b) . .	82
5-3	Comparison of Measured and Computed Concentration Curves for $S_o = 0.001$ and $i = 3$ (Experiment No. 2a) . .	83
5-4	Comparison of Measured and Computed Concentration Curves for $S_o = 0.001$ and $i = 3$ (Experiment No. 2b) . .	84
5-5	Comparison of Measured and Computed Concentration Curves for $S_o = 0.001$ and $i = 4$ (Experiment No. 3) . . .	85
5-6	Comparison of Measured and Computed Concentration Curves for $S_o = 0.001$ and $i = 5$ (Experiment No. 4) . . .	86
5-7	Comparison of Measured and Computed Concentration Curves for $S_o = 0.015$ and $i = 2$ (Experiment No. 5) . . .	87
5-8	Comparison of Measured and Computed Concentration Curves for $S_o = 0.015$ and $i = 3$ (Experiment No. 6) . . .	88
5-9	Comparison of Measured and Computed Concentration Curves for $S_o = 0.015$ and $i = 4$ (Experiment No. 7) . . .	89
5-10	Comparison of Measured and Computed Concentration Curves for $S_o = 0.015$ and $i = 5$ (Experiment No. 8) . . .	90
5-11	Comparison of Measured and Computed Concentration Curves for $S_o = 0.030$ and $i = 2$ (Experiment No. 9a) . .	91
5-12	Comparison of Measured and Computed Concentration Curves for $S_o = 0.030$ and $i = 2$ (Experiment No. 9b) . .	92
5-13	Comparison of Measured and Computed Concentration Curves for $S_o = 0.030$ and $i = 3$ (Experiment No. 10) . .	93
5-14	Comparison of Measured and Computed Concentration Curves for $S_o = 0.030$ and $i = 4$ (Experiment No. 11) . .	94
5-15	Comparison of Measured and Computed Concentration Curves for $S_o = 0.030$ and $i = 5$ (Experiment No. 12) . .	95
5-16	Typical Envelope of Computed Peak Concentrations	100

<u>Figure</u>		<u>Page</u>
5-17	ϵ_y from Eq. 5-3 for Laboratory Experiments $S_o = .001$. . .	114
5-18	ϵ_y from Eq. 5-3 for Laboratory Experiments $S_o = .015$ and $.030$	115
5-19	Variation of ϵ_y with Rainfall Intensity	116
5-20	Variation of ϵ_y with Distance	117
5-21	Variance of Dye Cloud Versus Time Since Injection for $S_o = .001$	123
5-22	Variance of Dye Cloud Versus Time Since Injection for $S_o = .015$	124
5-23	Variance of Dye Cloud Versus Time Since Injection for $S_o = .030$	125
5-24	D from Eq. 5-25 for Laboratory Experiments	129
5-25	Velocity Profile Which Yields Positive, Negative, and Zero Values for Dispersion Coefficient Using Eq. 2-6	132
A-1	Flow Chart for Numerical Model	147
B-1	Differences in Numerical Model and Cleary and Adrian Solution for Uniform Velocity Field	203
B-2	Results of Multiple Point Injections	204
B-3	Summation of Point-Source Solutions	204
E-1	Comparison of Measured and Computed Concentration Curves for $S_o = 0.001$ and $i = 2$ (Experiment No. 1a) . . .	225
E-2	Comparison of Measured and Computed Concentration Curves for $S_o = 0.001$ and $i = 2$ (Experiment No. 1b) . . .	226
E-3	Comparison of Measured and Computed Concentration Curves for $S_o = 0.001$ and $i = 3$ (Experiment No. 2a) . . .	227
E-4	Comparison of Measured and Computed Concentration Curves for $S_o = 0.001$ and $i = 3$ (Experiment No. 2b) . . .	228
E-5	Comparison of Measured and Computed Concentration Curves for $S_o = 0.001$ and $i = 4$ (Experiment No. 3) . . .	229
E-6	Comparison of Measured and Computed Concentration Curves for $S_o = 0.001$ and $i = 5$ (Experiment No. 4) . . .	230

<u>Figure</u>	<u>Page</u>
E-7	Comparison of Measured and Computed Concentration Curves for $S_o = 0.015$ and $i = 2$ (Experiment No. 5) . . . 231
E-8	Comparison of Measured and Computed Concentration Curves for $S_o = 0.015$ and $i = 3$ (Experiment No. 6) . . . 232
E-9	Comparison of Measured and Computed Concentration Curves for $S_o = 0.015$ and $i = 4$ (Experiment No. 7) . . . 233
E-10	Comparison of Measured and Computed Concentration Curves for $S_o = 0.015$ and $i = 5$ (Experiment No. 8) . . . 234
E-11	Comparison of Measured and Computed Concentration Curves for $S_o = 0.030$ and $i = 2$ (Experiment No. 9a) . . 235
E-12	Comparison of Measured and Computed Concentration Curves for $S_o = 0.030$ and $i = 2$ (Experiment No. 9b) . . 236
E-13	Comparison of Measured and Computed Concentration Curves for $S_o = 0.030$ and $i = 3$ (Experiment No. 10) . . 237
E-14	Comparison of Measured and Computed Concentration Curves for $S_o = 0.030$ and $i = 4$ (Experiment No. 11) . . 238
E-15	Comparison of Measured and Computed Concentration Curves for $S_o = 0.030$ and $i = 5$ (Experiment No. 12) . . 239

Chapter I

INTRODUCTION

The movement of pollutants over the land surface during a rainfall-runoff event can have a significant impact on the quality of the receiving water. This impact can be especially important from such pollutants as agricultural chemicals applied to cropland, bacterial and organic wastes from feedlots, drainage from surface mining activities, street surface contaminants from urban runoff, leachates from industrial stockpiles, and hazardous waste leakage or spills.

The State of Colorado is particularly susceptible to these overland flow water quality impacts. It is a State where unique and sensitive ecosystems abound and where quantities of high quality water are a precious commodity. Yet it is a state experiencing significant urban and industrial growth superimposed on an economy traditionally based heavily on agricultural and mining activities--all of which are potentially threatening to the quality of surface runoff. Therefore, in order to maintain and protect the existing water quality resources of Colorado, it is important to gain a better understanding of pollutant movement and pollutant concentrations in overland flow during rainfall-runoff events.

The typical approach to estimating pollutant concentrations in overland flow has been to divide the pollutant mass available at the land surface during a given time interval by the runoff volume during the same time interval. Little attention has been directed to the

transport processes involved or the influence of these processes on pollutant concentrations.

When overland flow occurs without raindrop impact, pollutant movement can be modeled using theories developed for wide, straight open channels with uniform discharge. However, the introduction of rainfall onto thin overland flow increases vertical mixing, changes the velocity profile, produces nonuniform flow, and provides continuous dilution. This study attempts to gain insight into these processes by investigating the following simplified case: an instantaneous, line-source injection of a soluble, conservative, dye tracer in steady, nonuniform overland flow over a smooth, impervious surface under rainfall impact.

First, an examination is made of those processes thought to be important in the transport of soluble pollutants in overland flow with rainfall impact: shear-flow convection, vertical mixing, and rainfall dilution. Second, a numerical model is proposed which attempts to describe these processes. Third, the model is calibrated to laboratory data using the vertical mixing coefficient as a calibration parameter. Finally, a mathematical relationship for the vertical mixing coefficient is obtained which is used to derive an expression for the one-dimensional, convective, dispersion coefficient for overland flow with rainfall.

Chapter II

LITERATURE REVIEW

A. Overland Flow Hydraulics

The momentum equation for shallow, steady, gradually-varied overland flow with rainfall as lateral inflow was presented in the following form by Yen and Wenzel (1970)

$$\frac{dy_s}{dx} = \frac{S_o - S_f + \frac{i}{gA} (V \cos\phi - 2\beta\bar{u}) - \frac{\bar{u}^2}{g} \frac{d\beta}{dx}}{\cos\theta - \frac{\beta\bar{u}^2}{gD_h}}$$

where y_s = depth of flow, x = distance along the flow direction, S_o = bed slope, S_f = friction slope, i = lateral inflow rate, g = acceleration of gravity, A = cross-sectional area of flow, V = velocity vector of lateral inflow, ϕ = angle between V and x , β = momentum coefficient, \bar{u} = mean velocity of flow, θ = angle between channel bed and the horizontal, and D_h = hydraulic depth, equal to the area A divided by the free surface width.

Robertson et al. (1966) and Yu and McNown (1964) experimentally evaluated the terms in the momentum equation and found that S_o and S_f were of much greater magnitude than the remaining terms, resulting in the following approximation to the momentum equation for shallow overland flow with rainfall,

$$S_o = S_f \tag{2-1}$$

The Darcy-Weisbach equation has been used (Robertson et al., 1966; Yu and McNown, 1964; Shen and Li, 1973; Woolhiser, 1975; Morgali, 1970; Kisisel et al., 1973; Emmett, 1970) to express Eq. 2-1 as

$$S_o = \frac{f \bar{u}^2}{8 g y_s} \quad (2-2)$$

where f = Darcy-Weisbach friction coefficient.

It can be theoretically shown that for laminar overland flow without rainfall,

$$f = \frac{24}{R_e}$$

where

$$R_e = \frac{q}{\nu} \quad (2-3)$$

and

$$q = \bar{u} y_s$$

with R_e = Reynolds number, q = discharge per unit width, and ν = kinematic viscosity. For low Reynolds number flows under rainfall, experimental data have been collected which show that f increases with increasing rainfall intensity (Emmett, 1970; Kisisel et al., 1973; Morgali, 1970; Shen and Li, 1973; Woo and Brater, 1962; Yoon and Wenzel, 1971; and Yu and McNown, 1964). For flow over a smooth surface, a relationship of the form

$$f = \frac{24 + 27.162 R_e^{0.407}}{R_e} \quad (2-4)$$

was found by Shen and Li (1973) for Reynolds numbers less than 900, while a relationship of the form

$$\frac{f}{f_e} = 1.048$$

was found for Reynolds numbers greater than 2000, where f_e = Darcy-Weisbach friction factor for equivalent flow without rainfall. For Reynolds numbers between 900 and 2000, an interpolated relationship was presented.

The transitional Reynolds number range between laminar and turbulent overland flow with rainfall was found to be 200 to 1000 by Yu and McNown (1964) over a concrete surface and 800 to 1000 by Yoon (1970) over a hydraulically smooth surface. Data presented by Morgali (1970) for asphalt and turf surfaces indicate a transition between about 100 and 300, while for a crushed slate surface, the transition appears to be between 200 and 300. Based on f vs. R_e plots for data collected over a smooth surface, Shen and Li (1973) chose to use the three Reynolds number ranges mentioned above (less than 900, 900 to 2000, and greater than 2000) for the derivation of friction coefficient expressions.

Velocity profiles in overland flow with rainfall have been measured by Kisisel (1971) and Yoon (1970). Kisisel measured velocities for flows in the Reynolds number range of 2673 to 5754 on a slope of 0.001 under a rainfall intensity of 5.00 inches per hour. He found that velocity profiles over a smooth surface followed a law-of-the-wall logarithmic relationship in the turbulent and buffer zones, while velocities measured closest to the bottom surface were somewhat less than that predicted by the law-of-the-wall for the viscous sublayer. Kisisel did not observe a velocity retardation close to the free surface.

Yoon measured velocities for flows in the Reynolds number range of 350 to 4000 on slopes of 0.005 and 0.010 under rainfall intensities ranging from 1.25 to 15.00 inches per hour. In all cases, the maximum velocity occurred some distance below the water surface. The velocity distribution law derived from von Karman's similarity hypothesis was used to develop velocity profile equations for both the lower profile (below the point of maximum velocity) and the upper profile (above the point of maximum velocity). For the lower profile, the value of von Karman's constant was varied between 0.19 to 0.29 (compared to the usually accepted value of about 0.4) to obtain the best-fit equation. For the upper profile, the slope of the velocity profile at the water surface was varied to obtain the best-fit equation while using the von Karman constant found for the lower profile.

In discussing the differences found in the Kisisel and Yoon studies related to velocity retardation near the water surface, Rao et al. (1972) and Yoon and Wenzel (1973) speculated that this velocity retardation exists for the lower Reynolds number range investigated by Yoon and is absent for the higher Reynolds number range investigated by Kisisel.

B. Raindrop Impact

Laws and Parsons (1943) measured raindrop size and intensity over a two-year period in the Washington, D.C. area and showed a general trend of increased drop size with increased rainfall intensity. Drop sizes ranged from 1.00 to 4.00 millimeters over a rainfall intensity range of 0.02 to 4.50 inches per hour. Drop sizes for rainfall intensities of 1.00 to 4.50 inches per hour ranged from 2.00 to 4.00 millimeters.

Impact velocities of raindrops have been studied by a number of investigators. Laws (1941) used high-speed photography to measure the fall velocity of raindrops ranging in size from 1.15 to 6.14 millimeters and falling from heights of 0.50 to 20.00 meters. Measured velocities for all drop sizes at a fall height of 0.50 meters were 2.7 to 3.1 meters per second. At the largest fall height of 20.00 meters, velocities ranged from 4.6 meters per second for a 1.17 millimeter diameter drop to 9.4 meters per second for a 6.10 millimeter diameter drop. Dingle and Lee (1972) developed a regression equation for the terminal velocity of a raindrop. Banks (1978) used this regression equation along with the data collected by Laws (1941) to obtain an expression for the velocity of accelerating raindrops as a function of fall height, terminal velocity, density and diameter of raindrop, density of air, and drag coefficient.

Based on energy considerations, Engle (1966, 1967) derived theoretical equations for initial pressure, initial flow velocity, maximum crater depth, and time dependence of crater depth for impacts of waterdrops in deep, stagnant, liquid layers. These equations were expressed as functions of the impact velocity, drop diameter, and the density, surface tension, and viscosity of the liquid.

Mutchler (1967) and Mutchler and Hansen (1970) examined raindrop splash behavior in stagnant, liquid layers using high-speed photography and showed how crown height, crater width, and two characteristic angles varied with depth of water layer and time to maximum crown height. They found that waterdrop size is the major variable affecting splash size and that surface-water depth is the major variable affecting splash shape. They further concluded that surface-water depth has

its greatest effect on raindrop splash at depths of about one-third drop diameter and that splash geometry changes very little at depths greater than one drop diameter.

Harlow and Shannon (1967a, 1967b) numerically solved the Navier-Stokes equations of motion for a number of raindrop impacts in stagnant liquid and presented the analytical results of pressures, velocities, and splash shape as a function of time. Wang and Wenzel (1970) extended Harlow and Shannon's results by numerically solving the Navier-Stokes equations for a range of raindrop sizes typical in storm intensities of one to six inches per hour impacting at speeds up to terminal velocity. Resulting pressures, velocities, and shear stresses compared favorably to experimental data.

Macklin and Metaxas (1976) used an energy approach similar to Engle (1966, 1967), but expressed in terms of the dimensionless Froude, Weber, and Reynolds numbers, to derive analytical expressions for maximum cavity radius and maximum crown height for both deep and shallow splashing. Deep splashing (where the bottom of the liquid layer does not affect the splash and where the cavity is approximately hemispherical) was experimentally found to occur at ratios of water layer depth (y_s) to maximum cavity radius (R_c) greater than 1.5. Shallow splashing (where the cavity is approximately cylindrical) was experimentally found to occur at y_s/R_c ratios less than 0.5.

C. Overland Flow Pollutant Concentration Models

A number of models have been developed for the simulation of pollutant concentrations in overland flow during rainfall. The Storm-water Management Model (SWMM) computes a "pollutograph" at a subbasin outlet by dividing the estimated pollutant mass washed off the surface

in any time interval by the volume of runoff in that time interval (Lager et al., 1971). The Pesticide Transport and Runoff (PTR) model (Crawford and Donigian, 1973) and its modified version, the Agricultural Runoff Management (ARM) model (Donigian and Crawford, 1976) determine the soluble pollutant concentration by dividing the estimated mass of pollutant available in soluble form during any time interval by the volume of flow in that time interval. The Nonpoint Source Pollutant (NPS) model relates pollutants to sediment transport which is modeled using empirical equations (Donigian and Crawford, 1976). The Cornell Nutrient Simulation (CNS) model estimates monthly losses of nutrients in runoff, thereby determining only a monthly average pollutant concentration (Haith and Loehr, 1979). The Agricultural Chemical Transport Model (ACTMO) simulates overland flow concentrations on the basis of pollutant mass available at the surface per runoff volume (Frere et al., 1975). The Field Scale Model for Chemicals, Runoff, and Erosion from Agricultural Management Systems (CREAMS) determines the amount of pollutant extracted from the top soil layer divided by runoff volume to estimate pollutant concentration in overland flow (Knisel, 1980). CREAMS is the only one of the above models which accounts for the nonuniform character of overland flow during rainfall.

D. Dispersion in Steady, Uniform, Open Channel Flow

Taylor (1953, 1954) published two important analyses of longitudinal dispersion. He showed that the combined action of convection and diffusion in shear flow can be modeled as an apparent one-dimensional diffusion process moving at the speed of the mean flow velocity. This process, called dispersion, can be described mathematically by the following one-dimensional, convective, dispersion equation

$$\frac{\partial \bar{c}}{\partial t} + \bar{u} \frac{\partial \bar{c}}{\partial x} = D \frac{\partial^2 \bar{c}}{\partial x^2} \quad (2-5)$$

where \bar{c} = cross-sectional average concentration, t = time, \bar{u} = mean flow velocity, x = distance in direction of flow, and D = longitudinal dispersion coefficient.

In order for Taylor to establish this analogy, he had to impose some conditions on the distribution of concentrations throughout the flow. The conditions included that the deviation of local concentration from \bar{c} must be small and that \bar{c} must vary slowly with time and distance. When these conditions are met, Taylor showed that the longitudinal dispersion coefficient (written here for open channel flow with infinite width, from Fischer, 1966) is

$$D = - \frac{1}{y_s} \int_0^{y_s} u' \int_0^y \frac{1}{\epsilon_y} \int_0^y u' dy dy dy \quad (2-6)$$

where y = distance in vertical direction measured above streambed, y_s = depth at water surface, ϵ_y = vertical mixing coefficient, and u' = point velocity deviation from the cross-sectional mean velocity.

Fischer (1966, 1967, 1968) emphasized that following an instantaneous injection of solute into shear flow, there is an initial time period, or "convective period," when Taylor's conditions are not met. During this time, the spreading of the solute cloud is dominated by convection, and the distribution along the channel of the cross-sectionally averaged concentration is highly skewed. For instance, at very short time periods after injection, the cloud will assume the shape of the velocity profile. Following the initial time period, the "diffusive period" or "Taylor period" begins. This period can be

experimentally verified by observing a linear growth rate of the variance of the solute cloud and by observing that the cross-sectionally averaged concentration distribution along the channel decays according to the dispersion equation, Eq. 2-5.

The time to the end of the convective period has been related to two time scales (Fischer, 1967). The Eulerian time scale is a measure of the time required for cross-sectional mixing and is defined as

$$T_E = \frac{\ell^2}{\varepsilon} \quad (2-7)$$

where ℓ is a characteristic length and ε is a characteristic mixing coefficient. The Lagrangian time scale for turbulent flow is a measure of how long a fluid particle takes to lose memory of its initial velocity. It is defined as

$$T_L = \int_0^{\infty} R(\tau) d\tau$$

where $R(\tau)$ is the Lagrangian autocorrelation function,

$$R(\tau) = \frac{\langle u''(t) u''(t + \tau) \rangle}{\langle u''(t)^2 \rangle}$$

and u'' is the instantaneous point velocity of a fluid particle, t and τ are values of time, and the angle brackets represent an average over a large number of particles. Fischer (1966b, 1967) derived the expression

$$D = \overline{u'^2} T_L \quad (2-8)$$

where the overbar represents a cross-sectional average. He showed that T_L could be computed from Eq. 2-8 by using Eq. 2-6 for D and using the velocity profile to compute u' .

These time scales have been used to approximate the transition between the convective and Taylor periods. In steady, laminar, Poiseuille pipe flow, Bailey and Gogarty (1962) and Lighthill (1966) found that Eq. 2-5 is a good approximation for times greater than $0.5 T_E$, and Chatwin (1970) showed that the concentration distribution became normally distributed approximately at $1.0 T_E$. In these studies, the characteristic length and mixing coefficient for T_E (Eq. 2-7) were the pipe radius and the molecular diffusion coefficient, respectively.

In steady, uniform, turbulent, laboratory, open channel flow, Sayre (1968a, 1968b, 1969) found that conditions necessary for establishment of the Taylor period were satisfied to within one percent at about $0.5 T_E$, where the characteristic length was the flow depth and the characteristic mixing coefficient was the vertical eddy diffusivity averaged over the flow depth. Sayre (1969) concluded that the rate of approach of the longitudinal concentration distribution from negative skewness to symmetry was quite slow, converging at times much greater than the beginning of the Taylor period. For natural streams, where transverse mixing usually controls longitudinal dispersion, Fischer (1967) concluded that 1) the convective period extends through $3 T_L$, 2) a transition period occurs between $3 T_L$ and $6 T_L$ during which time the growth of concentration variance is nearly linear but the one-dimensional dispersion equation (Eq. 2-5) does not apply, and 3) the Taylor period extends beyond $6 T_L$. Elsewhere (Fischer et al., 1979), results of experiments in uniform channels show 1) generation of skewed concentration distribution up to $0.2 T_E$, 2) decay of the skewed distribution from $0.2 T_E$ to $1.0 T_E$, 3) gradual approach toward Gaussian distribution beyond $1.0 T_E$, 4) linear growth of variance beyond $0.2 T_E$, and 5) validity of dispersion equation beyond $0.4 T_E$.

Several approaches to modeling concentration distributions during the convective period have been presented. Yotsukura and Fiering (1964, 1966) developed a numerical solution to the two-dimensional dispersion equation,

$$\frac{\partial c}{\partial t} + u \frac{\partial c}{\partial x} = \frac{\partial}{\partial y} \left(\epsilon_y \frac{\partial c}{\partial y} \right)$$

where c = point concentration, u = point velocity in x direction, and ϵ_y = point vertical diffusion coefficient. A logarithmic velocity profile was assumed. The results indicated that the characteristics of the longitudinal concentration distribution became approximately Gaussian at distances of several hundred times the depth. The authors questioned the feasibility of using this solution approach due to the substantial computer time required.

Because of this limitation, Fischer (1968b) developed a model which attempts to simulate the physical processes rather than solve the differential equation. The model divides the flow into streamtubes. Each time step consists of two parts: 1) the concentration is convected within each streamtube according to the velocity of that tube, and 2) mass is transferred between streamtubes using an appropriate mixing coefficient, ϵ , in a finite difference form of Fick's law,

$$F = - \epsilon \frac{\Delta c_{i,j}}{l_{i,j}}$$

where F = mass flux across boundary between streamtubes i and j , $\Delta c_{i,j}$ = difference in concentration between streamtubes i and j , and $l_{i,j}$ = distance between centerlines of streamtubes i and j . Fischer (1968b) applied this model to two cases. In natural streams where the transverse velocity profile dominates dispersion, streamtubes were

placed side by side across the channel width so that the common boundary between streamtubes was in the x-y plane, where x is the direction of flow and y is the vertical direction. For two-dimensional flow in an infinitely wide channel, streamtubes were stacked vertically so that the common boundary between streamtubes was in the x-z plane, where z is orthogonal to x and y. For the latter case, with a logarithmic velocity profile, the numerical solution converged to a linear rate of variance increase consistent with Elder's theoretical dispersion coefficient (Elder, 1959).

McQuivey and Keefer (1976) presented a pure convective model which moves an instantaneous, completely-mixed injection of mass downstream according to the vertical velocity profile and includes no diffusion processes. This approach was found to reasonably simulate the longitudinal concentration distribution during the initial stage of the convective period. For application in natural streams where transverse velocity variations are important, the flow was divided into streamtubes placed side by side across the channel width. The mass in each streamtube was then moved downstream by convection according to the unique vertical velocity profile in each streamtube. Again, this approach appeared satisfactory only for the initial stage of the convective period. A "multiple-convective-systems model" of the entire convective period was also presented. This consisted of 1) dividing the convective period into six or more subreaches, 2) convecting mass through the subreach according to the vertical velocity profile, 3) using the vertically-averaged concentrations at the end of the subreach as the initial "injection" into the following subreach, and 4) repeating steps 2 and 3. Comparison of model results to laboratory

data and river data indicated close agreement. However, the authors and others (Sayre, 1977; Fischer, 1977) have noted that this multiple-convective-systems approach is lacking in meaningful physical similarity to actual dispersion processes in real streams.

Two noteworthy analytical solutions to the concentration distribution in open channel flow are available. Cleary and Adrian (1973) presented analytical solutions to the two- and three-dimensional, convective-diffusive, partial differential equations which describe the concentration distribution of a tracer dye released as an instantaneous line source (two-dimensional case) or instantaneous point source (three-dimensional case) subject to no-flux boundary conditions at the river bottom, water surface, and banks. The channel was assumed rectangular with constant depth and infinite width for the two-dimensional case and finite width for the three-dimensional case. The velocity field was described by uniform velocity at all points in the flow. Directional diffusion coefficients were constant, but were not required to be identical. Longitudinal diffusion was included in both two- and three-dimensional solutions. Yeh (1976) and Yeh and Tsai (1976) presented analytical solutions to the two- and three-dimensional, convective-dispersive, partial differential equations which describe the steady-state concentration distribution of a continuously-released line source (two-dimensional case) or continuously-released point source (three-dimensional case) subject to the same no-flux boundary conditions and channel geometry as assumed by Cleary and Adrian. However, the spatial variation of velocity, vertical diffusion, and transverse diffusion were expressed as power functions of the vertical distance above the streambed. Longitudinal diffusion was neglected.

Buchberger (1979) and Buchberger and Sanders (1982) derived partial differential equations for one-dimensional dispersion in open channel flow with uniform lateral inflow (rainfall) assuming that the one-dimensional dispersion coefficient does not vary in the direction of flow. For the special case of a soluble pollutant applied uniformly over a dry impervious plane prior to rainfall, a solution to the dispersion equation for the rising hydrograph (unsteady, uniform flow) was shown to be

$$\bar{c} = \frac{w}{i t}$$

where \bar{c} = vertically-averaged pollutant concentration, w = pollutant mass initially applied per unit area, i = rainfall intensity, and t = time since beginning of rainfall. This solution assumes instantaneous uniform vertical mixing of the pollutant mass at the beginning of rainfall and is valid in the region bounded on the upstream end by the location of the kinematic wave front and on the downstream end by the limit of the initial pollutant application.

Chapter III

MATHEMATICAL MODEL

A. Introduction

Solute transport in two-dimensional, steady, nonuniform flow (overland flow during rainfall) can be described by the following equation assuming that velocity components orthogonal to the flow direction are zero and that the longitudinal diffusion term is negligible compared to the longitudinal convective term (Yotsukura and Fiering, 1964):

$$\frac{\partial c(x,y,t)}{\partial t} + u(x,y) \frac{\partial c(x,y,t)}{\partial x} = \frac{\partial}{\partial y} \left[\varepsilon_y(x,y) \frac{\partial c(x,y,t)}{\partial y} \right]$$

where c = point concentration, t = time, u = time-averaged point velocity, x = distance along the flow direction, y = vertical distance above the streambed, and ε_y = vertical mixing coefficient. The above equation is a second-order, linear, partial differential equation with variable coefficients for which an analytical solution is not available without restrictive assumptions regarding velocity profiles and uniformity of flow conditions. Therefore, numerical methods must be employed to model in general this type of solute transport.

This study approaches solute transport by attempting to mathematically simulate the dominant physical processes thought to be involved. The simulation takes the form of a two-dimensional, convection-dilution-diffusion model which assumes that conditions transverse to the flow direction are uniform.

The model is valid in both the convective and Taylor periods. Although the influence of rainfall mixing on the lengths of these periods in overland flow has not been previously studied, one can easily estimate an upper limit for the convective period and conclude that this time could be very large. For instance, as rainfall intensity approaches zero over laminar overland flow, the mixing coefficient would be expected to approach the molecular diffusivity--generally about 1×10^{-8} ft²/sec. If the depth of flow is 0.01 foot, the Eulerian time scale (T_E) is computed from Eq. 2-7 to be 2.8 hours. Using $0.4 T_E$ as an estimate for the convective period (Fischer et al., 1979) results in a period of 1.1 hours. Furthermore, in many field applications, travel distances to the nearest gulley, stream, or storm-sewer can be relatively short--reemphasizing the need to investigate both convective and Taylor periods.

The model developed for this study is patterned after the Fischer flow layer model (Fischer, 1968b; Fischer, 1977; Fischer et al., 1979). Flow layers, whose longitudinal axes are aligned in the direction of Streamtubes, whose longitudinal axes are aligned in the direction of flow, are stacked vertically such that boundaries between flow layers are in approximately horizontal planes. A three-part computational sequence is completed during each time step. First, mass is convected within each flow layer according to the velocity profile. Since overland flow with rainfall is nonuniform, the velocities in each flow layer increase with increasing distance downstream. Second, the mass in each flow layer is diluted based on the ratio of flow depths before and after convection. Third, mass is diffused vertically between flow layers based on an appropriate vertical mixing coefficient which

incorporates the effect of rainfall mixing. Longitudinal diffusion is generally considered to have a negligible effect on longitudinal dispersion (Fischer, 1968b; Fischer et al., 1979; Taylor, 1954; Yeh and Tsai, 1976; Yotsukura and Fiering, 1964) and is therefore not included in this study.

The model is used to investigate the following simplified case: an instantaneous, line-source injection of a soluble, conservative, dye tracer in steady, nonuniform, overland flow at Reynolds numbers in the laminar range occurring over a smooth, impervious surface subject to rainfall. The following assumptions are employed: The width-to-depth ratio is sufficiently large that lateral boundaries have negligible effect on flow or dispersion characteristics. The initial injection is instantaneously, uniformly mixed. A cross-sectionally averaged mixing coefficient can be applied throughout the depth of flow. Transport of mass by splash droplets can be neglected.

B. Velocities and Depths

The velocity profile measurements published by Yoon (1970) and Yoon and Wenzel (1973) were used to derive new velocity profile equations for overland flow with rainfall. These equations were developed using a different approach than Yoon for three reasons. First, Yoon used von Karman's mixing length for turbulent flow to derive the velocity profile; however, the turbulence created by a raindrop impacting a thin sheet of moving liquid at a laminar Reynolds number is a different physical phenomenon than the model of eddy turbulence assumed by von Karman. Second, Yoon's velocity profile is not valid near the bed surface where it results in negative velocities. Third, simpler mathematical expressions of the velocity profile are needed to

integrate Eq. 2-6 to theoretically derive a one-dimensional dispersion coefficient.

Yoon measured velocity profiles in overland flow under rainfall intensities of 1.25, 3.75, and 15.00 inches per hour over slopes of 0.005 and 0.010 at Reynolds numbers ranging from 350 to 4000. From a plot of Darcy-Weisbach friction factor versus Reynolds number for flows without rainfall, Yoon concluded that the upper limit for laminar flow in his experiments occurred at Reynolds numbers between 800 and 1000. Shen and Li (1973) used Yoon's data as well as their own to come to a similar conclusion. Therefore, in order to restrict the present study to flows in the laminar Reynolds number range, only those profiles measured at Reynolds numbers of 800 or less were analyzed.

To investigate similarities between profiles, Yoon's velocity data were transformed for the present study using the dimensionless variables

$$u^* = u/u_m$$

and

$$y^* = y/y_m$$

where u = point velocity at distance y from bed surface, u_m = maximum point velocity in the profile, and y_m = distance from bed surface to u_m . The transformed data are plotted in Figure 3-1. Separate profile curves were fit to the data below and above $y^* = 1.0$.

For the lower profiles, two comparisons were made. In the first case, each profile was fit by least-squares regression to a second-degree polynomial,

$$u^* = A_\ell + B_\ell y^* + C_\ell y^{*2}$$

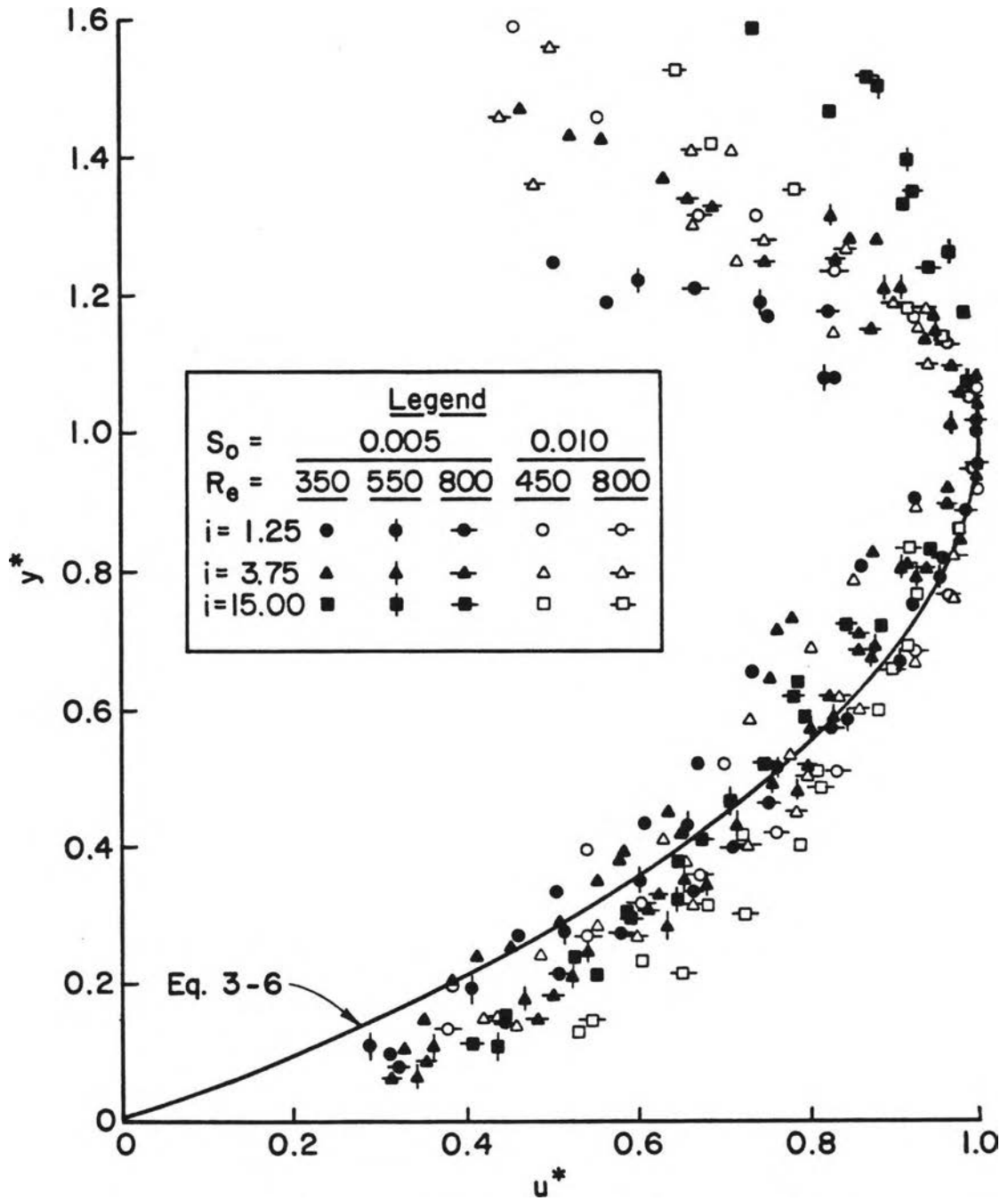


Figure 3-1. Plot of Transformed Velocity Profile Data
(Data Collected by Yoon, 1970)

where the subscript ℓ indicates the lower profile. In general, the resulting polynomials did not pass through the point (0,0) and (1,1), even though from the no-slip boundary condition and from physical reasoning, the actual velocity profiles must pass through these two points. Therefore, artificial data at these points were included in the velocity profile data sets. The results of the regression analyses are shown in Table 3-1. Because of the added artificial data, the resulting coefficients of determination, r^2 , for these regressions were not meaningful. Instead, Table 3-1 shows values for a Mean Residual defined as

$$\text{Mean Residual} = \sqrt{\frac{1}{n} \sum_{i=1}^n (u_i^* - \hat{u}_i^*)^2}$$

where u_i^* = i th measured value of u^* , \hat{u}_i^* = estimate of u_i^* based on polynomial equation, and n = total number of measured data points.

In order to obtain a general velocity profile equation for any flow condition within the range of those considered in Table 3-1, an attempt was made to correlate the polynomial coefficients to flow conditions. Since the values for coefficient A_ℓ were very small and since this coefficient should theoretically equal zero (zero velocity at bed surface), its value was taken as zero for the general velocity profile equation. Coefficients B_ℓ and C_ℓ were related to flow conditions by multiple linear regression.

The choice of flow parameters used in the regression of B_ℓ and C_ℓ was based on functional relationships used by Yoon (1970) and Shen and Li (1973). For overland flow under rainfall, Yoon presented

$$\tau_o = \text{function} (\bar{u}, y_s, S_o, k', \mu, \rho, i, v, d, \eta, \lambda, g)$$

Table 3-1

Results of Polynomial Regression for Lower Portion of Velocity Profile

Rainfall Intensity, i (in/hr)	Reynolds Number, R_e	Bed Slope, S_o	Best-Fit Polynomial Coefficients			Number of Measured Data Points, n	Mean Residual
			A_ℓ	B_ℓ	C_ℓ		
1.25	350	0.005	0.019	1.667	-0.711	10	0.057
1.25	450	0.010	0.010	1.680	-0.688	5	0.034
1.25	550	0.005	0.021	1.993	-1.022	11	0.026
1.25	800	0.005	0.027	2.224	-1.272	12	0.062
1.25	800	0.010	0.021	2.243	-1.281	11	0.028
3.75	350	0.005	0.029	1.663	-0.723	19	0.058
3.75	450	0.010	0.027	1.948	-0.996	15	0.072
3.75	550	0.005	0.044	2.095	-1.167	18	0.066
3.75	800	0.005	0.050	2.044	-1.124	19	0.069
3.75	800	0.010	0.030	2.221	-1.272	16	0.057
15.00	350	0.005	0.021	2.042	-1.079	8	0.064
15.00	450	0.010	0.035	2.291	-1.352	10	0.085
15.00	550	0.005	0.034	2.103	-1.156	7	0.099
15.00	800	0.005	0.028	1.979	-1.024	9	0.081
15.00	800	0.010	0.035	2.527	-1.594	8	0.104

where τ_o = boundary shear stress, \bar{u} = mean flow velocity, y_s = depth of flow, S_o = bed slope, k' = boundary roughness, μ = dynamic viscosity of water, ρ = density of water, i = rainfall intensity, v = impact velocity of raindrop, d = size of raindrop, η = parameter describing raindrop pattern, λ = parameter describing raindrop shape, and g = acceleration of gravity. He rearranged these variables into dimensionless groups as follows:

$$\frac{\tau_o}{\rho \bar{u}^2} = \text{function} \left(\frac{\rho \bar{u} y_s}{\mu}, \frac{\bar{u}}{\sqrt{g y_s}}, S_o, \frac{\rho i y_s}{\mu}, \frac{v}{\sqrt{g y_s}}, \frac{\rho i d}{\mu}, \frac{k'}{y_s}, \eta, \lambda \right) \quad (3-1)$$

Yoon concluded that 1) k'/y_s is negligible over a smooth surface, 2) λ was constant throughout the tests, 3) the effect of η on $\tau_o/(\rho \bar{u}^2)$ and on the velocity profile was negligible for the two raindrop patterns investigated, 4) $(\rho i y_s)/\mu$ and $v/\sqrt{g y_s}$ are poorly correlated to $\tau_o/(\rho \bar{u}^2)$, 5) the effect of $\bar{u}/\sqrt{g y_s}$ appears to be of secondary importance for the slopes tested, and 6) $(\rho i d)/\mu$ is essentially proportional to i , since raindrop size was held constant. Therefore, Eq. 3-1 was reduced to

$$\frac{\tau_o}{\rho \bar{u}^2} = \text{function} (R_e, S_o, i)$$

From a similar analysis, Shen and Li (1973) presented

$$\frac{y_s}{y_{s_e}} = \text{function} (R_e, S_o, i)$$

and

$$\frac{\bar{u}}{\bar{u}_e} = \text{function} (R_e, S_o, i)$$

where y_s = flow depth under rainfall, \bar{u} = flow velocity under rainfall, and the subscript e indicates the element of equivalent flow without rainfall.

Based on the above analyses, it was assumed for the present study that the polynomial coefficients describing the velocity profile under rainfall would be a function of R_e , S_o , and i . Results of the multiple linear regression for polynomial coefficients B_ℓ and C_ℓ are

$$B_\ell = 0.415 i^{0.047} R_e^{0.241} \quad (3-2)$$

and

$$C_\ell = -0.741 S_o^{0.323} R_e^{0.322} \quad (3-3)$$

with coefficients of determination, r^2 , of 0.60 and 0.57 respectively. The addition of a third independent variable in each regression did not increase the explained variation sufficiently to warrant its inclusion in the final equations, based on an F test at $\alpha = 0.01$. Therefore, the final general velocity profile from this approach is

$$u^* = (0.415 i^{0.047} R_e^{0.241}) y^* - (0.741 S_o^{0.323} R_e^{0.322}) y^{*2} \quad (3-4)$$

A second approach to obtaining a general velocity profile equation for $y^* < 1.0$ was also investigated. A second-degree polynomial equation was fit by regression to all data below $y^* = 1.0$, including artificial data points at (0,0) and (1,1). The resulting equation was

$$u^* = 0.056 + 1.957 y^* - 1.034 y^{*2} \quad (3-5)$$

with a Mean Residual of 0.075. This equation is very similar to the theoretical velocity profile equation for laminar flow,

$$u^* = 2 y^* - y^{*2} \quad (3-6)$$

A comparison of Eq. 3-6 to all data below $y^* = 1.0$ resulted in a mean residual of 0.091.

Equations 3-4, 3-5, and 3-6 are compared in Table 3-2, where it is shown that the lowest average Mean Residual results from the use of Eq. 3-5. However, at lower rainfall intensities and lower Reynolds numbers, where one would expect the flow to be the most laminar, Eq. 3-6 based on the theoretical laminar velocity profile appears to give an equal or better fit. Since the tests conducted for the present study covered the lower rainfall intensity range (2 to 5 inches per hour) and included a Reynolds number range (100 to 400) equal to and less than the lower range of Yoon's data, the theoretical laminar velocity profile equation, Eq. 3-6, was chosen to describe the lower portion of the profile. A plot of this equation is shown in Figure 3-1.

As shown in Figure 3-1, the upper portion of the profile ($y^* > 1.0$) displays significant scatter, partly because of measurement difficulties experienced by Yoon which were introduced by surface tension and water surface irregularities. An attempt to fit each profile to a polynomial equation and then correlate polynomial coefficients to flow parameters was not successful due to lack of correlation. The data were then grouped according to rainfall intensity, and a polynomial equation was fit to each group. However, when these equations were applied to the experimental flow conditions, negative velocities were computed near the water surface for some flows. To avoid this result, the depths were transformed using the dimensionless variable \tilde{y} defined as

Table 3-2

Comparison of General Velocity Profile Equations for Lower Profile

Rainfall Intensity, i (in/hr)	Reynolds Number, R_e	Bed Slope, S_o	Number of Measured Data Points, n	Mean Residual		
				Eq. 3-4 ⁽¹⁾	Eq. 3-5 ⁽²⁾	Eq. 3-6 ⁽³⁾
1.25	350	0.005	10	0.085	0.092	0.085
1.25	450	0.010	5	0.171	0.084	0.066
1.25	550	0.005	11	0.069	0.023	0.033
1.25	800	0.005	12	0.084	0.061	0.091
1.25	800	0.010	11	0.171	0.040	0.067
3.75	350	0.005	19	0.065	0.090	0.083
3.75	450	0.010	15	0.152	0.069	0.079
3.75	550	0.005	18	0.092	0.066	0.093
3.75	800	0.005	19	0.099	0.068	0.093
3.75	800	0.010	16	0.096	0.061	0.088
15.00	350	0.005	8	0.082	0.055	0.073
15.00	450	0.010	10	0.139	0.094	0.120
15.00	550	0.005	7	0.131	0.093	0.117
15.00	800	0.005	9	0.176	0.074	0.091
15.00	800	0.010	8	0.128	0.134	0.165
Average				0.116	0.074	0.090

$$(1) u^* = (0.415 i^{0.047} R_e^{0.241}) y^* - (0.741 S_o^{0.323} R_e^{0.322}) y^{*2}$$

$$(2) u^* = 0.056 + 1.957 y^* - 1.034 y^{*2}$$

$$(3) u^* = 2 y^* - y^{*2}$$

$$\tilde{y} = \frac{y - y_m}{y_s - y_m} \quad (3-7)$$

A plot of \tilde{y} versus u^* is shown in Figure 3-2. These data were grouped according to rainfall intensity. A regression analysis fit each data group to a second-degree polynomial,

$$u^* = A_u + B_u \tilde{y} + C_u \tilde{y}^2$$

where the subscript u indicates the upper profile. Since the profile must pass through point (1,0), artificial data points at this location were included in each data group. The results are shown in Table 3-3.

A general relationship for these polynomial coefficients was determined. A constant value of 1.0 was chosen for coefficient A_u since its value should theoretically be 1.0 ($u^* = 1.0$ at $\tilde{y} = 0$) and since the best-fit values of this coefficient were all close to 1.0. Coefficients B_u and C_u were related to rainfall intensity by fitting a straight line between coefficient values for 1.25 and 3.75 inches per hour and between coefficient values for 3.75 and 15.00 inches per hour. The following set of equations resulted,

$$B_u = \begin{cases} -0.404 + 0.0492i, & i \leq 3.75 \text{ in/hr} \\ -0.211 - 0.0022i, & i > 3.75 \text{ in/hr} \end{cases} \quad (3-8)$$

$$C_u = \begin{cases} -0.199 + 0.0060i, & i \leq 3.75 \text{ in/hr} \\ -0.217 + 0.0110i, & i > 3.75 \text{ in/hr} \end{cases} \quad (3-9)$$

Therefore, a general equation for the upper portion of the profile becomes

$$u^* = 1.0 + B_u \tilde{y} + C_u \tilde{y}^2 \quad (3-10)$$

where B_u and C_u are given in Eqs. 3-8 and 3-9. Plots of Eq. 3-10 for 1.25, 3.75, and 15.00 inches per hour are shown in Figure 3-2.

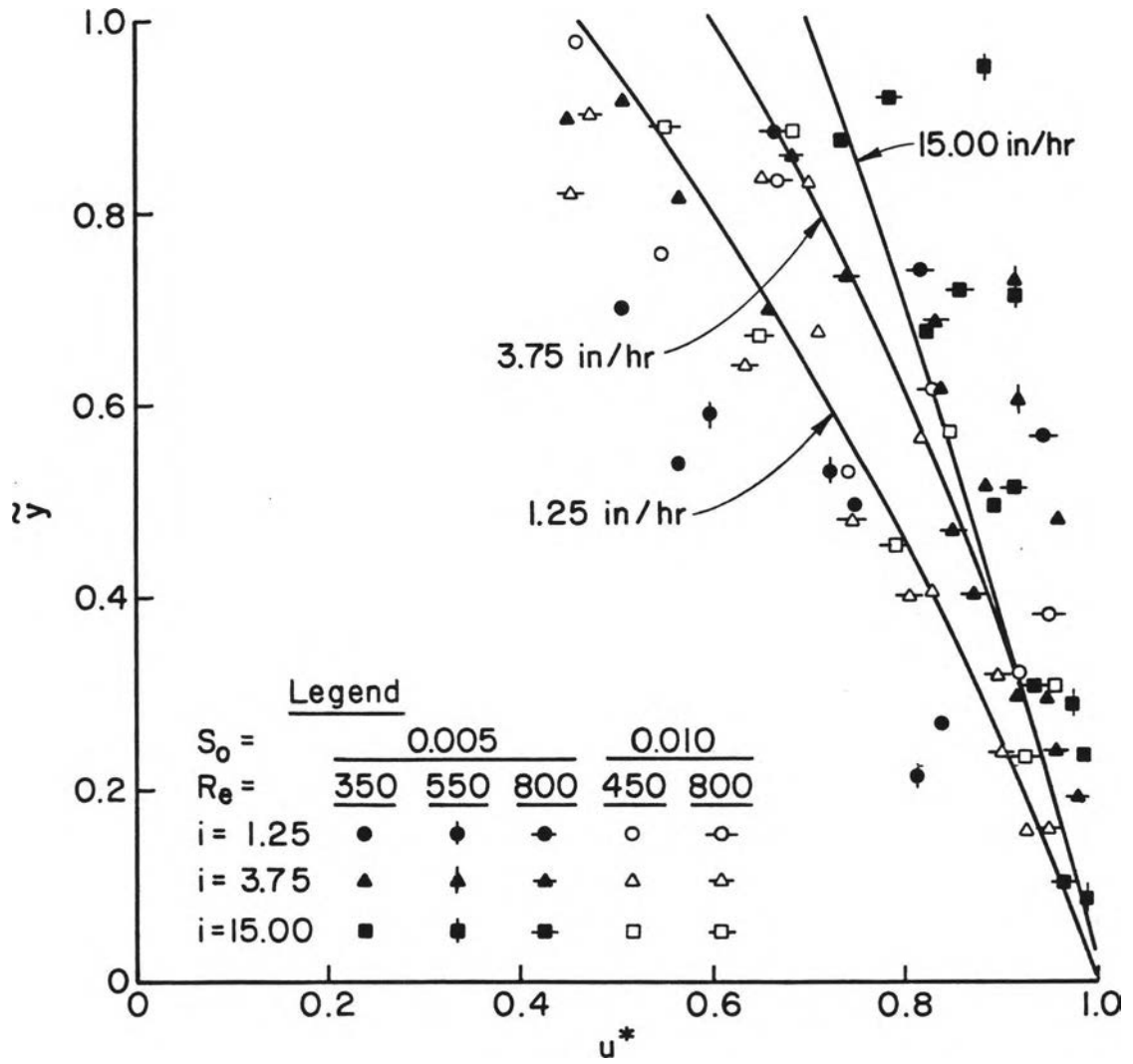


Figure 3-2. Plot of \bar{z} Versus u^*

Table 3-3

Results of Polynomial Regression for
Upper Portion of Velocity Profile

Rainfall Intensity, i (in/hr)	Best-Fit Polynomial ⁽¹⁾ Coefficients			Number of Measured Data Points, n	Mean Residual
	A_u	B_u	C_u		
1.25	1.005	-0.342	-0.191	17	0.116
3.75	0.992	-0.219	-0.176	32	0.095
15.00	1.006	-0.244	-0.053	20	0.081

(1) Polynomial coefficients defined by $u^* = A_u + B_u \tilde{y} + C_u \tilde{y}^2$.

To use these profile equations, a relationship for u_m and y_m must be found. Therefore, values of u_m and y_m from Yoon's measurements were related to flow and rainfall variables by regression. A functional relationship similar to that for the lower profile polynomial coefficients was assumed--that is, u_m and y_m are functions of R_e , S_o , and i . However, since a high correlation was expected between the maximum and mean velocities and between the depth of the maximum velocity and the flow depth, \bar{u} and y_s were used as independent variables in place of R_e in the regression, since

$$R_e = \frac{\bar{u} y_s}{\nu}$$

and ν remains essentially constant. The functional relationship becomes

$$u_m, y_m = \text{function} (\bar{u}, y_s, S_o, i)$$

The data are shown in Table 3-4. The resulting regression equations are

$$u_m = 1.216 \bar{u}^{0.801} i^{-0.071} \quad (3-11)$$

$$y_m = 1.361 y_s^{1.138} i^{-0.078} \quad (3-12)$$

with coefficients of determination, r^2 , of 0.96 and 0.86, respectively. In Eqs. 3-11 and 3-12, the units of u_m and \bar{u} are feet per second; the units of y_m and y_s are feet; and the units of i are inches per hour. The addition of a third independent variable in each regression did not increase the explained variation sufficiently to warrant its inclusion in the final equations, based on an F test at $\alpha = 0.01$.

Flow depths and mean velocities can be computed using the Darcy-Weisbach equation. Rearranging Eq. 2-2,

Table 3-4
Measured Velocities and Depths⁽¹⁾

Rainfall Intensity, i (in/hr)	Reynolds Number, R_e	Bed Slope, S_o	Mean Velocity, \bar{u} (ft/sec)	Maximum Velocity, u_m (ft/sec)	Flow Depth, y_s (ft)	Depth of Max Velocity, y_m (ft)
1.25	350	0.005	0.315	0.475	0.0118	0.0088
1.25	450	0.010	0.466	0.740	0.0102	0.0063
1.25	550	0.005	0.414	0.565	0.0143	0.0104
1.25	800	0.005	0.540	0.730	0.0160	0.0129
1.25	800	0.010	0.705	0.890	0.0127	0.0092
3.75	350	0.005	0.300	0.405	0.0129	0.0092
3.75	450	0.010	0.438	0.578	0.0118	0.0083
3.75	550	0.005	0.396	0.480	0.0155	0.0117
3.75	800	0.005	0.494	0.638	0.0179	0.0129
3.75	800	0.010	0.638	0.752	0.0143	0.0092
15.00	350	0.005	0.245	0.340	0.0168	0.0100
15.00	450	0.010	0.398	0.470	0.0135	0.0092
15.00	550	0.005	0.361	0.425	0.0178	0.0117
15.00	800	0.005	0.446	0.575	0.0206	0.0125
15.00	800	0.010	0.554	0.615	0.0171	0.0096

(1) From data measured by Yoon (1970).

$$y_s = \left[\frac{f q^2}{8 g S_o} \right]^{1/3} \quad (3-13)$$

The friction coefficient, f , can be computed from Eq. 2-4. The discharge per unit width, q , can be computed from

$$q = ix$$

where x = distance from top of the plane. When units of i are inches per hour, when units of x are feet, and when units of q are cubic feet per second per foot width, q can be computed from

$$q = (2.315 \times 10^{-5})ix \quad (3-14)$$

Mean velocity is then

$$\bar{u} = q/y_s \quad (3-15)$$

Mean velocity can also be computed from Eqs. 3-6 and 3-10.

Consider

$$\bar{u}_p = u_m \bar{u}^* \quad (3-16)$$

where \bar{u}_p = mean velocity (in units of feet per second) based on the previously derived velocity profile, u_m = maximum velocity in the profile (in units of feet per second), and \bar{u}^* = mean of the dimensionless velocity profile, u^* , throughout the flow depth. \bar{u}^* can be expressed as

$$\bar{u}^* = \omega_\ell \bar{u}_\ell^* + \omega_u \bar{u}_u^* \quad (3-17)$$

where ω_ℓ = fraction of total depth included in lower profile = y_m/y_s ;
 ω_u = fraction of total depth included in upper profile = $(y_s - y_m)/y_s$;
 and

$$\bar{u}_\ell^* = \int_0^1 u^* dy^* \quad (3-18)$$

and

$$\bar{u}_u^* = \int_0^1 u^* d\tilde{y} \quad (3-19)$$

Substituting Eqs. 3-6, 3-10, 3-17, 3-18, and 3-19 into Eq. 3-16,

$$\bar{u}_p = u_m \left[\frac{y_m}{y_s} \int_0^1 (2 y^* - y^{*2}) dy^* + \frac{y_s - y_m}{y_s} \int_0^1 (1.0 + B_u \tilde{y} + C_u \tilde{y}^2) d\tilde{y} \right]$$

After integrating and rearranging,

$$\bar{u}_p = \frac{u_m}{y_s} \left[\frac{2}{3} y_m + (y_s - y_m) \left(1.0 + \frac{1}{2} B_u + \frac{1}{3} C_u \right) \right] \quad (3-20)$$

Mean velocities computed from Eqs. 3-15 and 3-20 will not exactly coincide due to the different nature of their derivations. A comparison of these two equations is shown in Table 3-5 for a range of hypothetical flow conditions typical of the flows investigated for this study. Table 3-6 compares Eqs. 3-15 and 3-20 to measured data for the lower rainfall intensities and lower Reynolds numbers. To make the velocity profiles consistent with Darcy-Weisbach mean velocities, the ratio \bar{u}/\bar{u}_p was added to the profile equations as a correction factor. The final velocity profile equations are therefore written as

$$u^* = \begin{cases} (\bar{u}/\bar{u}_p)(2y^* - y^{*2}), & y^* \leq 1.0 \\ (\bar{u}/\bar{u}_p)(1.0 + B_u \tilde{y} + C_u \tilde{y}^2), & y^* > 1.0 \end{cases} \quad (3-21)$$

C. Dilution

Pollutant concentration will decrease as it travels down the overland flow plane due to the increasing depth of flow. Consider a parcel of fluid in flow layer j at point A on the overland flow plane as shown in Figure 3-3. The volume of this parcel of unit width is $\delta x \cdot \delta y_{j,A} \cdot 1$, where

Table 3-5

Comparison of Mean Velocity Equations for Hypothetical Flows

Rainfall Intensity, i (in/hr)	Bed Slope, S_o	Distance from Top of Plane, x (ft)	Reynolds Number ⁽¹⁾	Mean Velocity (ft/sec)	
				Eq. 3-15 ⁽²⁾	Eq. 3-20 ⁽³⁾
2.0	0.001	35	162	0.104	0.132
2.0	0.015	35	162	0.256	0.279
2.0	0.030	35	162	0.323	0.337
5.0	0.001	35	404	0.177	0.194
5.0	0.015	35	404	0.436	0.407
5.0	0.030	35	404	0.549	0.492

(1) Assuming kinematic viscosity is 1×10^{-5} ft²/sec.

(2) Using Eqs. 2-4, 3-13, and 3-14.

(3) Using Eqs. 3-8, 3-9, 3-11, 3-12, and 3-13.

Table 3-6
Comparison of Computed and Measured Velocities⁽¹⁾

Rainfall Intensity, i (in/hr)	Bed Slope, S_o	Reynolds Number, R_e	Mean Velocity (ft/sec)		
			Computed by Eq. 3-15	Computed by Eq. 3-20	Measured
1.25	0.005	350	0.315	0.329	0.315
1.25	0.010	450	0.475	0.458	0.466
3.75	0.005	350	0.291	0.297	0.300
3.75	0.010	450	0.440	0.414	0.438

(1) Measured velocities taken from data collected by Yoon (1970).

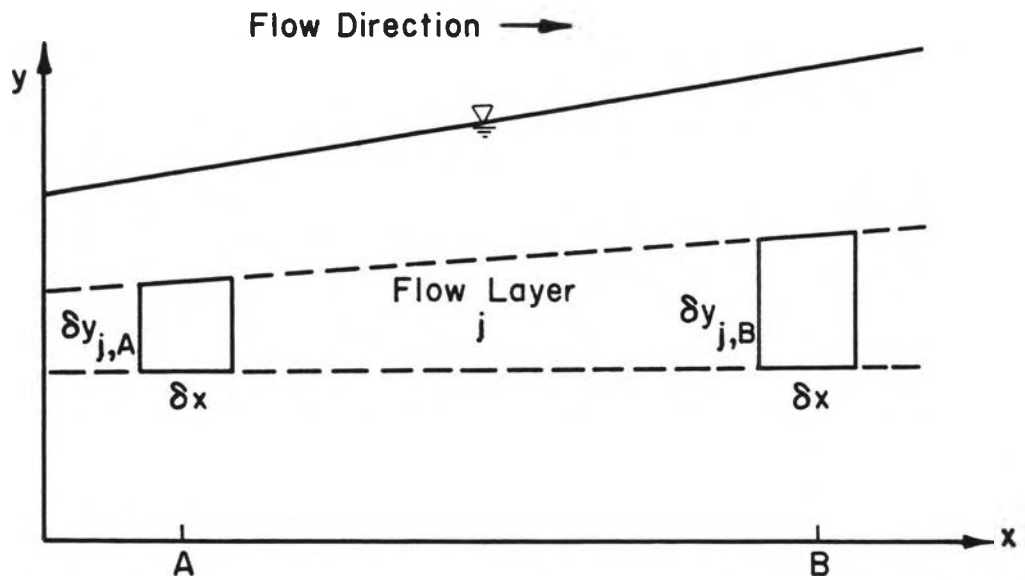


Figure 3-3. Change in Volume of a Parcel of Fluid of Fixed Length Moving Through Flow Layer in Nonuniform Flow

$$\delta y_{j,A} = \alpha_j y_{s,A} \quad (3-22)$$

and where $y_{s,A}$ = depth of water surface at point A, and α_j = fractional height of flow layer j relative to depth of water surface. For a given mass, M , contained within this parcel, the parcel concentration at point A is

$$C_{j,A} = \frac{M}{\delta x \cdot \delta y_{j,A} \cdot l} \quad (3-23)$$

Similarly, for point B,

$$C_{j,B} = \frac{M}{\delta x \cdot \delta y_{j,B} \cdot l} \quad (3-24)$$

From Eqs. 3-22, 3-23, and 3-24, the ratio of concentrations at points A and B is

$$\frac{C_{j,A}}{C_{j,B}} = \frac{\delta y_{j,B}}{\delta y_{j,A}} = \frac{y_{s,B}}{y_{s,A}}$$

Solving for the concentration at point B,

$$C_{j,B} = C_{j,A} \frac{y_{s,A}}{y_{s,B}} \quad (3-25)$$

or, the concentration of a fixed-length parcel traveling within a flow layer in nonuniform flow, considering only pure convection, is equal to its upstream concentration times the ratio of upstream to downstream flow depths.

D. Vertical Diffusion

For this study, vertical movement of solute in laminar, overland flow is assumed to be influenced by two processes: 1) continuous molecular diffusion, and 2) short-term, local mixing due to raindrop impact. For movement by molecular diffusion, Fick's law describes

solute mass flux as proportional to the concentration gradient in the direction of solute movement. Stated mathematically,

$$F_y = - \epsilon_m \frac{\partial C}{\partial y} \quad (3-26)$$

where F_y = solute mass flux in the vertical direction, ϵ_m = diffusion coefficient due to molecular diffusion, and C = solute concentration. Application of conservation of mass to a control volume using Fick's law results in the partial differential equation,

$$\frac{\partial C}{\partial t} = \epsilon_m \frac{\partial^2 C}{\partial y^2} \quad (3-27)$$

where t = time.

Solute mixing due to raindrop impact is more difficult to precisely describe quantitatively. However, qualitative descriptions of raindrop impact behavior in stagnant liquid have been presented by a number of authors (Macklin and Metaxas, 1976; Engle, 1966; Harlow and Shannon, 1967; Mutchler, 1967; Wang and Wenzel, 1970). Following drop impact, a crown of liquid is thrown upward along the perimeter of the drop. As the drop penetrates further, the height of the crown increases and a cavity formed in the liquid layer increases in size. During this time, local velocity directions are downward beneath the cavity, outward along the sides of the cavity, and upward into the crown. For shallow liquid depths, such as those considered in this study, the shape of the cavity is cylindrical and the bottom of the cavity penetrates to the bed surface. At maximum crown height, spray droplets are formed at the peak of the crown and are thrown outward, followed by recession and disintegration of the crown and collapse of the cavity. At this point, local velocities have reversed direction

and move radially inward. As the cavity collapses, a jet of liquid may rise above the water surface at the center of the former cavity. The time to maximum crater diameter for shallow liquid layers has been shown to be several hundredths of a second or less (Mutchler, 1967; Wang and Wenzel, 1970). Defining the effect of raindrops on vertical mixing is further complicated by their random nature in time and space.

Due to the complexity of mathematically describing these physical processes, simplifying assumptions were made. It was assumed that the vertical mixing of solute due to raindrops could be modeled using a Fickian-based diffusion model, similar to Eq. 3-27, with a vertically-averaged, time-averaged, vertical diffusion coefficient. Therefore, the effect of both molecular diffusion and raindrop mixing can be expressed as

$$\varepsilon_y = \varepsilon_m + \varepsilon_{y,r} \quad (3-28)$$

where ε_y = total vertical diffusion coefficient and $\varepsilon_{y,r}$ = vertical diffusion coefficient due to raindrop mixing. The general form of Eq. 3-27 for both molecular diffusion and raindrop mixing then becomes

$$\frac{\partial C}{\partial t} = \varepsilon_y \frac{\partial^2 C}{\partial y^2} \quad (3-29)$$

Consider the vertical diffusion of solute concentration C_j in flow layer j where the lower and upper boundaries of the flow layer are located r and s distances from the bed surface, respectively. The initial condition is

$$C(y,t) \Big|_{t=0} = C(y,0) = \begin{cases} 0, & y < r \\ C_j, & r \leq y \leq s \\ 0, & y > s \end{cases} \quad (3-30)$$

The solution to Eq. 3-29 becomes

$$C(y,t) = \int_r^s \frac{C_j}{\sqrt{4 \pi \epsilon_y t}} \exp \left[\frac{-(y - \xi)^2}{4 \epsilon_y t} \right] d\xi \quad (3-31)$$

where the integrand is the solution to Eq. 3-29 for

$$C(y,0) = C_j \delta(y - \xi)$$

with $\delta(\)$ representing the Dirac delta function. Transforming Eq. 3-31 by setting

$$z = \frac{(y - \xi)}{\sqrt{4 \epsilon_y t}}$$

results in

$$\begin{aligned} C(y,t) &= -\frac{C_j}{\sqrt{\pi}} \int_{\frac{y-r}{\sqrt{4 \epsilon_y t}}}^{\frac{y-s}{\sqrt{4 \epsilon_y t}}} e^{-z^2} dz \\ &= -\frac{C_j}{\sqrt{\pi}} \left[-\int_0^{\frac{y-r}{\sqrt{4 \epsilon_y t}}} e^{-z^2} dz + \int_0^{\frac{y-s}{\sqrt{4 \epsilon_y t}}} e^{-z^2} dz \right] \\ &= \frac{C_j}{2} \left[\operatorname{erf} \left(\frac{y-r}{\sqrt{4 \epsilon_y t}} \right) - \operatorname{erf} \left(\frac{y-s}{\sqrt{4 \epsilon_y t}} \right) \right] \quad (3-32) \end{aligned}$$

where erf is defined as the error function. With no-flux boundary conditions at the bed surface and water surface, the solution for $C(y,t)$ for $0 < y < y_s$ is the summation of Eq. 3-32 for sets of R and S which define the lower and upper boundaries of flow layer j as well as the lower and upper boundaries of all image sources of flow layer j . The resulting solution is written

$$C(y,t) = \frac{C_j}{2} \sum_{n=-\infty}^{\infty} \left[\operatorname{erf} \left(\frac{y - R(n)}{\sqrt{4 \epsilon_y t}} \right) - \operatorname{erf} \left(\frac{y - S(n)}{\sqrt{4 \epsilon_y t}} \right) \right] \quad (3-33)$$

where

$$R(n) = \begin{cases} ny_s + r, & \text{for all even } n \\ (n+1)y_s - r, & \text{for all odd } n \end{cases}$$

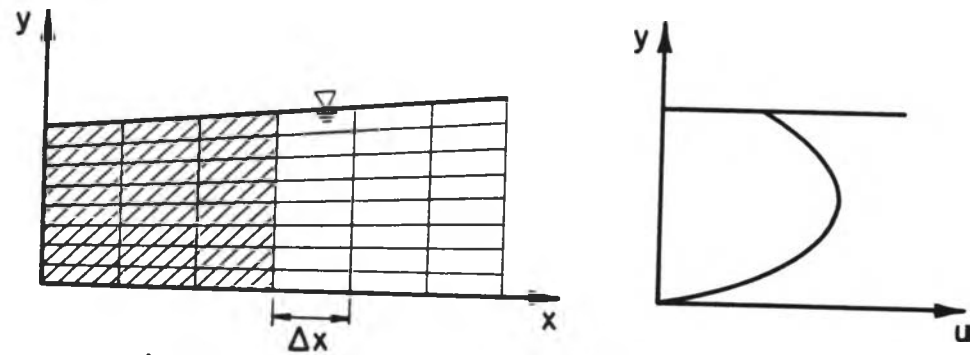
$$S(n) = \begin{cases} ny_s + s, & \text{for all even } n \\ (n+1)y_s - s, & \text{for all odd } n \end{cases}$$

and where n is an integer. In the application of Eq. 3-33, n is taken in steps beginning with 0, ± 1 , ± 2 , etc. until the incremental increase in $C(y,t)$ is below a predetermined cutoff level.

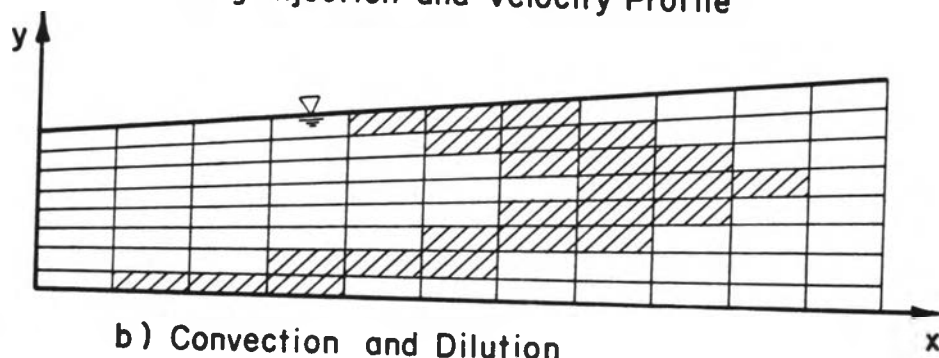
E. Proposed Model

A simplified schematic of the proposed model is shown in Figure 3-4. As shown in this figure, the flow field is divided into flow layers. Each flow layer is further divided into fixed grid cells of equal length, Δx . During each computational time step, ΔT , mass is convected within its flow layer, diluted due to the increase in depth, and vertically diffused. Details of the procedures are described below.

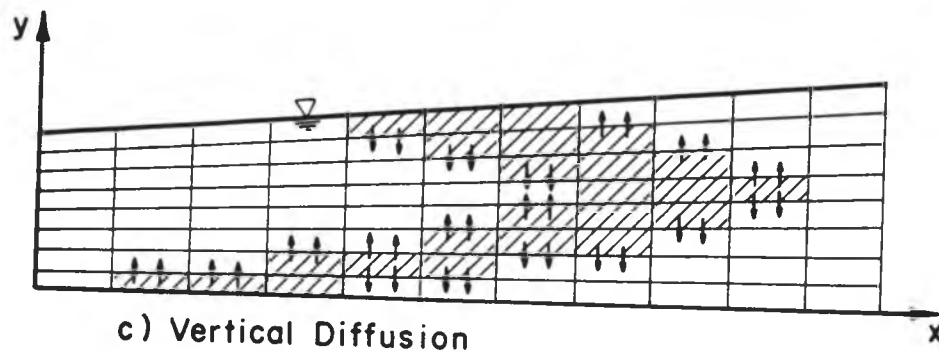
1. Convection. Due to the nonuniform nature of overland flow with rainfall, the velocity within a flow layer is a function of distance from the top of the plane. A velocity $U(j,k)$ is assigned to each grid cell, where j = flow layer number, counting from the bed surface up, and k = cell number, counting downstream from the point of injection. The value of $U(j,k)$ is determined from Eq. 3-21 at the center of the grid cell.



a) Slug Injection and Velocity Profile



b) Convection and Dilution



c) Vertical Diffusion

Figure 3-4. Simplified Schematic of Proposed Model for Solute Transport in Overland Flow with Rainfall

Pollutant mass is contained within pollutant cells. At injection, pollutant cell boundaries are identical to grid cell boundaries as shown in Figure 3-5a. However, during convection, pollutant cell boundaries move downstream at the velocity of the flow layer, and at the end of the computational time step, ΔT , the location of the pollutant cell boundary will not in general be identical to one of the fixed grid cell boundaries as shown in Figure 3-5b. Also, due to nonuniform velocities within the flow layer, pollutant cell boundaries tend to spread apart during convection. Therefore, each pollutant cell boundary is convected separately. The convection is simulated by moving the boundary through successive downstream grid cells until the summation of $\Delta x/U(j,k)$ equals ΔT . At that point, the distance between the pollutant cell boundary and the nearest grid cell boundary is recorded as a residual (Figure 3-5b). Then the pollutant cell boundary is temporarily adjusted to its nearest grid cell boundary (Figure 3-5c) for the dilution and diffusion steps. The pollutant cell is then returned to its exact location prior to the next convection step (Figure 3-5d). When adjacent pollutant cell boundaries spread far enough apart to span the distance of two grid cells, a new pollutant cell boundary is created, and the pollutant cell is split into two cells. The pollutant mass is equally divided between the two cells.

2. Dilution. Following convection, the concentration of the pollutant cell is adjusted due to the increase in flow depth in the downstream direction. This adjustment is made by multiplying the cell concentration by the ratio of flow depths before and after convection (Eq. 3-25). Flow depths are computed using the Darcy-Weisbach equation, Eq. 3-13, with a friction factor computed from Eq. 2-4.

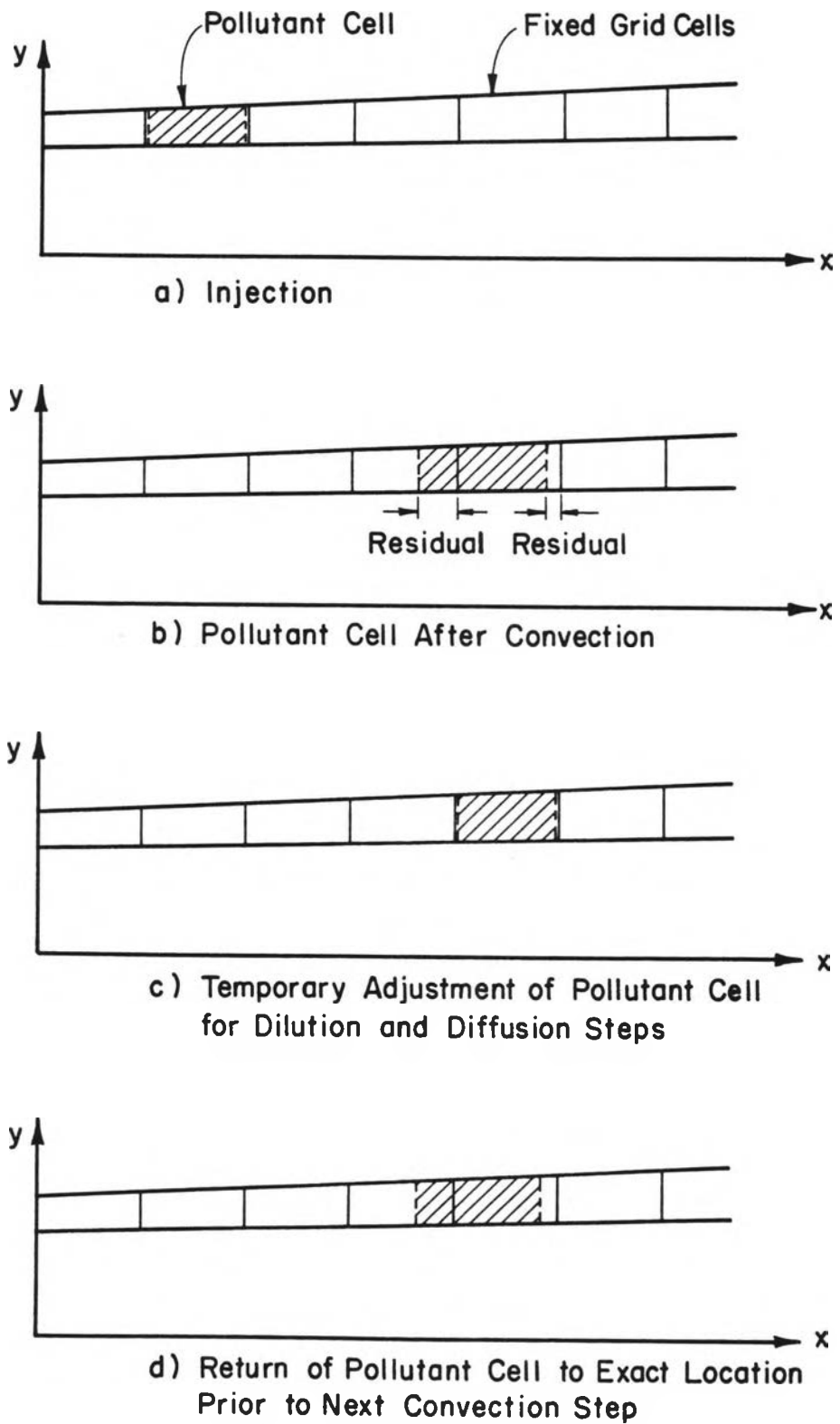


Figure 3-5. The Convection Step

3. Vertical Diffusion. To facilitate vertical diffusion computations, the location of a pollutant cell is adjusted as shown in Figure 3-5c to match the grid cell configuration. All cells which are then aligned in one vertical column comprise a "cell column." Vertical diffusion calculations proceed independently from one cell column to the next. Equation 3-33, with $t = \Delta T$, is applied separately to each pollutant cell within a cell column, and then the individual solutions are added to yield the final diffused concentrations. In applying Eq. 3-33 for the present study, the value of n was incremented from 0 to ± 1 , ± 2 , etc. until the incremental increase in $C(y, \Delta T)$ was less than 0.5 percent of C_j . The resulting truncation error was then distributed uniformly throughout the cell column. The concentration computed at the mid-depth of the cell was used as the concentration for the entire cell.

4. Computer Program. The procedures described above were coded into a FORTRAN V computer program. A program listing is included in Appendix A.

F. Model Testing

Analytical solutions are not available for model testing of nonuniform flow with rainfall impact. Instead, the model was tested for steady, uniform flow (no rainfall) using the analytical solutions described below.

1. Cleary and Adrian Solution. A two-dimensional, analytical solution for an instantaneous point source in a uniform velocity field was presented by Cleary and Adrian (1973). Figure 3-6 shows schematically the concentration distribution resulting from the solution when only vertical mixing is considered.

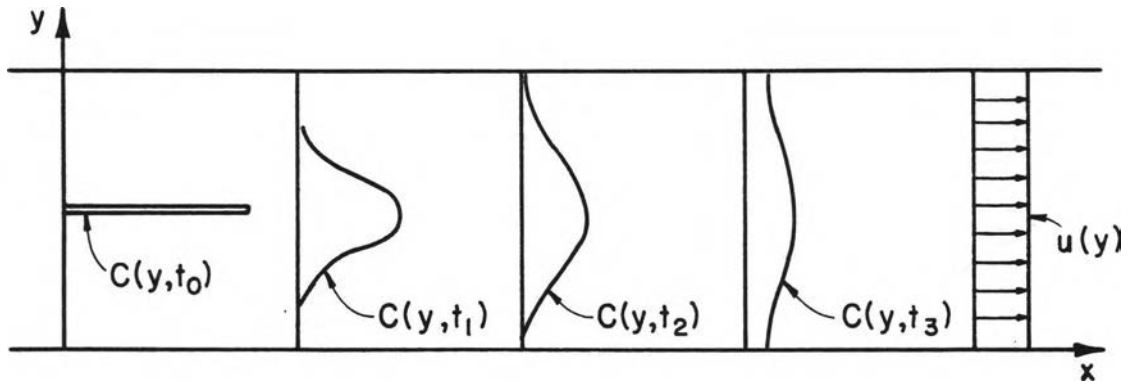


Figure 3-6. Concentration Distribution of Cleary and Adrian (Neglecting Longitudinal Diffusion)

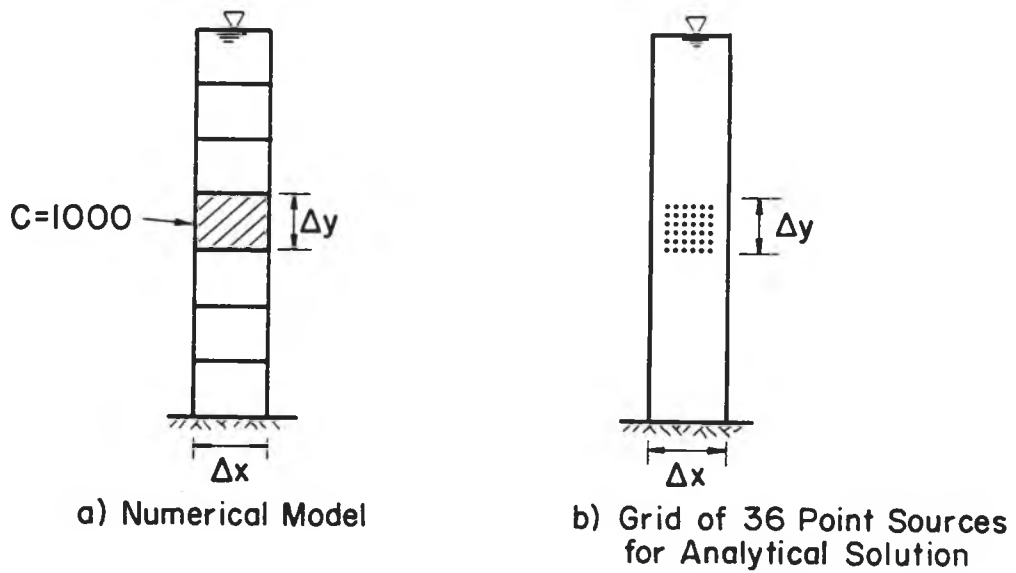


Figure 3-7. Middepth Injection Used for Cleary and Adrian Test

The numerical model was tested against the Cleary and Adrian solution for a source introduced instantaneously at flow middepth under the steady, uniform conditions described in Table 3-7. In this table, discharge was computed from Eq. 3-14 using $i = 3$ inches per hour and $x = 35$ feet. The parameter f was computed using Eq. 24 with $i = 3$ inches per hour. Depth of flow and mean velocity were computed from Eqs. 3-13 and 3-15, respectively. Longitudinal diffusion was assumed to be negligible.

To simulate a middepth injection, the source was introduced in the numerical model as a concentration of 1000 within a single grid cell located in the middle flow layer as shown in Figure 3-7a. Therefore, the total mass injected was

$$M_{\text{numerical}} = 1000(\Delta x \cdot \Delta y \cdot 1)$$

where Δx and Δy are defined in Figure 3-7.

Since the analytical solution is valid only for a point source (in two dimensions), a grid of point sources was used as shown in Figure 3-7b to represent a uniform concentration within the area equivalent to a grid cell. Therefore the mass of each point source was equal to

$$M_{\text{analytical}} = \frac{1000(\Delta x \cdot \Delta y \cdot 1)}{36}$$

The sum of the 36 individual solutions was compared against the numerical model results. Details are contained in Appendix B.

For each test, the value of the dimensionless group

$$\frac{(\Delta y)^2}{\Delta T \cdot \epsilon_y}$$

was varied until the difference between model result and analytical solution was minimized. The significance of this dimensionless group

Table 3-7

Flow Conditions for Cleary and Adrian Test
and Yeh and Tsai Test

Discharge Per Unit Width, q	0.0024255 ft ² /sec
Kinematic Viscosity, ν	0.00001 ft ² /sec
Friction Coefficient, f	0.2721
Acceleration of Gravity, g	32.2 ft/sec ²
Bed Slope, S_o	0.015
Depth of Flow, y_s	0.007455 ft
Mean Velocity, \bar{u}	0.3254 ft/sec
Vertical Mixing Coefficient, ϵ_y	30×10^{-8} ft ² /sec

in determining the accuracy of diffusion calculations can be explained as follows. The numerator is a measure of the distance between flow layers. The denominator is a measure of the distance over which the system is able to diffuse mass during the time interval ΔT . For a large value of $(\Delta y)^2/(\Delta T \cdot \epsilon_y)$, the distance between flow layers is large relative to the distance over which the system is able to diffuse mass. For a small value of $(\Delta y)^2/(\Delta T \cdot \epsilon_y)$, the system is able to diffuse mass over distances much greater than Δy . Because the computational scheme uses the concentration at middepth of the flow layer as the average cell concentration, accuracy is greater when the mass is spread over many flow layers than when spread over few flow layers.

Model tests were conducted using 7, 11, and 19 flow layers. All results are contained in Appendix B. The results using only 11 flow layers are shown graphically in Figure 3-8 and are typical of those obtained using 7 and 19 flow layers. A review of all tests indicates that the greatest accuracy is achieved when $(\Delta y)^2/(\Delta T \cdot \epsilon_y) \leq 1.25$. Within this range, the mean deviation was not greater than 0.6 percent of the cross-sectional average concentration. This value of 1.25 was therefore selected as the upper limit for $(\Delta y)^2/(\Delta T \cdot \epsilon_y)$ for all subsequent model runs presented in this study.

Based on these test results, it appears that the number of flow layers, within the range investigated, is not a major factor affecting accuracy. From the practical view of adequately defining the velocity profile, a minimum of 11 flow layers was used in all subsequent model runs.

2. Yeh and Tsai Solution. A two-dimensional, steady-state, analytical solution for a continuously-released point source in shear

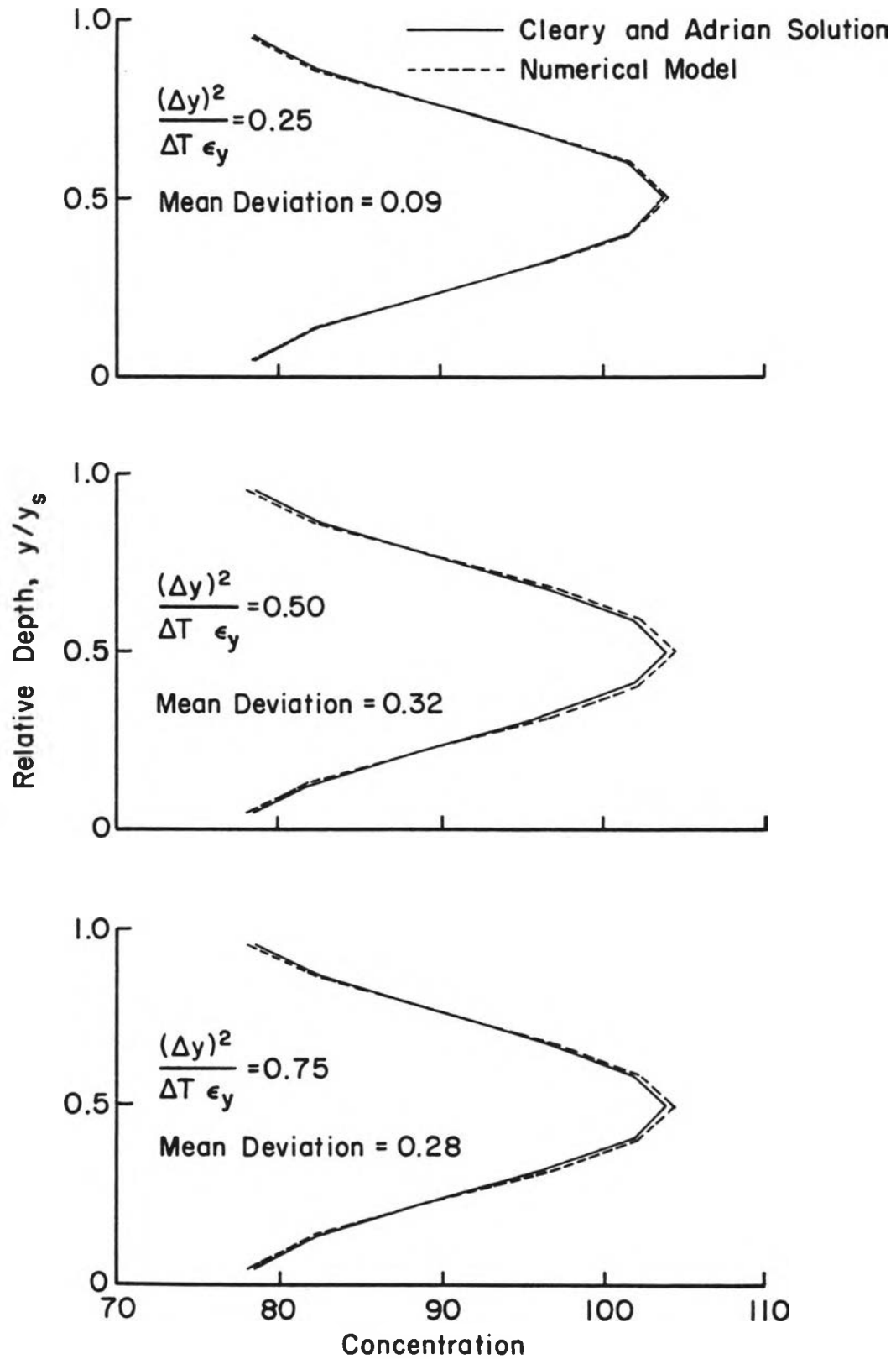


Figure 3-8. Comparison of Numerical Model (Using 11 Flow Layers) to Cleary and Adrian Solution

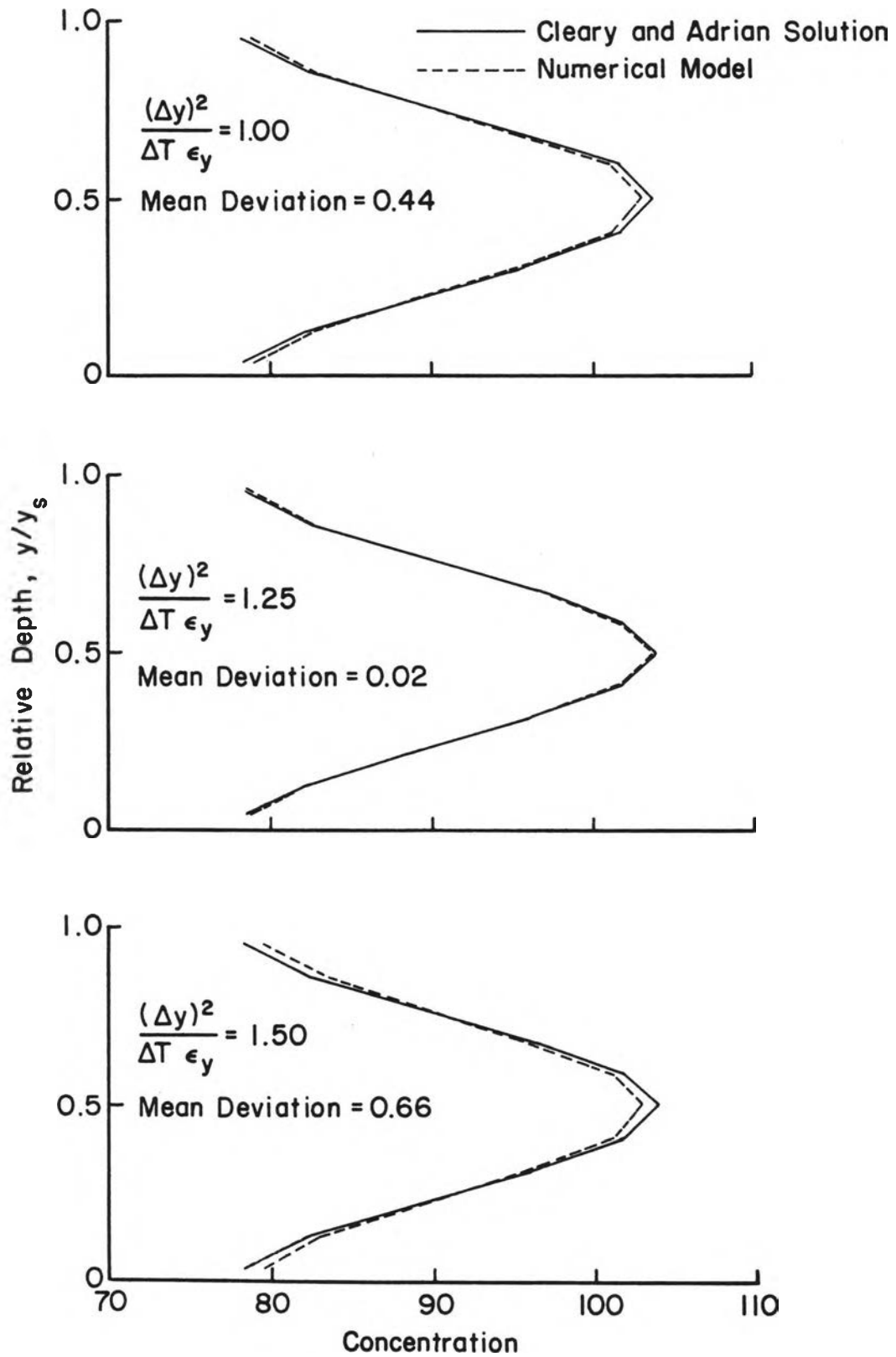


Figure 3-8. continued

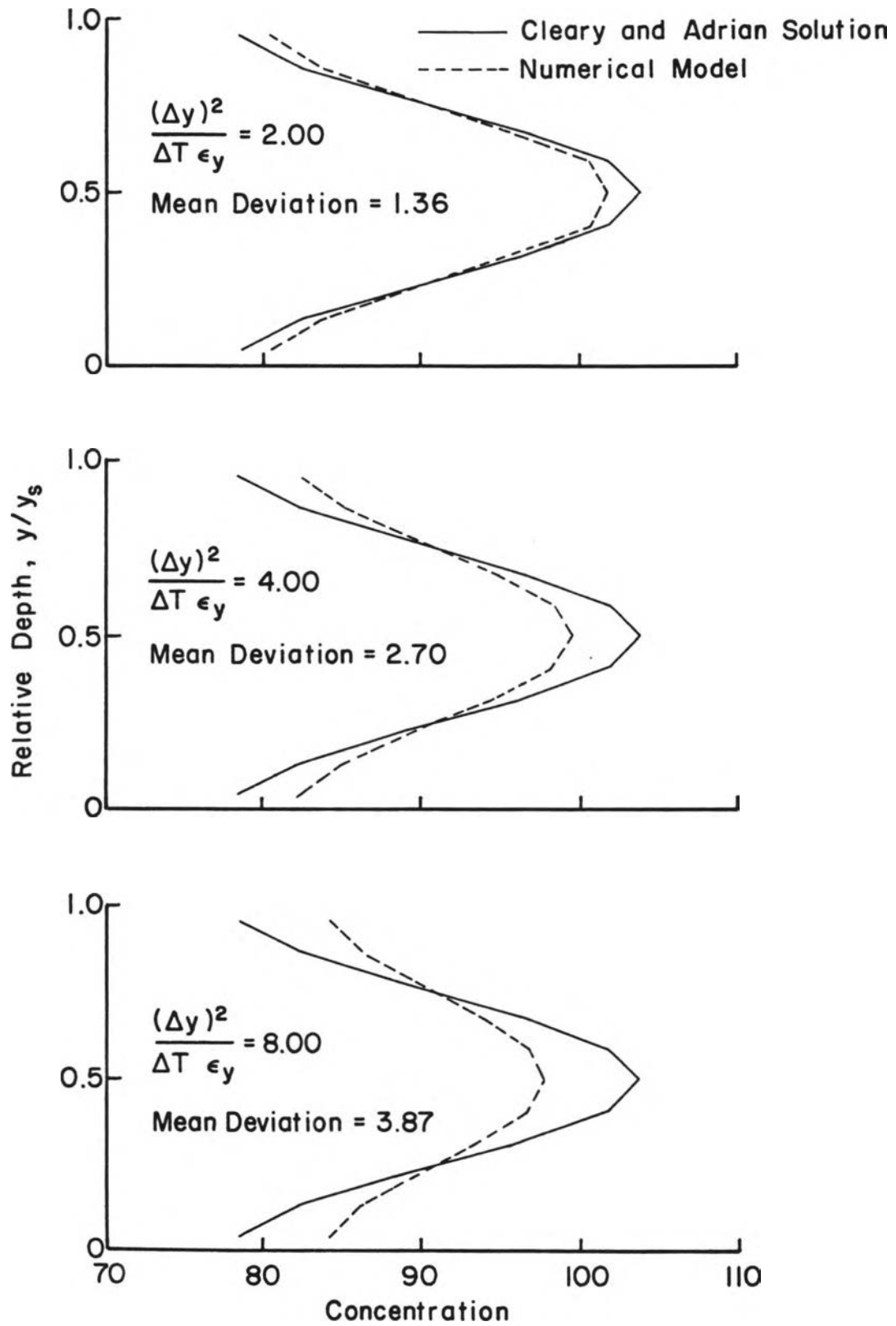


Figure 3-8. continued

flow was presented by Yeh and Tsai (1976). The velocity profile was expressed as a power function of the vertical distance above the streambed. Only diffusion in the vertical direction was considered.

The numerical model was tested against this solution for a source introduced continuously at flow middepth under the same steady, uniform flow conditions described in Table 3-7. Thirteen flow layers were used in these tests. The velocity profile was defined by

$$u = 0.7488 y^{1/7}$$

where u = local velocity at vertical distance y from the streambed.

The source was introduced in the numerical model as a continuous injection of concentration 1000 within the middepth grid cell. Therefore, the rate of mass injection was

$$M_{\text{numerical}} = \frac{1000(\Delta x \cdot \Delta y \cdot 1)}{\Delta x / u_{\text{midpt}}}$$

where Δx and Δy are defined in Figure 3-7a and u_{midpt} = local velocity at middepth.

For the analytical solution, multiple point sources were used to simulate the areal coverage of injection in the numerical model as done for the Cleary and Adrian test. So, the rate of mass injection of each point source was equal to $M_{\text{numerical}}$ divided by the total number of point source injections.

In each test, the ratio $\Delta x / \Delta T$ was varied to determine its influence on the response of the numerical model compared to the analytical solution. The response was examined for a point located eight feet down the plane from the point of injection. Results are shown in Figure 3-9 and Table 3-8 for $\Delta x / \Delta T$ values ranging from $0.5 \bar{u}$ to $3.0 \bar{u}$. These results indicate a mean deviation from the analytical

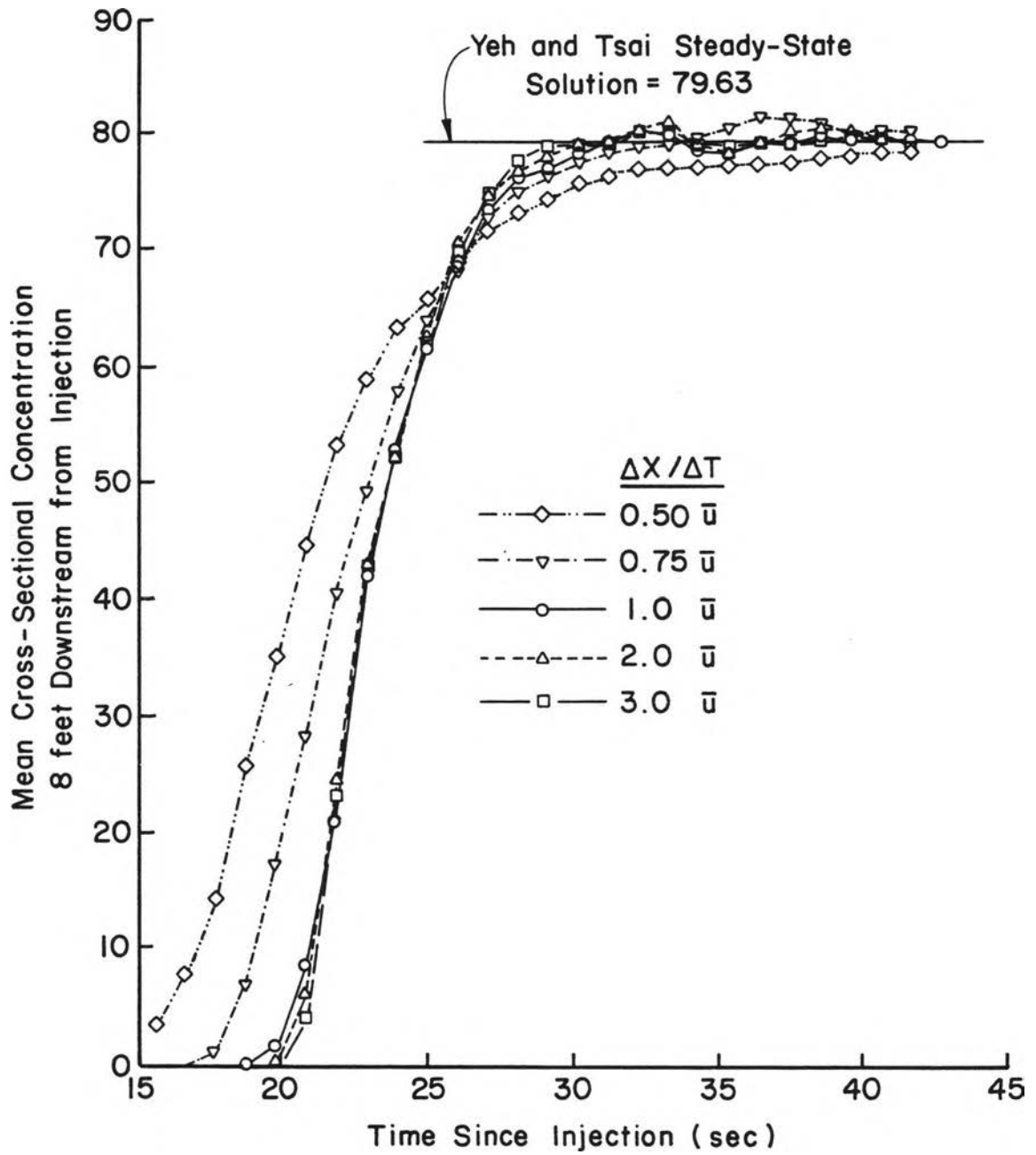


Figure 3-9. Graphical Comparison of Numerical Model to Yeh and Tsai Solution

Table 3-8
 Tabular Comparison of Numerical Model to
 Yeh and Tsai Solution⁽¹⁾

Time Since Injection (sec)	Mean Cross-Sectional Concentration Computed By Numerical Model 8 Feet Downstream from Injection				
	$\Delta x/\Delta T$				
	0.5 \bar{u}	0.75 \bar{u}	1.0 \bar{u}	2.0 \bar{u}	3.0 \bar{u}
31.2	76.41	78.51	79.57	79.70	79.42
32.2	77.23	78.96	80.42	80.35	80.37
33.3	77.31	79.26	80.17	81.27	80.38
34.3	77.30	79.76	78.71	79.31	79.35
35.3	77.62	80.72	78.33	78.17	79.26
36.4	77.68	81.61	79.58	79.55	79.40
37.4	77.81	81.55	79.65	80.54	79.41
38.5	78.18	80.86	79.73	80.68	79.80
39.5	78.36	80.23	79.93	80.64	80.30
40.5	78.81	80.44	79.98	79.96	80.15
41.6	78.89	80.48	79.73	78.94	79.43
Mean	77.78	80.22	79.62	79.91	79.75
Mean ⁽²⁾ Deviation	1.85	0.98	0.41	0.75	0.40
Mean ⁽³⁾ Deviation Percent	2.3	1.2	0.5	0.9	0.5

(1) Mean cross-sectional concentration from Yeh and Tsai solution = 79.63.

$$(2) \text{ Mean deviation} = (1/n) \sum_{i=1}^n C_i - 79.63$$

where n = number of concentration values
 C_i = concentration value

$$(3) \text{ Mean deviation percent} = \frac{\text{Mean deviation}}{79.63} \times 100$$

solution of less than 1.0 percent for $\Delta x/\Delta T > 1.0 \bar{u}$. A comparison of vertical concentration distributions for $\Delta x/\Delta T = 1.0 \bar{u}$ is shown in Figure 3-10. In all subsequent model runs presented in this study, $\Delta x/\Delta T$ was set between \bar{u} and u_m (u_m = maximum velocity within the cross section). The value of u_m generally ranged between $1.2 \bar{u}$ and $1.8 \bar{u}$.

Further details of these tests are included in Appendix C.

3. Elder's Theoretical Turbulent-Flow Dispersion Coefficient.

Elder (1959) investigated dispersion in steady, uniform, turbulent flow down an "infinitely-wide" plane. He used the following logarithmic velocity profile

$$u = \bar{u} + \frac{u_s}{\kappa} \left(1 + \ln \frac{y}{y_s} \right) \quad (3-34)$$

where \bar{u} = mean velocity, u_s = shear velocity = $\sqrt{g y_s S_o}$, g = acceleration of gravity, y_s = flow depth, S_o = bed slope, κ = von Karman constant, and y = vertical distance above bed surface. Assuming that the mixing coefficients for momentum and mass are the same in turbulent flow based on the Reynolds analogy, he derived

$$\varepsilon_y = \kappa y \left(1 - \frac{y}{y_s} \right) u_s \quad (3-35)$$

Elder substituted Eqs. 3-34 and 3-35 into Eq. 2-6 and solved for the longitudinal dispersion coefficient, D . Taking von Karman's constant to be 0.410, he found

$$D = 5.86 y_s u_s \quad (3-36)$$

Elder used a dye tracer in turbulent flow and experimentally measured D within eight percent of Eq. 3-36.

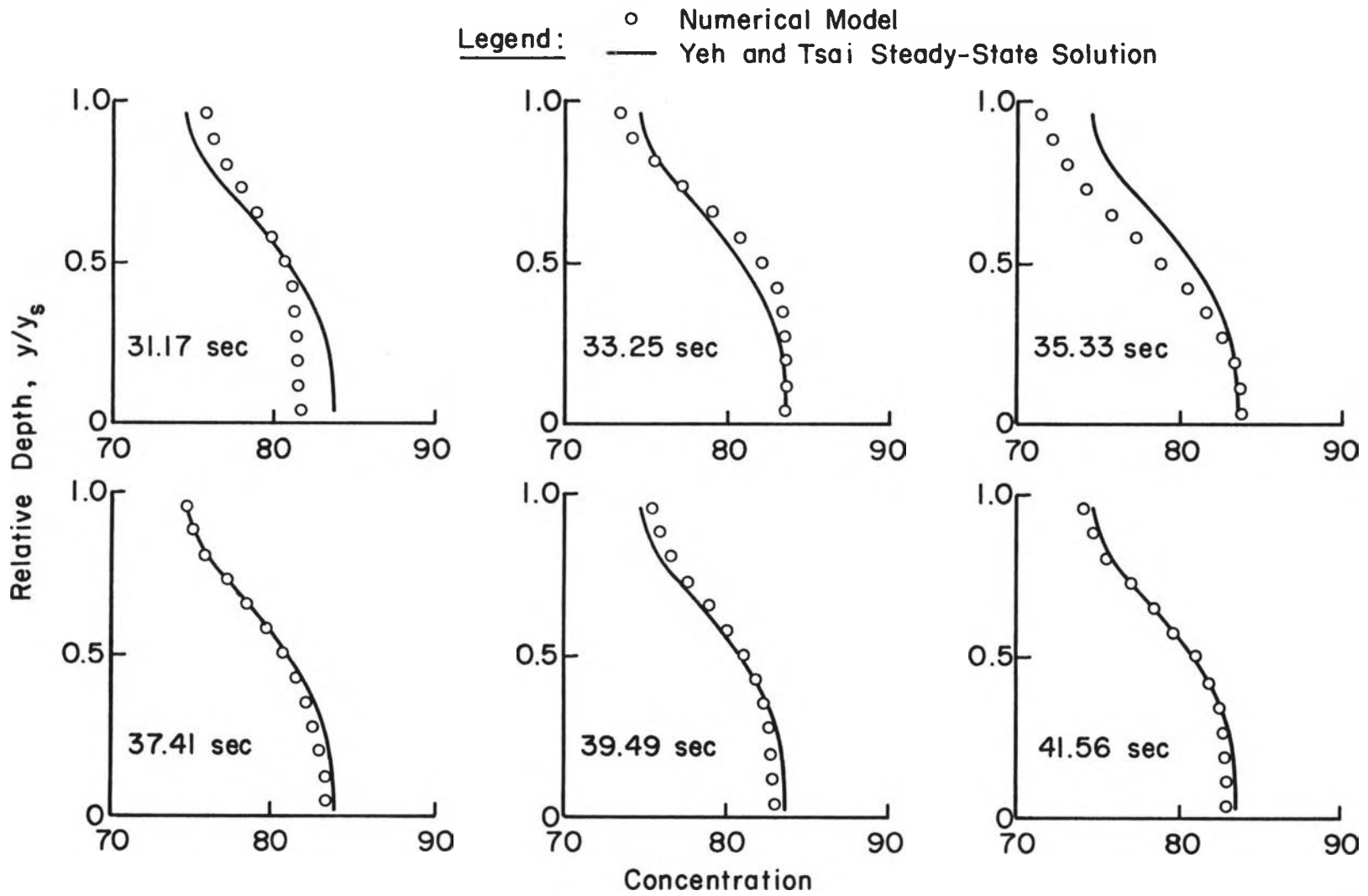


Figure 3-10. Comparison of Concentration Distributions of Numerical Model ($\Delta X/\Delta T = 1.0 \bar{u}$) and Yeh and Tsai Solution at 8 Feet Downstream from Injection

The mean cross-sectional value for ϵ_y using Eq. 3-35 is (Fischer et al., 1979)

$$\epsilon_y = 0.067 y_s u_s \quad (3-37)$$

This constant value for ϵ_y along with Eq. 3-34 can be substituted into Eq. 2-6, as shown in Appendix D, to yield

$$D = 6.58 y_s u_s \quad (3-38)$$

if von Karman's constant is taken to be 0.410 as assumed by Elder (1959), or

$$D = 6.91 y_s u_s \quad (3-39)$$

if von Karman's constant is taken to be 0.4 as assumed by Schlichting (1979).

Equations 3-38 and 3-39 were used to test the numerical model in a manner similar to Fischer (1968b). An instantaneous injection, completely mixed in the cross section, was simulated in the numerical model using Eq. 3-34 for the velocity profile and Eq. 3-37 for the vertical mixing coefficient. The variance of the distribution of the vertically-averaged concentration in the direction of flow is plotted versus time since injection. After the convective period, the variance should increase linearly with time according to Eq. 2-5, and the longitudinal dispersion coefficient can be computed from

$$D = \frac{1}{2} \frac{\Delta \sigma_x^2}{\Delta t} \quad (3-40)$$

where σ_x^2 = variance of the distribution of the vertically-averaged concentration along the x axis (Fischer, 1966; Holley and Harleman, 1965).

The numerical model was tested using similar flow conditions as investigated by Elder (1959). This included a relationship for the maximum velocity (at the water surface) found by Elder for his flow conditions,

$$u_o = 6.496 y_s^{0.63}$$

where units of y_s are feet and units of u_o are feet per second. Data used in the model test are listed in Table 3-9.

A plot of variance versus time since injection is shown in Figure 3-11. Application of Eq. 3-40 to Figure 3-11 results in a dispersion coefficient of approximately $0.0108 \text{ ft}^2/\text{sec}$. Equations 3-38 and 3-39 yield dispersion coefficients of 0.0094 and $0.0099 \text{ ft}^2/\text{sec}$, respectively--a difference of 13 and 8 percent from the numerical model result.

From Eq. 2-7, an estimate of the Eulerian time scale is

$$T_E = \frac{y_s^2}{\epsilon_y} = 19.3 \text{ sec}$$

From Fischer et al., (1979), an estimate of the time when the variance will begin to increase linearly is

$$0.2 T_E = 3.9 \text{ sec}$$

The variance plotted in Figure 3-11 appears to increase at a linear rate beyond about 3.0 seconds.

4. Theoretical Laminar-Flow Dispersion Coefficient. A procedure similar to that described above for turbulent flow can be used to theoretically derive a dispersion coefficient for laminar flow down a plane. Fischer et al., (1979) used the laminar flow velocity profile (a rearranged form of Eq. 3-6)

Table 3-9

Data Used in Numerical Model for Theoretical
Turbulent-Flow Dispersion Test

Reynolds Number, R_e	3500
Kinematic Viscosity, ν	0.00001 ft ² /sec
Discharge Per Unit Width, q	0.035 ft ² /sec
Bed Slope, S_o	0.0008029
Friction Coefficient, f	47
Depth of Flow, y_s	0.04302 ft
Mean Velocity, \bar{u}	0.81376 ft/sec
Acceleration of Gravity, g	32.2 ft/sec ²
Velocity Profile, $u = \bar{u} + \frac{u_s}{\kappa} (1 + \ln \frac{y}{y_s})$	
Vertical Mixing Coefficient, $\epsilon_y = 0.067 y_s u_s = 9610 \times 10^{-8}$ ft ² /sec	
Number of Flow layers = 9	
$\frac{(\Delta y)^2}{\epsilon_y \Delta T} = 1.19$	
$\frac{\Delta x}{\Delta T} = \bar{u}$	

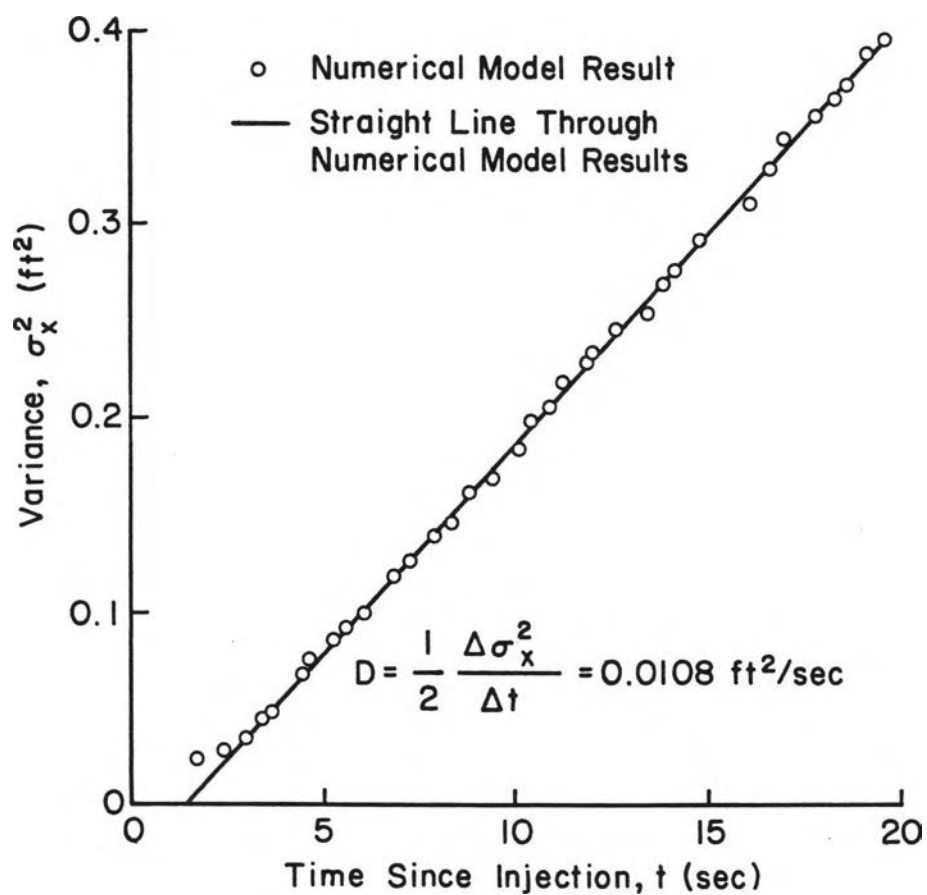


Figure 3-11. Variance of Vertically-Averaged Concentration Along x Axis Versus Time Since Injection for Turbulent Flow Dispersion Test

$$u = u_o \left[2\left(\frac{y}{y_s}\right) - \left(\frac{y}{y_s}\right)^2 \right] \quad (3-41)$$

along with a constant vertical mixing coefficient to derive

$$D = \frac{8}{945} \frac{y_s^2 u_o^2}{\epsilon_m} \quad (3-42)$$

where u_o is the maximum velocity (at water surface) computed from

$$u_o = \frac{1}{2} \frac{y_s^2 g S_o}{\nu}$$

and where ϵ_m = molecular diffusion coefficient, g = acceleration of gravity, S_o = bed slope, and ν = kinematic viscosity.

An instantaneous injection, completely mixed in the cross section, was simulated in the numerical model using Eq. 3-41 for the velocity profile. A steady, uniform discharge of 0.0018 ft²/sec was used. This value is equivalent to the discharge produced by a rainfall intensity of 3 inches per hour at a point 26 feet from the top of the runoff plane. Other data used in the model test are listed in Table 3-10.

A plot of variance versus time since injection is shown in Figure 3-12. Application of Eq. 3-40 to Figure 3-12 results in a dispersion coefficient of approximately 0.1573 ft²/sec. Equation 3-42 yields a dispersion coefficient of 0.1544 ft²/sec, a difference of 2 percent from the numerical model result.

From Eq. 2-7, an estimate of the Eulerian time scale is

$$T_e = \frac{y_s^2}{\epsilon_y} = 60.7 \text{ sec}$$

Table 3-10

Data Used in Numerical Model for Theoretical
Laminar-Flow Dispersion Test

Reynolds Number, R_e	168
Kinematic Viscosity, ν	0.0000107 ft ² /sec
Discharge per Unit Width, q	0.0018 ft ² /sec
Bed Slope, S_o	0.015
Friction Coefficient, f	0.1426
Depth of Flow, y_s	0.004928 ft
Mean Velocity, \bar{u}	0.3654 ft/sec
Acceleration of Gravity, g	32.2 ft/sec ²
Vertical Mixing Coefficient, ϵ_y	40 x 10 ⁻⁸ ft ² /sec
Velocity Profile, $u = u_o [2(\frac{y}{y_s}) - (\frac{y}{y_s})^2]$	
$\frac{(\Delta y)^2}{\epsilon_y \Delta T} = 0.76$	
$\frac{\Delta x}{\Delta T} = 1.2 \bar{u}$	

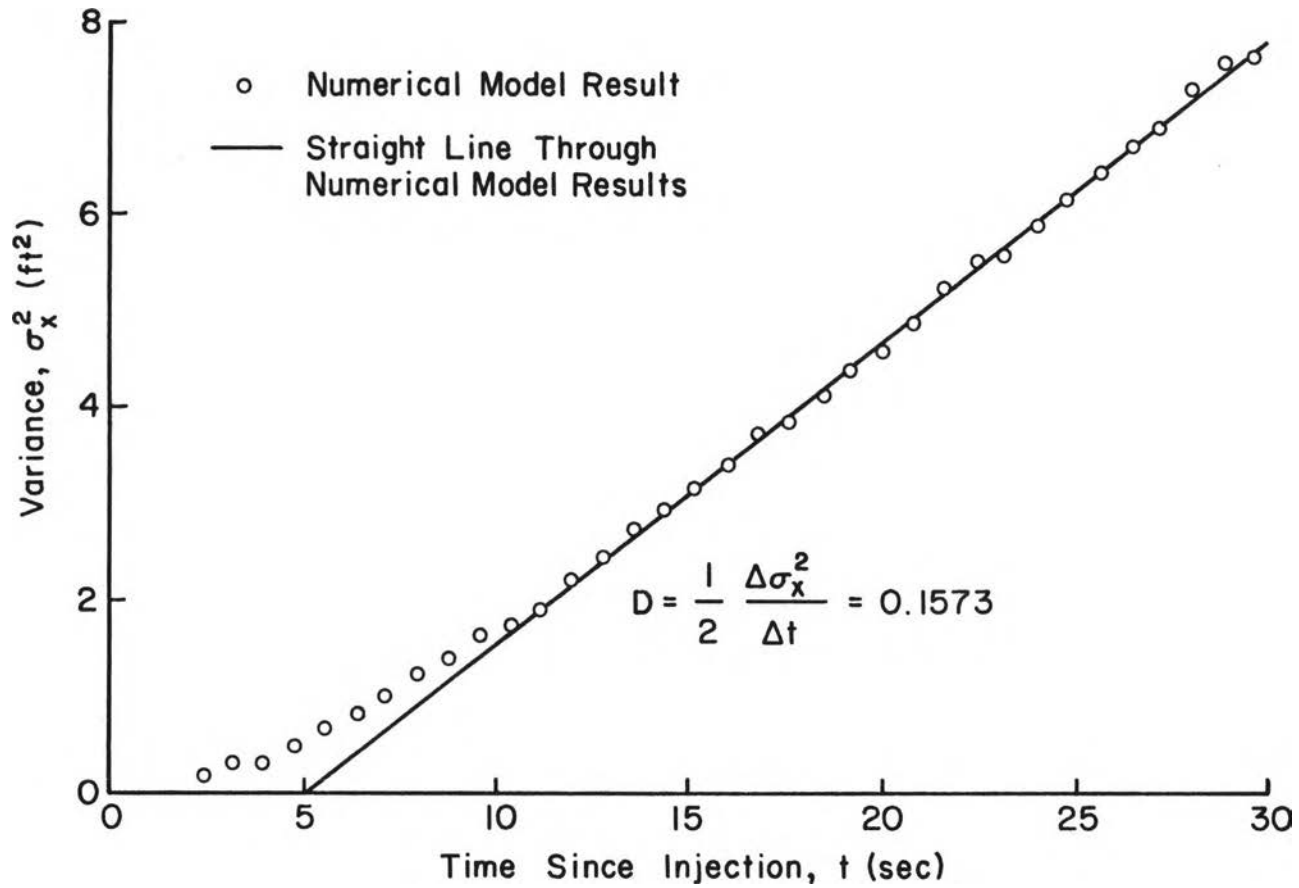


Figure 3-12. Variance of Vertically-Averaged Concentration Along x Axis Versus Time Since Injection for Laminar Flow Dispersion Test

From Fischer et al. (1979) an estimate of the time when the variance will begin to increase linearly is

$$0.2 T_E = 12.1 \text{ sec}$$

The variance plotted in Figure 3-12 appears to increase at a linear rate beyond about 11.0 seconds.

Chapter IV
LABORATORY EXPERIMENTS

A. Introduction

Dye tracer experiments were conducted in overland flow under simulated rainfall to provide data for the calibration of the numerical model. These experiments consisted of an instantaneous, line source injection of a soluble, conservative dye tracer in steady, nonuniform overland flow over a smooth, impervious surface under a constant, uniform rainfall intensity. This chapter describes the experimental facilities and procedures used to collect this data.

B. Indoor Rainfall-Runoff Simulator

The indoor rainfall-runoff simulator used for these experiments is described in detail by Peterson (1977) and Buchberger (1979). A general description follows.

1. Rainfall Modules. Rainfall was simulated using two feet by two feet Plexiglas modules, shown in Figure 4-1, suspended approximately ten feet above the floor of a tilted flume. Capillary tubes penetrated the bottom of the Plexiglas module to form water drops. One-half of the modules contained capillary tubes with 0.022 inch inside diameter; the other half contained tubes with 0.023 inch inside diameter. These tubes produced a mean spherical drop diameter of 3.63 millimeters which reached about 77 percent of terminal velocity prior to impact (Peterson, 1977). The tubes were spaced on a one-inch square grid system as shown in Figure 4-2 so that each module contained 576

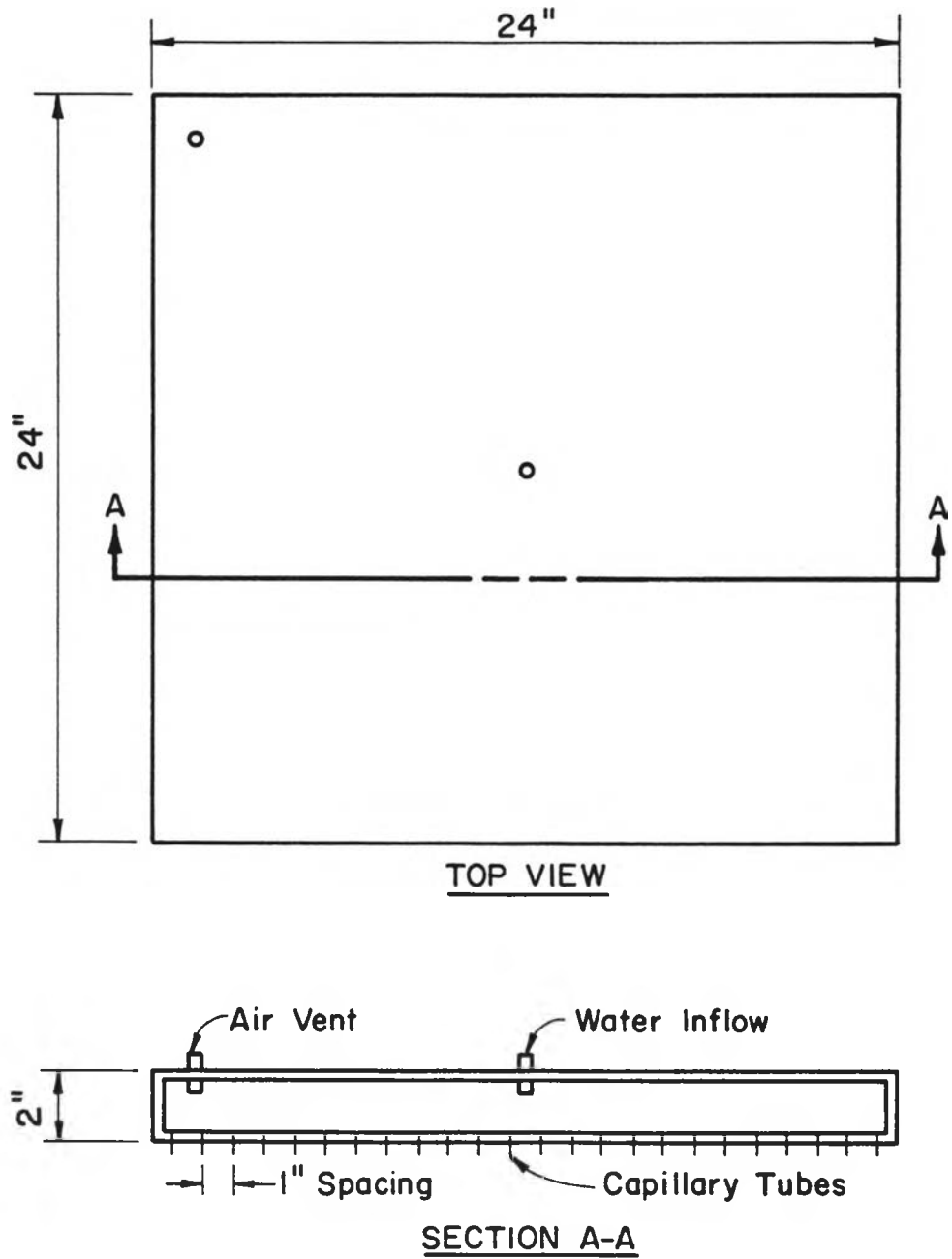


Figure 4-1. Rainfall Module

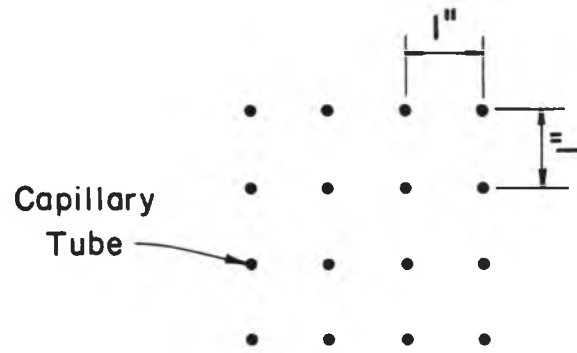


Figure 4-2. Capillary Tube Spacing

tubes. An estimated 20 percent of the capillary tubes functioned erratically due to clogging or structural inconsistencies.

Water entered the module through a hole at the top. An air vent at the top corner of the module relieved air pressure buildup. The depth of water inside the module determined rainfall intensity. The modules were placed side by side to produce uniform rainfall over a 4 feet by 41 feet area.

2. Water Supply. Water from the City of Fort Collins municipal water system was fed through a water softener unit and stored in an 800-gallon holding tank. Heating units were contained inside the tank to maintain water temperatures between 18 and 22°C. A pump delivered water from the tank to the rainfall modules.

3. Flow Controls. A schematic diagram of the flow control system is shown in Figure 4-3. The pump at the holding tank pressurized a 3-inch diameter feeder line which ran along the entire 41 feet of rainfall module coverage. Three-eighths inch diameter branch pipes tapped the feeder line at two-foot intervals. Each branch pipe provided two rainfall modules with their water supply. Needle valves were located in the branch pipes between the feeder line and the rainfall module to allow for flow control. A one-fourth inch diameter pressure line tapped each branch pipe downstream of the needle valve. The pressure line was connected to a "scanivalve" which was capable of scanning all pressure lines and connecting the desired line to a pressure transducer and transducer indicator. In this manner, the pressure in each branch pipe could be monitored and correlated to rainfall intensity to facilitate intensity control.

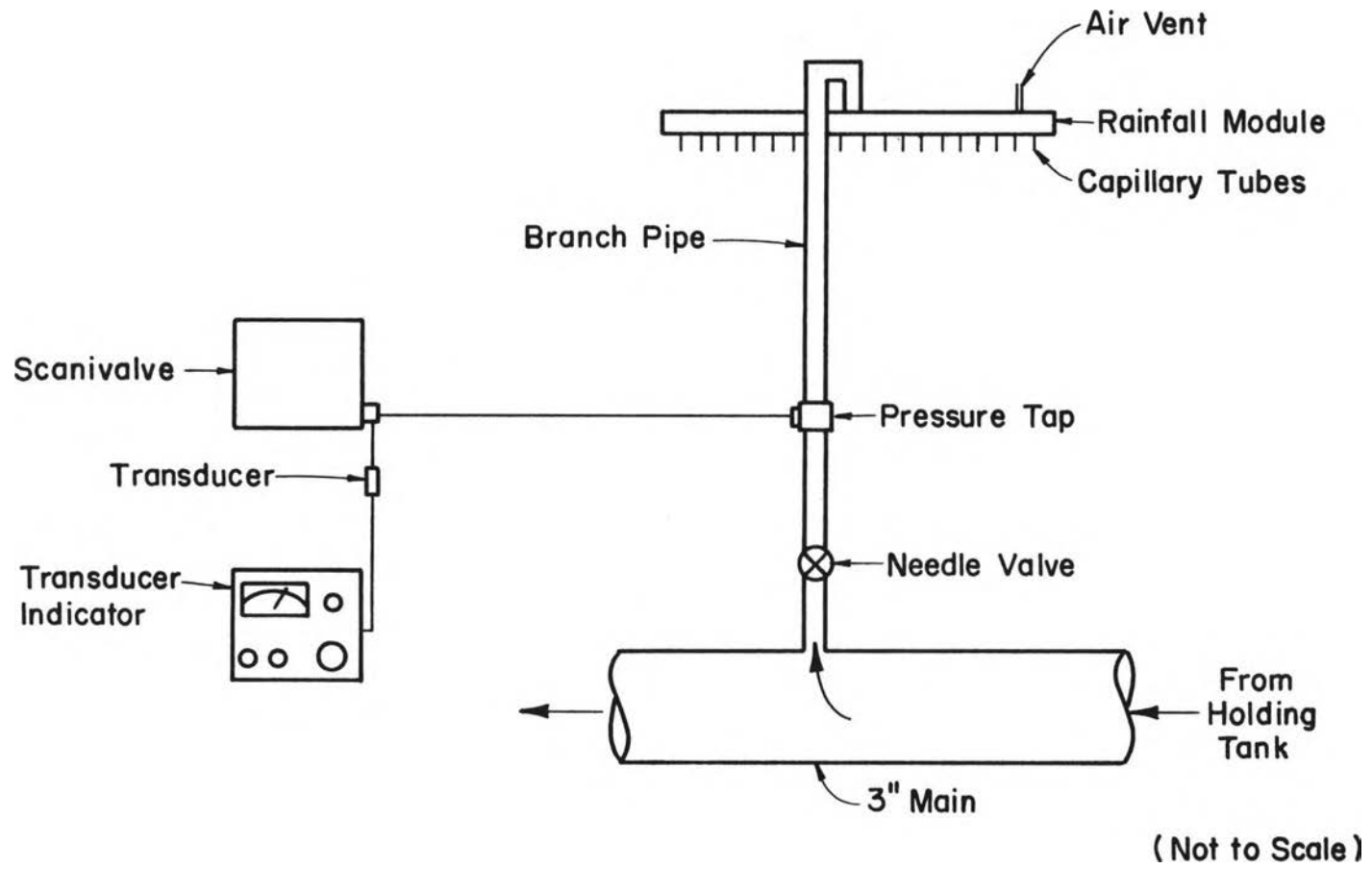


Figure 4-3. Flow Control System (from Buchberger, 1979)

4. Runoff Collection System. A 4 feet wide by 60 feet long flume served as the base for the runoff collection system. The flume could be tilted to produce slopes ranging from 0 to 0.0333. A six-inch high raised floor was constructed in the bottom of the flume directly below the rainfall modules. The floor was covered with a neoprene rubber surface painted with a white latex paint to increase surface wettability (that is, minimize formation of water beads and flow rivulets and facilitate the formation of sheet flow), to minimize adsorption of dye tracer, and to provide a suitable background color for viewing movement of the dye tracer.

The raised floor ended at the downstream limit of rainfall module coverage, providing a six-inch vertical drop at this location for convenient sampling. A collection box, containing two 22-1/2 degree triangular weirs along its downstream end, was placed beneath this drop-off as shown in Figure 4-4. The depth of water in the collection box was measured using a stage recorder and was calibrated to weir discharge. During rainfall-runoff simulations, the stage recorder was used to confirm steady flow conditions on the plane.

A triangular sampling trough, shown in Figure 4-4, was used for dye tracer sampling. This trough was approximately six inches long, one and one-half inches deep, and one and one-half inches wide and was open on both ends. It could easily be moved to any point along the overflow ledge. The trough provided for a temporary concentration of flow sufficient to submerge a one-fourth inch diameter fluorometer intake tube located in the bottom of the trough. A pump located on the discharge end of this intake tube forced a sample of the trough flow through the fluorometer which produced a continuous record of dye

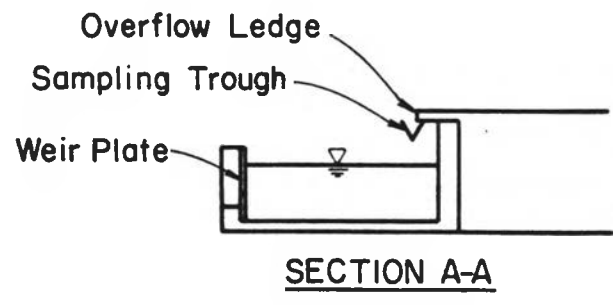
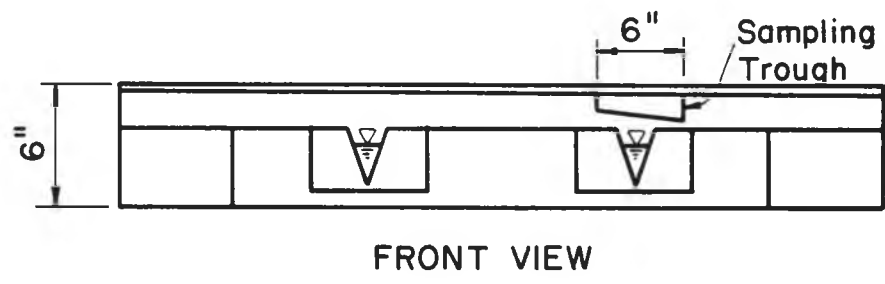
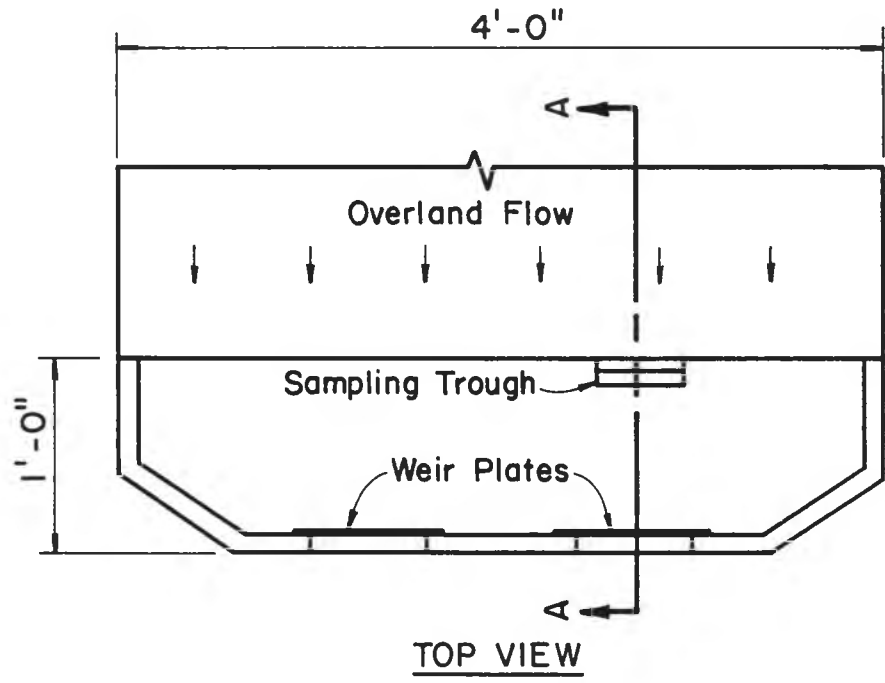


Figure 4-4. Overflow Collection Box

concentration on chart paper. Tests conducted to measure the time from dye entry into the intake tube to the time of response on the fluorometer chart recorder indicated a time of approximately one and one-half seconds.

C. Experimental Procedure

1. Facility Operation. Prior to each rainfall-runoff simulation, the rainfall supply holding tank was filled and the water was allowed to warm to 20-22°C. When rainfall simulation was begun, the inflow rate into the holding tank was set approximately equal to the outflow rate. However, due to limitations in the holding tank storage and limitations in the maximum inflow rate, outflow exceeded inflow when rainfall intensities greater than three inches per hour were simulated. For instance, at five inches per hour intensity, there was storage and inflow capacity for only 30 to 40 minutes of simulation--thus essentially restricting the maximum capacity of the rainfall simulator to this intensity.

After the three-inch diameter feeder line was pressurized, each needle valve (Figure 4-3) was adjusted until the downstream branch pipe pressure equaled the precalibrated pressure required for that pair of rainfall modules to generate the desired rainfall intensity. After all pressures were set and after a steady-state discharge had been reached at the overflow ledge (as indicated by the stage recorder chart), a discharge measurement was taken manually. This measurement consisted of collecting the flow in a container during a measured time period and then calculating discharge as the volume of water collected divided by the time of collection. If this discharge did not match the desired

rainfall intensity, all needle valves were adjusted uniformly until the desired flow rate (and therefore intensity) was reached.

Line-source injections of dye tracer were made using a 4.35 feet long, 2.0 inch diameter pipe, sealed on both ends, with a line of 1/4 inch diameter holes drilled along its length. These holes were spaced 3/8 inch apart. The pipe was placed inside a wooden frame, shown in Figure 4-5, which spanned across the flume width, rested on the top of the flume walls, and protected the pipe from contact with the rainfall. The pipe was positioned so that the line of drilled holes was on top and so that the pipe's longitudinal axis was in a horizontal plane and was perpendicular to the flow direction. Then 200 milliliters of a Rhodamine WT dye solution were poured into the pipe. A line-source injection into the overland flow was made by releasing the pipe from its fixed position and allowing it to roll forward one revolution under the force of its own weight--thus simulating an "instantaneous" injection which was easily reproducible in terms of volume of dye solution injected. The dye fell approximately two feet from the pipe to the overland flow.

2. Data Collection. The travel distance of the dye between the point of injection and the point of measurement varied from 8 to 13 feet. The injection location was chosen so that this travel distance was at the downstream end of the rainfall simulator. At this location, flow conditions changed slowly with distance down the plane--that is, the percent increase in discharge, depth of flow, and velocity of flow over this travel distance was the smallest compared to any other equivalent length of plane. One would therefore speculate that ϵ_y would also change slowly over this distance. Since a constant

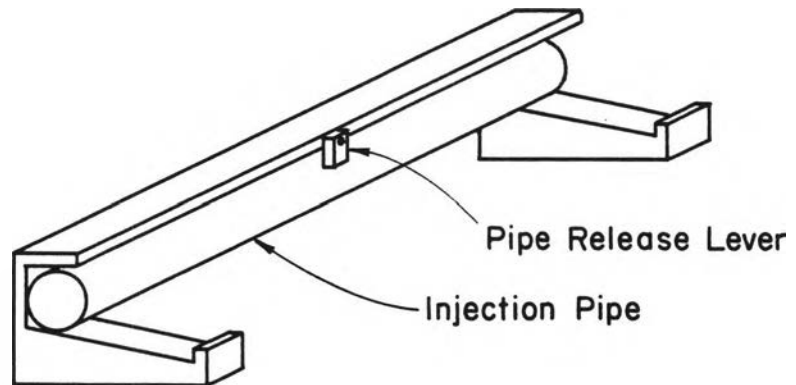


Figure 4-5. Wooden Frame Containing Injection Pipe

value of ε_y over the entire travel distance was used in the numerical model calibration, this "most uniform" flow condition was the most desirable location for data collection.

The dye concentration was measured at the overflow point using a Turner 111 fluorometer. Two methods of collecting and measuring samples were employed, continuous sampling and discrete sampling. The first involved continuous sampling from a trough attached to the overflow ledge as explained previously. This resulted in continuous concentration data being recorded by a strip chart recorder attached to the fluorometer. Experiments were repeated three times with the trough moved to a different location each time. These locations were $1/6$, $1/2$, and $5/6$ the distance across the overflow ledge. The data collected at each location was assumed to be representative of a strip of flow equal in width to $1/3$ of the flume width. A flow-weighted average concentration was computed from the data collected at the three locations and was used for subsequent numerical model calibration. Flows used in the flow weighting were collected at the overflow ledge for each one-third-width strip by measuring the volume of water flowing over the ledge in a known time period.

A second method involved collecting and measuring width-averaged samples at discrete time intervals. These were collected by manually moving a glass container at a constant speed underneath the entire width of the overflow ledge, thus collecting a single, flow-weighted, width-averaged sample. The travel time of the glass container across the width of the ledge was 1 to 2 seconds. Immediately after collection, the sample was poured into a cuvette and stored. This procedure was repeated every 10 seconds during the passage of the dye cloud

across the overflow ledge. At the conclusion of sampling, the cuvettes were individually placed into the fluorometer for concentration readings. This method was used when concentrations at the collection point were changing slowly with time.

The mass of dye injected was changed between many of the experiments so that the dye concentrations at the measurement location would fall within a convenient detection range of the fluorometer. The selection of the mass injected was based on preliminary trial-and-error runs. A comparison of dye mass injected to dye mass collected indicated that dye loss was negligible.

Chapter V

RESULTS AND DISCUSSION

A. Introduction

This chapter describes the simulation of laboratory experiments using the mathematical model presented in Chapter 3. The vertical mixing coefficient, ϵ_y , was used as a calibration parameter in the simulations. The results are discussed, and a regression relationship is presented relating ϵ_y to rainfall and flow characteristics. This predictive equation for ϵ_y completes the data set needed to apply the mathematical model. The study is then taken one step further by using the equation for ϵ_y to examine the convective period and the one-dimensional dispersion coefficient for overland flow.

B. Laboratory Measurements

Data were collected for 12 sets of rainfall intensities and slopes as listed in Table 5-1. Rainfall intensities less than 2 inches per hour were not investigated because of significant spatial nonuniformity in raindrop production at low intensities.

The results of the laboratory concentration-versus-time measurements are displayed in Figures 5-1 through 5-15. One of the measured curves in Figure 5-1 (as indicated on the figure) and the measured curve in Figure 5-3 represent width-averaged concentrations obtained from the discrete sampling method described in Chapter 4. The change in concentration with time at the measurement location was

Table 5-1
Summary of Experiments

Experiment No.	Slope	Rainfall Intensity (in/hr)	Injection Location from Top of Plane (ft)	Measurement Location from Top of Plane (ft)	Reynolds Number at Midpoint Between Injection and Collection
1a	0.001	2	27.7	40.8	138
1b	0.001	2	32.8	40.8	148
2a	0.001	3	27.7	40.8	221
2b	0.001	3	32.8	40.8	222
3	0.001	4	32.8	40.8	334
4	0.001	5	32.8	40.8	387
5	0.015	2	32.8	40.8	159
6	0.015	3	32.8	40.8	237
7	0.015	4	32.8	40.8	318
8	0.015	5	22.8	30.6	294
9a	0.030	2	27.7	40.8	153
9b	0.030	2	32.8	40.8	162
10	0.030	3	32.8	40.8	222
11	0.030	4	32.8	40.8	291
12	0.030	5	27.7	40.8	382

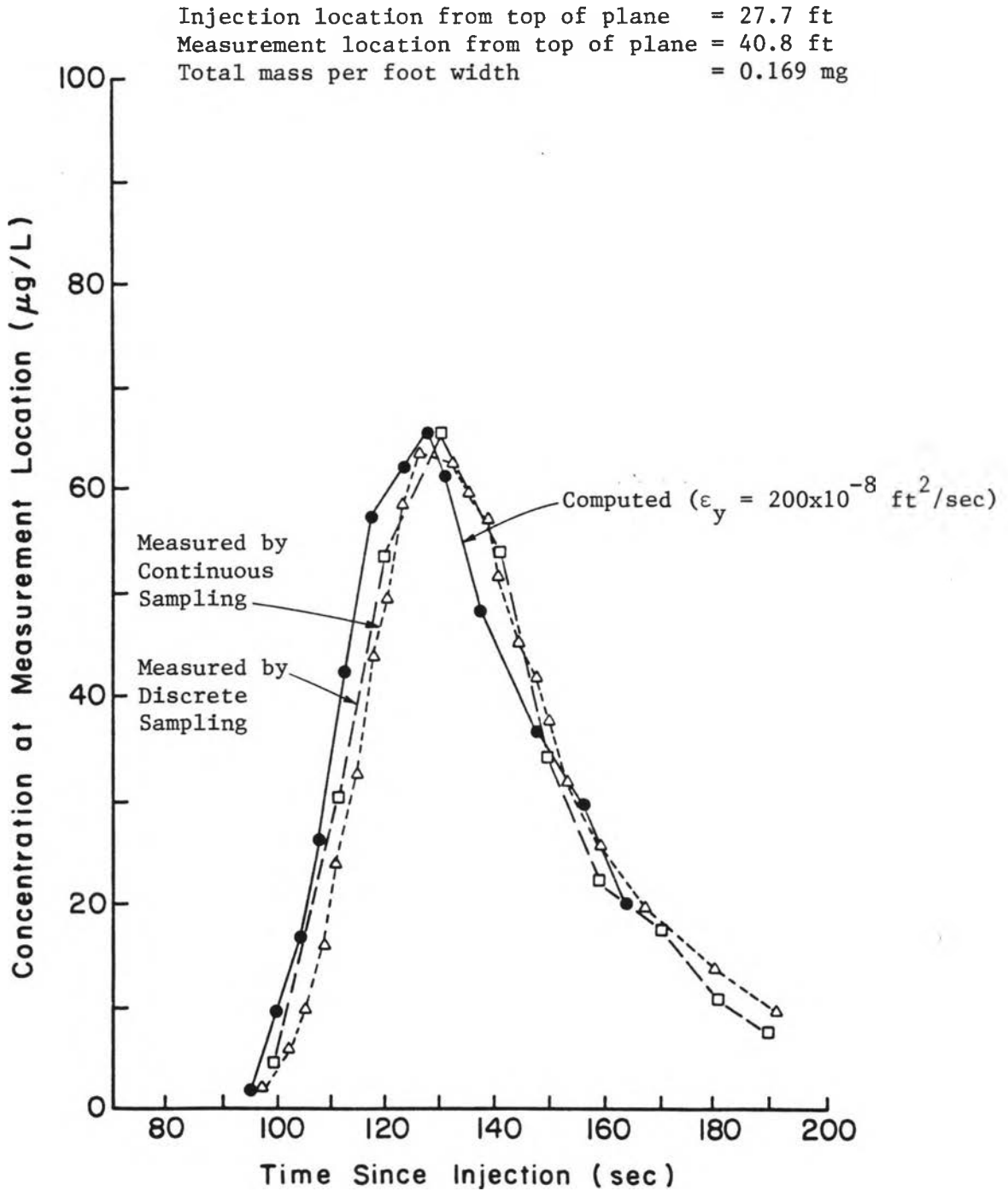


Figure 5-1. Comparison of Measured and Computed Concentration Curves for $S_0 = 0.001$ and $i = 2$ (Experiment No. 1a)

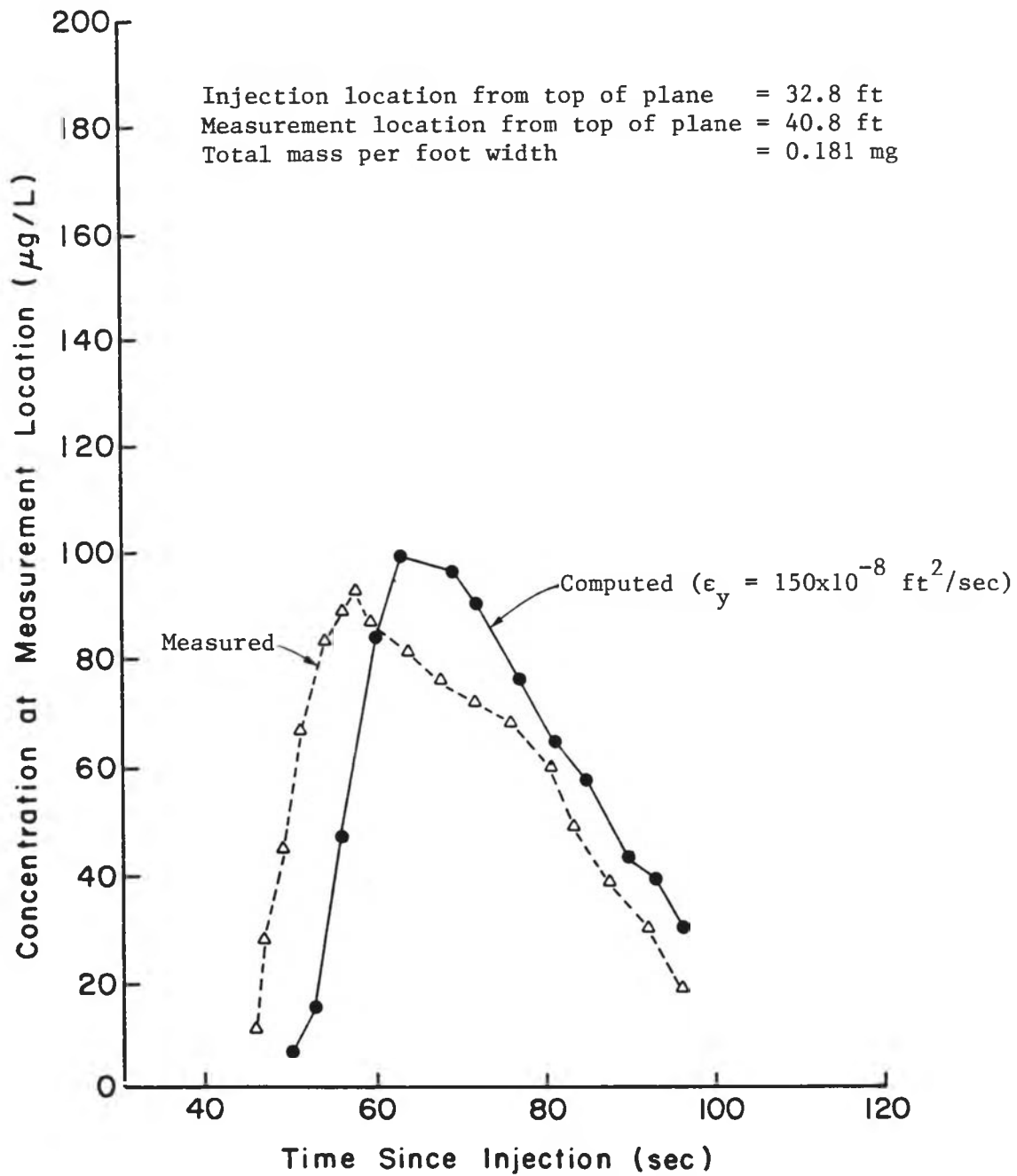


Figure 5-2. Comparison of Measured and Computed Concentration Curves for $S_o = 0.001$ and $i = 2$ (Experiment No. 1b)

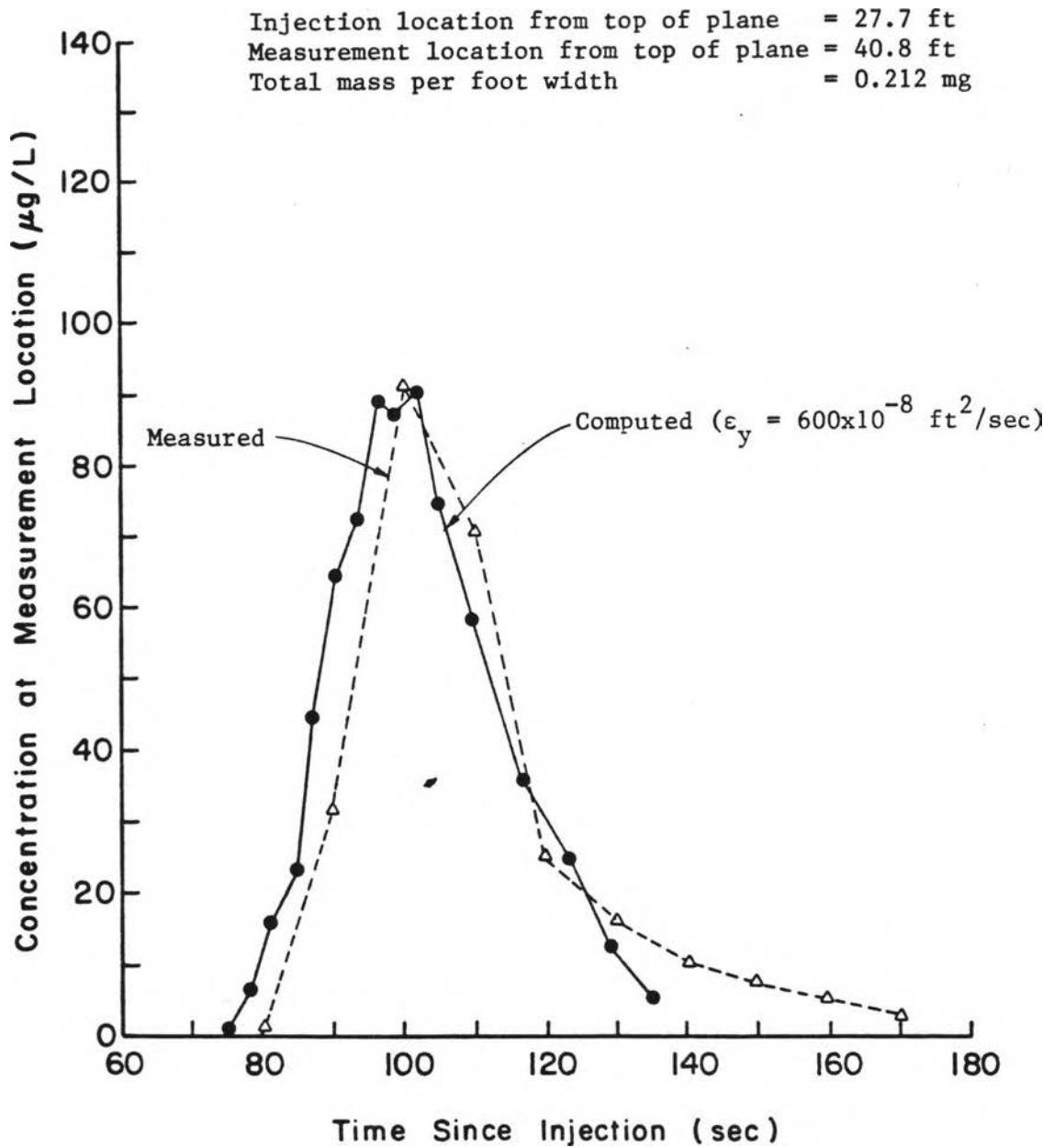


Figure 5-3. Comparison of Measured and Computed Concentration Curves for $S_0 = 0.001$ and $i = 3$ (Experiment No. 2a)

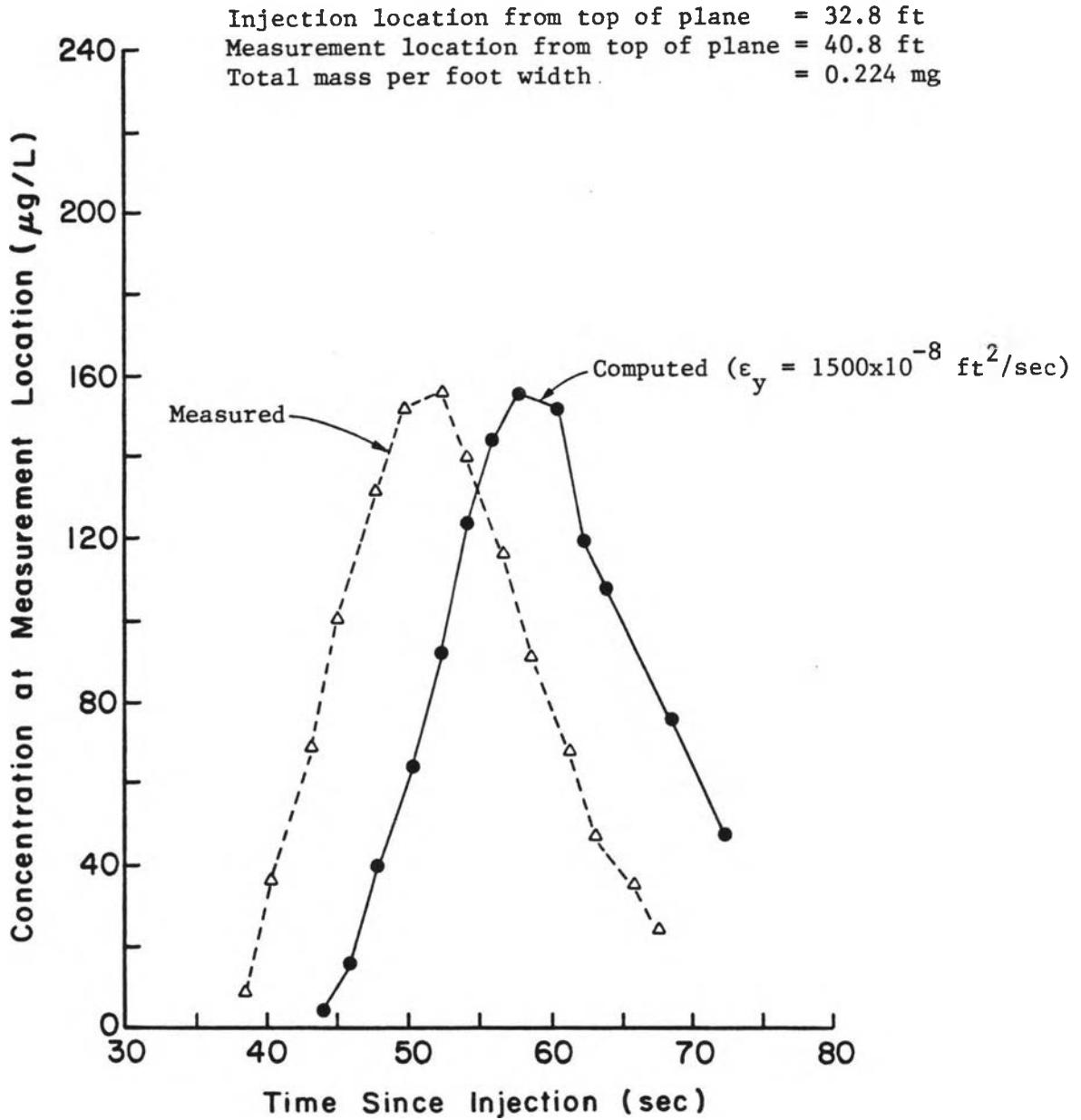


Figure 5-4. Comparison of Measured and Computed Concentration Curves for $S_o = 0.001$ and $i = 3$ (Experiment No. 2b)

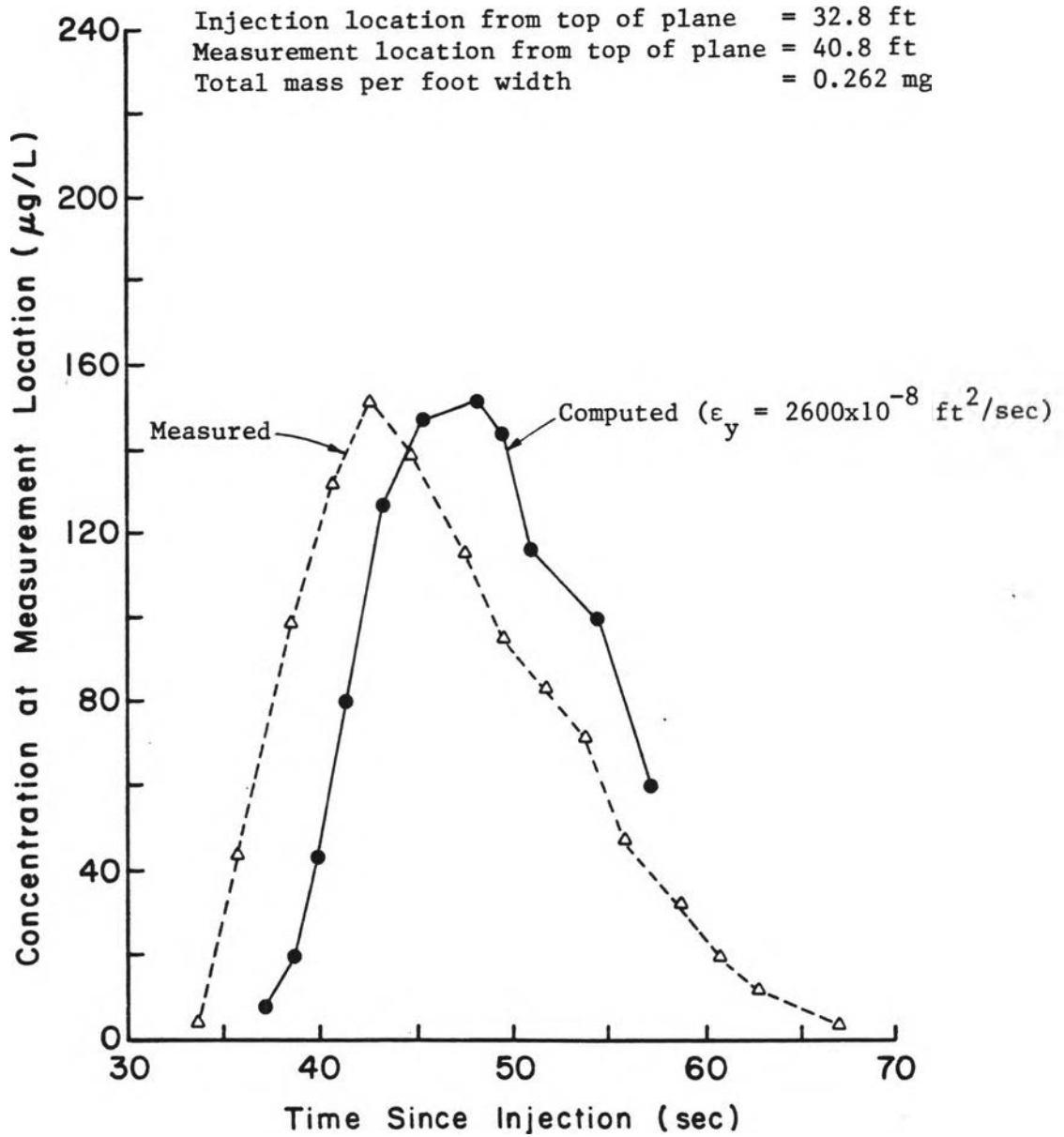


Figure 5-5. Comparison of Measured and Computed Concentration Curves for $S_o = 0.001$ and $i = 4$ (Experiment No. 3)

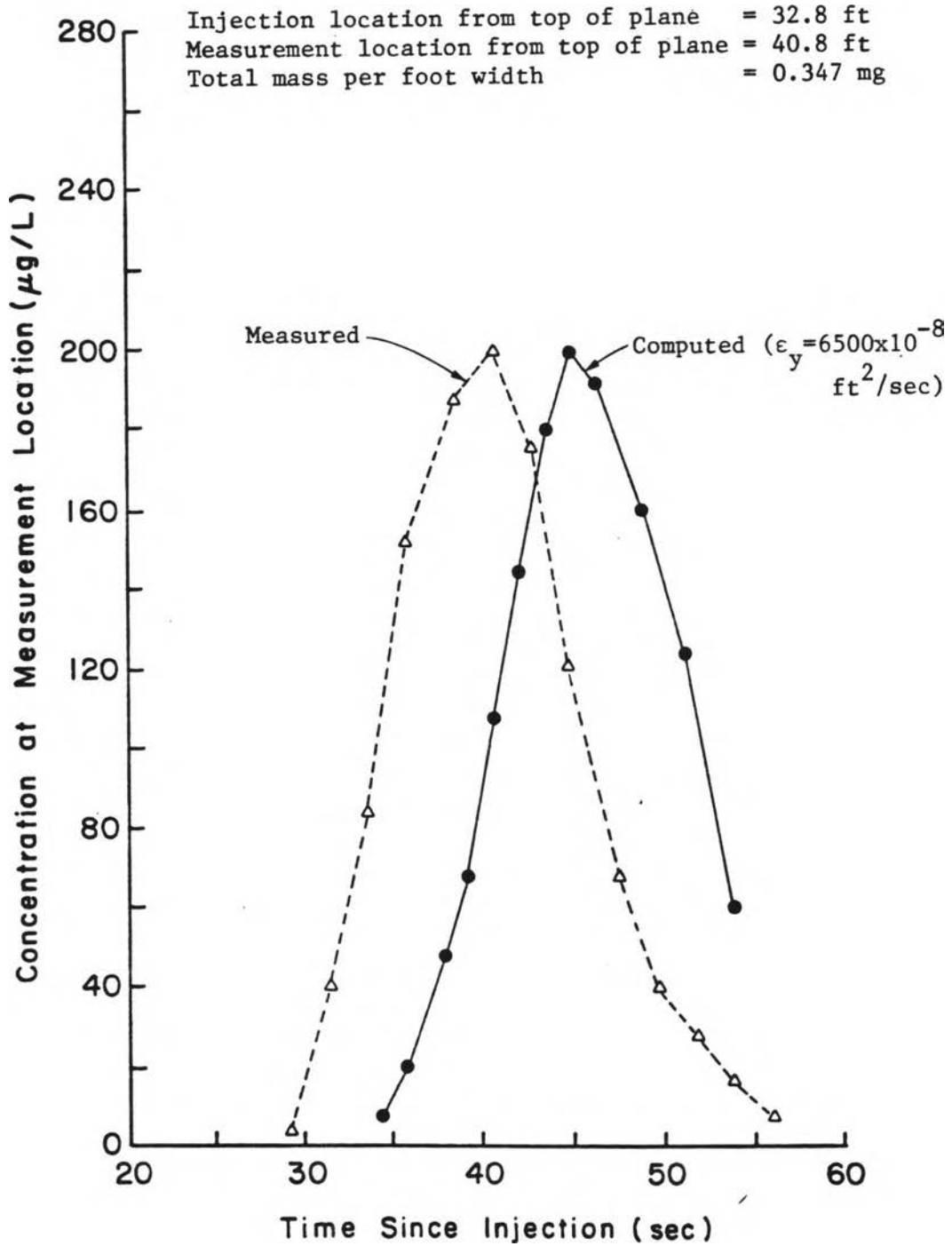


Figure 5-6. Comparison of Measured and Computed Concentration Curves for $S_0 = 0.001$ and $i = 5$ (Experiment No. 4)

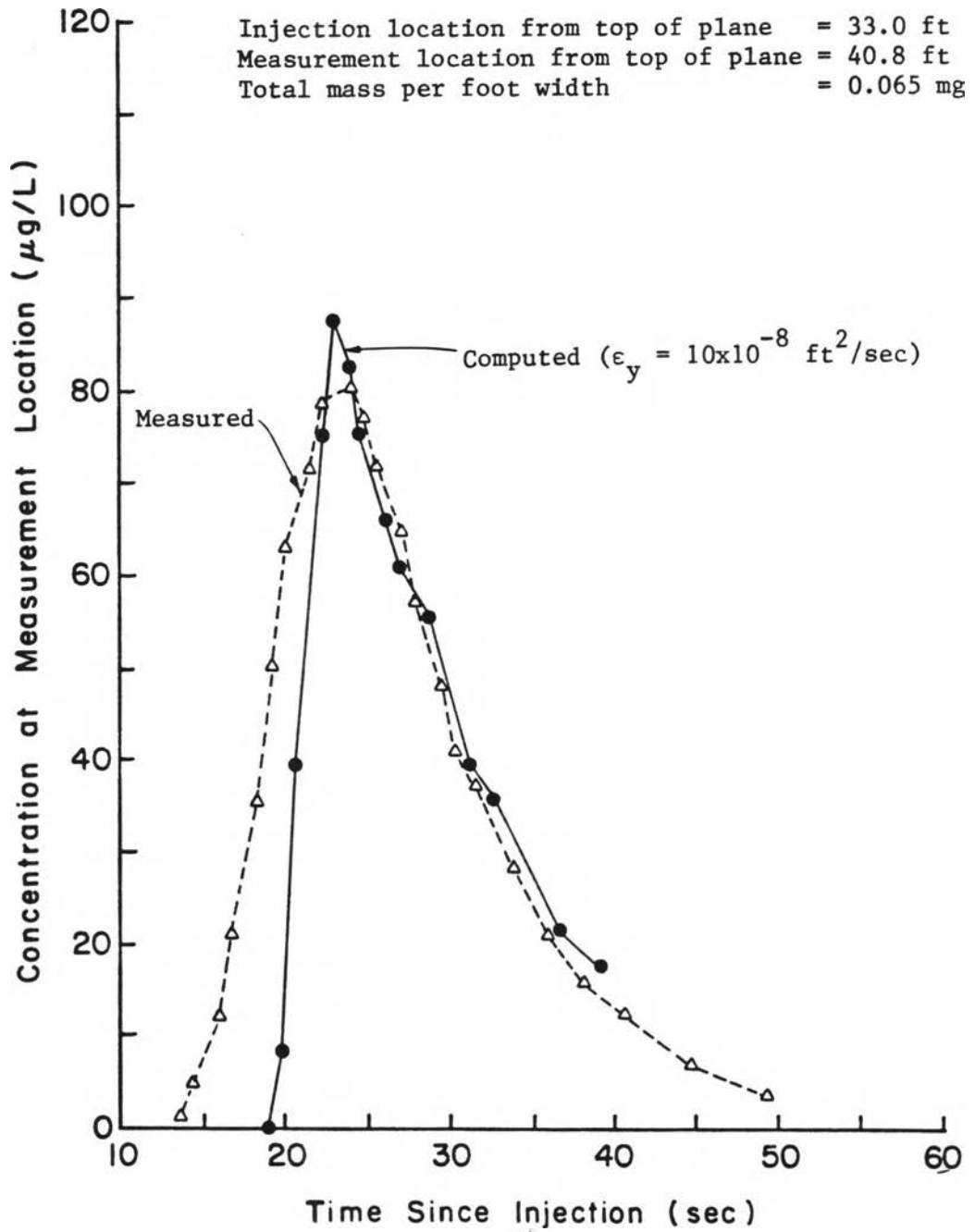


Figure 5-7. Comparison of Measured and Computed Concentration Curves for $S_0 = 0.015$ and $i = 2$ (Experiment No. 5)

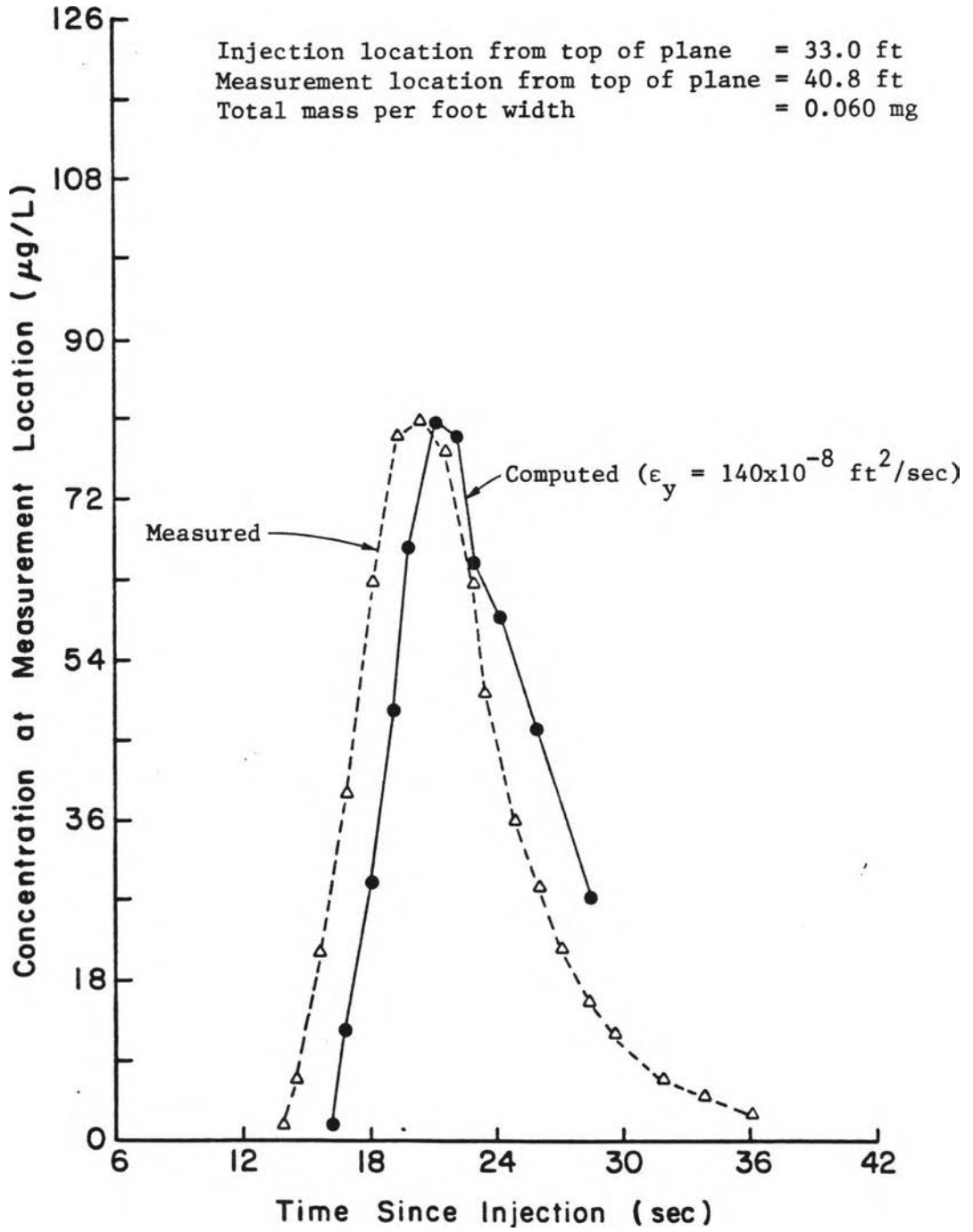


Figure 5-8. Comparison of Measured and Computed Concentration Curves for $S_0 = 0.015$ and $i = 3$ (Experiment No. 6)

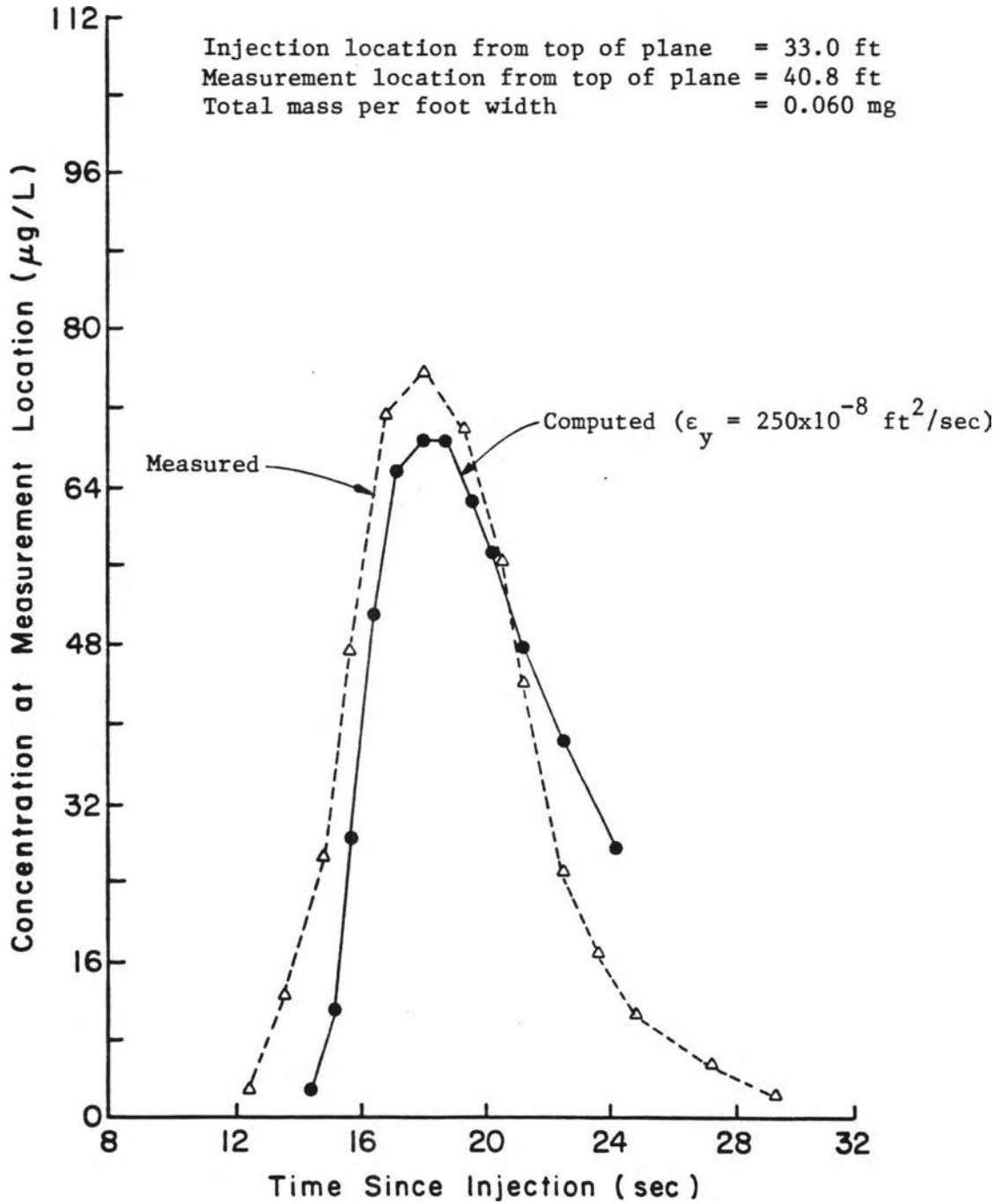


Figure 5-9. Comparison of Measured and Computed Concentration Curves for $S_0 = 0.015$ and $i = 4$ (Experiment No. 7)

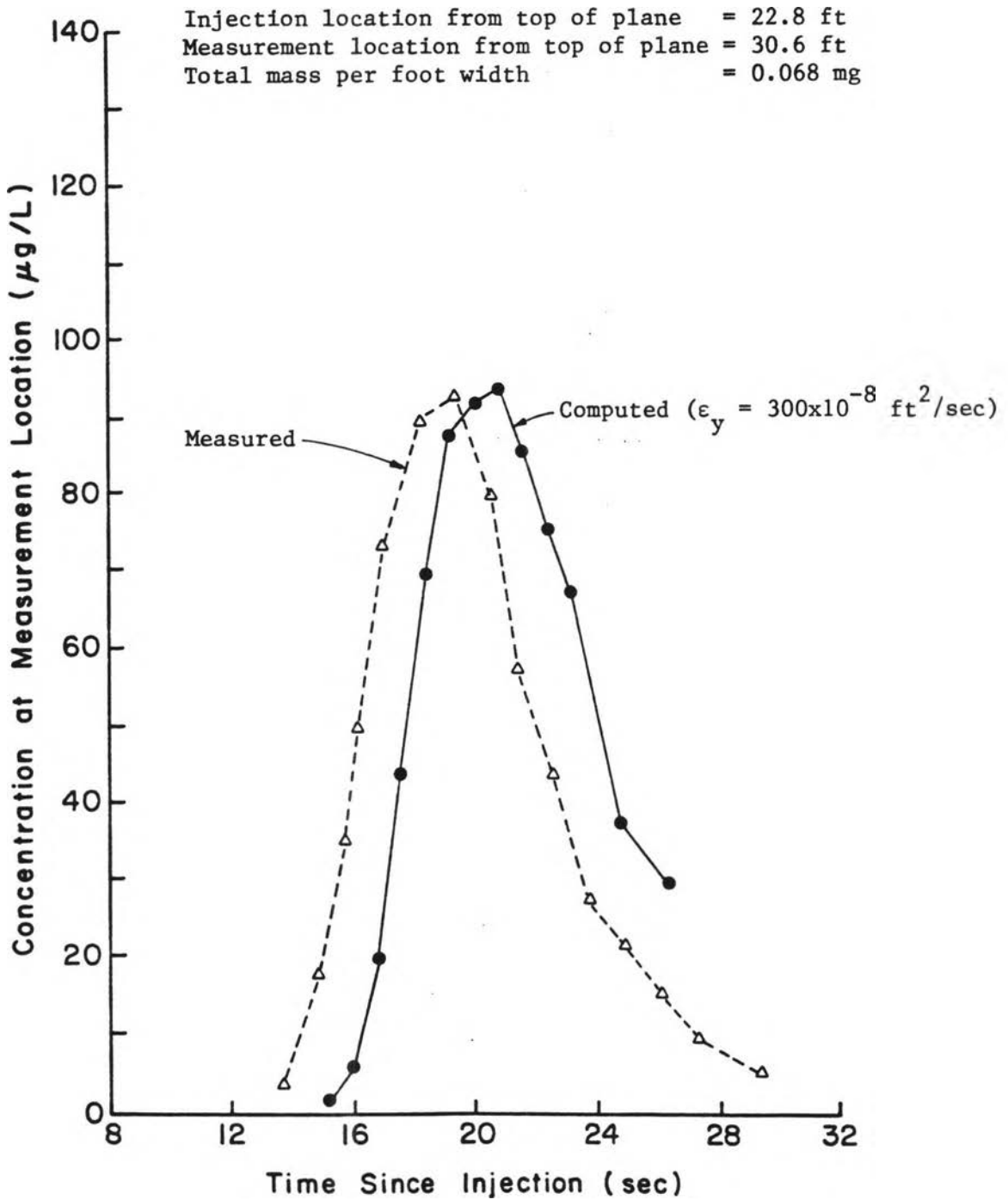


Figure 5-10. Comparison of Measured and Computed Concentration Curves for $S_0 = 0.015$ and $i = 5$ (Experiment No. 8)

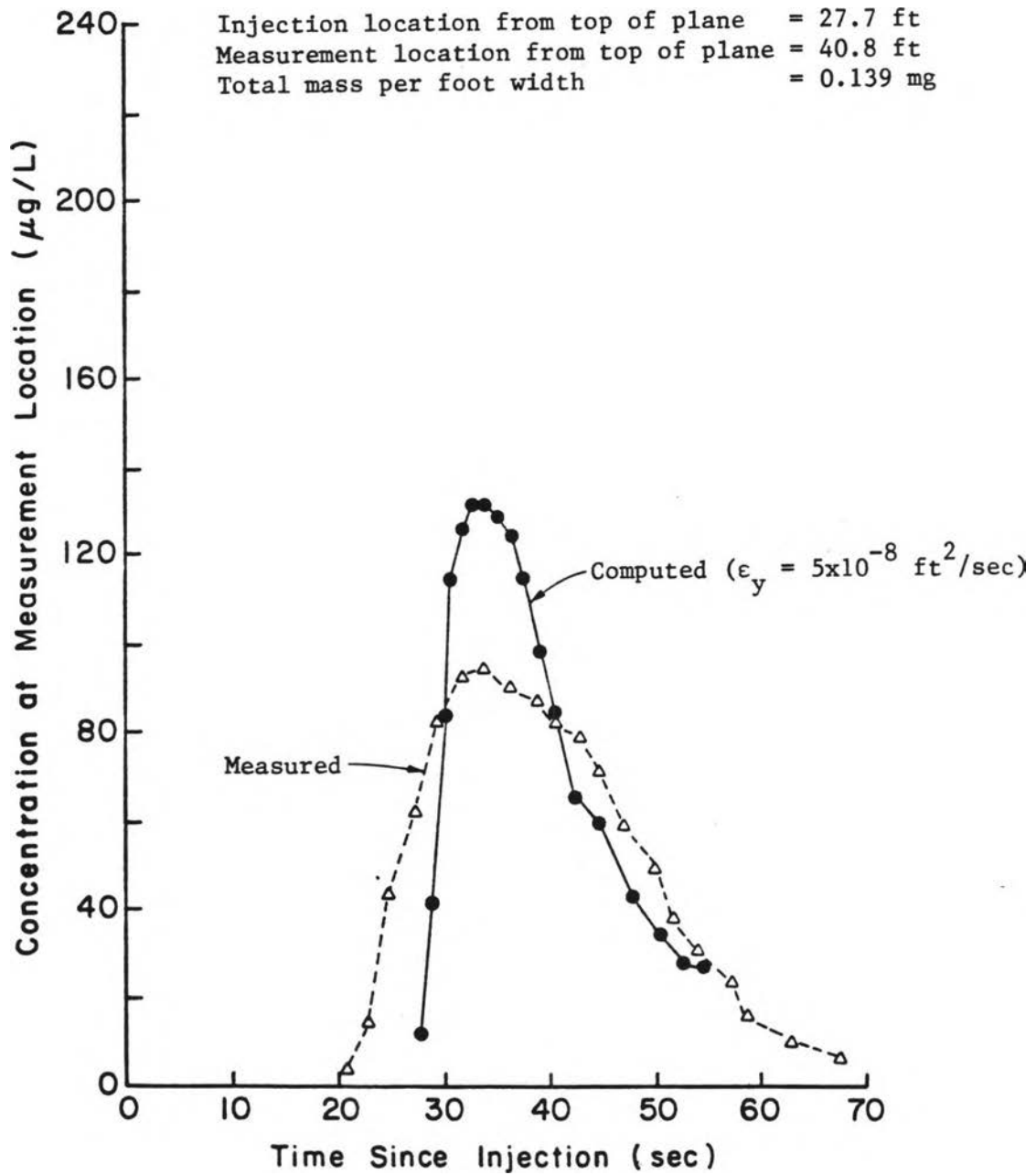


Figure 5-11. Comparison of Measured and Computed Concentration Curves for $S_0 = 0.030$ and $i = 2$ (Experiment 9a)

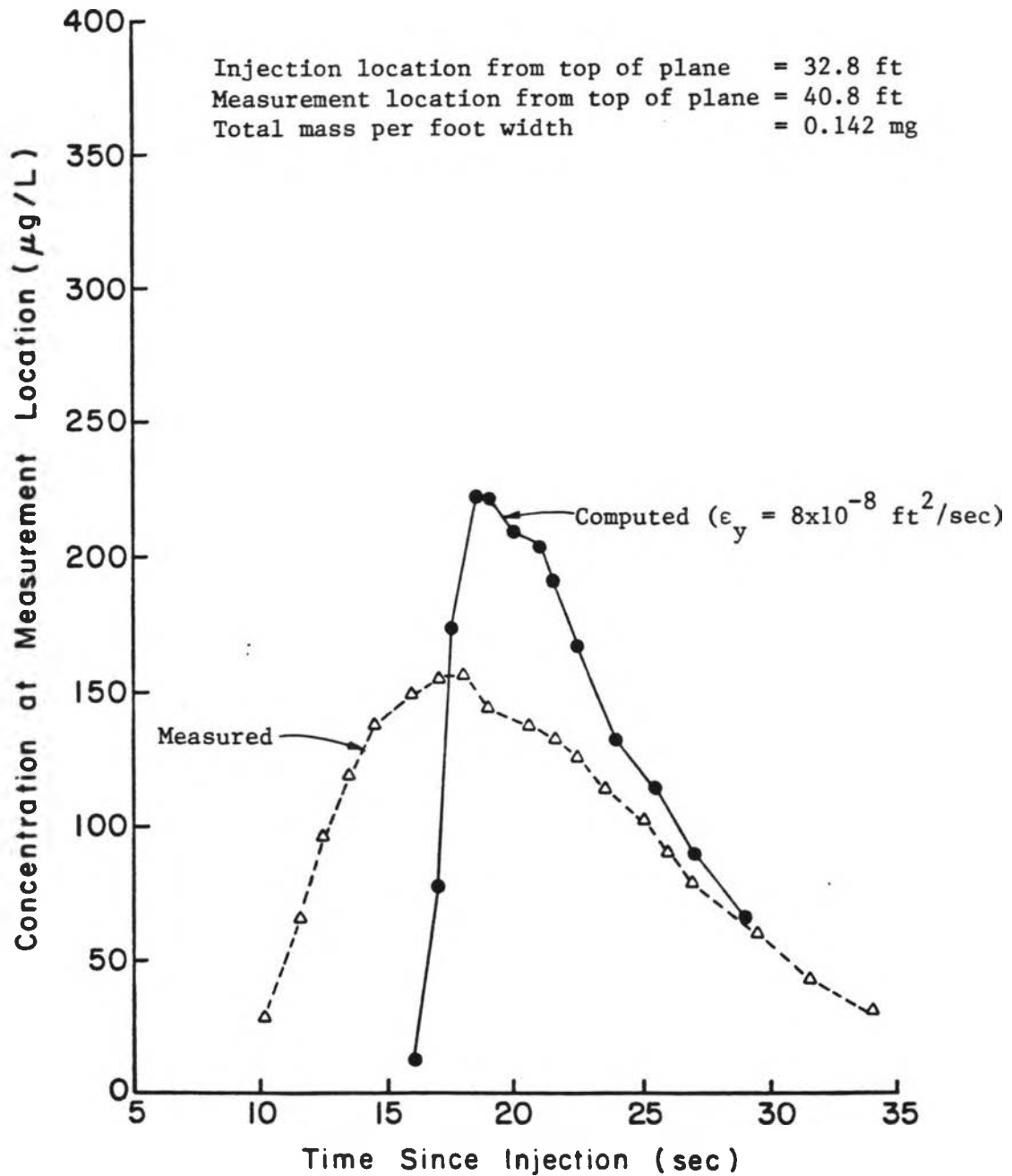


Figure 5-12. Comparison of Measured and Computed Concentration Curves for $S_o = 0.030$ and $i = 2$ (Experiment No. 9b)

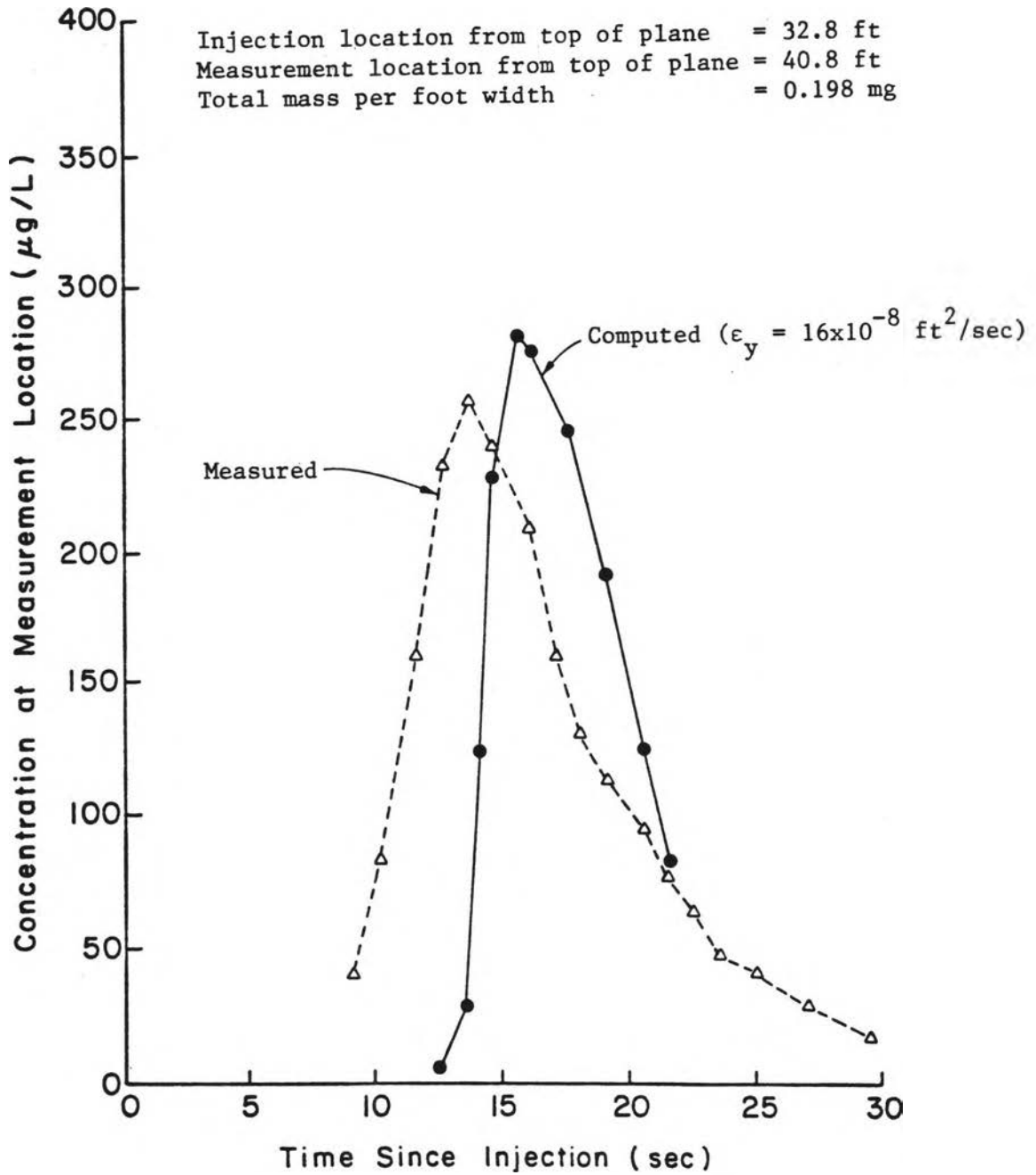


Figure 5-13. Comparison of Measured and Computed Concentration Curves for $S_0 = 0.030$ and $i = 3$ (Experiment No. 10)

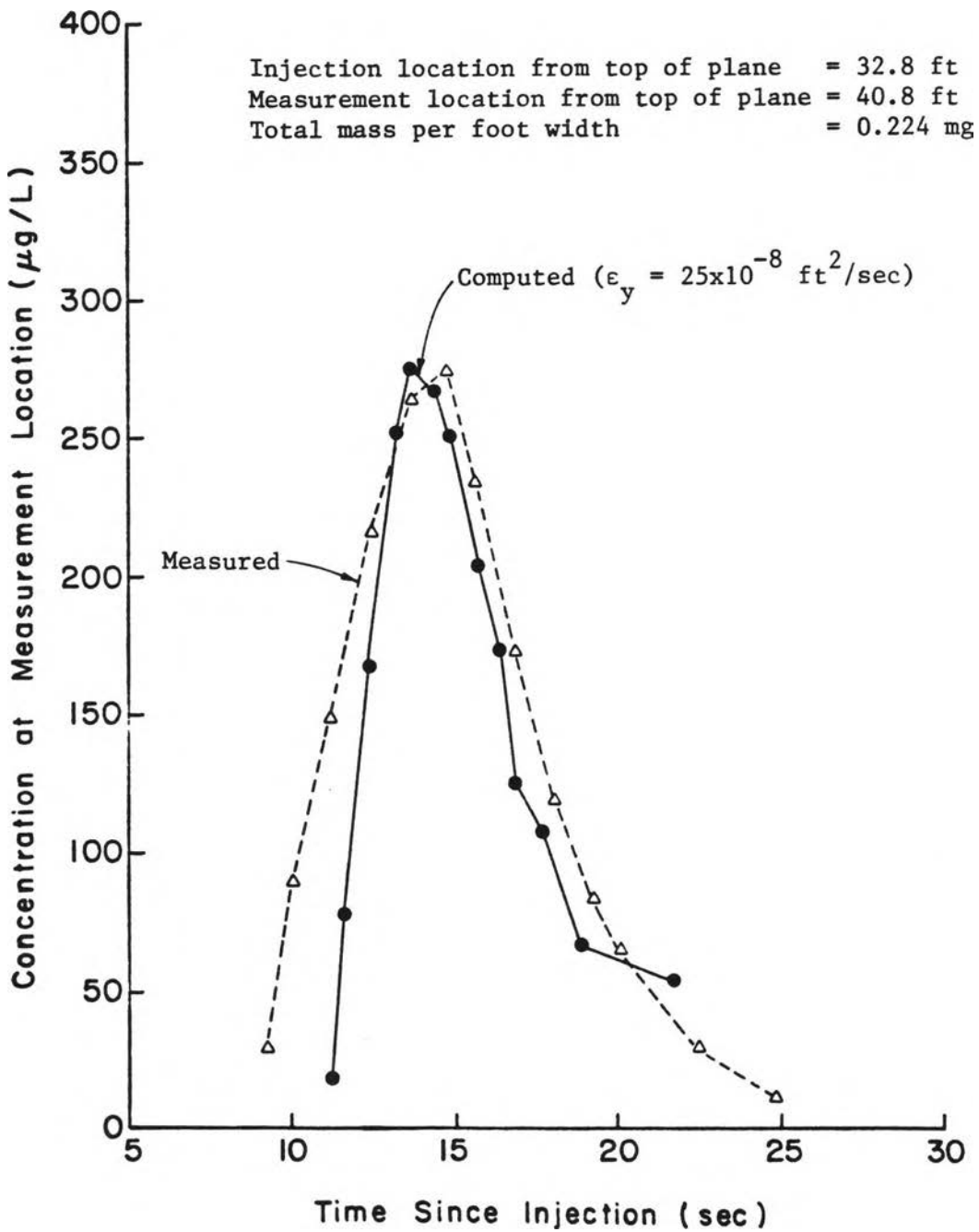


Figure 5-14. Comparison of Measured and Computed Concentration Curves for $S_0 = 0.030$ and $i = 4$ (Experiment No. 11)

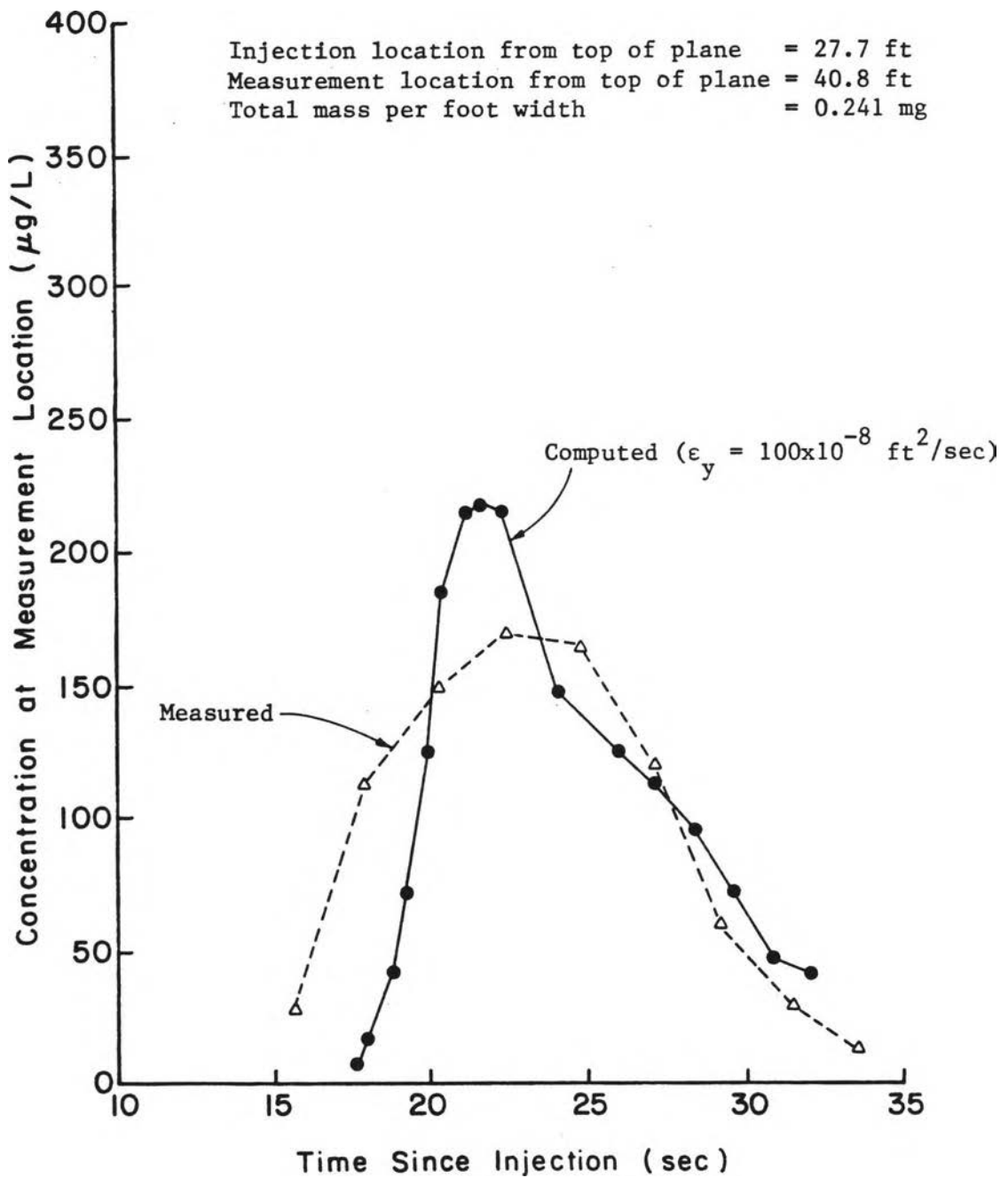


Figure 5-15. Comparison of Measured and Computed Concentration Curves for $S_0 = 0.030$ and $i = 5$ (Experiment No. 12)

sufficiently slow to allow this sampling method to describe these concentration-versus-time curves.

The measured curves shown in the remaining figures represent flow-weighted average concentrations obtained from the continuous sampling method. As described in Chapter 4, this method involves averaging the concentration measured at three different locations across the width of the overflow ledge. A comparison can be made in Appendix E between the averaged curve and the magnitude and timing of the peak concentrations from the three separate measurements. This comparison indicates that the concentrations were not always uniform transverse to the flow direction. Factors influencing this variation were that 1) the flume was slightly out of level in the transverse direction near the downstream end causing a transverse flow distribution of approximately 38, 34, and 28 percent across one-third width segments at the overflow ledge and 2) bed surface irregularities existed due to seams in the neoprene rubber surface and due to occasional small pockets of water which accumulated under the rubber surface after many hours of continuous rainfall simulation. Although much effort was expended to minimize these deviations from a theoretically plane surface, the deviations that remained were assumed to introduce variabilities which would be expected in natural overland flow.

Deviations of a width-averaged measured curve shown in Figures 5-1 through 5-15 from the true width-averaged curve could be influenced by a number of factors: 1) The use of only three measurement locations to determine a width-averaged concentration curve could have introduced errors since flow over only 38 percent of the ledge was actually sampled. 2) The three measurements were made from three separate injections as explained in Chapter IV. Variabilities due to the amount

of dye injected, fluctuation in rainfall module line pressures, changes in water temperature, and the random timing of raindrop impacts could have produced variations between the three dye clouds. 3) Fluorometer reproducibility was found to vary by a small amount. 4) Slight fluorometer fluctuations were experienced during steady-state measurements of constant concentrations. 5) Small changes in the fluorometer calibration were found to have occurred during the period that laboratory experiments were conducted. 6) The use of the collection trough for flow sampling allowed for a short period of local flow mixing within the trough prior to flow entry into the sampling intake tube. 7) The use of a 2-1/2 feet long sampling intake tube between the collection trough and the fluorometer allowed for additional dispersion of the dye during its travel through the tube. 8) The warming of the fluid during its travel through the sampling intake tube and the fluorometer was difficult to judge and correct for in analyzing the temperature-sensitive fluorometer readings.

The discrete sampling method was additionally susceptible to errors due to continually changing concentrations during the one-to-two-second period of collection, errors due to the long (10 seconds) interval between samples, errors introduced by sample storage conditions between the time of collection and the time of concentration readings, and errors related to fluorometer operation during the readings of the cuvette samples.

To emphasize the fact that the width-averaged measured concentrations shown in Figures 5-1 through 5-15 are influenced by these random and systematic measurement errors, a subjective assessment of percent variability was made. Variability in these concentrations up to ± 15 percent was estimated due to the averaging of three

measurement locations from three separate injections for the continuous sampling method and due to continually changing concentrations during and between sample collection for the discrete sampling method. Additional variability of up to ± 5 percent was estimated due to other factors. Therefore, the accuracy of the width-averaged measurements compared to the true width averaged values is roughly estimated to be up to ± 20 percent.

C. Numerical Model Results

1. Data Input. Appendix F summarizes the data used to generate the numerical model calibrations for each experiment listed in Table 5-1.

Initial concentration in the flow at time zero was determined as follows. Observations made during the laboratory experiments indicated that the length (in the direction of flow) of the line source immediately after injection was approximately 0.35 foot. The initial concentration was therefore computed as

$$\text{Initial Concentration} = \frac{(\text{mass injected per unit width})}{(\text{flow depth})(0.35 \text{ ft})}$$

where flow depth was computed from Eq. 3-13. To conveniently describe this initial concentration in the numerical model, Δx was set to 0.35 foot in all model calibrations.

2. Calibration Procedure and Results. For each experiment in Table 5-1, a series of numerical model runs were made, using a different value of ϵ_y for each run, until the computed concentration-time curve most closely matched the measured curve. The criterion chosen to establish the best fit was the closeness of the magnitude and timing of the peak concentrations. This criterion was selected because of the

importance of peak concentrations in environmental modeling and assessments and because the overall shapes of the two curves were generally very similar.

In the course of completing each series of numerical model runs, it was noted that as ϵ_y was changed from a high value approaching complete vertical mixing to a low value approaching molecular diffusion, the envelope of computed peak concentrations followed a shape similar to that shown in Figure 5-16 from point 1 to point 2. The value of ϵ_y which produced the point on the envelope closest to the measured peak concentration was selected as the appropriate ϵ_y value for that experiment. Appendix E shows the series of computed concentration-time curves which were generated for each experiment. The curves selected as the best fits are shown in Figures 5-1 through 5-15 along with the corresponding measured curve.

3. Discussion of Figures 5-1 through 5-15. The curves generated by the numerical model for $S_0 = 0.001$ were lagged behind the laboratory measurements when the dye injection occurred at 32.8 feet from the top of the plane. Two possible reasons for this exist. First, the low mean velocities produced on this slope were outside the range of data analyzed by Yoon (1970) and Shen and Li (1973). The data of these investigators were used to estimate maximum and mean flow velocities in the numerical model. Since this range was exceeded, the appropriateness of the model for $S_0 = 0.001$ could be subject to question. Second, the timing of the individually-measured peaks using the continuous sampling method, as shown in Appendix E, generally displayed the greatest variability for $S_0 = 0.001$ with the injection at 32.8 feet, indicating that these experiments may have been influenced more

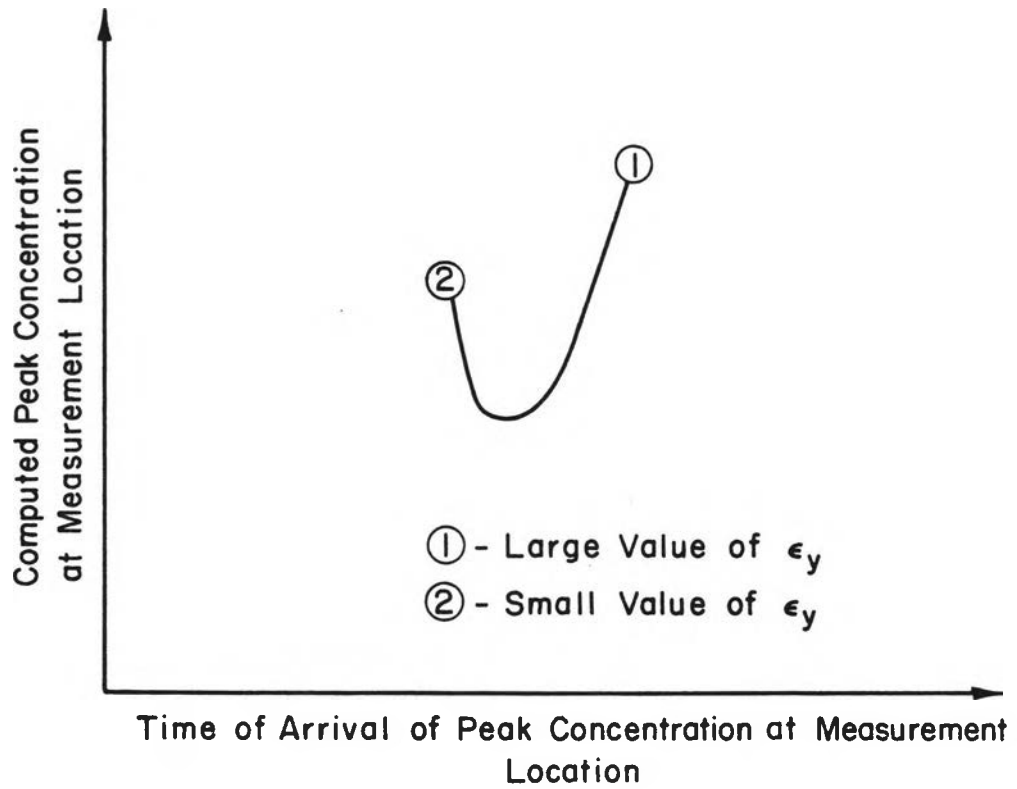


Figure 5-16. Typical Envelope of Computed Peak Concentrations

significantly by surface nonuniformities. A further test of the model was made using data obtained from injections at 27.7 feet from the top of the plane for rainfall intensities of 2 and 3 inches per hour (data were not available for 4 and 5 inches per hour at this injection location). Figures 5-1 and 5-3 show a much closer timing of the peak concentrations for these two additional experiments, justifying the use of the model's velocity equations and implicating the effect of surface nonuniformities downstream of the 32.8 feet injection as influencing the lag in modeled peak concentrations for the other $S_o = 0.001$ experiments.

Laboratory measurements for $S_o = 0.015$ had the least variability transverse to the flow, and the corresponding numerical model calibrations appear to produce reasonable fits.

A comparison of the curves for $S_o = 0.030$ indicates deviations in peak concentrations and in curve shapes for rainfall intensities of 2 and 5 inches per hour. In these two cases, the measured curve (an average curve based on continuous sampling at three different points across the flow width) has a wider base and lower peak than the computed curve. It is presumed that the relatively large differences in timing of the three individually-measured curves as seen by the plots of their peak concentrations in Appendix E, contributed substantially to the uncharacteristic shape of the averaged curves in these two cases.

4. Discussion of Figure 5-16. This figure is based on the apparent behavior of the peaks of the computed concentration-time curves shown in Appendix E. It indicates that as ϵ_y is decreased from a value representative of complete vertical mixing to a value

approaching molecular diffusion, the peak concentration will arrive earlier and will decrease to a minimum value before increasing again.

A physical explanation supports the above finding related to travel time. When the extent of vertical mixing is very small, mass tends to remain at its original depth (or in its original flow layer) and little is vertically diffused to other locations (to other flow layers). Therefore, the distribution of mass in the flow, following a completely-mixed, instantaneous injection, tends to take on a shape similar to the velocity profile. Since the slope of the velocity gradient is greatest near the point of maximum velocity, the greatest concentration of mass will reside in this vicinity and will travel at a speed near the maximum flow velocity--thus producing a peak concentration which arrives "early" at the measurement location.

When the extent of vertical mixing is very great, a particle of mass in the flow will change its vertical position very frequently, sampling a large range of velocities throughout the depth of flow. Thus, over a long time period, the speed of the particle of mass will tend toward the mean flow velocity. Summing this process over all the particles of mass which were injected instantaneously into the flow results in a peak concentration traveling near the speed of the mean flow velocity. This peak concentration will therefore arrive at the measurement location at a later time than for a flow with little vertical mixing. This implies that caution should be exercised in using dye tracer time-of-travel data to estimate mean flow velocities in overland flow.

When ε_y is between values representative of complete vertical mixing and molecular diffusion, the peak concentration will travel at a

speed between the maximum velocity and mean velocity. In this transition region, Figure 5-16 indicates that the magnitude of the peak concentration will be somewhat less than that for a peak concentration travel speed of either the maximum or mean velocity.

5. Calibrated ϵ_y Values. A summary is shown in Table 5-2 of the ϵ_y values which resulted in the best-fit concentration-time curves. Each ϵ_y value was assumed to be valid at the midpoint between injection and measurement locations. These midpoint distances are also listed in Table 5-2.

Calibrations were conducted for two different injection locations in Experiments 1, 2, and 9. These two injection locations produced travel distance midpoints which were 2.5 feet apart. The calibrated ϵ_y values for Experiment 1 (200 and 150 ft²/sec) and Experiment 9 (5 and 8 ft²/sec) were reasonably close. The much larger difference between ϵ_y values for Experiment 2 (600 versus 1500 ft²/sec) can be partly explained by the method of data collection. Concentrations in Experiment 2a were collected and measured by the discrete sampling method. The samples were collected at 10-second intervals. From Figure 5-3, it is seen that the measured concentration values immediately before the peak, at the peak, and immediately after the peak were approximately 32, 90 and 71. Because samples were collected only once every 10 seconds and because there are large jumps in concentration values between measurements, it seems very likely that the actual peak concentration was missed and was somewhat greater than 90. If this were the case, Figure E-3 in Appendix E indicates that ϵ_y would need to be increased to match a larger peak, thus converging more closely to the ϵ_y value of 1500 for Experiment 2b.

Table 5-2
Calibrated ϵ_y Values

Experiment No.	Slope	Rainfall Intensity (in/hr)	$\epsilon_y \times 10^8$ (ft ² /sec)	Distance to Midpoint ⁽¹⁾ (ft)	Computed Values at Midpoint ^(1,2)			
					Mean Velocity (ft/sec)	Depth of Flow (ft)	Ratio of ⁽³⁾ Depth of Flow to Drop Diameter	Reynolds Number
1a	0.001	2	200	34.3	0.098	0.0162	1.4	138
1b	0.001	2	150	36.8	0.103	0.0166	1.4	148
2a	0.001	3	600	34.3	0.127	0.0187	1.6	221
2b	0.001	3	1500	36.8	0.130	0.0196	1.7	222
3	0.001	4	2600	36.8	0.160	0.0213	1.8	334
4	0.001	5	6500	36.8	0.176	0.0242	2.0	387
5	0.015	2	10	36.8	0.260	0.0066	0.6	159
6	0.015	3	140	36.8	0.328	0.0078	0.7	237
7	0.015	4	250	36.8	0.388	0.0088	0.7	318
8	0.015	5	300	26.7	0.356	0.0087	0.7	294
9a	0.030	2	5	34.3	0.315	0.0050	0.4	153
9b	0.030	2	8	36.8	0.329	0.0052	0.4	162
10	0.030	3	16	36.8	0.405	0.0063	0.5	222
11	0.030	4	25	36.8	0.474	0.0072	0.6	291
12	0.030	5	100	34.3	0.531	0.0075	0.6	382

- (1) Midpoint between injection and measurement locations.
(2) Computed using Eqs. 2-4, 3-13, and 3-14.
(3) Drop diameter approximately equal to 3.63 mm, or 0.0119 ft.

A number of variables can be identified as having a possible influence on the calibrated values of ϵ_y . As discussed in Chapter 2, the pressures, velocities, and crater geometries experienced by a stagnant liquid layer due to the impact of a drop have been related to impact velocity, drop diameter, depth of the receiving liquid, and the density, surface tension, and viscosity of the liquid. For the present study, it is suggested that these pressures, velocities, and crater geometries are related to the magnitude and areal extent of local vertical mixing due to the impact of a raindrop in overland flow. If this is the case, then when impact velocity, drop diameter, and the density, surface tension, and viscosity of the liquid are held constant, as was done for the laboratory experiments reported herein, depth of the receiving liquid becomes a variable affecting ϵ_y . Mutchler (1967) and Mutchler and Hansen (1970), using water drops falling from a height of 40 feet, found that both the height of the splash crown and the width of the crater reached maximums when the water depth was approximately 1/3 of the drop diameter, and then they slowly decreased (by 30 and 15 percent, respectively) to relatively constant values above a water depth of one drop diameter. Palmer (1965) used a strain gage at the bottom of various depths of water to find that the maximum impact force from water drops falling from a height of 5 feet occurred at a water depth equal to one drop diameter. His data indicates that the impact force at depths equal to 1/3 of the drop diameter and 2 drop diameters was about 80 percent of the maximum. Wang and Wenzel (1970) used a pressure transducer mounted flush with the bottom surface of a tray to measure water-drop impact pressures under various depths of ponded water. They found that the maximum

pressure occurred at a zero depth of water and that pressures decreased as the depth of water increased. They used water drop fall heights ranging from 4.7 to 33.0 feet. Macklin and Metaxas (1976) classified the behavior of drop impacts into two unique categories: shallow splashing characterized by a cylindrical cavity which penetrates to the bed surface and deep splashing characterized by a hemispherical cavity which is not affected by the bed surface. The experiments conducted for the present study were at depths ranging from 0.4 to 2.0 times the drop diameter and were classified as shallow splashing according to the definitions of Macklin and Metaxas.

Another variable which would be expected to influence vertical mixing is the number of drops impacting the receiving liquid per unit time period. For the experiments conducted in the present study, the drop rate was linearly proportional to the rainfall intensity since drop size was constant. In nature, Laws and Parsons (1943) found that the median drop size tends to increase with increasing rainfall intensity. This finding was based primarily on data collected at rainfall intensities less than two inches per hour; an extrapolation of this relationship indicates a 20 percent increase in median drop size from 2 to 5 inches per hour rainfall intensity. For the present study, rainfall intensity was selected as the variable representing number of drops per unit time.

Mean flow velocity was a third variable which was expected to affect ϵ_y . As a parcel of water flows between two fixed points on the plane, the parcel will be impacted by fewer raindrops, resulting in less vertical mixing, as the velocity of the parcel is increased.

Finally, it is speculated that the Reynolds number may affect vertical mixing due to rainfall. As the Reynolds number of the flow

decreases, the influence of viscous forces over inertial forces becomes stronger. When this occurs, it seems reasonable to assume that the flow can more effectively dampen local perturbations created by the impact of a raindrop.

Table 5-2 lists values of the above variables for each calibration. In reviewing this table, it is difficult to deduce the effect of any single variable. In order to develop a quantitative relationship between ϵ_y and these variables, a regression analysis was performed as described later in this chapter.

An estimate of the molecular diffusion coefficient for Rhodamine WT dye can be made and compared to the ϵ_y values in Table 5-2. Rhodamine WT is an organic compound whose chemical structure was presented by Abidi (1982). Based on this structure, a molecular weight of 523 can be computed. A regression equation presented by Spalding (1963) relates the molecular weight of a substance (with the exception of inorganic acids and bromine) to the Schmidt Number,

$$S_c = \frac{v}{\epsilon_m}$$

where v = kinematic viscosity and ϵ_m = molecular diffusion coefficient. The regression equation is

$$S_c = 140(MW)^{0.397}$$

where MW = molecular weight. Spalding estimates that this equation is accurate within ± 20 percent. Using these relationships, an estimate of ϵ_m for Rhodamine WT dye is 0.65×10^{-8} ft²/sec. For laminar flow without rainfall,

$$\epsilon_y \cong \epsilon_m$$

The lowest calibrated values of ϵ_y in Table 5-2 (at a rainfall intensity of 2 inches per hour) are in the range of 5×10^{-8} to 10×10^{-8} ft²/sec--a reasonable comparison to ϵ_m considering that ϵ_y values in Table 5-2 increase by multiples of 1.5 to 14 for an increase in rainfall intensity of one inch per hour.

Another comparison can be made between ϵ_y values in Table 5-2 and estimated ϵ_y values for hypothetical, steady, uniform, turbulent flow at equivalent discharges. Using a Manning's n value of 0.01 and Manning's equation to compute depth, Eq. 3-37, written below, can be used to estimate ϵ_y for steady, uniform, turbulent flow:

$$\epsilon_y = 0.067 y_s u_*^3$$

where y_s = depth of flow and $u_* = \text{shear velocity} = \sqrt{g y_s S_o}$. A steady, uniform, turbulent discharge equivalent to 5 inches per hour rainfall intensity at 36.8 feet down the plane on a slope of 0.001 results in $\epsilon_y = 2200 \times 10^{-8}$ ft²/sec compared to 6500×10^{-8} ft²/sec in Table 5-2. A steady, uniform, turbulent discharge equivalent to 5 inches per hour rainfall intensity at 26.7 feet down the plane on a slope of 0.015 results in $\epsilon_y = 1900 \times 10^{-8}$ ft²/sec compared to 300×10^{-8} ft²/sec in Table 5-2. A steady, uniform, turbulent discharge equivalent to 5 inches per hour rainfall intensity at 34.3 feet down the plane on a slope of 0.030 results in $\epsilon_y = 2400 \times 10^{-8}$ ft²/sec compared to 100×10^{-8} ft²/sec in Table 5-2. This indicates that when rainfall occurs on overland flow moving at a laminar Reynolds number, vertical mixing under certain conditions can be equal to or greater than that predicted by the above turbulent flow ϵ_y equation for the same discharge without rainfall. Under different conditions, the

vertical mixing created by rainfall can be significantly less than expected in turbulent flow.

For purposes of comparison, the numerical model was run once for each experiment assuming "complete vertical mixing." This condition was simulated in the model by replacing the diffusion step with a complete mixing step: following convection and dilution during each time interval, the concentration in each cell was set equal to the average concentration of its vertical cell column. As can be seen from the plots in Figures 5-1 to 5-15 and in Appendix E, most of the calibrated ϵ_y values were significantly less than that required to approach the "completely-mixed," concentration-time curve. It is therefore concluded that for the range of conditions examined in this study, rainfall generally does not produce a continuous state of complete vertical mixing in overland flow.

6. Sensitivity and Limitations of the Numerical Model. Appendix E shows the sensitivity in the concentration-time curves computed by the numerical model due to changes in ϵ_y . Along the right-hand limb of the envelope of computed peak concentrations (Figure 5-16), a 1 percent decrease in ϵ_y generally resulted in a 1/3 percent decrease in peak concentration. The change in peak concentration was less near the minimum point on the envelope curve of Figure 5-16.

The model becomes more limited as it is applied closer to the top of the plane. This results from the difficulty in maintaining the relationships

$$\frac{(\Delta y)^2}{\Delta T \cdot \epsilon_y} \leq 1.25$$

and

$$\bar{u} \leq \frac{\Delta x}{\Delta T} \leq u_m$$

(as discussed in Chapter 3, Sections F1 and F2) where the flow conditions are changing most rapidly per unit length of plane.

Depth and velocity relationships used in the numerical model were based on data collected by others. These data were collected under restricted sets of conditions which thereby limit the applicability of the numerical model. These restrictions include the following. The data were collected in the shallow splashing zone as defined by Macklin and Metaxas (1976). The data chosen for use in the present study were limited to the laminar Reynolds number range (less than 900). The ranges in raindrop sizes and raindrop spacings were limited. The raindrop impact velocities were less than terminal velocity.

As can be seen in Figures 5-1 through 5-15 and in Appendix E, a certain degree of numerical "noise" was present in the results of the numerical model. A change in the number of flow layers or in the length of the time step would change this noise pattern. As seen in the computed concentration-time curves, the effect of this noise appears to be minor. In some cases it could have had a small influence on the selection of the calibrated ϵ_y value.

It was found that the numerical model was costly to run on the computer. The cost increased as the value of ϵ_y increased due to the increased number of iterations necessary to compute vertically-diffused concentrations down to the cutoff limit of 0.5 percent of C_j (see Section III-E-3). On the other hand, for very small values of ϵ_y , the required minimum number of flow layers was large (in order to satisfy $(\Delta y)^2 / (\Delta T \cdot \epsilon_y) < 1.25$), which also increased computer time.

D. Regression of Calibrated ϵ_y Values

Based on the previous discussion of variables likely to affect vertical mixing in the experiments conducted, the following independent variables were selected for use in a regression analysis: rainfall intensity, mean velocity, depth of flow, and Reynolds number. The calibrated values of $\log \epsilon_y$ were related to the logarithms of the values of the above variables in Table 5-2 by using the stepwise multiple linear regression program described by Dixon (1981). Details of the regression analyses discussed below are contained in Appendix G.

The resulting equation for ϵ_y was

$$\epsilon_y = 0.278 y_s^{3.23} i^{2.23} \quad (5-1)$$

with a coefficient of determination, r^2 , equal to 0.95. The units of y_s are feet, and the units of i are inches per hour. The addition of \bar{u} or R_e in the equation did not increase the explained variation sufficiently to warrant the inclusion of either in the final equation, based on an F test at $\alpha = 0.01$.

Equation 5-1 results in increased vertical mixing with increased depth of flow and with increased rainfall intensity. As discussed previously, one would rationally expect a greater degree of mixing when the frequency of drop impacts, or rainfall intensity, increases. However, increased mixing with increased depth of flow does not appear to be physically reasonable nor can it be justified from previous research findings related to measured splash geometry, forces, or pressures at depth-to-drop diameter ratios greater than about 1/3 to 1 (see discussion in Section 5-III-E). Since some of the depth-to-drop diameter ratios for the data in Table 5-2 fall between 1/3 and 1, a

second regression was conducted using only the data with ratios greater than 1 (data for $S_o = 0.001$). The resulting equation

$$\epsilon_y = 2.472 \times 10^{11} y_s^{9.59}$$

gives the same general relationship between ϵ_y and y_s , that is, increasing ϵ_y with increasing y_s . It is therefore assumed that this correlation between ϵ_y and y_s exhibited by the data in Table 5-2 is not a correlation between ϵ_y and splash geometry, forces, and pressures, but instead indicates that y_s is apparently serving as a surrogate for other independent variables in the analysis.

A third regression was conducted using all the data in Table 5-2 but using only rainfall intensity, mean velocity, and Reynolds number as independent variables. The following equation resulted,

$$\epsilon_y = 3.663 \times 10^{-11} i^{5.25} \bar{u}^{-3.25} \quad (5-2)$$

with a coefficient of determination, r^2 , equal to 0.94. The units of i are inches per hour, and the units of \bar{u} are feet per second. The addition of R_e in the equation did not increase the explained variation sufficiently to warrant its inclusion in the final equation, based on an F test at $\alpha = 0.01$. Equation 5-2 shows that vertical mixing increases with increasing rainfall intensity and with decreasing mean flow velocity--results which are physically reasonable. Therefore, Eq. 5-2 was selected for the present study.

Equation 5-2 can be rewritten to show how ϵ_y varies as a function of distance from the top of the plane, x , for a given rainfall intensity, slope, friction coefficient, viscosity, and acceleration of gravity. Substituting Eqs. 2-4, 3-13, 3-14, and 3-15 into Eq. 5-2 and rearranging,

$$\epsilon_y = 0.0427 \left(\frac{v}{g S_o}\right)^{1.08} (24 + 27.162 i^{0.407})^{1.08} i^{3.08} x^{-2.167} \quad (5-3)$$

A plot of Eq. 5-3 as a function of x is shown in Figures 5-17 and 5-18 for the range of travel distances used in the laboratory experiments of this study, indicating a decrease in ϵ_y of 38 and 57 percent over the travel distances of 8.0 and 13.1 feet, respectively.

An extrapolation of Eq. 5-3 outside the range of data used in its derivation is shown in Figure 5-19, where

$$\epsilon_{y,i}^* = \frac{\epsilon_y}{0.0427 \left(\frac{v}{g S_o}\right)^{1.08} x^{-2.167}}$$

This figure indicates the variation of ϵ_y with rainfall intensity. The plot includes the 2 to 5 inches per hour range as well as extrapolations beyond this range. Note that the largest change in ϵ_y per unit change in rainfall intensity occurs in the lower intensity range--the most often encountered intensity range in nature.

A third plot of Eq. 5-3 is shown in Figure 5-20 where

$$\epsilon_{y,x}^* = \frac{\epsilon_y}{0.0427 \left(\frac{v}{g S_o}\right)^{1.08} (24 + 27.162 i^{0.407})^{1.08} i^{3.08}}$$

This figure shows the radical changes in ϵ_y which Eq. 5-3 would predict near the top of the plane--the region where flow hydraulics are changing most rapidly and the region of special interest in urban hydrology where the travel distance to storm sewers or roadside drainage is frequently short.

The regression equation for ϵ_y found in this study, Eq. 5-2, is based on numerical model calibration of laboratory data. As discussed previously, these laboratory data include an amount of variability due to random and systematic experimental error which was roughly estimated to be up to ± 20 percent. Considering this experimental error, as well

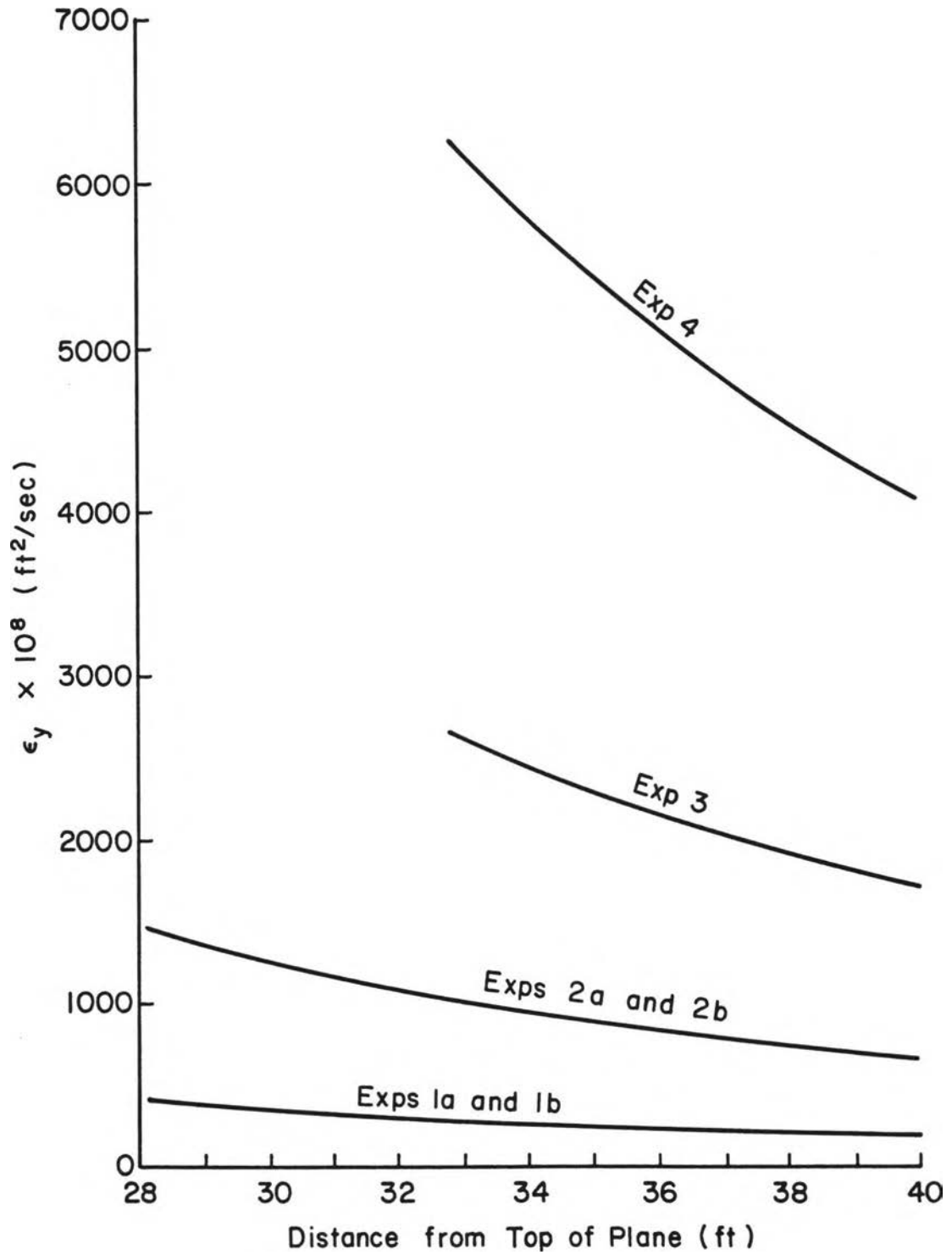


Figure 5-17. ϵ_y from Eq. 5-3 for Laboratory Experiments
 $s_o^y = .001$

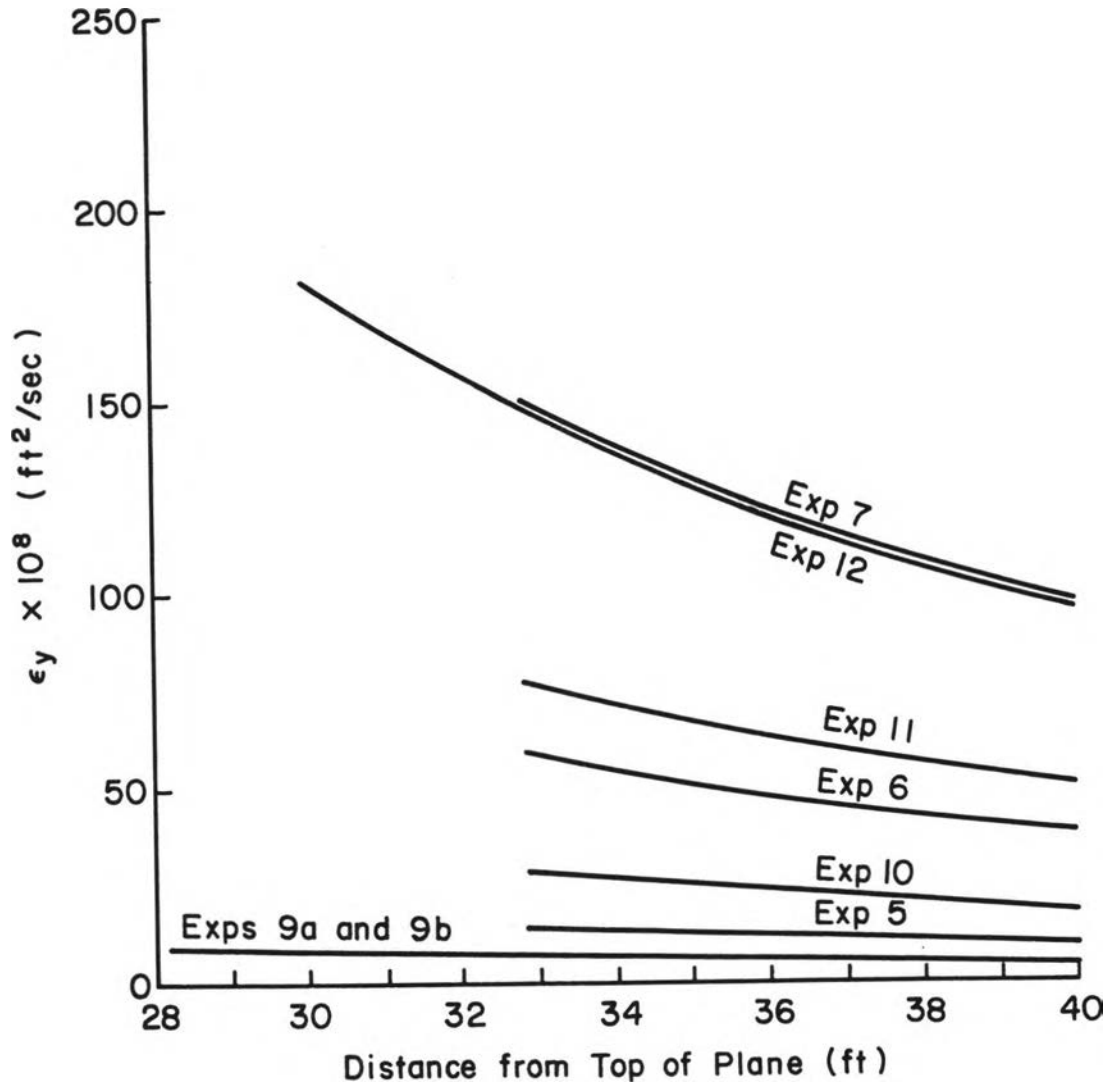


Figure 5-18. ϵ_y from Eq. 5-3 for Laboratory Experiments
 $S_o^y = .015$ and $.030$

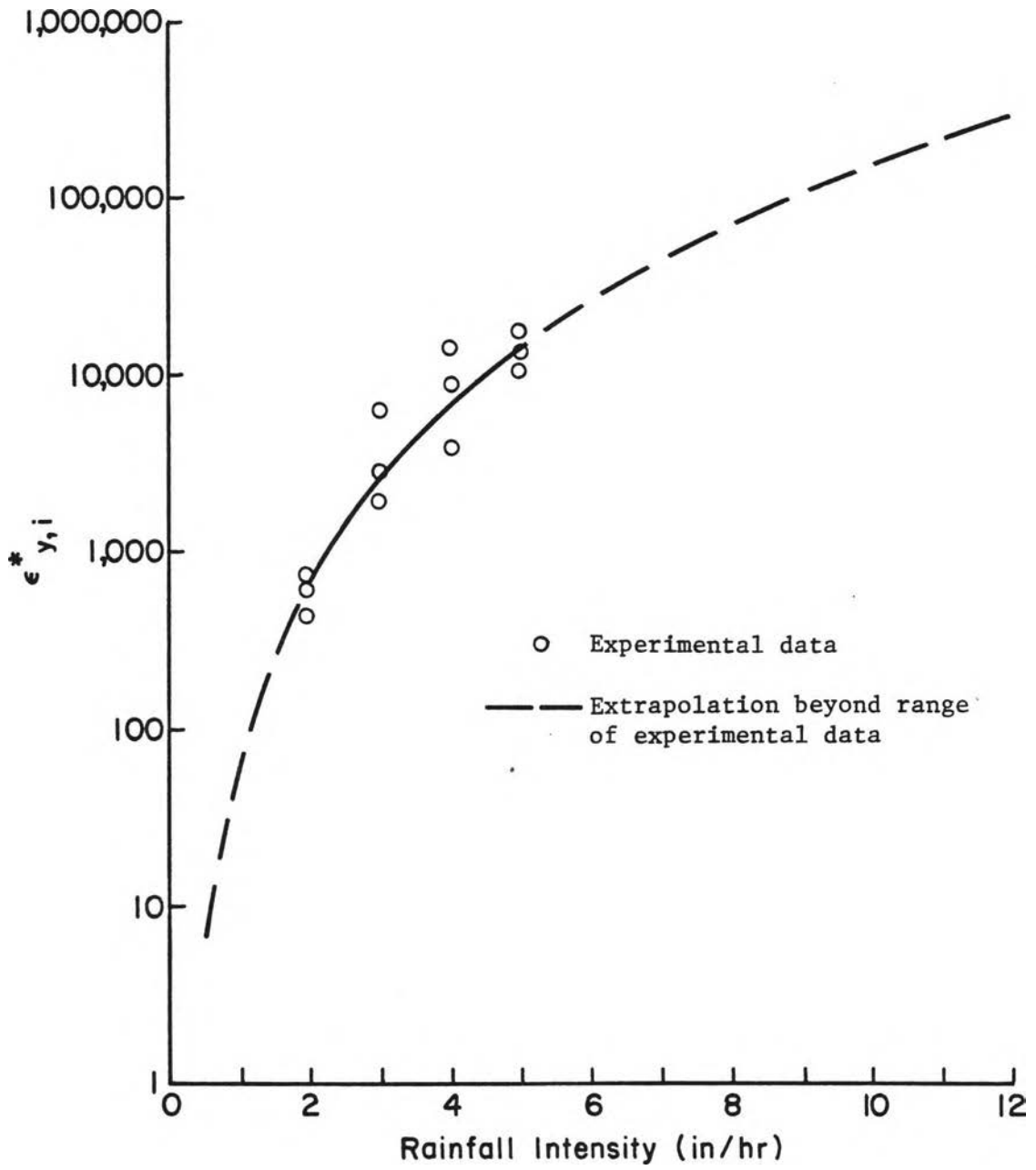


Figure 5-19. Variation of ϵ_y with Rainfall Intensity

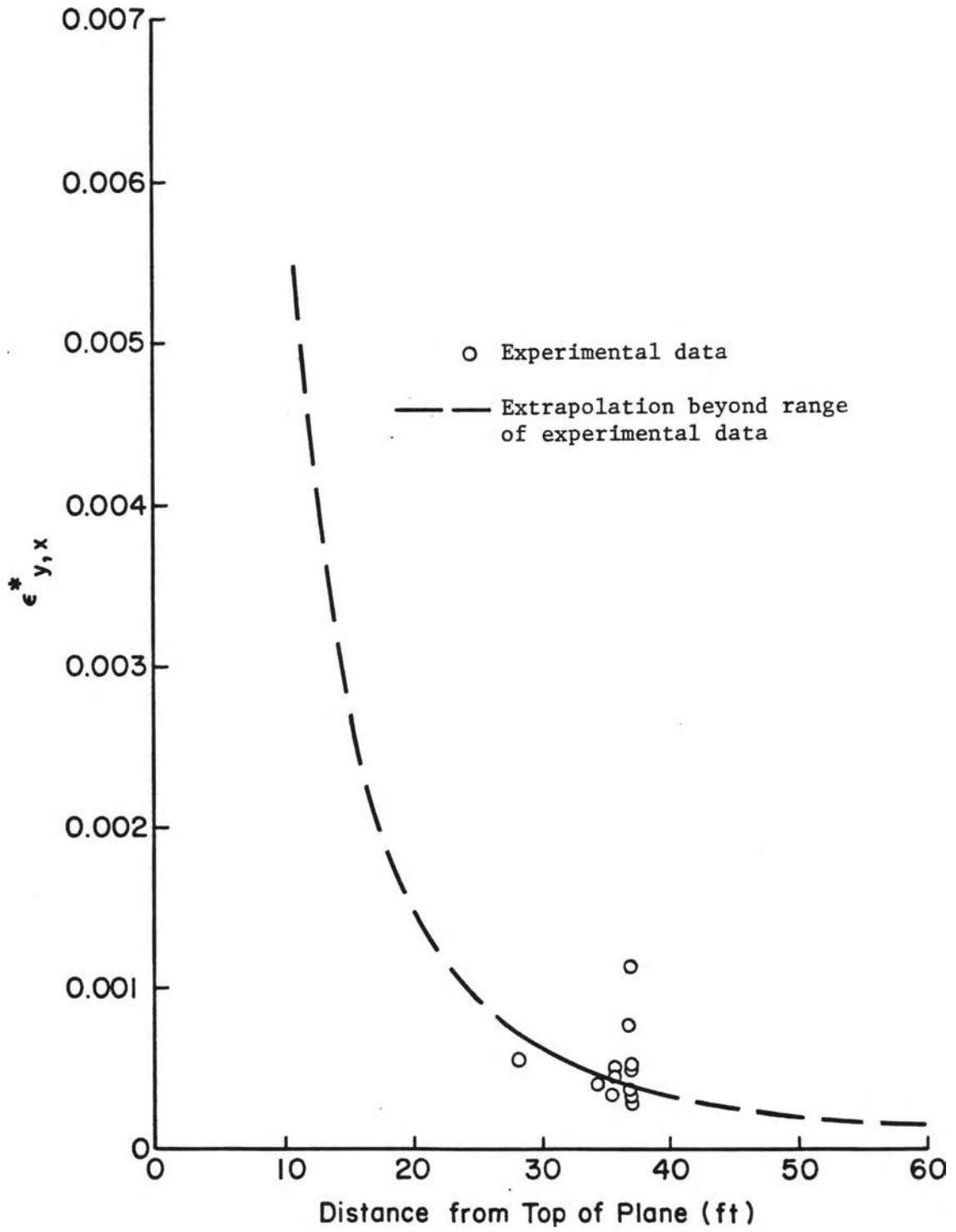


Figure 5-20. Variation of ϵ_y with Distance

as the sensitivity of ϵ_y to peak concentration in the numerical model calibration runs and the numerical noise present in the numerical model, the variability incorporated into the regression equation for ϵ_y could be up to 60 percent or more. However, note that the range in calibrated ϵ_y values found in this study varies by a factor of 1000.

E. Convective and Taylor Periods

These two periods have been defined to establish when the one-dimensional dispersion equation for steady, uniform flow (Eq. 2-5) can be correctly applied. The two periods are divided by the point at which the Taylor conditions are established. Though the equation itself is not theoretically valid for nonuniform overland flow during rainfall, an examination of these Taylor conditions and their relationship to ϵ_y as applied to this study may be useful.

As explained in Chapter 2, the Taylor conditions are that 1) only small deviations exist between local concentrations (c) and the vertically-averaged concentration (\bar{c}) and 2) vertically-averaged concentrations vary slowly with time and distance down the plane. The first condition will be met when injected particles have had a sufficient time to move significant distances in the vertical direction from their original position immediately after injection. For small ϵ_y , this time period could be very large; for large ϵ_y , the condition could be met very quickly. Regarding the second condition, \bar{c} at a fixed point near the injection location will vary greatly with time immediately following the injection regardless of the value of ϵ_y . The variation of \bar{c} with distance down the plane will be large when the peak concentration is traveling near the leading edge of the dye cloud, thus producing a large concentration gradient in this vicinity. This event

will occur when ε_y is small, resulting in a peak concentration traveling at a speed near the maximum velocity. Therefore, the convective period (the time between injection and the beginning of the Taylor period) is longer for small ε_y .

The Eulerian time scale is defined in Eq. 2-7 to be

$$T_E = \frac{l^2}{\varepsilon}$$

and is generally taken to be

$$T_E = \frac{y_s^2}{\varepsilon_y} \quad (5-4)$$

for infinitely-wide, open channel flow. As discussed in Chapter 2, this time scale has been used as a tool for estimating the travel time through the convective period in steady, uniform flow. The travel distance corresponding to T_E for steady, uniform flow can be written as

$$x_{T_E} = T_E \bar{u} \quad (5-5)$$

In order to develop similar time and distance scales for overland flow during rainfall, Eqs. 5-4 and 5-5 must be modified to account for the changing hydraulic conditions with distance down the plane. In the case of steady, uniform flow, the fraction of x_{T_E} represented by a subreach Δx is

$$w_{x_{T_E}} = \frac{\Delta x}{x_{T_E}} = \frac{\Delta x}{T_E \bar{u}} = \frac{\Delta x \varepsilon_y}{y_s^2 \bar{u}} \quad (5-6)$$

For steady, nonuniform flow, assume that the flow conditions change in a stepwise manner with step reaches equal to Δx . The fraction of x_{T_E} represented by the i th subreach is written as

$$w_{x_{T_E}}^i = \frac{\Delta x \varepsilon_y(x_i)}{y_s^2(x_i) \bar{u}(x_i)}$$

where x_i = distance from top of plane to midpoint of the i th subreach. Assuming that an injection is made at the beginning of the first subreach, x_{TE} can be computed as

$$x_{TE} = n \Delta x$$

where n is defined in the following equation,

$$\sum_{i=1}^n w_{x_{TE}}^i = 1 \quad (5-7)$$

Similarly, as Δx approaches zero, x_{TE} can be computed from

$$\int_{(x_{inj})}^{(x_{inj} + x_{TE})} \frac{\varepsilon_y(x)}{y_s^2(x) \bar{u}(x)} dx = 1 \quad (5-8)$$

where x_{inj} = distance from top of plane to injection location and where $y_s(x)$, $\bar{u}(x)$, and $\varepsilon_y(x)$ are defined by Eqs. 3-13, 3-15, and 5-3, respectively.

From Eqs. 2-3, 2-4, 3-13, and 3-14, $y_s(x)$ can further be expressed as

$$y_s(x) = K_{y_s} x^{1/3} \quad (5-9)$$

where

$$K_{y_s} = 0.01425 \left[\frac{v_i(24 + 27.162 i^{0.407})}{g S_o} \right]^{1/3} \quad (5-10)$$

Similarly, from Eqs. 2-3, 2-4, 3-13, 3-14, and 3-15,

$$\bar{u}(x) = K_u x^{2/3} \quad (5-11)$$

where

$$K_u^- = 0.00162 \left[\frac{i^2 g S_o}{v(24 + 27.162 i^{0.407})} \right]^{1/3} \quad (5-12)$$

and from Eq. 5-3,

$$\varepsilon(y) = K_{\varepsilon_y} x^{-2.167} \quad (5-13)$$

where

$$K_{\varepsilon_y} = 0.0427 \left(\frac{v}{g S_o} \right)^{1.08} (24 + 27.162 i^{0.407})^{1.08} i^{3.08} \quad (5-14)$$

Substituting Eqs. 5-9, 5-11, and 5-13 into Eq. 5-8 and integrating gives the following relationship for x_{T_E} ,

$$x_{T_E} = \left[x_{inj}^{-2.50} - \frac{2.50 K_{y_s}^2 K_u^-}{K_{\varepsilon_y}} \right]^{-0.40} - x_{inj} \quad (5-15)$$

An expression for T_E can now be written as

$$T_E = \int_{x_{inj}}^{x_{T_E}} \frac{dx}{\bar{u}(x)} \quad (5-16)$$

Substituting Eq. 5-11 into this expression and integrating,

$$T_E = \frac{3}{K_u^-} (x_{T_E}^{1/3} - x_{inj}^{1/3}) \quad (5-17)$$

Table 5-3 gives the results of Eqs. 5-15 and 5-17 for the experiments conducted in this study.

As mentioned in Chapter 2, Fischer et al. (1979) concluded from a review of field and laboratory studies in steady, uniform flow that a linear growth with time of the variance (σ_x^2) of \bar{c} with respect to x begins at about time $0.2 T_E$, or at about distance $0.2 x_{T_E}$, and that the Taylor conditions are generally met at time $0.4 T_E$, or at about

Table 5-3

Computed Values for x_{T_E} and T_E for Laboratory Experiments

Experiment No.	Slope	Rainfall Intensity (in/hr)	Injection Location From Top of Plane, x_{inj} (ft)	$x_{T_E}^{(1)}$ (ft)	$T_E^{(2)}$ (sec)
1a	0.001	2	27.7	2.0	23
1b	0.001	2	32.8	6.8	67
2a	0.001	3	27.7	2.5	22
2b	0.001	3	32.8	4.7	37
3	0.001	4	32.8	2.7	19
4	0.001	5	32.8	1.5	9
5	0.015	2	32.8	>200	>200
6	0.015	3	32.8	>200	>200
7	0.015	4	32.8	>200	>200
8	0.015	5	22.8	4.1	12
9a	0.030	2	27.7	>200	>200
9b	0.030	2	32.8	>200	>200
10	0.030	3	32.8	>200	>200
11	0.030	4	32.8	>200	>200
12	0.030	5	27.7	50.8	75

(1) Computed from Eq. 5-15 using data presented in Appendix F. Values for Experiments 5, 6, 7, 9a, 9b, 10, and 11 were approximated from Eq. 5-7 instead of Eq. 5-15 since the bracketed term in Eq. 5-15 was negative, producing a complex number.

(2) Computed from Eq. 5-17 using data presented in Appendix F.

distance $0.4 x_{T_E}$. For nonuniform flow, one would not expect to see a strictly linear growth rate of σ_x since ε_y , D (Eq. 2-6), y_s , u , and q are all changing in the direction of flow. However, for overland flow during rainfall, the degree of nonuniformity is decreasing with increasing distance down the plane. That is, the percent change in ε_y , D , y_s , \bar{u} , and q per unit length of plane is decreasing downstream, so that σ_x^2 might be expected to approach a linear growth rate in an asymptotic manner. Figures 5-21 through 5-23 show σ_x^2 versus time as computed by the numerical model for each experiment in this

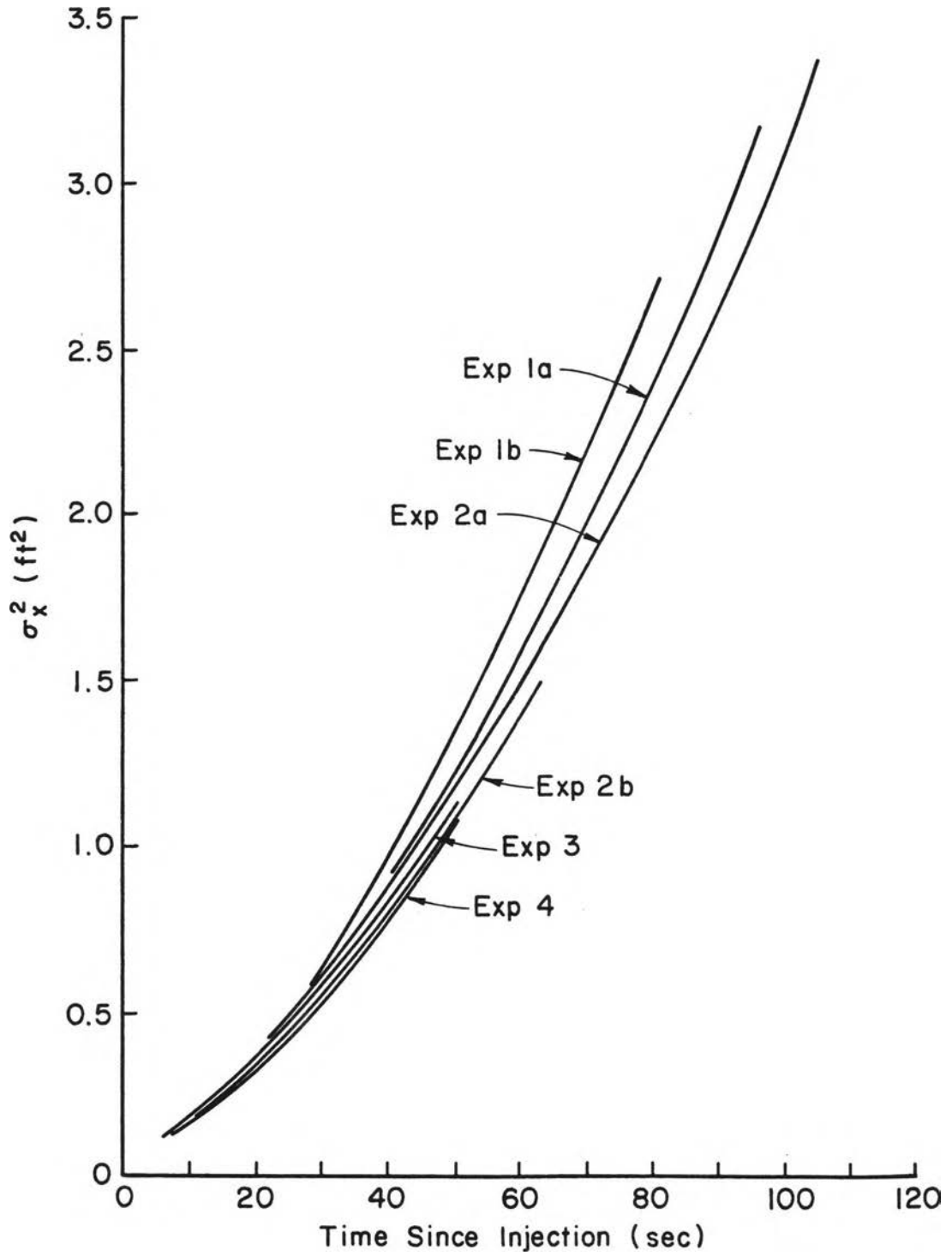


Figure 5-21. Variance of Dye Cloud Versus Time Since Injection for $S_0 = .001$

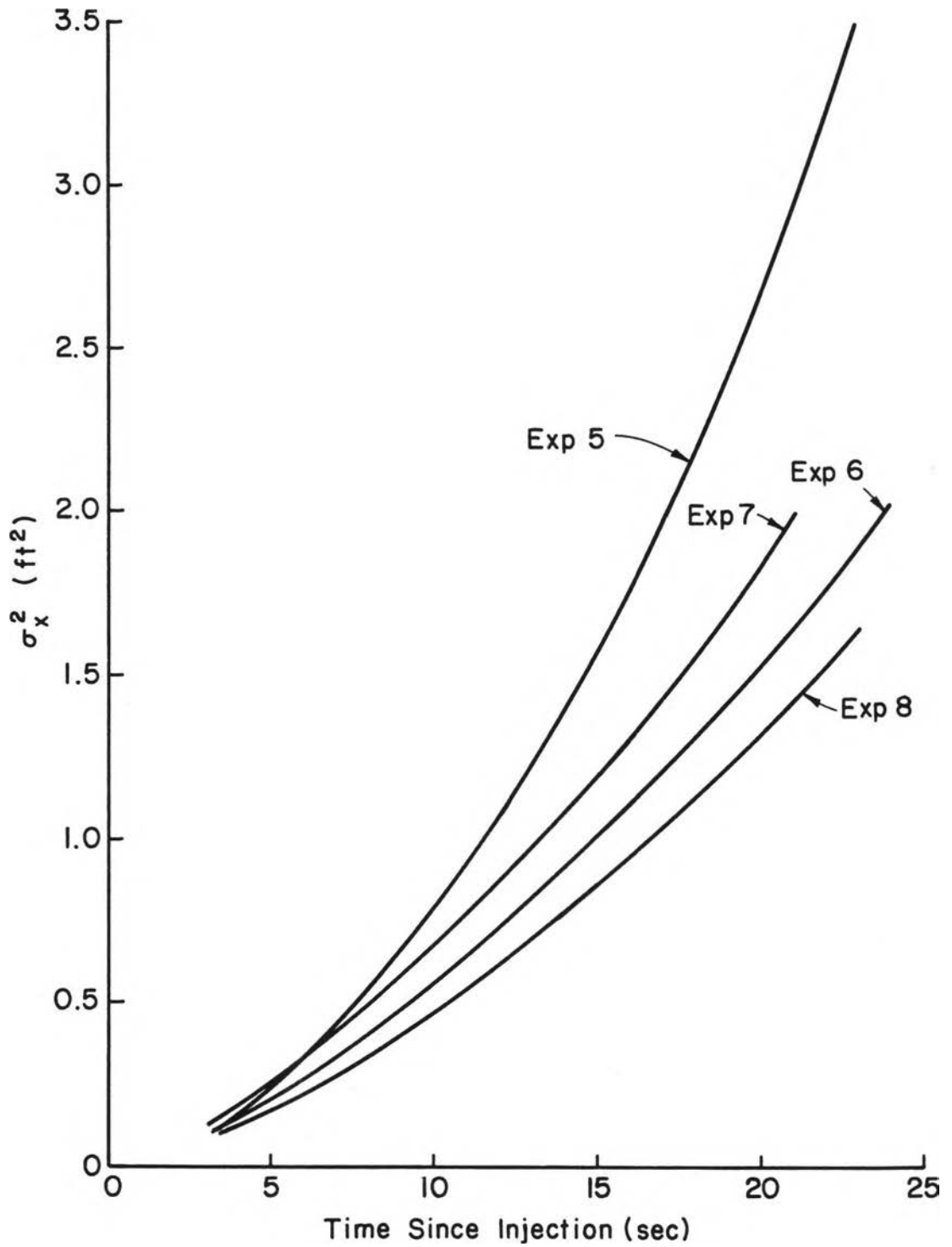


Figure 5-22. Variance of Dye Cloud Versus Time Since Injection for $S_o = .015$

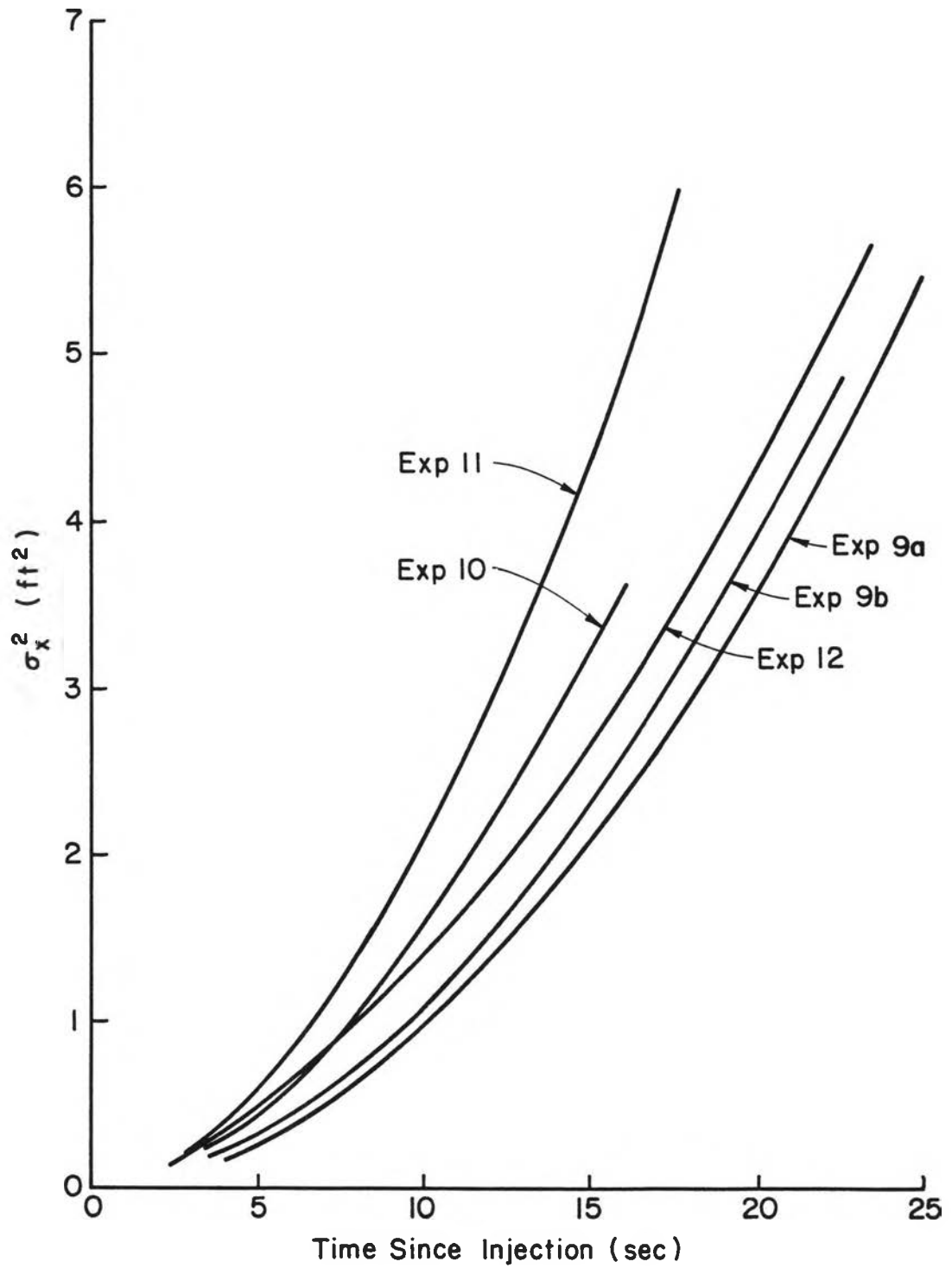


Figure 5-23. Variance of Dye Cloud Versus Time Since Injection for $S_0 = .030$

study. Compared to the values of T_E given in Table 5-3, it appears that the σ_x^2 -versus-time curves remain nonlinear beyond $0.2 T_E$ as expected; however, they seem to be moving toward a linear growth rate.

It is difficult to compare the experimental results of this study to the $0.4 T_E$ guideline for the beginning of the Taylor conditions. Though it was developed from steady, uniform flow data, it will be assumed that this guideline would not be significantly different over short reaches of slowly-varying, nonuniform flow. Comparison of this guideline to the x_{T_E} and T_E values shown in Table 5-3 and to the ϵ_y values in Figures 5-17 and 5-18 implies that the Taylor conditions are reached within a reasonable travel distance only for large ϵ_y .

F. Longitudinal Dispersion Coefficient

The velocity profile equation developed in Chapter 3, Eq. 3-21, can be substituted into the theoretical equation for the longitudinal dispersion coefficient, Eq. 2-6, to derive a relationship for this dispersion coefficient for overland flow during rainfall. From Eq. 2-6, the longitudinal dispersion coefficient is

$$D = - \frac{1}{y_s} \int_0^{y_s} u' \int_0^y \frac{1}{\epsilon_y} \int_0^y u' dy dy dy \quad (2-6)$$

where

$$u' = u - \bar{u} \quad (5-18)$$

and y = distance in vertical direction measured from streambed, y_s = depth at water surface, ϵ_y = vertical mixing coefficient, u = point velocity, and \bar{u} = vertically-averaged velocity. Define u_L as the lower velocity profile from $y = 0$ to $y = y_m$ (where y_m = vertical

distance above streambed to point of maximum velocity, u_m) and u_U as the upper velocity profile from $y = y_m$ to $y = y_s$. From Eq. 3-21,

$$u_L = \frac{\bar{u}}{\bar{u}_p} u_m \left(\frac{2}{y_m} y - \frac{1}{y_m^2} y^2 \right) \quad (5-19)$$

and

$$u_U = \frac{\bar{u}}{\bar{u}_p} u_m \left[1.0 + B_U \left(\frac{y - y_m}{y_s - y_m} \right) + C_U \left(\frac{y - y_m}{y_s - y_m} \right)^2 \right] \quad (5-20)$$

The equation for u' becomes

$$u' = \begin{cases} u_L - \bar{u}, & 0 < y < y_m \\ u_U - \bar{u}, & y_m < y < y_s \end{cases} \quad (5-21)$$

Substituting Eq. 5-21 into Eq. 2-6 and assuming ε_y is constant with respect to y ,

$$D = -\frac{1}{y_s \varepsilon_y} \left[\int_0^{y_m} (u_L - \bar{u}) \int_0^y \int_0^y (u_L - \bar{u}) dy dy dy + \int_{y_m}^{y_s} (u_U - \bar{u}) \int_0^y \int_0^y (u_U - \bar{u}) dy dy dy \right] \quad (5-22)$$

Define Terms 1 and 2 as

$$\text{Term 1} = \int_0^{y_m} (u_L - \bar{u}) \int_0^y \int_0^y (u_L - \bar{u}) dy dy dy \quad (5-23)$$

$$\text{Term 2} = \int_{y_m}^{y_s} (u_U - \bar{u}) \int_0^y \int_0^y (u_U - \bar{u}) dy dy dy \quad (5-24)$$

These terms are evaluated in Appendix H. Substituting these evaluated terms into Eq. 5-22 results in

$$\begin{aligned}
D = & -\frac{1}{y_s} \varepsilon_y \left(\frac{\bar{u}}{\bar{u}_p} \right)^2 \left[\frac{13}{210} u_m^2 y_m^3 - \frac{13}{60} u_m \bar{u}_p y_m^3 + \frac{1}{6} u_p^2 y_m^3 \right. \\
& + \frac{1}{6} k_1^2 (y_s^3 - y_m^3) + \frac{1}{6} k_1 k_2 (y_s^4 - y_m^4) \\
& + \left(\frac{7}{60} k_1 k_3 + \frac{1}{30} k_2^2 \right) (y_s^5 - y_m^5) + \frac{1}{24} k_2 k_3 (y_s^6 - y_m^6) \\
& \left. + \frac{1}{84} k_3^2 (y_s^7 - y_m^7) \right] \quad (5-25)
\end{aligned}$$

where

$$k_1 = u_m - \frac{u_m B_U y_m}{y_s - y_m} + \frac{u_m C_U y_m^2}{(y_s - y_m)^2} - \bar{u}_p \quad (5-26)$$

$$k_2 = \frac{u_m B_U}{y_s - y_m} - \frac{2 y_m u_m C_U}{(y_s - y_m)^2} \quad (5-27)$$

$$k_3 = \frac{u_m C_U}{(y_s - y_m)^2} \quad (5-28)$$

Equation 5-25 was evaluated for the experiments considered in this study, using Eqs. 2-3, 2-4, 3-8, 3-9, 3-11, 3-12, 3-13, 3-14, 3-15, 3-16, and 5-3 to determine values for B_U , C_U , u_m , y_m , y_s , \bar{u} , \bar{u}_p , and ε_y . Plots of D are shown in Figure 5-24. The results for Experiments 6, 7, 8, 10, 11, and 12 gave negative values for D .

A comparison is made in Table 5-4 between three different dispersion coefficients computed for the same discharge but representing different flow conditions. Equation 3-36 is the theoretical dispersion coefficient for infinitely-wide, steady, uniform turbulent flow down a smooth plane with a logarithmic velocity profile. Equation

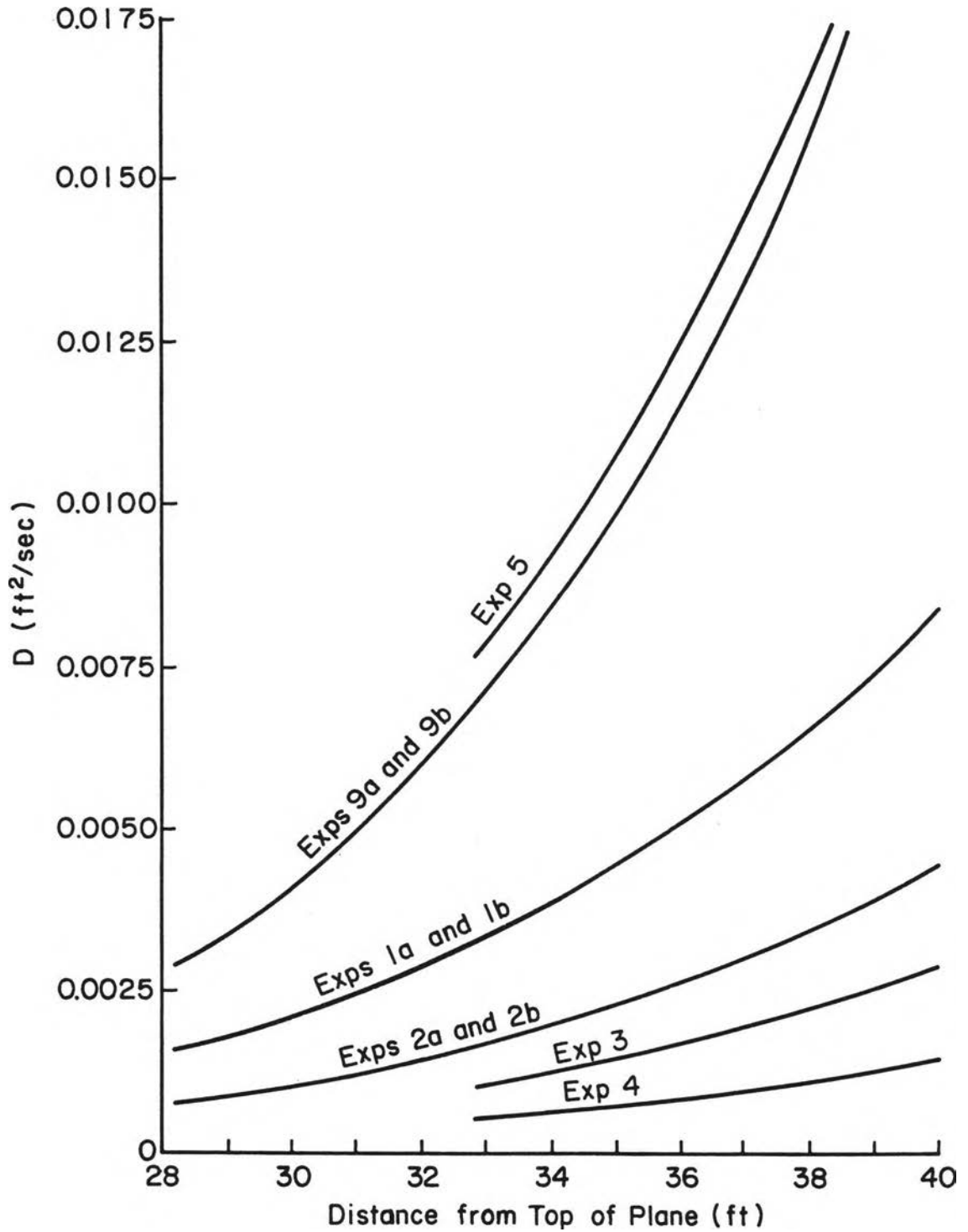


Figure 5-24. D from Eq. 5-25 for Laboratory Experiments

Table 5-4

Comparison of Dispersion Coefficients Computed from Eqs. 3-36, 3-42, and 5-25

Experiment No.	Slope	Rainfall Intensity (in/hr)	Discharge ⁽²⁾ (ft ³ /sec)	Dispersion Coefficient (ft ² /sec)		
				Eq. 3-36 ⁽³⁾	Eq. 3-42 ⁽⁴⁾	Eq. 5-25
1a	0.001	2	0.00159	0.0008	7.4	0.0040
1b	0.001	2	0.00170	0.0008	8.5	0.0056
2a	0.001	3	0.00238	0.0011	16.6	0.0021
2b	0.001	3	0.00256	0.0012	19.2	0.0030
3	0.001	4	0.00341	0.0016	34.1	0.0019
4	0.001	5	0.00426	0.0019	53.2	0.0010
5	0.015	2	0.00170	0.0010	8.5	0.0140
9a	0.030	2	0.00159	0.0009	7.4	0.0087
9b	0.030	2	0.00170	0.0010	8.5	0.0131

(1) Only those experiment numbers which produced a positive value for Eq. 5-25 are included.

(2) Computed at midpoint of laboratory travel distance.

(3) Flow depth computed using Manning's equation with $n = 0.01$.

(4) Flow depth computed using Eq. 3-13 with $f = 24/R_e$; molecular diffusion coefficient assumed to be 0.65×10^{-8} ft²/sec for Rhodamine WT dye.

3-42 is the theoretical dispersion coefficient for infinitely-wide, steady, uniform laminar flow down a smooth plane. Equation 5-25 represents dispersion in overland flow during rainfall. The dispersion coefficient values in this table for overland flow with rainfall are generally closer to those for steady, uniform turbulent flow than for steady, uniform laminar flow.

The large values shown for laminar flow are due in part to the use of the very small molecular diffusion coefficient as the vertical mixing coefficient. As seen in Eq. 2-6, from which the equations used in Table 5-4 were derived, the dispersion coefficient is inversely related to the vertical mixing coefficient. Since the molecular diffusion coefficient is generally several orders of magnitude lower than the vertical mixing coefficient for either overland flow with rainfall or steady, uniform turbulent flow, the dispersion coefficient for laminar flow might be expected to be significantly greater.

It is interesting to note that for small Reynolds number flows, these much larger dispersion coefficients will be approached as the rainfall approaches zero intensity, while the length of the convective period will approach a very large value.

The negative values computed for D for some of the experiments raise questions regarding the applicability of the dispersion coefficient equation, Eq. 2-6, to certain velocity profiles. To further check this applicability, dispersion coefficients were computed for the velocity profile shown in Figure 5-25 which also has the maximum velocity, u_m , located below the water surface. One could conceive of this profile occurring for steady, uniform, laminar flow between parallel plates where the bottom plate is fixed, the top plate is

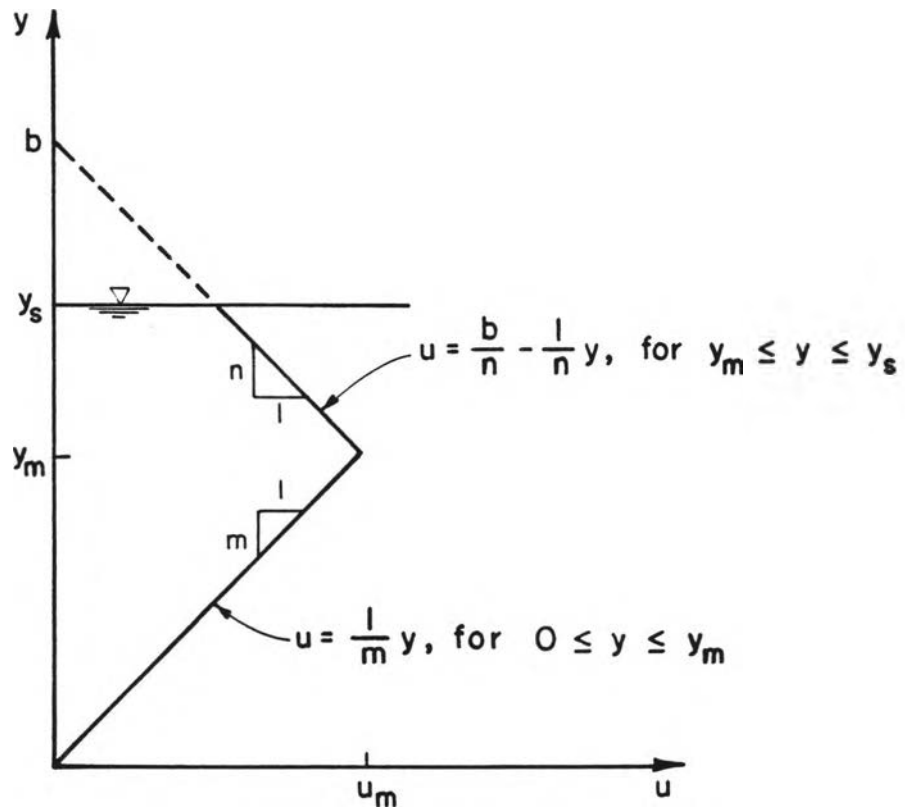


Figure 5-25. Velocity Profile Which Yields Positive, Negative, and Zero Values for Dispersion Coefficient Using Eq. 2-6

moving at a constant velocity, and a porous plate or screen located at depth y_m is moving at the maximum velocity, u_m . The following expression for D can be derived:

$$D = - \frac{1}{y_s \varepsilon_y} \left[\frac{1}{30 m^2} y_m^5 - \frac{1}{6m} \bar{u} y_m^4 + \frac{1}{6} \bar{u}^2 y_m^3 \right. \\ \left. + \frac{1}{6} \left(\frac{b}{n} - \bar{u} \right)^2 (y_s^3 - y_m^3) - \frac{1}{6n} \left(\frac{b}{n} - \bar{u} \right) (y_s^4 - y_m^4) \right. \\ \left. + \frac{1}{30 n^2} (y_s^5 - y_m^5) \right]$$

where \bar{u} = mean velocity, y_s = depth at water surface, y_m = depth at maximum velocity, ε_y = vertical mixing coefficient, and b , n , and m are defined in Figure 5-25. Calculations for the case of $u_m = 1.0$, $y_m = 1.0$, $y_s = 1.5$, and $m = 1.0$ indicate that the computed dispersion coefficients will be positive for $y_s \leq b < 1.60$, zero for $b = 1.60$, and negative for $b > 1.60$. This implies that Eq. 2-6 is not appropriate for all velocity profiles.

G. Approximation Methods for Peak Concentrations

The solution to Eq. 2-5 for the peak concentration in steady, uniform flow is (Fischer et al., 1979)

$$\bar{c}_p = \frac{M}{A \sqrt{4\pi Dt}} \quad (5-29)$$

where M = mass, A = cross-sectional area, D = longitudinal dispersion coefficient, and t = time. Since Eq. 2-5 is only valid for steady, uniform flow where the Taylor conditions are met, the solution is similarly restricted. However, an investigation was made into the possible use of Eq. 5-29 as a tool for estimating the peak concentrations measured in the laboratory experiments for this study, using

Eq. 5-25 to estimate the dispersion coefficient. The reasoning behind this investigation is that 1) flow conditions are changing slowly down the plane so that the use of average flow conditions over a short travel distance might be an acceptable approximation, and 2) the estimated travel distance to the point where the Taylor conditions are met is relatively short for some of the experiments based on calculations presented in Table 5-3.

Two approaches were taken. First, Eq. 5-29 was used to compute \bar{c}_p using an average cross-sectional area (Eq. 3-13) and average dispersion coefficient (Eq. 5-25) over the travel distance and using t equal to the travel time of the mean velocity,

$$t_{\bar{u}} = \int_{x_{inj}}^{x_{col}} \frac{dx}{\bar{u}(x)} \quad (5-30)$$

where x_{col} = distance from top of plane to sample collection location, and x_{inj} = distance from top of plane to injection location.

Second, Eq. 5-29 was modified to account for the changing cross-sectional area and changing dispersion coefficient over the travel distance. The modified equation is

$$\bar{c}_p = \frac{M}{\sqrt{4\pi \int_{x_{inj}}^{x_{col}} \frac{A^2(x) D(x)}{\bar{u}(x)} dx}} \quad (5-31)$$

For a unit width of flow,

$$A^2(x) = y_s^2(x)$$

so that

$$\bar{c}_p = \frac{M}{\sqrt{4\pi \int_{x_{inj}}^{x_{col}} \frac{y_s^2(x) D(x)}{\bar{u}(x)} dx}} \quad (5-32)$$

For the purposes of this comparison, Eq. 5-32 was approximated as

$$\bar{c}_p = \frac{M}{\sqrt{4\pi \sum_{i=1}^n \frac{y_s^2(x_i) D(x_i) \Delta x}{\bar{u}(x_i)}}} \quad (5-33)$$

where

$$n \cdot \Delta x = x_{col} - x_{inj}$$

A value of 0.5 foot was used for Δx .

The results are presented in Table 5-5 for those experiments with small x_{T_E} and T_E (Table 5-3) and with positive dispersion coefficients from Eq. 5-25. It is seen that both approximation methods give similar results and are greater than the measured peaks by a factor of 2 to 3. It therefore appears that even very short convective periods may cause significant deviations from the dispersion theory of Eqs. 2-5 and 5-29, and that the nonuniform conditions on the plane may be significantly influencing these approximations. However, for the cases examined, the two approximation methods could be used to obtain an upper limit of peak concentrations for planning studies.

Table 5-5

Peak Concentrations from Eqs. 5-29 and 5-33

Experiment No.	Slope	Rainfall Intensity (in/hr)	Computed Peak ($\mu\text{g/L}$)		Peak from Averaged Laboratory Conc.-Dist. Curve ($\mu\text{g/L}$)	Average of Individually Measured Laboratory Peaks ($\mu\text{g/L}$)
			Eq. 5-29	Eq. 5-33		
1a	0.001	2	134	135	65	79
1b	0.001	2	161	161	94	132
2a	0.001	3	225	223	93	192
2b	0.001	3	265	262	155	(1)
3	0.001	4	389	333	151	205
4	0.001	5	677	679	200	255

(1) Only width-averaged samples were collected for this experiment.

Chapter VI

CONCLUSIONS AND RECOMMENDATIONS

A. Conclusions

A numerical model was developed to simulate the movement of a solute in steady overland flow during rainfall. The flow layer approach used by the model, and the depth and velocity relationships adopted, produced concentration-time curves which reasonably reproduced measurements in the laboratory, given that a proper value for the vertical mixing coefficient, ϵ_y , was selected.

A study of these numerical model simulations concluded that the velocity of the peak concentration may vary between the mean cross-sectional velocity and the maximum point velocity, depending upon the ϵ_y value--implying that caution should be used in interpreting time-of-travel data to estimate velocities in overland flow. Based on these simulations, it is further concluded that for the conditions examined in this study, rainfall generally does not produce a continuous state of complete vertical mixing in overland flow.

The calibrated ϵ_y values were used in a regression analysis to determine their relationship to the rainfall and flow parameters thought to be most important in vertical mixing. It is concluded that the most important variables affecting ϵ_y (for the conditions of this study) are rainfall intensity and mean flow velocity. The regression equation showed that ϵ_y varies greatest at low rainfall intensities and near the top of the overland flow plane. The lower range of ϵ_y

values compared favorably with an estimate of the molecular diffusion coefficient for Rhodamine WT dye. The upper range of ϵ_y values was similar to estimated vertical mixing coefficient values for equivalent hypothetical turbulent flow.

The distance from the injection location to the point where the Taylor conditions are met was estimated to be very short where vertical mixing is great (high rainfall intensities and low flow velocities) and very long where vertical mixing is small (low rainfall intensities and high flow velocities). An expression for the longitudinal dispersion coefficient, D , (valid where the Taylor conditions apply) was derived using the integral equation for D presented by Fischer along with the flow relationships developed earlier in this study. In applying this expression to the flow conditions tested in the laboratory, the computed dispersion coefficients were generally closer in magnitude to turbulent dispersion coefficients than laminar dispersion coefficients. For some of these flow conditions, however, negative dispersion coefficients were computed. In further checking this finding, it was discovered that the integral equation for D can produce positive, negative, or zero values for D for the case of laminar flow between parallel plates where the bottom plate is fixed, the top plate is moving at a constant velocity, and a porous plate or screen located at an intermediate depth is moving at the maximum velocity. Therefore, it was concluded that this integral equation for D is not appropriate for all velocity profiles.

An investigation of approximate methods for estimating peak concentrations showed that they overestimate by a factor of 2 to 3. However, there may be cases when these approximate methods are appropriate as conservative estimates for planning studies.

The results and conclusions of this study are limited to the experimental conditions investigated. These conditions include a rainfall intensity range of 2 to 5 inches per hour; slopes of 0.001, 0.015, and 0.030; raindrop size of 3.64 millimeters; raindrop spacing on a 1-inch square grid; impact velocity at 77 percent of terminal velocity; a smooth, impervious bed surface; "shallow splashing" conditions; Rhodamine WT dye tracer; constant rainfall intensity; steady-state flow conditions; travel distances between 27.7 and 40.8 feet from the top of the plane; slightly nonuniform flow conditions transverse to the flow direction; and Reynolds numbers between about 100 and 400. Variability in the ϵ_y values presented in this study, due to experimental and numerical model variability, could range up to ± 60 percent or greater, based on subjective assessments.

B. Recommendations

As mentioned above, the experimental conditions investigated in this study are limited. In order to more completely describe vertical mixing coefficients and dispersion coefficients in overland flow found in nature, additional experimental investigations should include 1) a wider rainfall intensity range, 2) transport closer to the top of the plane, 3) transport throughout the runoff hydrograph, and 4) relationships for velocity profiles over rough surfaces.

The numerical model can be expanded with a modest amount of additional effort to include 1) initial solute distribution over an area rather than a line, 2) entrance of solute into the flow as a function of time rather than instantaneously, 3) infiltration of solute from bottom flow layer into bed surface, 3) entrance of solute from the bed surface into the bottom flow layer, 5) first-order decay of solute

due to sorption, volatilization, biodegradation, photolysis, etc., 6) rising and falling limbs of the runoff hydrograph, and 7) variable rainfall intensities. Expansion of the model to flow over rough surfaces would present special challenges. One of the major difficulties would be developing new relationships for velocity profiles, for which experimental data is lacking. Simulation of the "dead zones" created by a rough surface could be accomplished by adding an additional flow layer at the bed surface whose velocity would be zero and whose height could be correlated to the size of the roughness elements.

Additional need exists for development of approximate methods to estimate peak concentrations. For instance, in the case of hazardous waste spills, methods are needed which could be utilized quickly and easily to expedite decision-making. Also, the relative effect of various scenarios related to overland pollutant transport could be evaluated as effectively in many studies using approximate methods rather than computer simulations.

REFERENCES

- Abidi, S. L., 1982, "Detection of Diethylnitrosamine in Nitrite-Rich Water Following Treatment with Rhodamine Flow Tracers," Water Research, Vol. 16, pp. 199-204.
- Bailey, H. R. and Gogarty, W. B., 1962, "Numerical and Experimental Results on the Dispersion of a Solute in a Fluid in Laminar Flow through a Tube," Proceedings, Royal Society of London, Series A, Vol. 269, pp. 352-367.
- Banks, R. B., 1978, "Accelerations and Terminal Velocities of Raindrops," J. of Environmental Engr. Div., Am. Soc. of Civil Engrs., Vol. 104, No. EE3, June, pp. 527-531.
- Buchberger, S. G., 1979, "The Transport of Soluble Nonpoint Source Pollutants During the Rising Hydrograph," M.S. Thesis, Colorado State University, Fort Collins, Colorado.
- Buchberger, S. G., and Sanders, T. G., 1982, "A Kinematic Model for Pollutant Concentrations During the Rising Hydrograph," in Modeling Components of Hydrologic Cycle, Proceedings of the International Symposium on Rainfall-Runoff Modeling held May 18-21, 1981 at Mississippi State University, Water Resources Publications, Littleton, Colorado, pp. 405-426.
- Chatwin, P. C., 1970, "The Approach to Normality of the Concentration Distribution of a Solute in a Solvent Flowing Along a Straight Pipe," J. Fluid Mech., Vol. 43, Part 2, pp. 321-352.
- Cleary, R. W. and Adrian, D. D., 1973, "New Analytical Solutions for Dye Diffusion Equations," J. Environmental Engr. Div., Am. Soc. of Civil Engrs., Vol. 99, No. EE3, June, pp. 213-227.
- Crawford, N. H. and Donigian, A. S., Jr., 1973, "Pesticide Transport and Runoff Model for Agricultural Lands," U.S. Environmental Protection Agency, EPA-660/2-74-013.
- Dingle, A. N. and Lee, V., 1972, "Terminal Fallspeeds of Raindrops," J. of Applied Meteorology, Vol. 11, Aug., pp. 877-879.
- Dixon, W. J., Chief Editor, BMDP Statistical Software 1981, University of California Press, Berkeley, 1981.

- Donigian, A. S., Jr., and Crawford, N. H., 1976, "Modeling Pesticides and Nutrients on Agricultural Lands," U.S. Environmental Protection Agency, Environmental Protection Technology Series, EPA-600/2-76-043.
- Donigian, A. S., Jr., and Crawford, N. H., 1976, "Modeling Nonpoint Pollution from the Land Surface," U.S. Environmental Protection Agency, Ecological Research Series, EPA-600/3-76-083.
- Elder, J. W., 1959, "The Dispersion of Marked Fluid in Turbulent Shear Flow," J. of Fluid Mech., Vol. 5, No. 4, pp. 544-560.
- Emmett, W. W., 1970, "The Hydraulics of Overland Flow on Hillslopes," U.S. Geological Survey Professional Paper 662-A, U.S. Govt. Printing Office, Washington, D.C.
- Engle, O. G., 1966, "Crater Depths in Fluid Impacts," J. of Applied Physics, Vol. 37, No. 4, March 15, pp. 1798-1808.
- Engle, O. G., 1967, "Initial Pressure, Initial Flow Velocity, and the Time Dependence of Crater Depth in Fluid Impacts," J. of Applied Physics, Vol. 38, No. 10, Sept., pp. 3935-3940.
- Fischer, H. B., 1965, Discussion of "Numerical Solution to a Dispersion Equation," J. Hydraulics Div., Am. Soc. of Civil Engrs., Vol. 91, No. HY2, March, pp. 402-407.
- Fischer, H. B., 1966, "A Note on the One-Dimensional Dispersion Model," Air and Water Pollution International J., Vol. 10, pp. 443-452.
- Fischer, H. B., 1967, "The Mechanics of Dispersion in Natural Streams," J. Hydraulics Div., Am. Soc. of Civil Engrs., Vol. 93, No. HY6, Nov., pp. 187-216.
- Fischer, H. B., 1968a, "Dispersion Predictions in Natural Streams," J. Sanitary Engr. Div., Am. Soc. of Civil Engrs., Vol. 94, No. SA5, Oct., pp. 927-943.
- Fischer, H. B., 1968b, "Methods for Predicting Dispersion Coefficients in Natural Streams, With Applications to Lower Reaches of the Green and Duwamish Rivers, Washington," U.S. Geological Survey Professional Paper 582-A.
- Fischer, H. B., 1977, Discussion of "Convective Model of Longitudinal Dispersion," J. Hydraulics Div., Am. Soc. of Civil Engrs., Vol. 103, No. HY8, Aug., pp. 948-949.
- Fischer, H. B., List, E. J., Koh, R. C. Y., Imberger, J., and Brooks, N. H., 1979, Mixing in Inland and Coastal Waters, Academic Press, New York.
- Frere, M. H., Onstad, C. A., and Holtan, H. N., 1975, "ACTMO, An Agricultural Chemical Transport Model," U.S. Department of Agriculture, Agricultural Research Service, ARS-H-3.

- Haith, D. A. and Loehr, R. C., eds., 1979, "Effectiveness of Soil and Water Conservation Practices for Pollution Control," U.S. Environmental Protection Agency, Ecological Research Series, EPA-600/3-79-106.
- Harlow, F. H. and Shannon, J. P., 1967a, "Distortion of a Splashing Liquid Drop," Science, Vol. 157, No. 3788, Aug. 4, pp. 547-550.
- Harlow, F. H. and Shannon, J. P., 1967b, "The Splash of a Liquid Drop," J. of Applied Physics, Vol. 38, No. 10, Sept., pp. 3855-3866.
- Holley, E. R., Jr. and Harleman, D. R. F., "Dispersion of Pollutants in Estuary Type Flows," Report No. 74, Hydrodynamics Laboratory, Dept. of Civil Engr., Mass. Inst. of Tech., Cambridge, Mass., Jan. 1965.
- Kisisel, I. T., 1971, "An Experimental Investigation of the Effect of Rainfall on the Turbulence Characteristics of Shallow Water Flow," Thesis submitted in partial fulfillment of the requirements for the degree of Doctor of Philosophy, Purdue University, Lafayette, Indiana.
- Kisisel, I. T., Rao, R. A., Delleur, J. W., 1973, "Turbulence in Shallow Water Flow Under Rainfall," J. Engineering Mechanics Div., Am. Soc. of Civil Engrs., Vol. 99, No. EM1, Feb., pp. 31-53.
- Knisel, W. G., ed., 1980, "CREAMS: A Field Scale Model for Chemicals, Runoff, and Erosion from Agricultural Management Systems," U.S. Department of Agriculture, Conservation Research Report No. 26.
- Lager, J. A., Pyatt, E. E., and Shubinski, R. P., 1971, "Storm Water Management Model, Volume I - Final Report," U.S. Environmental Protection Agency, Water Pollution Control Research Series 11024 DOC 07/71.
- Laws, J. O., 1941, "Measurements of the Fall-Velocity of Water-Drops and Raindrops," Trans., Am. Geophysical Union, Part III, pp. 709-721.
- Laws, J. O. and Parsons, D. A., 1943, "The Relation of Raindrop-Size to Intensity," Trans., Am. Geophysical Union, Part II, pp. 452-460.
- Lighthill, M. J., 1966, "Initial Development of Diffusion in Poiseuille Flow," J. of the Institute of Mathematics and its Applications, Vol. 2, pp. 77-108.
- Macklin, W. C. and Metaxas, G. J., 1976, "Splashing of Drops on Liquid Layers," J. of Applied Physics, Vol. 47, No. 9, Sept., pp. 3963-3970.
- McQuivey, R. S. and Keefer, T. N., 1976, "Convective Model of Longitudinal Dispersion," J. Hydraulics Div., Am. Soc. of Civil Engrs., Vol. 102, No. HY10, Oct., pp. 1409-1424.

- Morgali, J. R., 1970, "Laminar and Turbulent Overland Flow Hydrographs," J. Hydraulics Div., Am. Soc. of Civil Engrs., Vol. 96, No. HY2, Feb., pp. 441-460.
- Mutchler, C. K., 1967, "Parameters for Describing Raindrop Splash," J. of Soil and Water Conservation, Vol. 22, No. 3, May-June, pp. 91-94.
- Mutchler, C. K. and Hansen, L. M., 1970, "Splash of a Waterdrop at Terminal Velocity," Science, Vol. 169, No. 3952, Sept. 25, pp. 1311-1312.
- Oliver, F. W. J., editor, 1960, Royal Society Mathematical Tables, Vol. 7, Bessel Functions, Part III, Zeros and Associated Values, University Press, Cambridge, 79 pp.
- Palmer, R. S., 1965, "Waterdrop Impact Forces," Trans. Am. Soc. of Agric. Engrs., Vol. 8, No. 1, pp. 69-70, 72.
- Rao, R. A., Kisisel, I. T., and Delleur, J. W., 1972, Discussion of "Mechanics of Sheet Flow Under Simulated Rainfall," J. Hydraulics Div., Am. Soc. of Civil Engrs., Vol. 98, No. HY6, June, pp. 1082-1089.
- Robertson, A. F., Turner, A. K., Crow, F. R., and Ree, W. O., 1966, "Runoff from Impervious Surfaces Under Conditions of Simulated Rainfall," Trans. Am. Soc. of Agric. Engrs., Vol. 9, No. 3, pp. 343-346, 351.
- Sayre, W. W., 1968a, "Dispersion of Mass in Open-Channel Flow," Colorado State University Hydraulics Paper No. 3, Colorado State University, Fort Collins, Colorado.
- Sayre, W. W., 1968b, Discussion of "The Mechanics of Dispersion in Natural Streams," J. Hydraulics Div., Am. Soc. of Civil Engrs., Vol. 94, No. HY6, Nov., pp. 1549-1556.
- Sayre, W. W., 1969, "Dispersion of Silt Particles in Open Channel Flow," J. Hydraulics Div., Am. Soc. of Civil Engrs., Vol. 95, No. HY3, May, pp. 1009-1038.
- Sayre, W. W., 1977, Discussion of "Convective Model of Longitudinal Dispersion," J. Hydraulics Div., Am. Soc. of Civil Engrs., Vol. 103, No. HY7, July, pp. 820-823.
- Schlichting, H., 1979, Boundary-Layer Theory, Seventh Edition, McGraw-Hill Book Company, New York.
- Shen, H. W. and Li, R. M., 1973, "Rainfall Effect on Sheet Flow Over Smooth Surface," J. Hydraulics Div., Am. Soc. of Civil Engrs., Vol. 99, No. HY5, May, pp. 771-792.
- Spalding, D. B., 1963, Convective Mass Transfer, McGraw-Hill Book Company, New York.

- Taylor, G. I., 1953, "Dispersion of Soluble Matter in Solvent Flowing Slowly Through a Tube," Proceedings, Royal Society of London, Series A, Vol. 219, pp. 186-203.
- Taylor, G. I., 1954, "The Dispersion of Matter in Turbulent Flow Through a Pipe," Proceedings, Royal Society of London, Series A, Vol. 223, pp. 446-468.
- Wang, R. C. and Wenzel, H. G., 1970, "The Mechanics of a Drop After Striking a Stagnant Water Layer," University of Illinois, Water Resources Center, Research Report No. 30, Urbana, Illinois.
- Woo, D. C. and Brater, E. F., 1962, "Spatially Varied Flow From Controlled Rainfall," J. Hydraulics Div., Am. Soc. of Civil Engrs., Vol. 88, No. HY6, Nov., pp. 31-56.
- Woolhiser, D. A., 1975, "Simulation of Unsteady Overland Flow," Chapter 12 in Unsteady Flow in Open Channels, Vol. II, by Mahmood, K. and Yevjevich, V., editors, Water Resources Publications, Fort Collins, Colorado.
- Yeh, G-T., 1976, "Three-Dimensional Pollutant Modeling in Shear Flow," J. Hydraulics Div., Am. Soc. of Civil Engrs., Vol. 102, No. HY3, March, pp. 351-365.
- Yeh, G-T and Tsai, Y-J., 1976, "Dispersion of Water Pollutants in a Turbulent Shear Flow," Water Resources Research, Vol. 12, No. 6, Dec., pp. 1265-1270.
- Yen, B. C. and Wenzel, H. G., Jr., 1970, "Dynamic Equations for Steady Spatially Varied Flow," J. Hydraulics Div., Am. Soc. of Civil Engrs., Vol. 96, No. HY3, March, pp. 801-814.
- Yoon, Y. N., 1970, "The Effect of Rainfall on the Mechanics of Steady Spatially Varied Sheet Flow on a Hydraulically Smooth Boundary," Thesis submitted in partial fulfillment of the requirements for the degree of Doctor of Philosophy in Civil Engineering, University of Illinois at Urbana-Champaign, Urbana, Illinois.
- Yoon, Y. N. and Wenzel, H. G., 1971, "Mechanics of Sheet Flow Under Simulated Rainfall," J. Hydraulics Div., Am. Soc. of Civil Engrs., Vol. 97, No. HY9, Sept., pp. 1367-1386.
- Yoon, Y. N. and Wenzel, H. G., 1973, Discussion Closure to "Mechanics of Sheet Flow Under Simulated Rainfall," J. Hydraulics Div., Am. Soc. of Civil Engrs., Vol. 99, No. HY4, April, pp. 675-677.
- Yotsukura, N. and Fiering, M. B., 1964, "Numerical Solution to a Dispersion Equation," J. Hydraulics Div., Am. Soc. of Civil Engrs., Vol. 90, No. HY5, Sept., pp. 83-104.
- Yotsukura, N. and Fiering, M. B., 1966, Discussion Closure to "Numerical Solution to a Dispersion Equation," J. Hydraulics Div., Am. Soc. of Civil Engrs., Vol. 92, No. HY3, May, pp. 67-72.

APPENDIX A
COMPUTER PRINTOUT OF
NUMERICAL MODEL

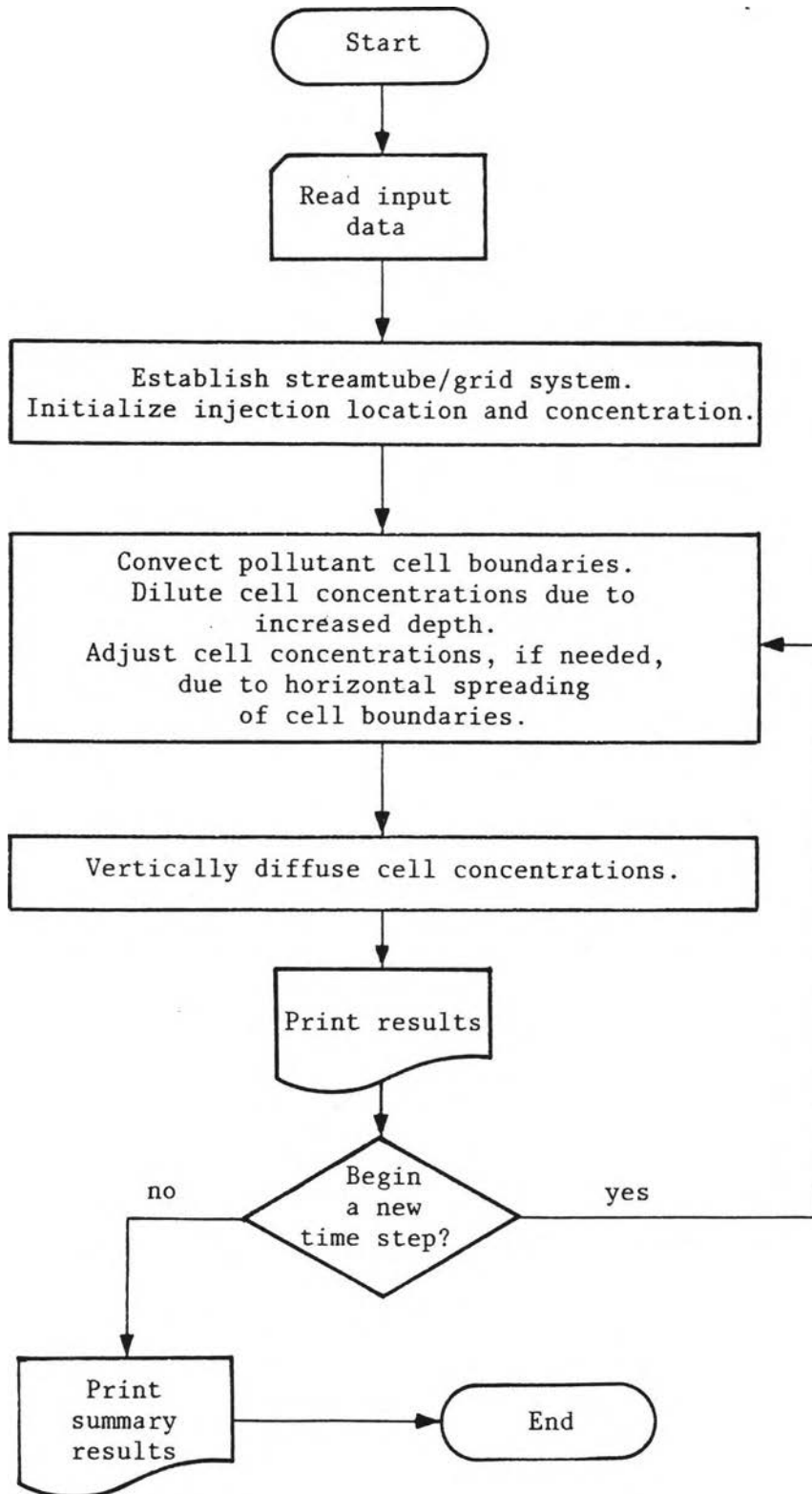


Figure A-1. Flow Chart for Numerical Model

PROGRAM DISPERS(INPUT,OUTPUT,TAPE5=INPUT,TAPE6=OUTPUT,TAPE7,
1 TAPE8)

*** THIS PROGRAM MODELS THE DISPERSION OF A POLLUTANT IN OVERLAND FLOW
 *** WITH RAINFALL. THE POLLUTANT IS WATER SOLUBLE AND CONSERVATIVE.
 *** THE INTRODUCTION OF THE POLLUTANT INTO THE FLOW TAKES PLACE
 *** INSTANTANEOUSLY WITH COMPLETE MIXING UPON INJECTION. THE AREAL
 *** COVERAGE OF THE SOURCE IS INFINITE IN THE DIRECTION TRANSVERSE
 *** TO THE FLOW AND FINITE IN THE DIRECTION LONGITUDINAL TO THE
 *** FLOW. THE RAINFALL HAS A CONSTANT AND UNIFORM INTENSITY, DROP
 *** SIZE, AND IMPACT VELOCITY OVER THE ENTIRE PLANE. THE OVERLAND
 *** FLOW IS STEADY AND NONUNIFORM ON A PLANE OF CONSTANT AND UNIFORM
 *** SLOPE AND ROUGHNESS. CONVECTION OF THE POLLUTANT OCCURS WITHIN
 *** STREAMTUBES WHOSE LONGITUDINAL AXIS IS PARALLEL TO THE FLOW,
 *** WHOSE TRANSVERSE DIMENSIONS ARE INFINITE, AND WHOSE VERTICAL
 *** DIMENSIONS ARE SPECIFIED BY THE USER.
 *** THE FLOW VELOCITY WITHIN STREAMTUBES IS DEFINED BY
 *** A DIMENSIONLESS VELOCITY DISTRIBUTION CURVE ALONG WITH THE MEAN
 *** CROSS-SECTIONAL VELOCITY COMPUTED FROM DARCY-WEISBACH FRICTION
 *** FACTOR EQUATION. VERTICAL DIFFUSION OF POLLUTANT BETWEEN STREAM-
 *** TUBES FOLLOWS FICKIAN-TYPE DIFFUSION PROCESS USING A CROSS-
 *** SECTIONAL MEAN VERTICAL MIXING COEFFICIENT WHICH
 *** INCLUDES THE EFFECT OF RAINDROP MIXING. DIFFUSION IN LONGITUDINAL
 *** DIRECTION IS ASSUMED NEGLIGIBLE COMPARED TO SHEAR FLOW DISPERSION.

 *** DEFINITIONS:

 *** AVGCON(J) = AVERAGE CONCENTRATION OF ALL CELLS IN THE VERTICAL
 *** CELL COLUMN (THAT IS, AVERAGE CROSS-SECTIONAL
 *** CONCENTRATION) LOCATED J CELLS DOWNSTREAM FROM
 *** BASELINE XO (UNITS = MG PER 1000L, OR PPB).

 *** CB(I,K) = POLLUTANT CELL BOUNDARY LOCATION, MEASURED FROM
 *** UPSTREAM POINT ON PLANE WHERE RAINFALL BEGINS, AND
 *** MEASURED ALONG X-AXIS (PARALLEL TO FLOW DIRECTION).
 *** 'I' REPRESENTS THE STREAMTUBE NUMBER, BEGINNING
 *** WITH THE TUBE ADJACENT TO THE STREAMBED LABELED '1'.
 *** 'K' REPRESENTS THE POLLUTANT CELL BOUNDARY NUMBER,
 *** BEGINNING WITH THE POLLUTANT CELL BOUNDARY LOCATED
 *** FURTHEREST DOWNSTREAM (WITHIN STREAMTUBE 'I')
 *** LABELED '1'. A POLLUTANT CELL BOUNDARY IS A
 *** VERTICAL BOUNDARY BETWEEN TWO ADJACENT COMPUTATIONAL
 *** CELLS WITHIN A STREAMTUBE, WITH AT LEAST ONE OF THE
 *** ADJACENT CELLS CONTAINING A POLLUTANT CONCENTRATION

*** GREATER THAN ZERO.

 *** CLPRT = TIME AT WHICH A PRINTOUT IS DESIRED OF
 *** INDIVIDUAL CELL CONCENTRATIONS (UNITS = SEC).

 *** CLPRTS = NUMBER OF CELL CONCENTRATION PRINTOUTS DESIRED.

 *** COMP = CONTROLS WHETHER TO COMPARE COMPUTED CONCENTRATION
 *** CURVE WITH LABORATORY CURVE. IF EQUAL TO '0',
 *** NO COMPARISON IS MADE. IF EQUAL TO '1', THE
 *** TWO CURVES WILL BE COMPARED BASED ON SUMMATION
 *** OF ABSOLUTE VALUES OF DIFFERENCES BETWEEN THE
 *** TWO CURVES.

 *** CONC(I,K) = THE POLLUTANT CONCENTRATION IN THE UPSTREAM
 *** CELL ADJACENT TO THE POLLUTANT CELL BOUNDARY,
 *** CB(I,K), (UNITS = MG PER 1000L, OR PPB).

 *** DEBUG = INTEGER VARIABLE CONTROLLING PRINTOUT OF INTERIM
 *** CALCULATIONS FOR DEBUGGING PURPOSES. IF EQUAL TO
 *** '0', NO INTERIM PRINTOUTS. IF EQUAL TO '1',
 *** INTERIM PRINTOUTS WILL BE PRINTED.

 *** DELT = THE COMPUTATIONAL TIME STEP (UNITS = SEC).

 *** DELX = THE LENGTH OF ALL COMPUTATIONAL CELLS, MEASURED IN
 *** FLOW DIRECTION (UNITS = FT).

 *** DELY = VERTICAL DIMENSION OF STREAMTUBE (UNITS = FT).

 *** DIFFUSION
 *** OPTION = OPTION ONE COMPUTES VERTICAL DIFFUSION
 *** RESULTS AT CENTERLINE OF EACH STREAMTUBE.
 *** OPTION TWO COMPUTES VERTICAL DIFFUSION RESULTS
 *** AT VERTICAL QUARTER POINTS WITHIN EACH STREAMTUBE,
 *** THEN AVERAGES THE RESULTS OVER THE HEIGHT OF
 *** THE STREAMTUBE.

 *** DIFUSE = VERTICALLY-DIFFUSED CONCENTRATION
 *** USING VERTICAL TURBULENT DIFFUSION COEFFICIENT,
 *** EPSLN (UNITS = MG PER 1000L, OR PPB).

 *** EPSLN = VERTICAL TURBULENT DIFFUSION COEFFICIENT (UNITS =
 *** SQ FT PER SEC).

 *** INTENS = RAINFALL INTENSITY (UNITS = INCHES PER HOUR).

 *** KPARAM = PARAMETER RELATED TO DARCY-WEISBACH FRICTION
 *** FACTOR (F) AND REYNOLDS NUMBER (R) SUCH THAT
 *** $KPARAM = F * R$.

 *** MAXT = MAXIMUM TIME FOR COMPUTER RUN (UNITS = SEC).

 *** Q = DISCHARGE PER FOOT WIDTH (UNITS = SQ FT PER SEC).

```

***
*** RES(I,K) = A RESIDUAL VALUE WHICH WHEN ADDED TO THE POLLUTANT
*** CELL BOUNDARY LOCATION, CB(I,K), RESULTS IN THE
*** CORRECT LOCATION FOR CB(I,K). THIS RESIDUAL
*** VALUE WILL ALWAYS BE LESS THAN PLUS OR MINUS
*** DELX (UNITS = FT).
***
*** SO = BED SLOPE
***
*** SOURCE = THE CONCENTRATION OF THE DYE IN THE FLOW THE
*** INSTANT FOLLOWING INJECTION AT TIME T=0
*** (UNITS = MG PER 1000L, OR PPB).
***
*** SUMT = TIME ELAPSED SINCE INJECTION (UNITS = SEC).
***
*** TPLOT = INTEGER VARIABLE CONTROLLING WHETHER CONCENTRA-
*** TION VS DISTANCE AND MASS VS DISTANCE CURVES
*** WILL BE PLOTTED AT TIMES SPECIFIED BY 'TPRINT'.
*** IF EQUAL TO '0', NO PLOT WILL BE PRODUCED. IF
*** EQUAL TO '1', A LINE PRINTER PLOT WILL BE MADE
*** USING 'MAPA' PLOT ROUTINE.
***
*** TPRT = TIME AT WHICH A CONCENTRATION-DISTANCE CURVE
*** PRINTOUT IS DESIRED.
***
*** TPRTS = NUMBER OF CONCENTRATION-DISTANCE CURVE PRINTOUTS
*** DESIRED.
***
*** TSUM = SUMMATION OF TRAVEL TIME OF A POLLUTANT CELL
*** BOUNDARY DURING CONVECTION (UNITS = SEC).
***
*** TUBES = NUMBER OF STREAMTUBES USED.
***
*** U(I,K) = VELOCITY WITHIN THE UPSTREAM CELL ADJACENT TO
*** THE POLLUTANT CELL BOUNDARY, CB(I,K), (UNITS =
*** FT PER SEC).
***
*** UAVG(J) = AVERAGE VELOCITY OF ALL CELLS IN THE VERTICAL
*** CELL COLUMN (THAT IS, AVERAGE CROSS-SECTIONAL
*** VELOCITY) LOCATED J CELLS DOWNSTREAM FROM
*** BASELINE XO (UNITS = FT PER SEC).
***
*** UNIFLO = DISCHARGE FOR STEADY UNIFORM FLOW CONDITIONS --
*** NO RAINFALL (UNITS = SQ FT PER SEC).
***
*** VCHECK = THE NUMBER OF CELLS DOWNSTREAM OF THE BASELINE,
*** XO, FOR WHICH VELOCITY VALUES ARE NEEDED TO
*** PROCEED WITH CONVECTION CALCULATIONS.
***
*** VEL = THE NUMBER OF CELLS DOWNSTREAM OF THE BASELINE,
*** XO, FOR WHICH VELOCITIES HAVE BEEN COMPUTED.
***
*** VISCOS = KINEMATIC VISCOSITY OF WATER (UNITS =
*** SQ FT PER SEC).

```

```

***
***   WHICHX   = CONTROLS WHICH LOCATION ON PLANE A COMPARISON
***             WILL BE MADE BETWEEN COMPUTED AND LABORATORY
***             CONCENTRATION CURVES.
***
***   WIDTH    = WIDTH OF LINE SOURCE INJECTION IN THE FLOW THE
***             INSTANT FOLLOWING INJECTION AT TIME T=0. THIS
***             WIDTH IS A DIMENSION MEASURED ALONG THE X-AXIS,
***             THAT IS, PARALLEL TO FLOW DIRECTION (UNITS =
***             FT).
***
***   XINJEC   = LOCATION OF CENTERLINE OF LINE SOURCE INJECTION,
***             MEASURED FROM UPSTREAM POINT ON PLANE WHERE
***             RAINFALL BEGINS. THE ORIENTATION OF THE LINE
***             SOURCE IS PERPENDICULAR TO X-AXIS, THAT IS,
***             PERPENDICULAR TO FLOW DIRECTION (UNITS = FT).
***
***   XO       = A BASELINE FOR COMPUTATIONS, EQUAL TO THE LOCATION
***             OF THE UPSTREAM-MOST CELL BOUNDARY WHICH CONTAINS
***             POLLUTANT (UNITS = FT).
***
***   XPLOT    = INTEGER VARIABLE CONTROLLING WHETHER CONCENTRATION
***             VS TIME AND MASS VS TIME CURVES WILL BE PLOTTED
***             FOR LOCATIONS SPECIFIED BY 'XPRINT'. IF EQUAL TO
***             '0', NO PLOT WILL BE PRODUCED. IF EQUAL TO '1',
***             A LINE PRINTER PLOT WILL BE MADE USING 'MAPA'
***             PLOT ROUTINE.
***
***   XPRINT   = LOCATIONS ALONG X-AXIS WHERE VALUES OF CONCENTRATION
***             VS TIME AND MASS VS TIME WILL BE PRINTED OUT.
***             UP TO FOUR LOCATIONS ARE ALLOWED. A ZERO VALUE
***             INPUT FOR ANY OF THE FOUR POSSIBLE XPRINT
***             LOCATION OPTIONS MEANS NO PRINTOUT WILL BE PRODUCED
***             FOR THAT XPRINT OPTION (UNITS = FT).
***
***   YS       = DEPTH OF FLOW AT WATER SURFACE (UNITS = FT).
***

```

```

DIMENSION AVGCN(150), CARAY1(200), CARAY2(4,150),
1 CB(41,100), CBS(58), CELL(58), CONC(41,100), CONCEN(400),
1 MARAY1(200), MARAY2(4,150), MASSS(400), NEWCB(150),
1 NEWCON(150), NEWRES(150), RES(41,100), TARAY(500),
1 TEMCON(58), TIME(150), U(41,100), UAVG(150), XARAY(200),
1 XOCBS(58), XPRINT(4), V(58), SUMUCY(150), LABTIM(150),
1 LABCON(150), DELY(58), YTUBE(58), CLPRT(90), TPRT(90),
1 CHANGT(58), NEWT(58), CHANGX(58), ARGMT(5), TERM(5)
1 ,DIFFAC(100), VV(58)

```

```

INTEGER ADVANC, ARAY1, ARAY2, BACKUP, CBS, CBSUM, CELL, COUNT,
1  DEBUG, ENDIT, EVEODD, GRDSUM, GRIDS, ODDEVE, OLD, OTHERL,
1  OTHERM, QUIT, REFLEC, STEPT, TOTAL, TPLT, TUBES, UPDOWN,

```

```

1  VCHECK, VEL, XOCBS, XPLOT, CARDS, DATA, POINTS, COMP, WHICHX,
1  OPTION, WHICH1, CLPRTS, TPRTS, CHOICE, DELTS, DELXS,
1  VPROFL, TEST, CEASE, REED, TIMEIN

REAL INTENS, KARMAN, KPARAM, LOCATE, MAXCB, MINCB, NEWCB,
1  NEWCON, NEWRES, NEWXO, MAXT, MASS, MARAY1, MARAY2, MASSS,
1  LABCON, LABTIM, NEWT, KPAR, INCRT, MAXU, MAXFAC

CHARACTER*10 DI, TI, CO, MA
CHARACTER*80 DICO, DIMA, TICO, TIMA

READ(5,1) WIDTH, XINJEC, SOURCE, TEST,
1  INCRT, REED, SURFU, MAXU,
1  DELX, DELT, MAXT, TUBES, DEBUG, OPTION, VPROFL,
1  KPARAM, SO, VISCOS, INTENS, EPSLN, UNIFLO, UMAX,
1  TPLOTT, XPRINT(1), XPRINT(2), XPRINT(3), XPRINT(4),
1  XPLOT, COMP, WHICHX
1  FORMAT(F10.4,2F10.3,I10,F10.3,I5,2F7.3/F10.7,F10.6,F10.3,
1  4I10/F10.3,F10.5,
1  F10.7,F10.3,F10.9,F10.8,F10.4/I10,4F10.3,3I3)
READ(5,3) DELTS, (CHANGT(I), NEWT(I), I=1,DELTS)
READ(5,3) DELXS, (CHANGX(I), I=1,DELXS)
READ(5,2) (DELY(I), I=1,TUBES)
2  FORMAT(10F7.3)
READ(5,3) CLPRTS, (CLPRT(I), I=1,CLPRTS)
READ(5,3) TPRTS, (TPRT(I), I=1,TPRTS)
3  FORMAT(I5,(8F8.3))
WRITE(6,4) WIDTH, XINJEC, SOURCE, TEST, INCRT, REED, SURFU,
1  MAXU,DELX,DELT,MAXT,TUBES,
1  DEBUG,OPTION,VPROFL,KPARAM, SO, VISCOS, INTENS, EPSLN, UNIFLO,
1  UMAX,TPLOT, XPRINT(1), XPRINT(2), XPRINT(3), XPRINT(4), XPLOT,
1  COMP, WHICHX, DELTS, (I, CHANGT(I), I, NEWT(I), I=1,DELTS)
4  FORMAT('1'///35X,'*****',
1  '*****'/35X,'*',19X,'DATA INPUT',
1  '*/35X,'*****',
1  '*****'/41X,'(SEE PROGRAM LISTING FOR DEFINITIONS)',
1  ///5X,'WIDTH(FT) =',F7.4/5X,'XINJEC(FT) =',F7.3/5X,
1  'SOURCE(PPB) =',F10.2/5X,'TEST =',I7/5X,'INCRT',8X,
1  '=',F8.3/5X,'REED',9X,'=',I7/5X,'SURFU',8X,'=',F7.3/5X,'MAXU'
1  ,9X,'=',F7.3///5X,'DELX(FT) =',2X,F10.7/5X,'DELT(SEC) =',
1  F8.6/5X,'MAXT(SEC) =',F8.3/5X,'TUBES =',I4/5X,'DEBUG =',
1  ,I4/5X,'DIFFUSION'/8X,'OPTION =',I4/5X,'VELOCITY'/8X,'PROFILE'
1  /8X,'OPTION =',I4///5X,'KPARAM',24X,'=',F6.1/5X,
1  'SO',28X,'=',F8.5/5X,'VISCOS(SQ FT PER SEC)',9X,'=',F12.7/
1  5X,'INTENS(IN PER HR)',13X,'=',F7.2/5X,'EPSLN(SQ FT PER SEC)'
1  ,10X,'=',F13.9/5X,'UNIFLO(CU FT PER SEC PER FT) =',F12.7
1  /5X,'UMAX(FT PER SEC)',14X,'=',F8.4///5X,'TPLOT',10X,'=',
1  I5/5X,'XPRINT(1) (FT) =',F10.4/5X,'XPRINT(2) (FT) =',
1  F10.4/5X,'XPRINT(3) (FT) =',F10.4/5X,'XPRINT(4) (FT) =',
1  F10.4/5X,'XPLOT',10X,'=',I5/5X,'COMP',11X,'=',I5/
1  5X,'WHICHX',9X,'=',I5///5X,'DELTS=',I3/(5X,'CHANGT(',I2,')='),
1  F8.3,' SEC',5X,'NEWT(',I2,')='),F8.3,' SEC'))
WRITE(6,6) DELXS, (I, CHANGX(I), I=1,DELXS)
6  FORMAT(5X,'DELXS=',I3/(5X,'CHANGX(',I2,')='),

```

```

1  F8.3,' SEC'))
  WRITE(6,7) (I, DELY(I), I=1,TUBES)
7  FORMAT(//5X,'DELY(' ,I2,' ) =' ,F6.2,' PERCENT OF DEPTH'))
  IF(CLPRTS.EQ.0) THEN
    WRITE(6,8)
8    FORMAT(//5X,'CLPRTS=  0')
  ELSE
    WRITE(6,9) CLPRTS, (I,CLPRT(I), I=1,CLPRTS)
9    FORMAT(//5X,'CLPRTS=' ,I5/(5X,'CLPRT(' ,I2,' )=' ,
1    F8.3,1X,'SEC'))
  ENDIF
  WRITE(6,10) TPRTS, (I,TPRT(I), I=1,TPRTS)
10  FORMAT(//5X,'TPRTS=' ,I5/(5X,'TPRT(' ,I2,' )=' ,
1    F8.3,1X,'SEC'))

  IF(COMP.EQ.1) THEN
    READ(5,11) CARDS, POINTS
11  FORMAT(2I5)
    DATA = CARDS * 3
    DO 13 I=1,DATA,3
      READ(5,12) LABTIM(I), LABCON(I), LABTIM(I+1),
1      LABCON(I+1), LABTIM(I+2), LABCON(I+2)
12  FORMAT(3(F10.2,F10.1))
13  CONTINUE
    ENDIF
    IF(REED.EQ.1) THEN
      READ(7,820) SUMT,DELT,DELX,X0,VEL,TOTAL,LIMIT,ARRAY1,
1      ARRAY2,KILL,ITIME,IX,STEPT,G,KARMAN
820  FORMAT(1X,2F10.3,2F10.5,3I10/1X,6I10/1X,2F10.5)
      DO 828 I=1,TUBES
        READ(7,822) CBS(I),(CB(I,K),K=1,CBS(I))
822  FORMAT(6X,I5/(1X,7F10.6))
        READ(7,824) (RES(I,K),K=1,CBS(I))
824  FORMAT((1X,7F10.6))
        READ(7,826) (CONC(I,K),K=1,(CBS(I)-1))
826  FORMAT((1X,7F10.4))
        READ(7,824) (U(I,J),J=1,VEL)
828  CONTINUE
        READ(7,824) (UAVG(J),J=1,VEL)
        READ(7,826) (AVGCON(J),J=1,TOTAL)
        IF(ARRAY1.GT.0) THEN
          READ(8,830) (XARRAY(J),CARAY1(J),MARAY1(J),J=1,ARRAY1)
830  FORMAT((1X,F10.6,F10.4,F10.8,F10.6,F10.4,F10.6))
        ENDIF
        IF(ARRAY2.GT.0) THEN
          DO 834 J=1,4
            IF(XPRINT(J).GT.0.) THEN
              READ(7,832) (TARAY(K),CARAY2(J,K),MARAY2(J,K),
1              K=1,ARRAY2)
832  FORMAT((1X,F10.3,F10.4,F10.8,F10.3,F10.4,F10.8))
            ENDIF
          CONTINUE
834  CONTINUE
        ENDIF
      ENDIF
    ENDIF
  ENDIF

```

```

WRITE(6,14)
14  FORMAT('1'////33X,'*****',
1    '*****'/33X,'*',19X,'PROGRAM OUTPUT',
1    19X,'*/33X,'*****',
1    '*****')

DI = 'DIST (FT) '
TI = 'TIME (SEC) '
CO = 'CONC (PPB) '
MA = 'MASS (MG) '
DICO = '          DISTANCE FROM BEGINNING OF RAIN * VERSUS * CONCE
INTRATION AT TIME T
DIMA = '          DISTANCE FROM BEGINNING OF RAIN * VERSUS * MASS
1 AT TIME T
TICO = '          TIME SINCE INJECTION * VERSUS * CONCENTRATION
1 AT FIXED POINT X
TIMA = '          TIME SINCE INJECTION * VERSUS * MASS AT FIXED
1 POINT X
IF(REED.EQ.1) GO TO 840

LIMIT = 0
ARAY1=0
ARAY2=0
SUMT=DELT
KILL=0
G=32.2
KARMAN = .41
ITIME = 1
IX = 1
STEPT = 1
TIMEIN = 0
C
C ***
C *** IF THE FLOW IS STEADY AND UNIFORM (NO RAINFALL),
C *** THEN COMPUTE:
C ***
C ***      1) DEPTH = DEPTH OF FLOW USING DARCY-WEISBACH
C ***          EQUATION WITH KPARAM WHERE
C ***          KPARAM = (FRICTION FACTOR) * (REYNOLDS NO.).
C ***
C ***      2) TAU(BOUNDARY SHEAR STRESS) = SO(BED SLOPE) TIMES
C ***          DEPTH(DEPTH OF FLOW) TIMES 62.3(SPECIFIC WEIGHT
C ***          OF WATER).
C ***
C ***      3) USTAR(SHEAR VELOCITY) = SQUARE ROOT OF (BOUNDARY
C ***          SHEAR STRESS DIVIDED BY DENSITY IN SLUGS).
C ***
C ***      4) V(LOCAL VELOCITY IN CROSS SECTION) = VELOCITY
C ***          DISTRIBUTION AS DERIVED FOR LAMINAR OR TURBULENT
C ***          FLOW OVER A PLANE.
C ***
C ***
840 IF(INTENS.EQ.0.) THEN
      DEPTH = ((KPARAM*VISCOS*UNIFLO)/(8.*G*SO))**(1./3.)
      TAU = SO * DEPTH * 62.3

```

```

USTAR = SQRT(TAU/1.937)
AVGVEL = UNIFLO/DEPTH
RYNDLS = UNIFLO/VISCOS
FRICTN = KPARAM/RYNDLS
WRITE(6,15) DEPTH, TAU, USTAR, AVGVEL, RYNDLS, FRICTN
15  FORMAT(////5X,'THE FLOW IS STEADY, UNIFORM (NO RAINFALL). '
1      /5X,'COMPUTED FLOW CHARACTERISTICS ARE AS FOLLOWS: '//
1      10X,'DEPTH OF FLOW(FT) =' ,F10.7/10X,
1      'BOUNDARY SHEAR STRESS(LB PER SQ FT) =' ,F10.7/10X,
1      'SHEAR VELOCITY(FT PER SEC) =' ,F9.6/10X,
1      'MEAN VELOCITY(FT PER SEC) =' ,F8.5/10X,'REYNOLDS NUMBER'
1      ,' =' ,F8.2/10X,'DARCY-WEISBACH FRICTION FACTOR ='
1      ,F8.4//)
YBASE = 0.
IF(TEST.EQ.3.OR.TEST.EQ.4.OR.TEST.EQ.5.OR.TEST.EQ.6
1      .OR.TEST.EQ.7) THEN
500  WRITE(6,500)
      FORMAT(/10X,'STREAMTUBE VELOCITIES BASED ON ',
1          '1/7 POWER LAW. ')
      ELSE IF(VPROFL.EQ.0) THEN
16   WRITE(6,16)
      FORMAT(/10X,'VELOCITY DISTRIBUTION IS UNIFORM. ',
1          'ALL STREAMTUBE VELOCITIES EQUAL TO ',
1          'CROSS-SECTIONAL MEAN VELOCITY. '//)
      ELSE IF(VPROFL.EQ.3) THEN
501  WRITE(6,501)
      FORMAT(/10X,'VELOCITY PROFILE IS PARABOLIC',
1          ' WITH A MAXIMUM VELOCITY AT .80 DEPTH. '//52X,
1          'LAMINAR PROFILE',8X,'ADJUSTED PROFILE')
      GO TO 505
      ELSE IF(RYNDLS.GE.950..OR.VPROFL.EQ.2) THEN
17   WRITE(6,17)
      FORMAT(/10X,'STREAMTUBE VELOCITIES BASED ON LOGARITHMIC'
1          ', ' VELOCITY PROFILE FOR'/10X,'TURBULENT FLOW OVER AN ',
1          'INCLINED PLANE ARE AS FOLLOWS: '//15X,'TUBE NO.',10X,
1          'DEPTH(FT)',10X,'VELOCITY(FT PER SEC) '//)
      GO TO 505
      ELSE IF(RYNDLS.LT.950.) THEN
18   WRITE(6,18)
      FORMAT(/10X,'STREAMTUBE VELOCITIES BASED ON VELOCITY ',
1          'PROFILE FOR'/10X,'LAMINAR FLOW OVER AN INCLINED',
1          ' PLANE ARE AS FOLLOWS: '//15X,'TUBE NO.',10X,'DEPTH(FT)'
1          ',10X,'VELOCITY(FT PER SEC) '//)
      ENDIF
505  IF(VPROFL.EQ.3) THEN
      Y = .8*DEPTH
      VMAX = (((USTAR**2)*Y)/VISCOS)-
1          ((G*SO*(Y**2))/(2.*VISCOS))
      MAXFAC = MAXU/VMAX
      P = (.25*((.2*DEPTH)**2))/(MAXU-SURFU)
      ENDIF
      DO 20 I=1,TUBES
      YTUBE(I) = (DELY(I)/100.)*DEPTH
      Y = (.5*YTUBE(I))+YBASE

```

```

YBASE = (.5*YTUBE(I))+Y
IF(TEST.EQ.3.OR.TEST.EQ.4.OR.TEST.EQ.5.OR.TEST.EQ.6
1 .OR.TEST.EQ.7) THEN
  V(I) = .748765*(Y**.1428571)
ELSE IF(VPROFL.EQ.0) THEN
  V(I) = AVGVEL
ELSE IF(VPROFL.EQ.3) THEN
  VV(I) = (((USTAR**2)*Y)/VISCOS)-((G*SO*(Y**2))/
1 (2.*VISCOS))
  IF(Y.LE.(.8*DEPTH)) THEN
    V(I) = MAXFAC*(((USTAR**2)*Y)/VISCOS)-
1 ((G*SO*(Y**2))/(2.*VISCOS)))
  ELSE
    V(I) = MAXU-(((Y-(.8*DEPTH))**2)/(4.*P))
  ENDIF
  WRITE(6,508) I,Y,VV(I),V(I)
508 FORMAT(15X,I3,13X,F9.6,16X,F8.5,16X,F8.5)
  GO TO 20
ELSE IF(RYNDLS.GE.950..OR.VPROFL.EQ.2) THEN
  V(I) = AVGVEL + ((USTAR/KARMAN)*(1.+LOG(Y/DEPTH)))
  GO TO 510
ELSE IF(RYNDLS.LT.950.) THEN
  V(I) = (((USTAR**2)*Y)/VISCOS)-((G*SO*(Y**2))/
1 (2.*VISCOS))
  ENDIF
510 WRITE(6,19) I, Y, V(I)
19 FORMAT(15X,I3,13X,F9.6,16X,F8.5)
20 CONTINUE
ENDIF
IF(VPROFL.EQ.3) THEN
  SUM=0.
  DO 509 I=1,TUBES
    SUM = V(I)+SUM
509 CONTINUE
  AVGVEL = SUM/TUBES
  DEPTH = UNIFLO/AVGVEL
  KPARAM = ((DEPTH**3)*8.*G*SO)/(VISCOS*UNIFLO)
  TAU = SO*DEPTH*62.3
  USTAR = SQRT(TAU/1.937)
  WRITE(6,511) KPARAM,DEPTH,TAU,USTAR,AVGVEL
511 FORMAT(///5X,'NEW KPARAM =',F8.2/5X,'NEW DEPTH =',
1 F10.7/5X,'NEW BOUNDARY SHEAR STRESS =',F10.7/
1 5X,'NEW SHEAR VELOCITY =',F9.6/5X,'NEW MEAN',
1 ' VELOCITY =',F8.5)
  ENDIF
512 IF(INTENS.EQ.0..AND.OPTION.EQ.5) THEN
  I = 0
  FAC1 = -3.
  FAC2 = -1.
  DT4 = SQRT(4.*EPSLN*DELT)
  YDEL = YTUBE(1)
514 I = I+1
  FAC1 = FAC1+2.
  FAC2 = FAC2+2.

```

```

      DIFFAC(I) = .5*(-ERF((FAC1*YDEL)/(2.*DT4))+
1      ERF((FAC2*YDEL)/(2.*DT4)))
      IF(DIFFAC(I).GT..001) GO TO 514
      MAXI = I
      ENDIF
      IF(TIMEIN.EQ.1) GO TO 30
      IF(REED.EQ.1) GO TO 30
C      ***
C      *** COMPUTE NUMBER OF GRID COLUMNS OCCUPIED BY
C      *** INJECTED DYE AT TIME T=0.
C      ***
      GRIDS=NINT(WIDTH/DELX)
C      ***
C      *** COMPUTE LOCATION OF UPSTREAM-MOST CELL BOUNDARY
C      *** OCCUPYING INJECTED DYE AT TIME T=0. LET THIS
C      *** LOCATION BE BASELINE, XO.
C      ***
      BACKUP=GRIDS/2
      XO=XINJEC-(BACKUP*DELX)

      IF(DEBUG.EQ.1) THEN
        WRITE(6,21) GRIDS, BACKUP, XO
21      FORMAT(/5X,'GRIDS =',I3,5X,'BACKUP =',I3,5X,'XO =',F7.3)
      ENDIF
C      ***
C      *** ESTABLISH LOCATION OF POLLUTANT CELL BOUNDARIES
C      *** (CB(I,K)) WHICH CONTAIN THE LINE SOURCE IN THE
C      *** FLOW AT TIME T=0. SET RESIDUAL VALUE (RES(I,K))
C      *** OF EACH CELL BOUNDARY TO ZERO. INITIALIZE
C      *** CONCENTRATION (CONC(I,K)) IN EACH CELL TO THE
C      *** VALUE OF 'SOURCE'.
C      ***
      KGRIDS = GRIDS + 1
      DO 23 I=1,TUBES
        DO 22 K=1,KGRIDS
          CB(I,K) = XO + ((KGRIDS)*DELX) - (K*DELX)
          RES(I,K) = 0.
          IF(K.EQ.KGRIDS) GO TO 22
          IF(TEST.EQ.1.OR.TEST.EQ.2.OR.TEST.EQ.3.OR.TEST.EQ.6)
1          THEN
            L = (TUBES + 1)/2
            IF(I.EQ.L) THEN
              CONC(I,K) = SOURCE
              GO TO 22
            ELSE
              CONC(I,K) = 0.
              GO TO 22
            ENDIF
          ELSE IF(TEST.EQ.4.OR.TEST.EQ.5) THEN
            IF(I.EQ.TUBES) THEN
              CONC(I,K) = SOURCE
              GO TO 22
            ELSE
              CONC(I,K) = 0.

```

```

                GO TO 22
            ENDIF
        ENDIF
        CONC(I,K) = SOURCE
22     CONTINUE
        CBS(I) = KGRIDS
23     CONTINUE

        IF(DEBUG.EQ.1) THEN
            WRITE(6,24)
24     FORMAT(5X,'IMMEDIATELY AFTER INJECTION:')
            DO 27 I=1,TUBES,2
                DO 26 K=1,KGRIDS,2
                    WRITE(6,25) I, K, CB(I,K), RES(I,K), CONC(I,K)
25     FORMAT(5X,'TUBE NO. =',I2,5X,'CELL BNDRY NO. =',I3,
1         5X,'CELL BNDRY LOCATION =',F7.3,5X,'RESIDUAL =',
1         F5.3,5X,'CONC =',F8.1)
26     CONTINUE
27     CONTINUE
        ENDIF
        DO 28 I=1,CLPRTS
            IF(SUMT.GE.CLPRT(I).AND.(SUMT-DELT).LT.CLPRT(I)) THEN
                ENDIT = GRIDS
                CHOICE = 1
                CALL CELLCON(CONC, CB, ENDIT, XO, DELX,TUBES,CBS,
1         DEBUG, SUMT,CHOICE)
            ENDIF
28     CONTINUE
C     ***
C     *** COMPUTE DOWNSTREAM CELL VELOCITIES FOR FIRST
C     *** 20 CELL COLUMNS.
C     ***
        VEL = 0
        VCHECK = 0
        CALL VELCTY (VCHECK, KPARAM, VISCOS, SO, DELT, DELX, INTENS,
1     XO, U, VEL, TUBES, UAVG, DEBUG, KILL, WHERE,AVGVEL,V,DELY,
1     UMAX, UPINJ, UINJ, KPAR)
        IF(KILL.EQ.1) GO TO 425
        IF(INTENS.GT.0.) THEN
            WRITE(6,520)
520    FORMAT(//////////5X,'VELOCITY DISTRIBUTION AT',
1        ' INJECTION LOCATION: '//10X,'TUBE NO.',5X,
1        'VELOCITY(FT/SEC) '//)
            DO 540 I=1,TUBES
                WRITE(6,530) I,U(I,1)
530    FORMAT(13X,I2,11X,F9.6)
540    CONTINUE
                WRITE(6,550) UINJ,UPINJ,KPAR
550    FORMAT(///' MEAN VELOCITY OF ABOVE CORRECTED PROFILE (CORR',
1        'ECTED TO INPUT K VALUE) IS',2X,F7.4/' MEAN VELOCITY OF',
1        ' UNCORRECTED PROFILE WAS',2X,F7.4/' K VALUE',
1        ' CORRESPONDING TO UNCORRECTED PROFILE WAS',F6.1)
            ENDIF
        IF(EPSLN.EQ..99) IEPSLN=1

```

```

30   IF (INCRT.GE.SUMT.AND.(INCRT-DELT).LT.SUMT) THEN
      WRITE(8,850) SUMT,DELT,DELX,XO,VEL,TOTAL,LIMIT,
1     ARAY1,ARAY2,KILL,ITIME,IX,STEPT,G,KARMAN
850  FORMAT(1X,2F10.3,2F10.5,3I10/1X,6I10/1X,2F10.5)
      DO 858 I=1,TUBES
          WRITE(8,852) I,CBS(I),(CB(I,K),K=1,CBS(I))
852  FORMAT(1X,2I5/(1X,7F10.6))
          WRITE(8,854) (RES(I,K),K=1,CBS(I))
854  FORMAT((1X,7F10.6))
          WRITE(8,856) (CONC(I,K),K=1,(CBS(I)-1))
856  FORMAT((1X,7F10.4))
          WRITE(8,854) (U(I,J),J=1,VEL)
858  CONTINUE
      WRITE(8,854) (UAVG(J),J=1,VEL)
      WRITE(8,856) (AVGCON(J),J=1,TOTAL)
      IF(ARAY1.GT.0) THEN
          WRITE(8,860) (XARAY(J),CARAY1(J),MARAY1(J),
1             J=1,ARAY1)
860  FORMAT((1X,F10.6,F10.4,F10.8,F10.6,F10.4,F10.6))
      ENDIF
      IF(ARAY2.GT.0) THEN
          DO 864 J=1,4
              IF(XPRINT(J).GT.0.) THEN
                  WRITE(8,862) (TARAY(K),CARAY2(J,K),
1                     MARAY2(J,K),K=1,ARAY2)
862  FORMAT((1X,F10.3,F10.4,F10.8,F10.3,F10.4,
1             F10.8))
              ENDIF
864  CONTINUE
          ENDIF
          GO TO 430
      ENDIF

C           *** CONVECT POLLUTANT CELL BOUNDARIES FOR TIME
C           *** STEP 'DELT' AND DILUTE CONCENTRATION DUE TO
C           *** RAINFALL (SPATIALLY-VARIED FLOW).

      DO 70 I=1,TUBES
C         ***
C         *** CHECK TO SEE IF SUFFICIENT NUMBER OF DOWNSTREAM
C         *** CELL VELOCITIES HAVE BEEN PREVIOUSLY COMPUTED.
C         *** IF NOT, COMPUTE THEM.
C         ***
          VCHECK = NINT((CB(I,1) - XO) /DELX) + 1
          CALL VELCTY ( VCHECK, KPARAM, VISCOS, SO, DELT, DELX, INTENS,
1             XO, U, VEL, TUBES, UAVG, DEBUG, KILL, WHERE, AVGVEL, V,DELY,

```

```

1      UMAX, UPINJ, UINJ, KPAR)
      IF(KILL.EQ.1) GO TO 425
      IF(DEBUG.EQ.1.AND.(I.EQ.4.OR.I.EQ.5).AND.SUMT.GT.0..AND.
1      SUMT.LE.4.) THEN
          WRITE(6,31)
31      FORMAT(/5X,'AFTER CONVECTION AND DILUTION ADJUSTMENT',1X,
1          '(PROG STATEMENT 34):'/5X,'STREAMTUBE',5X,'CELL BNDRY',
1          1X,'NO.',5X,'LOCATION',5X,'RESIDUAL',5X,'CONC')
      ENDIF
      DO 36 K=1,CBS(I)
C      ***
C      *** FIND CELL NUMBER, J, OF THE POLLUTANT CELL
C      *** WHOSE DOWNSTREAM POLLUTANT CELL BOUNDARY IS TO
C      *** BE CONVECTED. CELL NUMBER, J, REPRESENTS THE
C      *** JTH COMPUTATIONAL CELL DOWNSTREAM FROM
C      *** BASELINE, XO.
C      ***
          J = NINT((CB(I,K) - XO) / DELX)
          IF(DEBUG.EQ.1.AND.(I.EQ.4.OR.I.EQ.5).AND.SUMT.GT.0.
1          .AND.SUMT.LE.4.) THEN
              WRITE(6,29) I,K,CB(I,K),XO,DELX,J
29      FORMAT(/5X,'I=',I4,2X,'K=',I4,2X,'CB=',F9.5,2X,'XO=',
1          F9.5,2X,'DELX=',F9.5,2X,'J=',I4)
          ENDIF
C      ***
C      *** INITIALLY, SET VALUE OF 'TSUM' TO THE TRAVEL
C      *** TIME EQUIVALENT OF THIS POLLUTANT CELL
C      *** BOUNDARY RESIDUAL.
C      ***
          IF(RES(I,K).LT.0..AND.J.EQ.0) THEN
              TSUM = -RES(I,K) / U(I,J+1)
          ELSE IF(RES(I,K).LT.0.) THEN
              TSUM = -RES(I,K) / U(I,J)
          ELSE IF(RES(I,K).GT.0.) THEN
              TSUM = -RES(I,K) / U(I,J+1)
          ELSE
              TSUM = 0.
          ENDIF
          GRDSUM = 0
33      J = J + 1
          GRDSUM = GRDSUM + 1
C      ***
C      *** CHECK TO SEE IF SUFFICIENT NUMBER OF DOWNSTREAM
C      *** CELL VELOCITIES HAVE BEEN PREVIOUSLY COMPUTED.
C      *** IF NOT, COMPUTE THEM.
C      ***
          VCHECK = J + 2
          CALL VELCTY ( VCHECK, KPARAM, VISCOS, SO, DELT, DELX,
1          INTENS,XO, U, VEL, TUBES, UAVG, DEBUG, KILL, WHERE,
1          AVGVEL, V,DELY, UMAX, UPINJ, UINJ, KPAR)
          IF(KILL.EQ.1) GO TO 425
C      ***
C      *** COMPUTE TRAVEL TIME (TRAVEL) THROUGH EACH DOWN-
C      *** STREAM CELL WHILE SUMMING THESE TRAVEL TIMES

```

```

C      *** (TSUM). WHEN THE SUM EQUALS OR EXCEEDS THE
C      *** COMPUTATIONAL TIME STEP (DELT), STOP.
C      ***
C      *** THEN COMPUTE THE FOLLOWING FRACTION (FRAC):
C      *** THE DIFFERENCE BETWEEN THE TRAVEL TIME SUM
C      *** (TSUM) AND THE COMPUTATIONAL TIME STEP (DELT)
C      *** DIVIDED BY THE TRAVEL TIME (TRAVEL) THROUGH
C      *** THE LAST CELL.
C      ***
C      *** USE THIS FRACTION TO DECIDE WHICH COMPUTATIONAL
C      *** GRID LINE TO ASSIGN THE CONVECTED POLLUTANT CELL
C      *** BOUNDARY (CB(I,K)) AND TO COMPUTE ITS RESIDUAL
C      *** VALUE ( RES(I,K): THE DIFFERENCE BETWEEN THE
C      *** POLLUTANT CELL BOUNDARY'S ASSIGNED LOCATION AND
C      *** ITS ACTUAL CONVECTED LOCATION).
C      ***
C      *** THEN ADJUST CELL CONCENTRATION DUE TO RAINFALL
C      *** DILUTION ENCOUNTERED AS CELL WAS CONVECTED.
C      *** ACCOMPLISH THIS BY MULTIPLYING CONCENTRATION AT
C      *** OLD LOCATION BY THE RATIO OF DEPTH AT OLD
C      *** LOCATION (YOLD) TO DEPTH AT NEW LOCATION (YNEW).
C      *** FIND THIS RATIO FROM THE DARCY-WEISBACH EQUATION
C      ***  $Y = (F * (UAVG**2)) / (8. * SO * G)$ 
C      *** WHERE F = DARCY-WEISBACH FRICTION FACTOR = K/R;
C      *** K = PARAMETER; R = REYNOLDS NUMBER = Q/VISCOSITY;
C      *** Q = DISCHARGE PER FOOT WIDTH; UAVG = AVERAGE
C      *** CROSS-SECTIONAL VELOCITY; SO = BED SLOPE;
C      *** G = ACCELERATION OF GRAVITY; SO THAT
C      ***  $Y = (K * VISCOSITY * Q) / (8. * SO * G) ** (1/3)$ 
C      *** AND
C      ***  $YOLD/YNEW = (UAVG(OLD) / UAVG(NEW)) ** .5$ 
C      ***
TRAVEL = DELX / U(I,J)
TSUM = TSUM + TRAVEL
IF (TSUM.LT.DELT) GO TO 33
FRAC = (TSUM - DELT) / TRAVEL
IF (FRAC.GT..5) THEN
    CB(I,K) = XO + ((J-1) * DELX)
    RES(I,K) = (1. - FRAC) * DELX
    IF(K.EQ.CBS(I)) GO TO 34
    OLD = J - GRDSUM
    NEW = J-1
    CONC(I,K) = CONC(I,K) * ((UAVG(OLD)/UAVG(NEW))**.5)
ELSE
    CB(I,K) = XO + (J * DELX)
    RES(I,K) = -FRAC * DELX
    IF(K.EQ.CBS(I)) GO TO 34
    OLD = J - GRDSUM
    NEW = J
    CONC(I,K) = CONC(I,K) * ((UAVG(OLD)/UAVG(NEW))**.5)
ENDIF
34      IF (DEBUG.EQ.1.AND.(I.EQ.4.OR.I.EQ.5).AND.SUMT.GT.0.
1          .AND.SUMT.LE.4.) THEN

```

```

        WRITE(6,35) I, K, CB(I,K), RES(I,K), CONC(I,K)
35      FORMAT(/9X,I3,14X,I4,10X,F7.3,6X,F6.3,4X,F8.2)
        ENDIF
36      CONTINUE

        IF (DEBUG.EQ.1.AND.(I.EQ.4.OR.I.EQ.5).AND.SUMT.GT.0.
1          .AND.SUMT.LE.4.) THEN
            WRITE(6,37)
37          FORMAT(/5X,'AFTER ADJUSTMENT DUE TO HORIZONTAL SPREAD',
1              1X,'(PROG STATEMENT 37):'/5X,'STREAMTUBE',5X,
1              'CELL BNDRY NO.',31X,'CONC')
            ENDIF
        IF(DEBUG.EQ.9.OR.DEBUG.EQ.8) THEN
            IF(I.EQ.8.AND.(SUMT.EQ.40..OR.SUMT.EQ.48..OR.SUMT.EQ.52.
1              .OR.SUMT.EQ.56..OR.SUMT.EQ.60..OR.SUMT.EQ.64.)) THEN
                CONC(I,CBS(I))=0.
                DO 600 K=CBS(I),1,-1
                    WRITE(6,610) CONC(I,K), CB(I,K), RES(I,K)
610                FORMAT(20X,'CONC=',F10.4/10X,'CB=',F8.4/10X,
1                    'RES=',F8.4)
600            CONTINUE
            ENDIF
        ENDIF

        CBSUM = 1
        K = 0
620      K = K + 1
        IF(K.EQ.CBS(I)) GO TO 51
C          ***
C          *** ADJUST CONCENTRATIONS DUE TO HORIZONTAL SPREAD
C          *** OF CELL BOUNDARIES WHICH OCCURRED DURING CONVEC-
C          *** TION OF STEADY, NONUNIFORM FLOW. HORIZONTAL SPREAD
C          *** IS MEASURED BY COMPUTING CELL BOUNDARY WIDTH (CBW).
C          ***
46          CBW = CB(I,K) - CB(I,K+1)
            IF(DEBUG.EQ.1.AND.(I.EQ.4.OR.I.EQ.5).AND.SUMT.GT.0..AND.
1              SUMT.LE.4.) THEN
38              WRITE(6,38) I, K, CB(I,K),CB(I,K+1),CBW,CONC(I,K)
                FORMAT(I5,I5,3F10.4,F10.2)
            ENDIF
            IF(ANINT(CBW/DELX).EQ.0.) THEN
                IF(K.EQ.1) THEN
                    CONC(I,1) = CONC(I,1) + CONC(I,2)
                    DO 39 KK=2,(CBS(I)-1)
                        CB(I,KK) = CB(I,(KK+1))
                        RES(I,KK) = RES(I,(KK+1))
                        IF(KK.EQ.(CBS(I)-1)) GO TO 39
                        CONC(I,KK) = CONC(I,(KK+1))
39                    CONTINUE
                ELSE IF(K.EQ.(CBS(I)-1)) THEN
                    NEW = NINT((CB(I,(CBS(I)-2))-XO)/DELX)
                    OLD = NEW-1
                    CONC(I,(CBS(I)-2)) = CONC(I,(CBS(I)-2)) +
1                    (((UAVG(OLD)/UAVG(NEW))**.5)*CONC(I,(CBS(I)-1)))

```

```

NEWCON(CBS(I)-2) = CONC(I,(CBS(I)-2))
RES(I,(CBS(I)-1)) = RES(I,CBS(I))
NEWRES(CBS(I)-1) = RES(I,(CBS(I)-1))
CBS(I) = CBS(I) - 1
GO TO 51
ELSE
1 CHECK1 = CB(I,(K-1)) + RES(I,(K-1)) -
      (CB(I,K) + RES(I,K))
1 CHECK2 = CB(I,(K+1)) + RES(I,(K+1)) -
      (CB(I,(K+2)) + RES(I,(K+2)))
IF(CHECK1.LT.CHECK2) THEN
  NEW = NINT((CB(I,(K-1))-XO)/DELX)
  OLD = NEW-1
1 CONC(I,(K-1)) = CONC(I,(K-1)) +
      ((UAVG(OLD)/UAVG(NEW))**.5)*CONC(I,K)
  NEWCON(CBSUM-1) = CONC(I,(K-1))
  DO 40 KK=K,(CBS(I)-1)
    CB(I,KK) = CB(I,(KK+1))
    RES(I,KK) = RES(I,(KK+1))
    IF(KK.EQ.(CBS(I)-1)) GO TO 40
    CONC(I,KK) = CONC(I,(KK+1))
40 CONTINUE
  NEWRES(CBSUM) = RES(I,K)
ELSE IF(CHECK1.GT.CHECK2) THEN
  CONC(I,K) = CONC(I,K) + CONC(I,K+1)
  DO 41 KK=(K+1),(CBS(I)-1)
    CB(I,KK) = CB(I,(KK+1))
    RES(I,KK) = RES(I,(KK+1))
    IF(KK.EQ.(CBS(I)-1)) GO TO 41
    CONC(I,KK) = CONC(I,(KK+1))
41 CONTINUE
ELSE
  IF(ABS(RES(I,K)).GE.ABS(RES(I,K+1))) THEN
    NEW = NINT((CB(I,(K-1))-XO)/DELX)
    OLD = NEW-1
1 CONC(I,(K-1))=CONC(I,(K-1))+
      ((UAVG(OLD)/UAVG(NEW))**.5)*CONC(I,K)
  NEWCON(CBSUM-1)=CONC(I,(K-1))
  DO 47 KK=K,(CBS(I)-1)
    CB(I,KK)=CB(I,(KK+1))
    RES(I,KK)=RES(I,(KK+1))
    IF(KK.EQ.(CBS(I)-1)) GO TO 47
    CONC(I,KK)=CONC(I,(KK+1))
47 CONTINUE
  NEWRES(CBSUM)=RES(I,K)
ELSE
  CONC(I,K)=CONC(I,K)+CONC(I,(K+1))
  DO 48 KK=(K+1),(CBS(I)-1)
    CB(I,KK)=CB(I,(KK+1))
    RES(I,KK)=RES(I,(KK+1))
    IF(KK.EQ.(CBS(I)-1)) GO TO 48
    CONC(I,KK)=CONC(I,(KK+1))
48 CONTINUE
ENDIF

```

```

        ENDIF
        ENDIF
        CBS(I) = CBS(I) - 1
        GO TO 46
ENDIF
CONC(I,K) = CONC(I,K) * (1./ANINT(CBW/DELX))
IF (DEBUG.EQ.1.AND.(I.EQ.4.OR.I.EQ.5).AND.SUMT.GT.0.
1      .AND.SUMT.LE.4.) THEN
43      WRITE(6,43) I, K, CONC(I,K)
        FORMAT(9X,I3,14X,I4,33X,F10.2)
ENDIF
C      ***
C      *** IF HORIZONTAL SPREAD OF CELL BOUNDARIES EQUALS
C      *** OR EXCEEDS WIDTH OF TWO COMPUTATIONAL CELLS
C      *** (2 * DELX), THEN NEW CELL BOUNDARIES (NEWCB(N))
C      *** NEED TO BE ESTABLISHED BETWEEN THE OLD CELL
C      *** BOUNDARIES (CB(I,K) AND CB(I,K+1)). ALSO, THE
C      *** CONCENTRATION OF THESE NEW POLLUTANT CELLS
C      *** SHOULD BE ADJUSTED SLIGHTLY (NEWCON(N)) DUE TO
C      *** THEIR SLIGHTLY SHALLOWER DEPTH OF FLOW UPSTREAM
C      *** OF THE OLD CELL BOUNDARY, CB(I,K).
C      ***
C      ***      NEWCBS = NUMBER OF NEW CELL BOUNDARIES TO
C      ***      BE ESTABLISHED BETWEEN ONE SET OF
C      ***      OLD CELL BOUNDARIES.
C      ***
NEWCBS = ( NINT( CBW / DELX ) ) - 1
IF (NEWCBS.EQ.0) GO TO 45
CBS(I) = CBS(I)+NEWCBS
IF((K+NEWCBS+1).EQ.CBS(I)) THEN
    CB(I,CBS(I)) = CB(I,(CBS(I)-1))
    RES(I,CBS(I)) = RES(I,(CBS(I)-1))
    GO TO 660
ENDIF
DO 650 KL=CBS(I),(K+NEWCBS+1),-1
    CB(I,KL) = CB(I,(KL-NEWCBS))
    RES(I,KL) = RES(I,(KL-NEWCBS))
    IF(KL.EQ.CBS(I)) GO TO 650
    CONC(I,KL) = CONC(I,(KL-NEWCBS))
650 CONTINUE
660 DO 44 L=1,NEWCBS
    N = CBSUM + L
    NEWCB(N) = CB(I,K) - (L * DELX)
    NEWRES(N) = 0.
    OLD = NINT(( CB(I,K) - XO) / DELX)
    NEW = OLD - L
    NEWCON(N) = CONC(I,K) * ((UAVG(OLD)/UAVG(NEW))**.5)
    CB(I,(K+L)) = NEWCB(N)
    RES(I,(K+L)) = NEWRES(N)
    CONC(I,(K+L)) = NEWCON(N)
44 CONTINUE
NEWCON(N-NEWCBS) = CONC(I,K)
CBSUM = CBSUM+1
GO TO 620

```

```

C      ***
C      *** RELABEL THE SEQUENCE NUMBER OF THE OLD CELL
C      *** BOUNDARIES, RESIDUALS, AND CONCENTRATIONS
C      *** (SEQUENCE NUMBER = K IN THE (I,K) ARRAY)
C      *** DUE TO THE ADDITION OF NEW CELL BOUNDARIES.
C      ***
45     N = CBSUM + 1
        NEWCB(N) = CB(I,K+1)
        NEWRES(N) = RES(I,K+1)
        NEWCON(CBSUM) = CONC(I,K)
        CBSUM = CBSUM + 1
        IF(K.EQ.(CBS(I)-1)) GO TO 51
GO TO 620

51     IF(DEBUG.EQ.1.AND.(I.EQ.4.OR.I.EQ.5).AND.SUMT.GT.0.
1       .AND.SUMT.LE.4.) THEN
        WRITE(6,55)
55     FORMAT(/5X,'AFTER ADDING NEW CELL BOUNDARIES AND ADJUST'
1       , 'ING CONC IN NEW CELLS'/5X,'(PROG STATEMENT 56):'/5X,
1       'STREAMTUBE',5X,'CELL BNDRY NO.',5X,'LOCATION',5X,
1       'RESIDUAL',5X,'CONC')
        ENDIF
C      ***
C      *** REPLACE OLD VALUES WITH NEW ONES FOR POLLUTANT
C      *** CELL BOUNDARY LOCATION (CB(I,K)), POLLUTANT CELL
C      *** BOUNDARY RESIDUAL (RES(I,K)), AND POLLUTANT CELL
C      *** CONCENTRATION (CONC(I,K)).
C      ***
DO 60 K=2,CBSUM
        CB(I,K) = NEWCB(K)
        RES(I,K) = NEWRES(K)
        IF (K.EQ.CBSUM) GO TO 60
        CONC(I,K) = NEWCON(K)
        IF(DEBUG.EQ.1.AND.(I.EQ.4.OR.I.EQ.5).AND.SUMT.GT.0.
1       .AND.SUMT.LE.4.) THEN
56     WRITE(6,56) I, K, CB(I,K), RES(I,K), CONC(I,K)
        FORMAT(9X,I3,14X,I4,10X,F7.3,6X,F6.3,4X,F8.2)
        ENDIF
60     CONTINUE
        CBS(I) = CBSUM
        IF(TEST.EQ.2.OR.TEST.EQ.3.OR.TEST.EQ.4) THEN
            IF(TEST.EQ.2) ICELL=(TUBES+1)/2
            IF(TEST.EQ.3) ICELL=(TUBES+1)/2
            IF(TEST.EQ.4) ICELL=TUBES
            IF(I.EQ.ICELL) THEN
65     IF(NINT((CB(I,CBS(I))-XO)/DELX).EQ.0) GO TO 70
                CONC(I,CBS(I)) = SOURCE
                CBS(I) = CBS(I)+1
                CB(I,CBS(I)) = CB(I,(CBS(I)-1))-DELX
                RES(I,CBS(I)) = RES(I,(CBS(I)-1))
                IF(DEBUG.EQ.1) THEN
1       WRITE(6,68) I, CBS(I), CB(I,CBS(I)), RES(I,CBS(I)),
                    CONC(I,(CBS(I)-1))
68     FORMAT(/5X,'I=',I4,5X,'CBS(I)=',I4,5X,

```

```

1          'CB(I,CBS(I))=',F10.5,5X,'RES(I,CBS(I))=',
1          F10.5,5X,'CONC(I,(CBS(I)-1))=',F12.5)
          ENDIF
          GO TO 65
        ENDIF
      ENDIF
70 CONTINUE
C     ***
C     *** FIND LOCATION OF LEADING-MOST DYE CLOUD CELL
C     *** BOUNDARY (MAXCB) AND TRAILING-MOST DYE CLOUD
C     *** CELL BOUNDARY (MINCB).
C     ***
C     *** SET PRELIMINARY VALUES FOR 'MINCB' AND 'MAXCB'
C     ***
73 MINCB = CB(1,CBS(1))
   MAXCB = CB(1,1)
C     ***
C     *** FIND ACTUAL VALUES FOR 'MINCB' AND 'MAXCB'.
C     ***
DO 80 I=1,TUBES
   IF (CB(I,CBS(I)).GE.MINCB) GO TO 75
     MINCB = CB(I,CBS(I))
75   IF (CB(I,1).LE.MAXCB) GO TO 80
     MAXCB = CB(I,1)
80 CONTINUE
   IF(TEST.EQ.2.OR.TEST.EQ.3.OR.TEST.EQ.4) THEN
     TOTAL = NINT((MAXCB-XO)/DELX)
     IF(DEBUG.LE.2) THEN
       WRITE(6,82) MAXCB, MINCB, XO, TOTAL
82     FORMAT(/,5X,'MAXCB=',F10.5,5X,'MINCB=',F10.5,5X,
1       'XO=',F10.5,5X,'TOTAL=',I4)
       ENDIT = NINT((MAXCB-XO)/DELX)
       CHOICE = 2
       CALL CELLCON(CONC, CB, ENDIT, XO, DELX, TUBES,
1       CBS, DEBUG, SUMT, CHOICE)
     ENDIF
     GO TO 90
   ENDIF
C     ***
C     *** RESET VALUE FOR BASELINE XO. BASELINE XO IS
C     *** RESET FOLLOWING EACH CONVECTION CYCLE SO THAT
C     *** IT IS EQUAL TO THE TRAILING-MOST DYE CLOUD CELL
C     *** BOUNDARY (MINCB). THEN THE SEQUENCE NUMBERS FOR
C     *** CELL VELOCITIES AND AVERAGE VELOCITIES ARE ALSO
C     *** RESET. THIS PROCEDURE OF RESETTING XO IS USED TO
C     *** MINIMIZE COMPUTER MEMORY REQUIREMENTS FOR THESE
C     *** VELOCITY ARRAYS.
C     ***
NEWXO = MINCB
ADVANC = NINT((NEWXO-XO)/DELX)
NEWVEL = VEL - ADVANC
TOTAL = NINT((MAXCB-MINCB)/DELX)
IF (DEBUG.LE.2.AND.TOTAL.LT.50) THEN
  WRITE(6,85) MAXCB, MINCB, NEWXO, NEWVEL, TOTAL

```

```

85     FORMAT(//5X,'MAXCB =',F7.3,5X,'MINCB =',F7.3,5X,'NEWXO =',
1       F7.3,5X,'NEWVEL =',I4,5X,'TOTAL =',I4)
       ENDIT = NINT((MAXCB-XO)/DELX)
       CHOICE = 2
       CALL CELLCON(CONC, CB, ENDIT, XO, DELX, TUBES,CBS,
1       DEBUG, SUMT, CHOICE)
       ENDIF
       IF(DEBUG.EQ.1.AND.SUMT.GT.0..AND.SUMT.LE.2.) THEN
         WRITE(6,86)
86     FORMAT(/////5X,'CELL NO. (STARTING AT XO)',5X,'UAVG',
1       5X,'U IN TUBE AT BED',5X,'U IN TUBE AT SURFACE')
       ENDIF

       DO 89 M=1,NEWVEL
         N = M + ADVANC
         DO 87 I=1,TUBES
           U(I,M) = U(I,N)
87     CONTINUE
         UAVG(M) = UAVG(N)
         MODD = M - (2*INT( M/2))
         IF (DEBUG.EQ.1.AND.MODD.EQ.1.AND.SUMT.GT.0..AND.
1       SUMT.LE.2.) THEN
           WRITE(6,88) M, UAVG(M), U(1,M), U(TUBES,M)
88     FORMAT(15X,I4,13X,F6.4,8X,F6.4,19X,F6.4)
         ENDIF
89     CONTINUE

       XO = NEWXO
       VEL = NEWVEL
C     ***
C     *** INITIALIZE CONCENTRATION VALUE OF CELLS BETWEEN
C     *** XO AND CB(I,CBS(I)).
C     ***
90     DO 104 I=1,TUBES
         JEND = NINT((CB(I,CBS(I))-XO)/DELX)
         XOCBS(I) = CBS(I) + JEND
         IF(JEND.EQ.0) GO TO 104
         DO 91 J=1,JEND
           CB(I,(CBS(I)+J)) = CB(I,CBS(I)) - (J*DELX)
           RES(I,(CBS(I)+J)) = RES(I,CBS(I))
           CONC(I,(CBS(I)+J-1)) = 0.
91     CONTINUE
         CBS(I) = XOCBS(I)
104    CONTINUE
C     ***
C     *** INITIALIZE CONCENTRATION VALUE OF CELLS
C     *** BETWEEN MAXCB AND CB(I,1)
C     ***
       DO 96 I=1,TUBES
93     IF(MAXCB.GT.(CB(I,1)+(.5*DELX))) THEN
         NEWCB(1) = CB(I,1) + DELX
         NEWCON(1) = 0.
         NEWRES(1) = RES(I,1)
         DO 94 K=1,CBS(I)

```

```

NEWCB(K+1) = CB(I,K)
NEWRES(K+1) = RES(I,K)
IF(K.EQ.CBS(I)) GO TO 94
NEWCON(K+1) = CONC(I,K)
94  CONTINUE
    CBS(I) = CBS(I) + 1
    DO 95 K=1,CBS(I)
        CB(I,K) = NEWCB(K)
        RES(I,K) = NEWRES(K)
        IF(K.EQ.CBS(I)) GO TO 95
        CONC(I,K) = NEWCON(K)
95  CONTINUE
    GO TO 93
ELSE
    GO TO 96
ENDIF
96  CONTINUE
DO 103 I=1,CLPRTS
    IF(SUMT.GE.CLPRT(I).AND.(SUMT-DELT).LT.CLPRT(I)) THEN
        ENDIT = TOTAL
        CHOICE = 2
        CALL CELLCON (CONC, CB, ENDIT,XO, DELX, TUBES, CBS,
1      DEBUG, SUMT,CHOICE)
    ENDIF
103 CONTINUE

```

```

C      *** BEGIN PROCEDURE FOR DIFFUSING DYE IN VERTICAL
C      *** DIRECTION.  START WITH THE VERTICAL CELL COLUMN
C      *** CORRESPONDING TO THE TRAILING-MOST POLLUTANT
C      *** CELL.  DIFFUSE THE DYE VERTICALLY IN THIS
C      *** COLUMN.  REPEAT THE PROCESS IN A DOWNSTREAM
C      *** DIRECTION, ENDING WITH THE CELL COLUMN CORRES-
C      *** PONDING TO THE LEADING-MOST POLLUTANT CELL.

```

```

ISWICH = 0
IDROP = 0
DO 290 J=1,TOTAL
C      ***
C      *** FIND THE CELL COLUMN TO BE DIFFUSED.
C      ***
    LOCATE = XO + (J * DELX)
C      ***
C      *** FIND THE VERTICAL HEIGHT OF EACH STREAMTUBE (YTUBE(I))
C      ***
    IF(INTENS.EQ.0.) THEN
        Q = UNIFLO

```

```

        YS = DEPTH
        GO TO 101
    ENDIF
    Q = (LOCATE - (DELX / 2.)) * INTENS * .00002315
    YS = Q / UAVG(J)
    IF(IEPSLN.EQ.1) THEN
        EPSLN = .0000000001754*(INTENS**4.15)*(UAVG(J)**(-3.41))
    ENDIF
    IF(DEBUG.EQ.10.AND.STEPT.LE.5) THEN
        WRITE(6,899) EPSLN
899        FORMAT(5X,'EPSLN=',F20.15)
    ENDIF
101    DO 92 I=1,TUBES
        YTUBE(I) = (DELY(I)/100.)*YS
    92    CONTINUE
    IF (DEBUG.EQ.1.AND.J.LT.3.AND.SUMT.GT.0..AND.
1        SUMT.LE.2.) THEN
        WRITE(6,97) LOCATE, Q, YS, (YTUBE(I), I=1,TUBES)
97        FORMAT(/////5X,'VERTICAL DIFFUSION (PROG STATEMENT 92):'/5X,
1            'LOCATE =',F10.6,5X,'Q =',F10.7,5X,'YS =',F8.5,5X,
1            'YTUBE =',(F8.5))
    ENDIF
C        ***
C        *** INITIALIZE INTERIM CELL CONCENTRATION
C        *** VALUES (NEWCON).
C        ***
    DO 98 N=1,TUBES
        NEWCON(N) = 0.
    98    CONTINUE

    OPT4 = 0.
    DO 260 I=1,TUBES
C        ***
C        *** FIND THE CORRECT POLLUTANT CELL WITHIN
C        *** STREAMTUBE 'I' WHICH IS TO BE DIFFUSED.
C        ***
        CELL(I) = 0
        DO 102 K=1,(CBS(I)-1)
            IF (CB(I,K).EQ.LOCATE) THEN
                CELL(I) = K
                GO TO 110
            ELSE IF(CB(I,K).GT.(LOCATE+(.05*DELX))) THEN
                GO TO 99
            ELSE
                DIFF = ABS(LOCATE - CB(I,K))
                IF(DIFF.LT.(.05*DELX)) THEN
                    CELL(I) = K
                    GO TO 110
                ELSE IF(DIFF.GT.(.95*DELX).AND.DIFF.LT.(1.05*
1                    DELX)) THEN
                    CELL(I) = K-1
                    GO TO 110
                ENDIF
            ENDIF
        ENDIF
    ENDIF

```

```

99          IF (DEBUG.EQ.1 .AND. J.LT.3 .AND. SUMT.GT.0 .AND.
1           SUMT.LE.2.) THEN
100         WRITE (6,100) I,K,CB(I,K),LOCATE,CELL(I),DELX
1           FORMAT(5X,'I=',I2,2X,'K=',I2,2X,'CB=',F15.12,
1           5X,'LOCATE=',F15.12,5X,'CELL(I)=' ,I2,2X,
1           'DELX=',F9.6)
           ENDIF
102        CONTINUE
           IF (CELL(I).EQ.0) THEN
105         WRITE(6,105) I, J, SUMT
1           FORMAT(5X,'***TERMINATED***'/5X,'PROGRAM CANNOT LOCATE'
1           ,1X,'PROPER CELL FOR VERTICAL DIFFUSION AT PROG',
1           1X,'STATEMENT 100.'/5X,'TUBE =' ,5X,I3,'CELL NO.',
1           1X,'(STARTING FROM XO) =' ,I4,5X,'TIME =' ,F7.2)
           GO TO 430
           ENDIF
110        IF (DEBUG.EQ.1 .AND. J.LT.3 .AND. SUMT.GT.0 .AND.
1           SUMT.LE.2.) THEN
1           WRITE(6,115) I, K, CELL(I), CONC(I,CELL(I)), CBS(I),
1           CB(I,K)
115         FORMAT(5X,' I,K =' ,2I3,5X,'CELL BNDRY NO. =' ,I4,5X,
1           'PRE-DIFFUSED CONC =' ,F10.2,'CELLS=' ,I3,5X,
1           'CB(I,K) =' ,F8.4)
           ENDIF
C          ***
C          *** SKIP THIS CELL IF ITS CONCENTRATION IS ZERO.
C          ***
           IF (CONC(I,CELL(I)).EQ.0.) GO TO 260
           IF (EPSLN.EQ.0.) GO TO 260
C          ***
C          *** ESTABLISH CUTOFF VALUE FOR ENDING THE DIFFUSION
C          *** CALCULATIONS. (TO PRESERVE
C          *** CONSERVATION OF MASS, THE MASS LEFT OVER DUE TO
C          *** CUTOFF REQUIREMENT WILL BE PROPORTIONALLY ADDED
C          *** BACK TO THE OTHER DIFFUSED CONCENTRATIONS AT A
C          *** LATER POINT IN THE COMPUTER PROGRAM.)
C          ***
           IF (OPTION.EQ.1) CUTOFF=.01*CONC(I,CELL(I))
           IF (OPTION.EQ.2) CUTOFF=.005*CONC(I,CELL(I))
           IF (OPTION.EQ.3) CUTOFF=.005*CONC(I,CELL(I))
C          ***
C          *** COMPUTE DIFFUSED CONCENTRATIONS (DIFUSE) AT
C          *** DISTANCES AWAY FROM THE HORIZONTAL
C          *** CENTERLINE OF THE POLLUTANT SOURCE CELL.
C          *** USE THE VERTICAL DIFFUSION COEFFICIENT, EPSLN.
C          *** USE THE SOLUTION TO THE ONE-DIMENSIONAL, PARTIAL
C          *** DIFFERENTIAL DIFFUSION EQUATION. DUE TO
C          *** ASSUMPTION OF SYMMETRY, VALUES COMPUTED ON ONE
C          *** SIDE OF THE SOURCE CELL WILL APPLY TO BOTH SIDES.
C          ***
130         DO 120 M=1,TUBES
           TEMCON(M) = 0.
120        CONTINUE
C          ***

```

```

C      *** COMPUTE DIFFUSED CONCENTRATIONS IN VERTICAL CELL
C      *** COLUMN BEFORE IMAGE REFLECTION.
C      ***
C      IF(OPTION.EQ.2) THEN
C          ***
C          *** OPTION 2 COMPUTES DIFFUSED CONCENTRATIONS AT
C          *** QUARTER POINTS WITHIN EACH STREAMTUBE, THEN
C          *** AVERAGES THE FOUR CONCENTRATIONS TO OBTAIN THE
C          *** CELL CONCENTRATION. THIS LEVEL OF DETAIL IS NEEDED
C          *** FOR DIFFUSION COEFFICIENT VALUES ON THE ORDER OF THE
C          *** MOLECULAR DIFFUSION COEFFICIENT (LAMINAR FLOW WITH-
C          *** OUT RAINFALL).
C          ***
C          DY4 = YTUBE(I)/4.
C          A = (CONC(I,CELL(I)) * DY4)/SQRT(12.5664*EPSLN*DELT)
C          B = 4. * EPSLN * DELT
C          CEASE = 0
C          S = 0.
C          DO 136 L=1,(TUBES-I+1)
C              M = I+L-1
C              IF(L.EQ.1) THEN
C                  DIFUSE = 0.
C                  DO 122 JJ=1,4
C                      ARGMT(JJ) = (((REAL(JJ)-.5)*DY4)**2)/B
C                      IF(ARGMT(JJ).GT.100.) THEN
C                          TERM(JJ) = 0.
C                      ELSE
C                          TERM(JJ) = (9.-(2.*REAL(JJ)))*A*EXP
C                                  (-ARGMT(JJ))
C                      ENDIF
C                      DIFUSE = TERM(JJ) + DIFUSE
C          122 CONTINUE
C          DIFUSE = DIFUSE/4.
C          IF(DEBUG.EQ.3.AND.J.EQ.1.AND.(I.EQ.1.OR.I.EQ.2)
C          1 .AND.SUMT.LE.DELT) THEN
C              WRITE(6,124) J,I,L,M,DIFUSE
C          124 FORMAT(5X,'132 ',2X,'J=',I3,2X,'I=',I3,2X,'L=',
C          1 I3,2X,'M=',I3,2X,'DIFUSE=',F10.5)
C          ENDIF
C          GO TO 135
C      ENDIF
C      DIFUSE = 0.
C      W = YTUBE(M)/4.
C      DO 128 N=1,4
C          R=(N-.5)*DY4
C          DO 126 JJ=1,5
C              ARGMT(JJ) = ((R+S+((REAL(JJ)-1.)*W))**2)/B
C              IF(ARGMT(JJ).GT.100.) THEN
C                  TERM(JJ) = 0.
C              ELSE
C                  IF(JJ.EQ.1.OR.JJ.EQ.5) THEN
C                      COEF = .5
C                  ELSE
C                      COEF = 1.

```

```

                ENDIF
                TERM(JJ) = COEF*A*EXP(-ARGMT(JJ))
                ENDIF
                DIFUSE = TERM(JJ)+DIFUSE
126          CONTINUE
128          CONTINUE
                DIFUSE = DIFUSE/4.
                IF(DEBUG.EQ.3.AND.J.EQ.1.AND.(I.EQ.1.OR.I.EQ.2)
1          .AND.SUMT.LE.DELT) THEN
                WRITE(6,133) J,I,L,M,DIFUSE
133          FORMAT(5X,'133',2X,'J=',I3,2X,'K=',I3,2X,'L=',
1          I3,2X,'M=',I3,2X,'DIFUSE=',F10.5)
                ENDIF
                IF(DIFUSE.LT.CUTOFF.AND.L.GT.2) THEN
                    CEASE = 1
                    GO TO 138
                ENDIF
                S = S + YTUBE(M)
135          TEMCON(M) = DIFUSE
136          CONTINUE
138          S = 0.
                DO 142 L=2,I
                    M = I-L+1
                    DIFUSE = 0.
                    W = YTUBE(M)/4.
                    DO 140 N=1,4
                        R = (N-.5)*DY4
                        DO 139 JJ=1,5
                            ARGMT(JJ) = ((R+S+((REAL(JJ)-1.)*W))**2)/B
                            IF(ARGMT(JJ).GT.100.) THEN
                                TERM(JJ) = 0.
                            ELSE
                                IF(JJ.EQ.1.OR.JJ.EQ.5) THEN
                                    COEF = .5
                                ELSE
                                    COEF = 1.
                                ENDIF
                                TERM(JJ) = COEF*A*EXP(-ARGMT(JJ))
                            ENDIF
                            DIFUSE = TERM(JJ) + DIFUSE
                        ENDIF
                    ENDIF
                CONTINUE
139          CONTINUE
140          CONTINUE
                DIFUSE = DIFUSE/4.
                IF(DIFUSE.LT.CUTOFF.AND.L.GT.2.AND.CEASE.EQ.1)THEN
                    GO TO 200
                ELSE IF(DIFUSE.LT.CUTOFF.AND.L.GT.2.AND.
1          CEASE.EQ.0) THEN
                    GO TO 152
                ENDIF
                S = S + YTUBE(M)
                TEMCON(M) = DIFUSE
                IF(DEBUG.LE.3.AND.J.EQ.1.AND.(I.EQ.1.OR.I.EQ.2)
1          .AND.SUMT.EQ.DELT) THEN
                    WRITE(6,141) DY4, J, I, CELL(I), CONC(I,CELL(I)),

```

```

1          L, DIFUSE, TEMCON(M)
141      FORMAT(5X,'DY4=',F10.8,5X,'CELL COL.=' ,I3,5X,
1          'TUBE=', I3,5X,'CELL(I)=' ,I3,5X,'CONC(I,CELL',
1          '(I))=' ,F10.3/5X,'L=' ,I2,5X,'DIFUSE=' ,F10.3,5X,
1          'TEMCON(M)=' ,F10.3)
          ENDIF
142      CONTINUE
          ELSE IF(OPTION.EQ.1.OR.OPTION.EQ.3) THEN
C          ***
C          *** OPTION 1 COMPUTES DIFFUSED CONCENTRATIONS
C          *** ONLY AT CENTERLINE OF STREAMTUBES BASED ON MASS IN
C          *** SOURCE CELL CONCENTRATED AT CELL CENTERLINE.
C          ***
C          *** OPTION 3 COMPUTES DIFFUSED CONCENTRATIONS AT
C          *** CENTERLINE OF STREAMTUBES BASED ON STEP FUNCTION
C          *** CONCENTRATION AT SOURCE CELL.
C          ***
          IF(OPTION.EQ.3) THEN
              A = -YTUBE(I)/2.
              B = YTUBE(I)/2.
              C = SQRT(4.*EPSLN*DELTA)
          ELSE IF(OPTION.EQ.1) THEN
              A=(CONC(I,CELL(I))*YTUBE(I))/SQRT(12.5664*EPSLN*DELTA)
              B=4.*EPSLN*DELTA
          ENDIF
          S = 0.
          DO 144 L=1,(TUBES-I+1)
              M = I+L-1
              IF(L.EQ.1) GO TO 143
              S = S+(.5*YTUBE(M-1))+(.5*YTUBE(M))
143          IF(OPTION.EQ.3) THEN
              DIFUSE = (CONC(I,CELL(I))/2.)*(ERF((S-A)
1          /C)-ERF((S-B)/C))
              ELSE IF(OPTION.EQ.1) THEN
              DIFUSE = A*EXP(-(S**2)/B)
              ENDIF
              IF(DIFUSE.LT.CUTOFF.AND.L.GT.2) GO TO 146
              TEMCON(M) = DIFUSE
144          CONTINUE
146          S = 0.
          DO 149 L=2,I
              M = I-L+1
              S = S + (.5*YTUBE(M+1))+(.5*YTUBE(M))
              IF(OPTION.EQ.3) THEN
              DIFUSE = (CONC(I,CELL(I))/2.)*(ERF((S-A)/C)
1          -ERF((S-B)/C))
              ELSE IF(OPTION.EQ.1) THEN
              DIFUSE=A*EXP(-(S**2)/B)
              ENDIF
              IF(DIFUSE.LT.CUTOFF.AND.L.GT.2) GO TO 152
              TEMCON(M) = DIFUSE
              IF(DEBUG.EQ.3.AND.J.EQ.1.AND.(I.EQ.1.OR.I.EQ.2)
1          .AND.SUMT.GT.0..AND.SUMT.LE.2.) THEN
              WRITE(6,148) J, I, M, TEMCON(M)

```

```

148          FORMAT(/5X,'AT PROG STATEMENT 145:',5X,'J =',I4,5X,
1          'I =',I4,5X,'M =',I4,5X,'TEMCON(M) =',F9.2)
          ENDIF
149          CONTINUE
          ELSE IF(OPTION.EQ.4) THEN
C          ***
C          *** OPTION 4 ASSUMES COMPLETE VERTICAL MIXING
C          ***
          OPT4 = (CONC(I,CELL(I))*YTUBE(I))+OPT4
          GO TO 260
          ELSE IF(OPTION.EQ.5) THEN
C          ***
C          *** OPTION 5 REDUCES THE NUMBER OF COMPUTATIONS FOR
C          *** STEADY, UNIFORM FLOW WITH STREAMTUBES OF EQUAL HEIGHT.
C          *** THIS OPTION USES A STEP FUNCTION CONCENTRATION AT
C          *** SOURCE CELL AS IN OPTION 3.
C          ***
          JJ = 0
          DO 570 L=I,TUBES
              JJ = JJ+1
              TEMCON(L) = TEMCON(L)+(CONC(I,CELL(I))*DIFFAC(JJ))
              IF(JJ.EQ.MAXI) GO TO 580
570          CONTINUE
572          DO 574 L=TUBES,1,-1
              JJ = JJ+1
              TEMCON(L) = TEMCON(L)+(CONC(I,CELL(I))*DIFFAC(JJ))
              IF(JJ.EQ.MAXI) GO TO 580
574          CONTINUE
          DO 576 L=1,TUBES
              JJ = JJ+1
              TEMCON(L) = TEMCON(L)+(CONC(I,CELL(I))*DIFFAC(JJ))
              IF(JJ.EQ.MAXI) GO TO 580
576          CONTINUE
          GO TO 572
580          JJ = 1
          DO 582 L=(I-1),1,-1
              JJ = JJ+1
              TEMCON(L) = TEMCON(L)+(CONC(I,CELL(I))*DIFFAC(JJ))
              IF(JJ.EQ.MAXI) GO TO 200
582          CONTINUE
584          DO 586 L=1,TUBES
              JJ = JJ+1
              TEMCON(L) = TEMCON(L)+(CONC(I,CELL(I))*DIFFAC(JJ))
              IF(JJ.EQ.MAXI) GO TO 200
586          CONTINUE
          DO 588 L=TUBES,1,-1
              JJ =N JJ+1
              TEMCON(L) = TEMCON(L)+(CONC(I,CELL(I))*DIFFAC(JJ))
              IF(JJ.EQ.MAXI) GO TO 200
588          CONTINUE
          GO TO 584
          ENDIF
C          ***
C          *** COMPUTE DIFFUSED CONCENTRATIONS DUE TO IMAGE REFLECTION.

```

```

C      ***
152     SUP = 0.
        SDOWN = 0.
        DO 154 N=1, (TUBES-I)
            SUP = YTUBE(I+N)+SUP
154     CONTINUE
        DO 156 N=1, (I-1)
            SDOWN = YTUBE(N) + SDOWN
156     CONTINUE
        IF (REAL(TUBES-I) .GE. (.5*TUBES)) UPDOWN = 0
        IF (REAL(TUBES-I) .LT. (.5*TUBES)) UPDOWN = 1
        REFLEC = 0
        IF (UPDOWN.EQ.0) THEN
            LSTART = I
            OTHERL = TUBES - I + 1
            ODDEVE = 0
            COUNT = 0
            OTHERM = TUBES + 1
            EVEODD = 1
            S = SDOWN
            T = SUP
            SS = SDOWN+(.5*YTUBE(I))
            TT = SUP+(.5*YTUBE(I))
        ELSE
            LSTART = TUBES - I + 1
            OTHERL = I
            ODDEVE = 1
            COUNT = 1
            OTHERM = 0
            EVEODD = 0
            S = SUP
            T = SDOWN
            SS = SUP+(.5*YTUBE(I))
            TT = SDOWN+(.5*YTUBE(I))
        ENDIF
        DIFUS1 = SOURCE
        DIFUS2 = SOURCE

160     DO 170 NUM=1, TUBES
        IF (ODDEVE.EQ.1) M=TUBES+1-NUM
        IF (ODDEVE.EQ.0) M=NUM
        L = LSTART + (REFLEC*TUBES) + NUM
        IF (DIFUS1.LT.CUTOFF.AND.L.GT.2) GO TO 166
        IF (OPTION.EQ.2) THEN
            DIFUS1 = 0.
            W = YTUBE(M)/4.
            DO 163 N=1, 4
                R = (N-.5)*DY4
                DO 161 JJ=1, 5
                    ARGMT(JJ) = ((R+S+((REAL(JJ)-1.)*W))**2)/B
                    IF (ARGMT(JJ) .GT. 100.) THEN
                        TERM(JJ) = 0.
                    ELSE
                        IF (JJ.EQ.1.OR.JJ.EQ.5) THEN

```

```

        COEF = .5
        ELSE
        COEF = 1.
        ENDIF
        TERM(JJ) = COEF*A*EXP(-ARGMT(JJ))
        ENDIF
        DIFUS1 = TERM(JJ) + DIFUS1
161      CONTINUE
        IF (DEBUG.EQ.3.AND.SUMT.LE.2.) THEN
162          WRITE(6,162) A,B,R,S,W,DIFUS1
          FORMAT(5X,'162',2X,'A=',F12.9,2X,'B=',F12.9
1          ,2X,'R=',F12.9,2X,'S=',F12.9,2X,'W=',
1          F12.9,2X,'DIFUS1=',F18.12)
        ENDIF
163      CONTINUE
        S = S + YTUBE(M)
        DIFUS1 = DIFUS1/4.
        ELSE IF (OPTION.EQ.1.OR.OPTION.EQ.3) THEN
        SS = SS + (.5*YTUBE(M))
        IF (OPTION.EQ.3) THEN
1          DIFUS1 = (CONC(I,CELL(I))/2.)*(ERF((SS-A)/C)
          -ERF((SS-B)/C))
        ELSE IF (OPTION.EQ.1) THEN
        DIFUS1=A*EXP(-(SS**2)/B)
        ENDIF
        SS = SS + (.5*YTUBE(M))
        ENDIF
1          IF (DIFUS1.LT.CUTOFF.AND.DIFUS2.LT.CUTOFF.AND.L.GT.2)
          GO TO 200
        IF (DIFUS1.LT.CUTOFF.AND.L.GT.2) GO TO 166
        TEMCON(M) = TEMCON(M) + DIFUS1
        IF (DEBUG.EQ.3.AND.J.EQ.1.AND.COUNT.LT.3.AND.(I.EQ.1.OR.
1          I.EQ.2).AND.SUMT.GT.0..AND.SUMT.LE.2.) THEN
        WRITE(6,164) J, I, M, TEMCON(M)
164      FORMAT(/5X,'AT PROG STATEMENT 165:',5X,'J =',I4,5X,
1          'I =',I4,5X,'M =',I4,5X,'TEMCON(M) =',F9.2)
        ENDIF
166      IF (DIFUS2.LT.CUTOFF.AND.L.GT.2) GO TO 170
        IF (L.LE.OTHERL) GO TO 170
        IF (EVEODD.EQ.1) OTHERM=OTHERM-1
        IF (EVEODD.EQ.0) OTHERM=OTHERM+1
        IF (OTHERM.EQ.0) THEN
        OTHERM = 1
        EVEODD = 0
        ELSE IF (OTHERM.EQ.(TUBES+1)) THEN
        OTHERM = TUBES
        EVEODD = 1
        ENDIF
        IF (OPTION.EQ.2) THEN
        DIFUS2 = 0.
        W = YTUBE(OTHERM)/4.
        DO 167 N=1,4
        R = (N-.5)*DY4
        DO 165 JJ=1,5

```

```

ARGMT(JJ) = ((R+T+((REAL(JJ)-1.)*W))**2)/B
IF (ARGMT(JJ).GT.100.) THEN
  TERM(JJ) = 0.
ELSE
  IF (JJ.EQ.1.OR.JJ.EQ.5) THEN
    COEF = .5
  ELSE
    COEF = 1.
  ENDIF
  TERM(JJ) = COEF*A*EXP(-ARGMT(JJ))
ENDIF
DIFUS2 = TERM(JJ) + DIFUS2
165 CONTINUE
IF (DEBUG.EQ.3.AND.SUMT.LE.2.) THEN
  WRITE(6,169) A,B,R,T,W,DIFUS2
169 FORMAT(5X,'167',2X,'A=',F12.9,2X,'B=',F12.9,
1      2X,'R=',F12.9,2X,'S=',F12.9,2X,'W=',
1      F12.9,2X,'DIFUS2=',F18.12)
ENDIF
167 CONTINUE
T = T + YTUBE(OTHERM)
DIFUS2 = DIFUS2/4.
ELSE IF (OPTION.EQ.1.OR.OPTION.EQ.3) THEN
  TT = TT + (.5*YTUBE(OTHERM))
  IF (OPTION.EQ.3) THEN
    DIFUS2 = (CONC(I,CELL(I))/2.)*(ERF((TT-A)/C)
1      -ERF((TT-B)/C))
  ELSE IF (OPTION.EQ.1) THEN
    DIFUS2 = A*EXP(-(TT**2)/B)
  ENDIF
  TT = TT + (.5*YTUBE(OTHERM))
ENDIF
IF (DIFUS1.LT.CUTOFF.AND.DIFUS2.LT.CUTOFF.AND.L.GT.2)
1 GO TO 200
TEMCON(OTHERM) = TEMCON(OTHERM) + DIFUS2
IF (DEBUG.EQ.1.AND.J.EQ.1.AND.COUNT.LT.3.AND.(I.EQ.1.
1 OR.I.EQ.2).AND.SUMT.GT.0..AND.SUMT.LE.2.) THEN
  WRITE(6,168) J, I, OTHERM, TEMCON(OTHERM)
168 FORMAT(/5X,'AT PROG STATEMENT 168:',5X,'J =',I4,
1      5X,'I =',I4,5X,'OTHERM =',I4,5X,'TEMCON(OTHERM) ='
1      ,F9.2)
ENDIF
170 CONTINUE
COUNT = COUNT + 1
ODDEVE = COUNT - (2*INT(COUNT/2))
REFLEC = REFLEC + 1
IF (COUNT.EQ.15) THEN
  WRITE(6,180)
180 FORMAT(/5X,'***TERMINATED***'/5X,'COUNT EXCEEDED 15'
1      , ' AT PROG STATEMENT 170.')
  GO TO 430
ENDIF
GO TO 160
C ***

```

```

C      *** SUM ALL THE DIFFUSED CONCENTRATIONS IN THE
C      *** CELL COLUMN (SUMCON).
C      ***
200    SUMCON = 0.
      DO 210 N=1,TUBES
        SUMCON = SUMCON + (TEMCON(N)*YTUBE(N))
        IF (DEBUG.EQ.1.AND.J.LT.3.AND.SUMT.GT.0..AND.
1          SUMT.LE.2.) THEN
          WRITE(6,205) N, TEMCON(N)
205          FORMAT(10X,'TUBE =',I3,5X,'TEMCON(DIFFUSED CONC) ='
1            ,F10.2)
          ENDIF
210    CONTINUE
C      ***
C      *** COMPARE SUM OF ALL THE DIFFUSED CONCENTRATIONS
C      *** TO THE ORIGINAL CONCENTRATION OF THE SOURCE CELL.
C      *** (THIS IS EQUIVALENT TO A CHECK FOR MASS CONSER-
C      *** VATION.) IF SUM OF DIFFUSED
C      *** CONCENTRATIONS (SUMCON) IS GREATER THAN CONCEN-
C      *** TRATION OF SOURCE CELL (CONC(I,K)), PRINT NOTE.
C      ***
      IF (SUMCON.GT.(CONC(I,CELL(I))*YTUBE(I))) THEN
        IF(LIMIT.EQ.0) THEN
          WRITE(6,220) SUMCON, CONC(I,CELL(I)), I,
1            CELL(I), SUMT
220          FORMAT(/10X,'***NOTE***'/10X,'SUM OF DIFF',
1            'USED CONCENTRATIONS IN CELL COLUMN GREA',
1            'TER THAN'/10X,'SOURCE CONCENTRATION BECA',
1            'USE OF NUMERICAL APPROXIMATION TO DIRAC',
1            ' DELTA FUNCTION'/10X,'COMBINED WITH ',
1            'VERY SMALL DIFFUSION COEFFICIENT',
1            ' AND/OR TIME STEP.'/10X,'THIS WILL',
1            ' BE CORRECTED WITH APPROPRIATE',
1            ' REDUCTION FACTOR. NO OTHER NOTES',
1            ' WILL BE PRINTED.'/10X,'SUMCON=' ,
1            F10.3,5X,'CONC(I,CELL(I))=' ,F10.3,5X,
1            'I=' ,I2,3X,'CELL(I)=' ,I3,3X,'SUMT=' ,F8.3)
          LIMIT = 1
        ENDIF
C      ***
C      *** IF SUM OF DIFFUSED CONCENTRATIONS (SUMCON) IS
C      *** GREATER THAN SOURCE CONCENTRATION (CONC(I,K)),
C      *** COMPUTE REDUCTION FACTOR (FACTOR) TO APPLY TO
C      *** ALL DIFFUSED CONCENTRATIONS.
C      ***
      FACTOR = (CONC(I,CELL(I))*YTUBE(I)) / SUMCON
      GO TO 230
      ELSE IF (SUMCON.EQ.(CONC(I,CELL(I))*YTUBE(I))) THEN
        FACTOR = 1.
        GO TO 245
      ELSE
C      ***
C      *** IF SUM OF DIFFUSED CONCENTRATIONS ( SUMCON)
C      *** IS LESS THAN SOURCE CONCENTRATION (CONC(I,K)),

```

```

C      *** COMPUTE INFLATION FACTOR (FACTOR) TO APPLY
C      *** TO ALL DIFFUSED CONCENTRATIONS.
C      ***
      FACTOR = (CONC(I,CELL(I))*YTUBE(I)) / SUMCON
      GO TO 230
    ENDIF
C      ***
C      *** APPLY CORRECTION FACTOR (FACTOR) TO ALL
C      *** DIFFUSED CONCENTRATIONS.
C      ***
230    DO 240 N=1,TUBES
      TEMCON(N) = FACTOR * TEMCON(N)
240    CONTINUE
C      ***
C      *** STORE DIFFUSED CONCENTRATIONS IN VARIABLE
C      *** NAME 'NEWCON'.
C      ***
245    IF (DEBUG.EQ.1.AND.J.LT.3.AND.SUMT.GT.0..AND.
1      SUMT.LE.2.) THEN
246      WRITE(6,246) FACTOR
      FORMAT(10X,'FACTOR =',F10.7)
    ENDIF
    DO 250 N=1,TUBES
      NEWCON(N) = NEWCON(N) + TEMCON(N)
      IF (DEBUG.EQ.1.AND.J.LT.3.AND.SUMT.GT.0..AND.
1      SUMT.LE.2.) THEN
248      WRITE(6,248) N, NEWCON(N)
      FORMAT(10X,'TUBE =',I3,5X,'NEWCON =',F10.2)
    ENDIF
250    CONTINUE
260    CONTINUE
    IF (EPSLN.EQ.0.) GO TO 275
    IF (OPTION.EQ.4) THEN
      DO 265 I=1,TUBES
        CONC(I,CELL(I)) = OPT4/YS
265    CONTINUE
      AVGCON(J) = OPT4/YS
      GO TO 282
    ENDIF
C      ***
C      *** PLACE INTO THE 'PERMANENT' CONCENTRATION
C      *** VARIABLE 'CONC(I,K)' THE RESULT FROM THIS
C      *** DIFFUSION COMPUTATION CYCLE (NEWCON(I)).
C      ***
      DO 270 N=1,TUBES
        CONC(N,CELL(N)) = NEWCON(N)
270    CONTINUE
C      ***
C      *** COMPUTE AVERAGE CROSS-SECTIONAL CONCENTRATION.
C      ***
275    SUM = 0.
      DO 280 N=1,TUBES
        SUM = SUM + (CONC(N,CELL(N))*YTUBE(N))
280    CONTINUE

```

```

AVGCON(J) = SUM / YS
2 82 IF (AVGCON(J) .LT. .005 .AND. ISWICH.EQ.0) THEN
      IF (J.EQ.1) IDROP=1
      IF (J.GT.1) IDROP=IDROP+1
      ELSE
        ISWICH = 1
      ENDIF
      IF (DEBUG.EQ.1 .AND. SUMT.GT.0 .AND. SUMT.LE.2.)
1      THEN
        WRITE(6,285) J, AVGCON(J)
2 85      FORMAT(/5X, '*** CELL COLUMN NO. (MEASURED FROM XO) =', I4,
1      10X, 'AVGCON (AVG CONC FOR THIS CELL COLUMN) =', F10.2)
      ENDIF
C      ***
C      *** COMPUTE SUMMATION OF CPRIME*UPRIME*YTUBE
C      *** FOR USE IN COMPUTING LONGITUDINAL DISPERSION
C      *** COEFFICIENT LATER IN PROGRAM. (LOOK BETWEEN PROG
C      *** STATEMENTS 322 AND 325.)
C      ***
SUMUCY(J) = 0.
DO 289 N=1, TUBES
  CPRIME = CONC(N, CELL(N)) - AVGCON(J)
  UPRIME = U(N, J) - UAVG(J)
  SUMUCY(J) = SUMUCY(J) + (CPRIME*UPRIME*YTUBE(N))
  IF (DEBUG.LE.1 .AND. SUMT.EQ.12 .AND. J.LT.19 .AND. J.GT.15) THEN
1      WRITE(6,288) N, J, CONC(N, CELL(N)), AVGCON(J),
2 88      U(N, J)
1      FORMAT(5X, 'I=', I2, 2X, 'J=', I3, 2X, 'CONC(I, CELL(I))='
1      , F10.3, 4X, 'AVGCON(J)=' , F10.3, 4X, 'U(I, J)=' ,
1      F10.6)
      ENDIF
2 89 CONTINUE
2 90 CONTINUE
DO 294 N=1, CLPRTS
  IF (SUMT.GE. CLPRT(N) .AND. (SUMT-DELT) .LT. CLPRT(N)) THEN
    ENDIT = TOTAL
    CHOICE = 3
    CALL CELLCON(CONC, CB, ENDIT, XO, DELX, TUBES, CBS,
1      DEBUG, SUMT, CHOICE)
      ENDIF
2 94 CONTINUE
  IF ((CB(1,1) .GE. 5 .AND. CB(1,2) .LT. 5) .OR. (CB(1,1) .GE.
1 10 .AND. CB(1,2) .LT. 10) .OR. (CB(1,1) .GE. 15 .AND.
1 15 .AND. CB(1,2) .LT. 15)) THEN
    WRITE(6,292) CB(1,1)
2 92    FORMAT(/////5X, 'VELOCITY DISTRIBUTION', F9.4,
1      ' FEET FROM TOP OF PLANE: '//
1      10X, 'TUBE NO. ', 5X, 'VELOCITY(FT/SEC) '//
    J = NINT((CB(1,1) - XO) / DELX)
    DO 295 I=1, TUBES
      WRITE(6,293) I, U(I, J)
2 93      FORMAT(/13X, I2, 11X, F9.6////)
2 95 CONTINUE
      ENDIF

```

```

IF (DEBUG.EQ.8) THEN
  DO 299 I=1,TOTAL
    X = XO+(I*DELX)-( .5*DELX)
    Q = X*INTENS*.00002315
    YS = Q/UAVG(I)
    WRITE (6,297) I,XO,X,Q,AVGCON(I),UAVG(I),YS,U(1,I),U(TUBES,I)
297  FORMAT(/5X,'I=',I3,'XO=',F8.3,3X,'X=',F8.3,3X,'Q=',
1      F9.6,3X,'AVGCON=',F10.4,3X,'UAVG=',F7.4,3X,'YS=',F8.5,3X,
1      'U(1,I)=' ,F7.4,3X,'U(TUBES,I)=' ,F7.4)
299  CONTINUE
    IF (STEPT.EQ.1) GO TO 301
    WHICH1=1
    CALL STATS (AVGCON,XO,TOTAL,DELX,INTENS,UAVG,SUMT,STEPT,
1      DEPTH,TARAY,CARAY2,MARAY2,WHICH1,ARAY2,DELT,WHICHX,
1      UNIFLO,DEBUG,XPRINT)
    ENDIF

C      *** IF TPRTS GREATER THAN ZERO, PRINT RESULTS
C      *** OF AVERAGE CROSS-SECTIONAL CONCENTRATIONS
C      *** (AVGCON) ALONG X-AXIS AT TIME INTERVALS
C      *** SPECIFIED BY TPRT(I) (IN SECONDS).

301  DO 296 I=1,TPRTS
    IF (SUMT.GE.TPRT(I).AND.(SUMT-DELT).LT.TPRT(I)) GO TO 298
296  CONTINUE
    GO TO 340
C      ***
C      *** LIMIT THE NUMBER OF VALUES TO BE PRINTED
C      *** TO 100. ACCOMPLISH THIS BY DEFINING AN INTERVAL
C      *** (INTERV) FOR PRINTOUT VALUES.
C      ***
298  INTERV = 0
    DO 300 I=150,3000,150
      IF (TOTAL.LE.I.AND.TOTAL.GT.(I-150)) THEN
        INTERV = I / 150
        GO TO 312
      ENDIF
300  CONTINUE
    IF (INTERV.EQ.0) THEN
      WRITE (6,310)
310  FORMAT(/5X,'***WARNING***'/5X,'TOTAL NUMBER OF POLLUTANT',
1      1X,'CELLS IN X DIRECTION GREATER THAN 3000.'/5X,
1      'COMPUTER PROGRAM CANNOT PRINT CONCENTRATION CURVE',
1      1X,'THIS LARGE UNLESS PROGRAM IS MODIFIED.')
      GO TO 340
    ENDIF

```

```

C      ***
C      *** PRINT VALUES OF CONCENTRATION AND MASS
C      *** ALONG X-AXIS.
C      ***
312    WRITE(6,313) SUMT
313    FORMAT('1',20X,'*****CONCENTRATION-DISTANCE CURVE',
1      F6.2,' SECONDS AFTER INJECTION*****')
      WRITE(6,315) SUMT,STEPT, XINJEC
315    FORMAT(/////5X,'TIME (SEC) =',3X,F8.3/5X,'TIME STEP',
1      1X,'NUMBER =',2X,I4/5X,'INJECTION LOCATION FROM ',
1      'TOP OF PLANE(FT) =',F8.2)
      WRITE(6,320)
320    FORMAT(/81X,'APPROXIMATION OF'/9X,
1      'DISTANCE FROM TOP',10X,'MEAN CROSS-SECTIONAL',22X,
1      'LONGITUDINAL DISPERSION'/11X,'OF PLANE (FT)',12X,
1      'CONC(MG/1000L, OR PPB)      MASS (MG)      ',
1      'COEFFICIENT (SQ FT PER SEC)')
      DO 330 I=1,TOTAL,INTERV
      X = (I * DELX) - (.5 * DELX)
      TOTALX = XO + X
      IF(INTENS.EQ.0.) THEN
          Q = UNIFLO
          YS = DEPTH
          GO TO 322
      ENDIF
      Q = TOTALX * INTENS * .00002315
      YS = Q / UAVG(I)
322    MASS = AVGCN(I) * YS * DELX * .02832
C      ***
C      *** SAVE VALUES FOR PLOTTING.
C      ***
C      *** XARAY = LOCATION ON X AXIS (FT)
C      *** CARAY1 = CONC AT X (PPB)
C      *** MARAY1 = MASS AT X (MG)
C      ***
      IF (TPLOT.EQ.1) THEN
          ARAY1 = ARAY1 + 1
          XARAY(ARAY1) = TOTALX
          CARAY1(ARAY1) = AVGCN(I)
          MARAY1(ARAY1) = MASS
      ENDIF
C      ***
C      *** COMPUTE LONGITUDINAL DISPERSION COEFFICIENT, DISPER.
C      ***
C      *** DISPER = 1/(DC/DX) * 1/YS * (SUMMATION FROM Y=0
C      *** TO Y=YS OF (UPRIME*CPRIME*YTUBE) )
C      ***
C      *** WHERE:
C      *** DC/DX = GRADIENT (GRAD) OF AVERAGE CROSS-
C      *** SECTIONAL CONCENTRATION (AVGCN) WITH
C      *** RESPECT TO X.
C      *** YS = DEPTH OF FLOW
C      *** YTUBE = HEIGHT OF STREAMTUBE
C      *** UPRIME = U(I,J) - UAVG(J)

```

```

C      ***      CPRIME = CONC(I,J) - AVGCON(J)
C      ***      SUMUCY = SUMMATION OF (UPRIME*CPRIME*YTUBE)
C      ***      (SEE PROG. STATEMENT 288)
C      ***
      IF(TOTAL.LE.2) THEN
        DISPER = 0.
        GO TO 325
      ENDIF
      IF(I.EQ.1) THEN
        GRAD = (AVGCON(2)-AVGCON(1))/DELX
      ELSE IF(I.EQ.TOTAL) THEN
        GRAD = (AVGCON(TOTAL)-AVGCON(TOTAL-1))/DELX
      ELSE
        GRAD = (.5*((AVGCON(I)-AVGCON(I-1))/DELX))+
1         (.5*((AVGCON(I+1)-AVGCON(I))/DELX))
      ENDIF
      IF(GRAD.EQ.0.) THEN
        DISPER = 0.
        GO TO 325
      ENDIF
      DISPER = -SUMUCY(I)/(GRAD*YS)
      IF(DEBUG.LE.1.AND.SUMT.EQ.12..AND.I.LT.20.AND.I.GT.15)THEN
324      WRITE(6,324) I, GRAD, YS, SUMUCY(I)
1         FORMAT(/5X,'I=',I3,5X,'GRAD=',F15.8,5X,'YS=',F10.7,
           3X,'SUMUCY(I/)',F15.7)
      ENDIF
325      WRITE(6,326) TOTALX, AVGCON(I), MASS, DISPER
326      FORMAT(15X,F6.2,21X,F8.2,9X,F10.5,12X,F12.8)
330      CONTINUE
      WHICH1 = 1
      IF(TOTAL.EQ.1) GO TO 340
      CALL STATS(AVGCON, XO, TOTAL, DELX, INTENS,
1         UAVG, SUMT, STEPT, DEPTH, TARAY, CARAY2, MARAY2, WHICH1,
1         ARAY2, DELT, WHICHX, UNIFLO,DEBUG, XPRINT)

C      *** IF 'XPRINT' GREATER THAN ZERO, SAVE CONCENTRA-
C      *** TION AND MASS VALUES TO BE PRINTED OUT LATER.

C      ***
C      *** IF 'XPRINT' GREATER THAN ZERO, SAVE CONCENTRATION
C      *** AND MASS VALUES FOR ALL TIME STEPS AT A FIXED
C      *** LOCATION ON X-AXIS. THIS FIXED LOCATION EQUAL TO
C      *** THE VALUE OF 'XPRINT'. UP TO FOUR LOCATIONS
C      *** ARE ALLOWED IN THE PROGRAM.
C      ***
C      ***      TARAY = TIME (SEC)
C      ***      CARAY2 = CONC AT TIME TARAY (PPB)

```

```

C      ***      MARAY2 = MASS AT TIME TARAY (MG)
C      ***
340    ARAY2 = ARAY2 + 1
      TARAY(ARAY2) = SUMT
      DO 346 I=1,4
        IF (XPRINT(I).EQ.0.) GO TO 346
        IF (XPRINT(I).GT.MAXCB) GO TO 344
        IF (XPRINT(I).LT.MINCB) GO TO 344
        EXACT = (XPRINT(I)-XO)/DELX
        J = NINT(EXACT)
        IF(J.EQ.0) GO TO 344
        IF(J.EQ.TOTAL) AVGCN(J+1)=0.
        DFRNCE = (EXACT-REAL(J))*DELX
        CARAY2(I,ARAY2) = AVGCN(J)+((DFRNCE+(DELX/2.))/DELX)
1      * (AVGCN(J+1)-AVGCN(J))
        IF(INTENS.EQ.0.) THEN
          Q = UNIFLO
          YS = DEPTH
          UEXACT = AVGVEL
          GO TO 342
        ENDIF
        Q = XPRINT(I) * INTENS * .00002315
        UEXACT = UAVG(J)+(((DFRNCE+(DELX/2.))/DELX)*
1      (UAVG(J+1)-UAVG(J)))
        YS = Q / UEXACT
342    MASS = CARAY2(I,ARAY2) * UEXACT * DELT * YS * .02832
        MARAY2(I,ARAY2) = MASS
        GO TO 346
344    CARAY2(I,ARAY2) = 0.
        MARAY2(I,ARAY2) = 0.
346    CONTINUE

```

```

C      *** CHECK TO SEE IF DELX SHOULD BE CHANGED.

```

```

IF(IX.GT.DELXS) GO TO 350
IF(SUMT.GE.CHANGX(IX).AND.(SUMT-DELT).LT.CHANGX(IX)) THEN
  DO 349 I=1,TUBES
    J=0
    DO 347 K=1,CBS(I),2
      J=J+1
      NEWCB(J)=CB(I,K)
      NEWRES(J)=RES(I,K)
      IF((K+1).EQ.CBS(I)) THEN
        NEWCB(J+1) = NEWCB(J)-(2.*DELX)
        NEWRES(J+1) = RES(I,K)
        OLD = NINT((CB(I,K)-XO)/DELX)

```

```

NEW = OLD+1
NEWCON(J) = (((UAVG(NEW)/((UAVG(NEW)+UAVG(OLD))
1      /2.))**.5)*CONC(I,K))/2.
      ICBS = J+1
      XO = NEWCB(J+1)
      GO TO 347
ELSE IF(K.EQ.CBS(I)) THEN
      ICBS = J
      GO TO 347
ENDIF
OLD = NINT((CB(I,K)-XO)/DELX)
NEWCON(J) = (((UAVG(OLD)/((UAVG(OLD)+UAVG(OLD-1))
1      /2.))**.5)*CONC(I,K))+(((UAVG(OLD-1)/((UAVG(OLD)
1      +UAVG(OLD-1))/2.))**.5)*CONC(I,(K+1))))/2.
347  CONTINUE
      CBS(I) = ICBS
      DO 348 K=1,ICBS
          CB(I,K) = NEWCB(K)
          RES(I,K) = NEWRES(K)
          IF(K.EQ.CBS(I)) GO TO 348
          CONC(I,K) = NEWCON(K)
348  CONTINUE
349  CONTINUE
      DELX = 2.*DELX
      IX = IX+1
      VEL = 0
      VCHECK = 0
      CALL VELCTY(VCHECK,KPARAM,VISCOS, SO,DELT,DELX,
1          INTENS,XO,U,VEL,TUBES,UAVG,DEBUG,KILL,
1          WHERE,AVGVEL,V,DELY, UMAX, UPINJ, UINJ, KPAR)
      IF(KILL.EQ.1) GO TO 425
ENDIF

C          *** CHECK TO SEE IF TIME INCREMENT (DELT)
C          *** SHOULD BE CHANGED.

350  IF(ITIME.GT.DELTS) THEN
      TIMEIN = 0
      GO TO 351
ENDIF
IF((SUMT+.00000001).GE.CHANGT(ITIME).AND.(SUMT-DELT).LT.
1  CHANGT(ITIME)) THEN
      DELT = NEWT(ITIME)
      ITIME = ITIME+1
      TIMEIN = 1
      GO TO 351

```

```

ENDIF
TIMEIN = 0

```

```

C          *** IF THE TIME SINCE INJECTION (SUMT) IS LESS THAN
C          *** THE SPECIFIED MAXIMUM TIME FOR THIS COMPUTER
C          *** RUN (MAXT), THEN ADVANCE ONE TIME STEP AND
C          *** BEGIN ANOTHER COMPUTATION CYCLE.

```

```

351  IF(MAXT.GE.SUMT.AND.(MAXT-DELT).LT.SUMT) GO TO 353
      SUMT = SUMT + DELT
      STEPT = STEPT+1
      IF(DEBUG.LE.7) THEN
        WRITE(6,352) SUMT
352  FORMAT(/////5X,'***BEGIN NEW TIME STEP***'/
1      8X,'TIME (SEC) =',F8.3)
      ENDIF
      IF(IX.EQ.1) GO TO 359
      IF((SUMT-DELT).GE.CHANGX(IX-1).AND.(SUMT-(2.*DELT)).LT.
1  CHANGX(IX-1)) GO TO 742
359  IF(IDROP.GT.0) THEN
      XO = XO+(IDROP*DELX)
      VEL = VEL-IDROP
      TOTAL = TOTAL-IDROP
      DO 354 I=1,TUBES
        CBS(I) = CBS(I)-IDROP
      DO 356 J=1,VEL
        U(I,J) = U(I,(J+IDROP))
356  CONTINUE
354  CONTINUE
      DO 357 J=1,VEL
        UAVG(J) = UAVG(J+IDROP)
357  CONTINUE
      DO 358 J=1,TOTAL
        AVGCON(J) = AVGCON(J+IDROP)
358  CONTINUE
      ENDIF
      I = 0
      JDROP = 0
700  IF(AVGCON(TOTAL-I).LT..005) THEN
      JDROP = JDROP+1
      ELSE
      GO TO 710
      ENDIF
      I = I+1
      GO TO 700
710  IF(JDROP.EQ.0) GO TO 742

```

```

TOTAL = TOTAL-JDROP
DO 740 I=1,TUBES
  CBS(I) = CBS(I)-JDROP
  DO 730 K=1,CBS(I)
    CB(I,K) = CB(I,(K+JDROP))
    RES(I,K) = RES(I,(K+JDROP))
    IF(K.EQ.CBS(I)) GO TO 730
    CONC(I,K) = CONC(I,(K+JDROP))
730    CONTINUE
740  CONTINUE
742  IF(TIMEIN.EQ.0) GO TO 30
    IF(TIMEIN.EQ.1) GO TO 512

C          *** IF 'T PLOT' EQUALS 1, USE 'MAPA' (LIBRARY LINE
C          *** PRINTER PLOT ROUTINE) TO PLOT CONCENTRATION AND
C          *** MASS VS DISTANCE ALONG X AXIS.

353  IF (T PLOT.EQ.0) GO TO 355
      CALL MAPA(5,XARAY,CARAY1,1,ARAY1,XMIN,XMAX,YMIN,YMAX,
1      DI,CO,DICO,1)
      CALL MAPA (5,XARAY,MARAY1,1,ARAY1,XMIN,XMAX,YMIN,YMAX,
1      DI,MA,DIMA,1)

C          *** IF 'XPRINT' GREATER THAN ZERO, PRINT OUT CONC
C          *** VS TIME AND MASS VS TIME CURVES AT FIXED VALUES
C          *** OF X.

355  NEWJ = 0
      DO 420 I=1,4
        IF (XPRINT(I).EQ.0.) GO TO 420
        INTERV = 0
        DO 360 L=100,3000,100
          IF(ARAY2.LE.L.AND.ARAY2.GT.(L-100)) THEN
            INTERV = L/100
            GO TO 375
          ENDIF
360    CONTINUE
        IF (INTERV.EQ.0) THEN

```

```

        WRITE(6,370)
370      FORMAT(/5X,'***WARNING***'/5X,'TOTAL NUMBER OF',1X,
1         'XPRINT VALUES GREATER THAN 3000.'/5X,'COMPUTER',1X,
1         'PROGRAM MUST BE MODIFIED FOR MORE VALUES.')
        GO TO 420
      ENDIF
375      WRITE(6,380) XPRINT(I), XINJEC
380      FORMAT('1'/////22X,'*****CONCENTRATION-TIME CURVE ',
1         'AT ',F6.2,' FEET FROM TOP OF PLANE*****'/////5X,
1         'INJECTION LOCATION FROM TOP OF PLANE(FT) =',F6.2
1         '//36X,'MEAN CROSS-SECTIONAL')
      WRITE(6,390)
390      FORMAT(14X,'TIME (SEC)',12X,'CONC (MG/1000L, OR PPB)',5X,
1         'MASS (MG)')
      DO 410 J=1,ARAY2,INTERV
      WRITE(6,400) TARAY(J), CARAY2(I,J), MARAY2(I,J)
400      FORMAT(15X,F7.2,21X,F8.2,9X,F10.5)
      NEWJ = NEWJ + 1
      TIME(NEWJ) = TARAY(J)
      CONCEN(NEWJ) = CARAY2(I,J)
      MASSS(NEWJ) = MARAY2(I,J)
410      CONTINUE
      WHICH1 = 0
      CALL STATS (AVGCON, XO, TOTAL, DELX, INTENS, UAVG,
1         SUMT, STEPT, DEPTH, TARAY, CARAY2, MARAY2, WHICH1,
1         ARAY2, DELT, WHICHX, UNIFLO, DEBUG, XPRINT)
420      CONTINUE

C          *** IF 'XPLOT' EQUALS 1, USE 'MAPA' LIBRARY LINE
C          *** PRINTER PLOT ROUTINE TO PLOT CONC AND MASS
C          *** VS TIME.

      IF (XPLOT.EQ.0) GO TO 422
      CALL MAPA (5,TIME,CONCEN,1,NEWJ,XMIN,XMAX,YMIN,YMAX,
1  TI,CO,TICO,1)
      CALL MAPA (5,TIME,MASSS,1,NEWJ,XMIN,XMAX,YMIN,YMAX,
1  TI,MA,TIMA,1)

C          *** IF 'COMP' EQUALS 1, CALL SUBROUTINE COMPAR
C          *** TO COMPARE DIFFERENCE BETWEEN COMPUTED
C          *** CONCENTRATION-TIME CURVE VS LABORATORY

```

C

*** CONCENTRATION-TIME CURVE.

```

422  IF (COMP.EQ.1) THEN
      CALL COMPAR(CARAY2, TARAY, LABCON, LABTIM, POINTS,
1     ARAY2, DEBUG, WHICHX)
      ENDIF
      GO TO 430

425  WRITE(6,426) WHERE
426  FORMAT(///5X, '***TERMINATED***'/5X, 'VELOCITY IN STREAMTUBE AT',
1     1X, 'WATER SURFACE IS NEGATIVE.'/5X, 'LOCATION ON PLANE =',
1     F9.4,2X, 'FT')

430  STOP
      END

```

***** SUBROUTINE VELCTY *****

```

      SUBROUTINE VELCTY (VCHECK, KPARAM, VISCOS, SO, DELT, DELX,
1     INTENS, XO, U, VEL, TUBES, UAVG, DEBUG, KILL, WHERE,
1     AVGVEL, V,DELY, UMAX, UPINJ, UINJ, KPAR)

C     *** THIS SUBROUTINE COMPUTES THE FLOW VELOCITY WITHIN EACH COMPU-
C     *** TATIONAL CELL. SINCE OVERLAND FLOW WITH RAINFALL IS NONUNIFORM
C     *** FLOW, THE VELOCITY WITHIN A STREAMTUBE WILL VARY IN THE FLOW
C     *** DIRECTION. PLUS, VELOCITY VARIES IN THE VERTICAL DIRECTION DUE
C     *** TO THE VERTICAL VELOCITY DISTRIBUTION. THIS SUBROUTINE USES
C     *** A POLYNOMIAL EQUATION TO DESCRIBE THE VERTICAL VELOCITY
C     *** DISTRIBUTION, AND IT USES THE DARCY-WEISBACH FRICTION RELATION-
C     *** SHIP TO COMPUTE FLOW DEPTHS, WHERE K/R IS SUBSTITUTED FOR THE
C     *** DARCY-WEISBACH FRICTION FACTOR ( $K=KPARAM_{\mu}$   $R=REYNOLDS\ NUMBER=$ 
C     ***  $Q/VISCOS$ ).
C     ***
C     ***
C     *** DEFINITIONS:
C     ***
C     ***     YMAX     = THE DEPTH AT WHICH THE MAXIMUM LOCAL VELOCITY
C     ***                 (UMAX) OCCURS. (UNITS = FT)
C     ***

```

```

C     ***      UMAX   = MAXIMUM LOCAL VELOCITY IN CROSS-SECTION
C     ***
C     ***
C     ***      A,B,C  = POLYNOMIAL COEFFICIENTS IN EQUATION FOR
C     ***
C     ***
C     ***      YMAX   = DEPTH OF A POINT WITHIN CROSS SECTION DIVIDED
C     ***
C     ***
C     ***

```

```

INTEGER FORWAR, VEL, VCHECK, DEBUG, TUBES
REAL INTENS, KPARAM, KPAR, KFAC
DIMENSION U(41,100),UAVG(300), V(58), DELY(58)

```

```

G = 32.2
IF (VCHECK.LT.VEL) GO TO 100
XBEGIN = XO + (VEL * DELX)
FORWAR = VCHECK - VEL + 20
IF (DEBUG.EQ.1) THEN
5     WRITE(6,5) VEL,VCHECK, XBEGIN, FORWAR
1     FORMAT(/////5X,'SUBROUTINE VELCTY: '/5X,'VEL = ',I3,5X,
1     'VCHECK = ',I3,5X,'XBEGIN = ',F7.3,5X,
1     'FORWAR = ',I3)
ENDIF
IF(INTENS.EQ.0.) THEN
DO 7 L=1,FORWAR
J = VEL + L
UAVG(J) = AVGVEL
DO 6 I=1,TUBES
U(I,J) = V(I)
6     CONTINUE
7     CONTINUE
GO TO 90
ENDIF
IF(INTENS.LT.3.75) THEN
BU = -.404+(.0492*INTENS)
CU = -.199+(.0060*INTENS)
ELSE IF(INTENS.GE.3.75) THEN
BU = -.211-(.00222*INTENS)
CU = -.217+(.0110*INTENS)
ENDIF
DO 20 L = 1,FORWAR
DISTNC = (XBEGIN-DELX)+(L*DELX)+(DELX/2.)
Q = DISTNC * INTENS * .00002315
YS = ((KPARAM*VISCOS*Q)/(8.*G*S0))**(1./3.)
UMEAN = Q/YS
YSIN = YS * 12.
YMAXIN = .966*(YSIN**1.14)*(INTENS**(-.08))
YMAX = YMAXIN / 12.
IF(UMAX.GT.0.) UMAX1=UMAX*UMEAN
IF(UMAX.EQ.0.) UMAX1=1.216*(INTENS**(-.07))*(UMEAN**.80)

```

```

      J= VEL + L
      UAVG(J) = UMEAN
      UMEANP = (UMAX1/YS)*(((2./3.)*YMAX)+((YS-YMAX)*
1      (1.+(.5*BU)+((1./3.)*CU))))
      VELFAC = UMEAN/UMEANP
      IF(L.EQ.1) THEN
          UPINJ = UMEANP
          UINJ = UMEAN
          KPAR = ((8.*SO*G*Q)/(UMEANP**3))*(Q/VISCOS)
      ENDIF
      IF (DEBUG.EQ.1.AND.(L.EQ.1.OR.L.EQ.10)) THEN
          WRITE(6,8) L, J, DISTNC, Q, YS, UMEAN, YMAX, UMAX1
8          FORMAT(5X, 'L =', I3, 5X, 'J =', I3, 5X, 'DISTNC =', F7.3, 5X, 'Q ='
1          , F9.7, 5X, 'YS =', F7.5, 5X, 'UMEAN =', F6.4/10X,
1          'YMAX =', F7.5, 5X, 'UMAX1 =', F6.4, 5X)
      ENDIF
      YBASE = 0.
      DO 10 I=1, TUBES
          YYMAX = ((.5*(DELY(I)/100.)*YS)+YBASE)/YMAX
          YBASE = (.5*(DELY(I)/100.)*YS)+(YYMAX*YMAX)
          YXYS = ((YYMAX*YMAX)-YMAX)/(YS-YMAX)
          IF(YYMAX.LT.1.) U(I,J) = VELFAC*UMAX1*((2.*YYMAX)-
1          (YYMAX**2))
          IF(YYMAX.GE.1.) U(I,J) = VELFAC*UMAX1*(1.+(BU*YXYS)+
1          (CU*(YXYS**2)))
          IF (DEBUG.EQ.1.AND.(L.EQ.1.OR.L.EQ.10)) THEN
              WRITE(6,9) I, U(I,J)
9              FORMAT(5X, 'TUBE NO. =', I2, 5X, 'CELL VELOCITY =',
1              F6.4)
          ENDIF
10      CONTINUE
          IF(U(TUBES,J).GT.0.) GO TO 12
              KILL = 1
              WHERE = DISTNC
12      IF(U(TUBES,J).GT.U(1,J)) GO TO 20
          WRITE(6,15) DISTNC
15      FORMAT(10X, '***WARNING***'/10X, 'VELOCITY OF'
1          , 1X, 'STREAMTUBE AT SURFACE IS LESS THAN VELOCITY'
1          , 1X, 'OF STREAMTUBE AT THE BED.  DISTANCE =', F7.3/)
20      CONTINUE
90      VEL = VEL + FORWAR
100     RETURN
      END

```

***** SUBROUTINE CELLCON *****

```

SUBROUTINE CELLCON(CONC, CB, ENDIT, XO, DELX, TUBES,CBS,DEBUG,
1  SUMT, CHOICE)

C  *** THIS SUBROUTINE PRINTS OUT CELL CONCENTRATIONS IN FORM OF A
C  *** LONGITUDINAL CROSS-SECTION OF THE FLOW.
C  ***
      INTEGER ENDIT, TUBES, CBS, DEBUG, CHOICE
      DIMENSION CONC(41,100), CB(41,100), K(58), C(58), CBS(58)
      IF(CHOICE.EQ.1) THEN
2        WRITE(6,2)
1        FORMAT(/////34X,'*****CELL CONCENTRATIONS AT ',
          ' INJECTION*****')
      ELSE IF(CHOICE.EQ.2) THEN
3        WRITE(6,3) SUMT
1        FORMAT(/////23X,'*****CELL CONCENTRATIONS AFTER ',
          ' CONVECTION AT ',F6.2,1X,'SECONDS*****')
      ELSE IF(CHOICE.EQ.3) THEN
4        WRITE(6,4) SUMT
1        FORMAT(/////19X,'*****CELL CONCENTRATIONS AFTER ',
          ' VERTICAL DIFFUSION AT ',F6.2,1X,'SECONDS*****')
      ENDIF
      WRITE(6,6)
6      FORMAT(/2X,'DISTANCE FROM',35X,'STREAMTUBE NUMBER'/
1      2X,'TOP OF PLANE'/6X,'(FT)',11X,'1',9X,'2',9X,'3',
1      9X,'4',9X,'5',9X,'6',9X,'7',9X,'8',9X,'9',9X,'10'////)
      DO 10 I=50,2000,50
          IF(ENDIT.LE.I.AND.ENDIT.GT.(I-50)) THEN
              INTERV = I/50
              GO TO 10
          ENDIF
10     CONTINUE
      DO 50 J=1,ENDIT,INTERV
          DO 15 I=1,TUBES
              K(I) = NINT((CB(I,1)-(XO+(J*DELX)))/DELX) + 1
              IF(K(I).LT.1.OR.K(I).GE.CBS(I)) THEN
                  C(I) = 0.
              ELSE
                  C(I) = CONC(I,K(I))
              ENDIF
              IF(DEBUG.LE.2.AND.SUMT.GT.8..AND.SUMT.LE.10.
1              .AND.(I.EQ.4.OR.I.EQ.5)) THEN
12              WRITE(6,12) I, CB(I,1), XO, K(I)
1          FORMAT(/5X,'TUBE =',I2,5X,'CB(I,1) =',F8.4,5X,
1          'XO =',F8.4,5X,'K(I) =',I4)
              ENDIF
15          CONTINUE
              X = XO + (J*DELX)-(.5*DELX)
              WRITE(6,20) X, (C(I), I=1,TUBES)
20          FORMAT(/1X,F10.5,3X,10F10.2/14X,10F10.2)
50     CONTINUE
      RETURN

```

END

***** SUBROUTINE STATS *****

*** THIS SUBROUTINE COMPUTES THREE SETS OF MOMENTS FOR THE DYE CLOUD:

*** 1) MOMENTS OF CONCENTRATION DISTRIBUTION ALONG X-AXIS.

*** 2) MOMENTS OF MASS DISTRIBUTION ALONG X-AXIS.

*** 3) MOMENTS OF CONCENTRATION-TIME CURVE.

*** THE FOLLOWING MOMENTS ARE COMPUTED:

*** FOR CONCENTRATION:

*** 0TH MOMENT (MOCON)

*** 1ST MOMENT (M1CON)

*** 2ND MOMENT (M2CON)

*** 3RD MOMENT (M3CON)

*** FOR MASS:

*** 0TH MOMENT (MOMAS)

*** 1ST MOMENT (M1MAS)

*** 2ND MOMENT (M2MAS)

*** 3RD MOMENT (M3MAS)

*** THE FOLLOWING VARIABLES ARE COMPUTED:

*** FOR CONCENTRATION:

*** MASS (MASCON) = MOCON (UNITS = (MG-FT)/1000 LITERS)

*** CENTROID (CENCON) = M1CON / MOCON

*** VARIANCE (VARCON) = M2CON / MOCON

*** SKEW COEF (SKECON) = (M3CON/MOCON) / ((M2CON/MOCON)**1.5)

*** FOR MASS:

*** MASS (MASMAS) = MOMAS (UNITS = MG-FT)

*** CENTROID (CENMAS) = M1MAS / MOMAS

*** VARIANCE (VARMAS) = M2MAS / MOMAS

*** SKEW COEF (SKEMAS) = (M3MAS/MOMAS) / ((M2MAS/MOMAS)**1.5)

SUBROUTINE STATS(AVGCON,XO,TOTAL,DELX,INTENS,UAVG,SUMT,STEPT,
1 DEPTH,TARAY,CARAY2,MARAY2,WHICH1,ARAY2,
1 DELT,WHICHX,UNIFLO,DEBUG,XPRINT)
DIMENSION AVGCN(300),UAVG(300),TARAY(300),CARAY2(4,300),
1 MARAY2(4,300),XPRINT(4)
INTEGER TOTAL,STEPT,WHICH1,WHICHX,ARAY2,DEBUG
REAL MOCON,M1CON,M2CON,M3CON,MOMAS,M1MAS,M2MAS,M3MAS,
1 MASS,INTENS,MARAY2,MEDIAN

C *** INITIALIZE VALUES FOR MOMENTS

MOCON = 0.

M1CON = 0.

M2CON = 0.

```

M3CON = 0.
MOMAS = 0.
M1MAS = 0.
M2MAS = 0.
M3MAS = 0.
SUMASS = 0.

```

C *** COMPUTE 0TH AND 1ST MOMENTS

```

IF(WHICH1.EQ.0) THEN
  Q = XPRINT(WHICHX)*INTENS*.00002315
  DO 2 I=1, ARAY2
    IF(I.EQ.1) THEN
      DELT1 = TARAY(2)-TARAY(1)
    ELSE IF(I.EQ.ARAY2) THEN
      DELT1 = TARAY(ARAY2) - TARAY(ARAY2-1)
    ELSE
      DELT1 = .5*(TARAY(I+1)-TARAY(I-1))
    ENDIF
    MOCON = MOCON + (DELT1*CARAY2(WHICHX, I))
    IF(INTENS.EQ.0.) GO TO 1
    SUMASS = SUMASS + MARAY2(WHICHX, I)
1    M1CON = M1CON + (TARAY(I)*DELT1*CARAY2(WHICHX, I))
2    CONTINUE
    IF(INTENS.GT.0.) GO TO 12
    SUMASS = MOCON*UNIFLO*.02832
    GO TO 12
  ENDIF
DO 10 I=1, TOTAL
  X = (I*DELX) - (.5*DELX)
  MOCON = MOCON + (AVGCON(I)*DELX)
  M1CON = M1CON + (X*AVGCON(I)*DELX)
  IF(INTENS.EQ.0.) THEN
    YS = DEPTH
    GO TO 5
  ENDIF
  Q = (XO + X) * INTENS * .00002315
  YS = Q / UAVG(I)
5  MASS = AVGCON(I) * YS * DELX * .02832
  MOMAS = MOMAS + (MASS * DELX)
  M1MAS = M1MAS + (X * MASS * DELX)
10 CONTINUE

```

C *** COMPUTE CENTROIDS

```

12 IF(MOCON.EQ.0.) GO TO 38
  IF(WHICH1.EQ.0) THEN
    CENCON = M1CON/MOCON
    GO TO 13
  ENDIF
  CENCON = M1CON/MOCON
  CENMAS = M1MAS/MOMAS
  CENTRC = CENCON + XO
  CENTRM = CENMAS + XO

```

C *** COMPUTE 2ND AND 3RD MOMENTS

```

13 IF(WHICH1.EQ.0) THEN
    DO 14 I=1, ARAY2
        IF(I.EQ.1) THEN
            DELT1 = TARAY(2)-TARAY(1)
        ELSE IF(I.EQ.ARAY2) THEN
            DELT1 = TARAY(ARAY2)-TARAY(ARAY2-1)
        ELSE
            DELT1 = .5*(TARAY(I+1)-TARAY(I-1))
        ENDIF
        M2CON = M2CON+(((TARAY(I)-CENCON)**2)*
1          CARAY2(WHICHX,I)*DELT1)
        M3CON = M3CON+(((TARAY(I)-CENCON)**3)*
1          CARAY2(WHICHX,I)*DELT1)
14 CONTINUE
    GO TO 22
ENDIF
DO 20 I=1, TOTAL
    X = (I * DELX) - (.5 * DELX)
    M2CON = M2CON+(((X-CENCON)**2)*AVGCON(I)*DELX)
    M3CON = M3CON+(((X-CENCON)**3)*AVGCON(I)*DELX)
    IF(INTENS.EQ.0.) THEN
        YS = DEPTH
        GO TO 15
    ENDIF
    Q = (XO + X) * INTENS * .00002315
    YS = Q / UAVG(I)
15 MASS = AVGCON(I) * YS * DELX * .02832
    SUMASS = SUMASS + MASS
    M2MAS = M2MAS + (((X-CENMAS)**2)*MASS*DELX)
    M3MAS = M3MAS + (((X-CENMAS)**3)*MASS*DELX)
    IF(DEBUG.EQ.7) THEN
        WRITE(6,18) I,X,XO,Q,UAVG(I),YS,AVGCON(I),SUMASS
18 FORMAT(/5X,'I=',I4,3X,'X=',F9.4,3X,'XO=',F10.5,3X,
1      'Q=',F10.6,3X,'UAVG(I)=' ,F10.6/5X,'YS=',F10.6,3X,
1      'AVGCON(I)=' ,F8.2,3X,'SUMASS=' ,F10.6)
    ENDIF
20 CONTINUE

```

C *** COMPUTE VARIANCES

```

22 VARCON = M2CON / MOCON
    IF(WHICH1.EQ.0) GO TO 24
    VARMAS = M2MAS / MOMAS

```

C *** COMPUTE SKEW COEFFICIENTS

```

24 SKECON = (M3CON/MOCON)/((M2CON/MOCON)**1.5)
    IF(WHICH1.EQ.0) GO TO 26
    SKEMAS = (M3MAS/MOMAS)/((M2MAS/MOMAS)**1.5)

```

C *** COMPUTE MEDIAN TIME FOR TIME-CONCENTRATION CURVE.

```

26  IF(WHICH1.EQ.0) THEN
      SUM = 0.
      DO 28 I=1, ARAY2
          IF(I.EQ.1) THEN
              DELT1 = TARAY(2)-TARAY(1)
          ELSE IF(I.EQ.ARAY2) THEN
              DELT1 = TARAY(ARAY2)-TARAY(ARAY2-1)
          ELSE
              DELT1 = .5*(TARAY(I+1)-TARAY(I-1))
          ENDIF
          SUM = SUM + (DELT1*CARAY2(WHICHX,I))
          IF(SUM.GE.(MOCON/2.)) THEN
              IF(I.EQ.1) GO TO 38
              FRAC = ((MOCON/2.)-(SUM-(DELT1*CARAY2(WHICHX,I))))/
1              (DELT1*CARAY2(WHICHX,I))
              MEDIAN = ((TARAY(I)+TARAY(I-1))/2.)+(FRAC*DELT1)
              GO TO 29
          ENDIF
28  CONTINUE

C  *** PRINT RESULTS

29  WRITE(6,30) SUMASS, CENCON, VARCON, SKECON, MEDIAN
30  FORMAT(////5X,'STATISTICS OF CONCENTRATION-TIME CURVE: '//
1      5X,'TOTAL MASS (MG) =' ,F8.5/5X,
1      'CENTROID(SEC) =' ,F8.4/5X,'VARIANCE(SECONDS SQUARED)='
1      ,F8.4/5X,'SKEW COEF =' ,F8.4/5X,'MEDIAN(SEC)=' ,
1      F9.4/8X,'(MEDIAN = TIME WHEN 50 PERCENT OF' ,
1      ' MASS PASSED)')
      GO TO 38
      ENDIF

      WRITE(6,35)
35  FORMAT(////5X,'STATISTICS OF CONCENTRATION-DISTANCE CURVE:')
      WRITE(6,36) SUMT, STEPT, SUMASS, CENTRC, VARCON, SKECON,
1      CENTRM, VARMAS, SKEMAS
36  FORMAT(/5X,'TIME IN SECONDS =' ,11X,F10.2/5X,'TIME STEP NUMBER ='
1      ,15X,I4/5X,'TOTAL MASS IN MILLIGRAMS =' ,F10.5//5X,
1      'CONCENTRATION DISTRIBUTION: ' ,5X,'CENTROID(FT) =' ,2X,F8.4,5X,
1      'VARIANCE(SQ FT) =' ,2X,F8.4,5X,'SKEW COEF =' ,2X,F8.4/5X,
1      'MASS DISTRIBUTION: ' ,14X,'CENTROID(FT) =' ,2X,F8.4,5X,
1      'VARIANCE(SQ FT) =' ,2X,F8.4,5X,'SKEW COEF =' ,2X,F8.4)
38  RETURN
      END

```

***** SUBROUTINE COMPAR *****

*** THIS SUBROUTINE COMPARES THE CONCENTRATION-TIME CURVE COMPUTED
 *** IN THE MAIN PROGRAM (COMCON(L) VS COMTIM(L)) WITH THE
 *** CONCENTRATION-TIME CURVE MEASURED IN LABORATORY (LABCON(L) VS
 *** LABTIM(L)). THE MEASURE OF COMPARISON IS THE AVERAGE OF THE
 *** ABSOLUTE VALUES OF COMPUTED CONCENTRATION MINUS MEASURED CONCENTRATION.

```

SUBROUTINE COMPAR(COMCON, COMTIM, LABCON, LABTIM, POINTS,
1  ARAY2, DEBUG, WHICHX)

  DIMENSION COMCON(4,300), COMTIM(300), LABCON(300), LABTIM(300),
1  X(200), Y(200)
  CHARACTER*10 XT, YT
  CHARACTER*80 MTIT
  INTEGER POINTS, ARAY2, START, COUNT, DEBUG, WHICHX
  REAL LABCON, LABTIM

  CONMAX = 0.
  DELC = 0.
  COUNT = 1
  DELT1 = COMTIM(2)-COMTIM(1)
  DO 100 L=1,POINTS
    IF(COMTIM(1).GE.(LABTIM(L)+DELT1)) THEN
      DELC = DELC + LABCON(L)
      GO TO 80
    ELSE IF(COMTIM(1).GT.LABTIM(L).AND.COMTIM(1).LT.
1    (LABTIM(L)+DELT1)) THEN
      FRAC = (DELT1-(COMTIM(1)-LABTIM(L)))/DELT1
      DELC = DELC+ABS(LABCON(L)-(FRAC*COMCON(WHICHX,1)))
      GO TO 80
    ELSE IF(COMTIM(1).EQ.LABTIM(L)) THEN
      DELC = DELC+ABS(COMCON(WHICHX,1)-LABCON(L))
      GO TO 80
    ENDIF
    START = COUNT
    DO 20 M=START,ARAY2
      IF(COMTIM(M).EQ.LABTIM(L)) THEN
        DELC = DELC+ABS(COMCON(WHICHX,M)-LABCON(L))
        COUNT = M - 1
        GO TO 80
      ELSE IF(COMTIM(M).GT.LABTIM(L)) THEN
        FRAC = (COMTIM(M)-LABTIM(L))/(COMTIM(M)-
1          COMTIM(M-1))
        DELC = DELC+ABS(LABCON(L)-(COMCON(WHICHX,M)-
1          (FRAC*(COMCON(WHICHX,M)-COMCON(WHICHX,(M-1))
1          ))))
        COUNT = M - 1
        GO TO 80
      ENDIF
20  CONTINUE

```

```

      IF(LABTIM(L).GT.COMTIM(ARRAY2)) THEN
        AVERAG = DELC/(L-1)
        GO TO 105
      ENDIF
      WRITE(6,30) L
30     FORMAT(//5X,'***TERMINATED***'/5X,'SUBROUTINE COMPAR',
1       ' COULD NOT COMPUTE A DIFFERENCE BETWEEN LAB CONC',
1       ' AND COMPUTED CONC AT LABTIM(',I2,').')
      GO TO 120
80     IF(DEBUG.EQ.7) THEN
        WRITE(6,90) L, LABTIM(L), DELC
90     FORMAT(5X,'L=',I3,5X,'LABTIM(L)=' ,F8.3,5X,
1       'DELC=' ,F12.4)
      ENDIF
      IF(LABCON(L).GT.CONMAX) CONMAX=LABCON(L)
100    CONTINUE
C     ***
C     *** COMPUTE AVERAGE ABSOLUTE VALUE OF COMPUTED
C     *** CONCENTRATION MINUS MEASURED CONCENTRATION.
C     ***
      AVERAG = DELC / POINTS
105    WRITE(6,110) AVERAG
110    FORMAT(/////5X,'*** COMPARISON OF COMPUTED CURVE VS LAB CURVE'
1      , '***'/5X,'AVERAGE ABSOLUTE VALUE OF COMPUTED CONCENTRATION'
1      , ' MINUS LAB CONCENTRATION (PPB) =',F8.2)

      DO 114 I=1,POINTS
        X(I) = LABTIM(I)
        Y(I) = LABCON(I)
114    CONTINUE
      DO 116 I=1,ARRAY2
        X(POINTS+I) = COMTIM(I)
        Y(POINTS+I) = COMCON(WHICHX,I)
116    CONTINUE
      ITOTAL = POINTS + ARRAY2
      XT='TIME (SEC) '
      YT = 'CONC (PPB) '
      MTIT = '
CONCENTRATION VS TIME CURVES
1     YMIN = 0.
      YMAX = 2.0*CONMAX
      XMIN = LABTIM(1)-(.5*(LABTIM(POINTS)-LABTIM(1)))
      XMAX = LABTIM(POINTS)+(.5*(LABTIM(POINTS)-LABTIM(1)))
      CALL MAPA(5,X,Y,1,ITOTAL,XMIN,XMAX,YMIN,YMAX,
1     XT,YT,MTIT,1)
120    RETURN
      END

```

APPENDIX B

COMPARISON OF NUMERICAL MODEL
TO CLEARY AND ADRIAN SOLUTION

Appendix B

COMPARISON OF NUMERICAL MODEL TO CLEARY AND ADRIAN SOLUTION

Cleary and Adrian (1973) presented an analytical solution to the two-dimensional, convective-diffusive, partial differential equation,

$$\frac{\partial C}{\partial t} + U \frac{\partial C}{\partial x} = D_x \frac{\partial^2 C}{\partial x^2} + D_y \frac{\partial^2 C}{\partial y^2} + M \delta(x-x_1) \delta(y-y_1) \delta(t-\tau) \quad (B-1)$$

for an instantaneous, line-source injection (equivalent to a point source in two dimensions) in a uniform velocity field subject to no-flux boundary conditions at the streambed and water surface. The solution is

$$C(x,y,t) = \frac{M \exp \left[- \frac{(x - x_1 - Ut)^2}{4 D_x t} \right]}{H(4 \pi D_x t)^{1/2}} \cdot \left[1 + 2 \sum_{n=1}^{\infty} \exp(-D_y \mu_n^2 t) \cos(\mu_n y) \cos(\mu_n y_1) \right] \quad (B-2)$$

The symbols in the above two equations are given in Table B-1.

The numerical model in the present study is limited to a source with finite dimensions equivalent to the dimensions of one grid cell or a combination of grid cells, while the Cleary and Adrian solution is limited to a source at a point. Also, the numerical model simulates only vertical diffusion; thus, when this method is applied in a uniform velocity field, mass is diffused in the vertical direction only. The Cleary and Adrian solution requires a non-zero value for the

Table B-1

List of Symbols Used in Equations B-1 and B-2

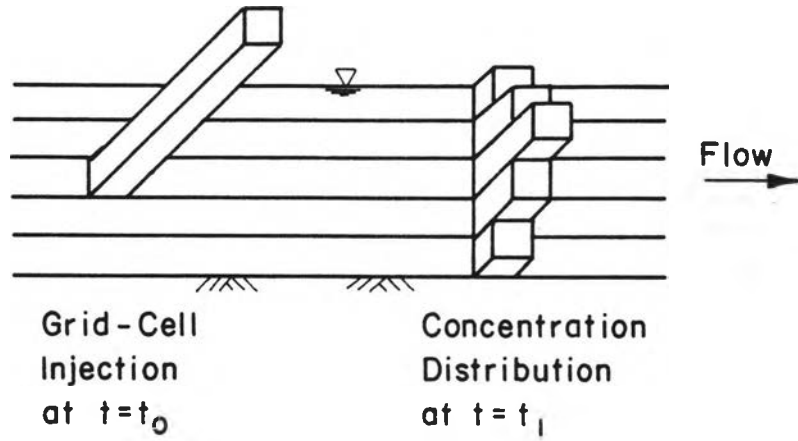
C	= concentration
x	= distance along flow direction
y	= vertical distance above streambed
t	= time
U	= uniform velocity
D_x	= longitudinal diffusion coefficient
D_y	= vertical diffusion coefficient
M	= mass per unit width of stream instantaneously injected at a point (in two dimensions)
$\delta()$	= Dirac delta function
τ	= time of source release
x_1	= longitudinal location of point source
y_1	= vertical location of point source
H	= depth of flow
μ_n	= $(n\pi)/H$
n	= integer

longitudinal diffusion coefficient and therefore models the spread of the point source both longitudinally and vertically. These concepts are shown schematically in Figure B-1.

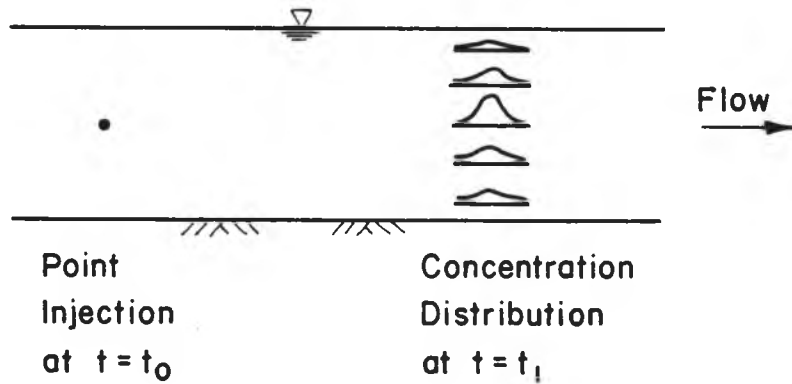
To provide for a valid test, the Cleary and Adrian solution was applied in such a way as to simulate the conditions in the numerical model. This was accomplished by using multiple point sources spaced uniformly over the area of the grid-cell injection. The mass of each point source was set equal to the total mass injected in the numerical model divided by the number of point sources used for the Cleary and Adrian simulation. This result is shown schematically in Figure B-2. By appropriately choosing the number of point sources and the value of the longitudinal diffusion coefficient, the sum of the individual point-source solutions, shown in Figure B-3, yields a concentration distribution with a spatial coverage approximating one cell column and with approximately uniform concentrations over the width of the cell column.

The number of point sources used in this test was 36. The longitudinal diffusion coefficient used was equal to about 0.1 percent of the vertical diffusion coefficient. Other data are given in Chapter 3.

The Cleary and Adrian solution for multiple point sources was coded into a FORTRAN V computer program listed in Attachment B-1. The summation in Eq. B-2 was truncated when the argument of its exponential function fell below -100. Concentrations were computed at points throughout the cell column. The distance between these points was the same as the distances between the multiple point sources. The computed concentrations were averaged over equivalent grid-cell areas.



a) Numerical Model



b) Cleary and Adrian Solution

Figure B-1. Differences in Numerical Model and Cleary and Adrian Solution for Uniform Velocity Field

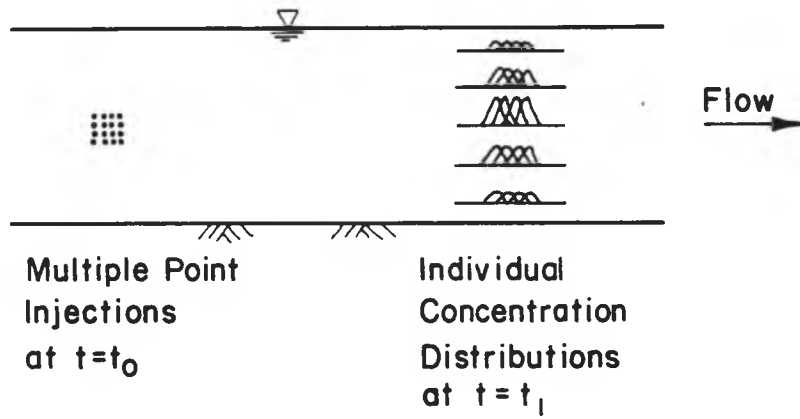


Figure B-2. Results of Multiple Point Injections

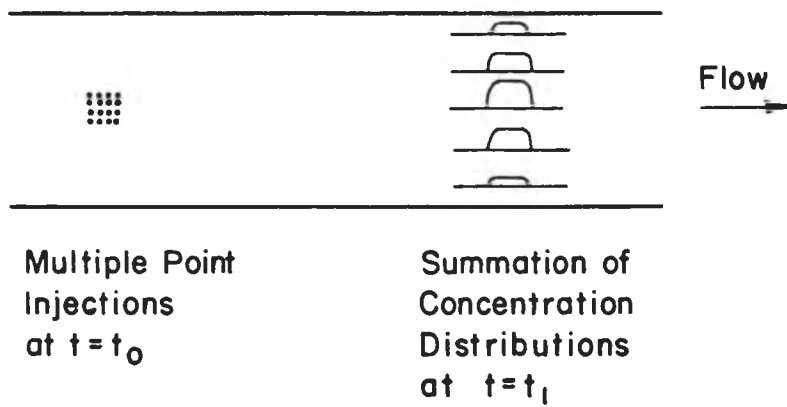


Figure B-3. Summation of Point-Source Solutions

Tests were conducted using 7, 11, and 19 streamtubes in the numerical model. For each test, the value of the dimensionless group

$$\frac{(\Delta y)^2}{\Delta T \cdot \epsilon_y}$$

was varied to determine its effect on the accuracy of the numerical model. The accuracy was measured by computing the Mean Deviation and the Mean Deviation Percent defined as

$$\text{Mean Deviation} = \frac{1}{n} \sum_{i=1}^n |C_{A,i} - C_{N,i}|$$

where

n = number of streamtubes,

$C_{A,i}$ = concentration in streamtube i based on analytical solution,

$C_{N,i}$ = concentration in streamtube i based on numerical model.

and

$$\text{Mean Deviation Percent} = \frac{\text{Mean Deviation}}{\bar{c}} \times 100$$

where

\bar{c} = cross-sectional average concentration.

The results are shown in Tables B-2, B-3, and B-4.

Table B-2

Comparison of Cleary and Adrian Solution to Numerical Model Using 7 Streamtubes

$\frac{(\Delta y)^2}{\Delta T \cdot \epsilon_y}$	Concentrations At 12.25 Seconds After Injection ⁽¹⁾				Mean Deviation	Mean Deviation Percent
	Streamtube No.					
	1	2	3	4		
(Cleary and Adrian Solution)	(124.99)	(138.44)	(155.22)	(162.70)		
0.62	125.30	138.51	155.01	162.35	0.22	0.2
0.93	125.61	138.59	154.79	162.01	0.44	0.3
1.23	125.24	138.50	155.05	162.42	0.18	0.1
1.54	126.45	138.80	154.21	161.07	1.04	0.7
1.85	127.24	139.00	153.66	160.19	1.61	1.1
2.47	126.90	138.91	153.90	160.57	1.36	1.0
3.70	130.01	139.68	151.75	157.12	3.58	2.5
7.41	132.56	140.31	149.98	154.29	5.40	3.8
	Concentrations At 24.50 Seconds After Injection ⁽¹⁾					
(Cleary and Adrian Solution)	(141.54)	(142.53)	(143.76)	(144.32)		
0.62	141.66	142.56	143.69	144.19	0.08	0.1
0.93	141.70	142.57	143.66	144.14	0.11	0.1
1.23	141.65	142.56	143.69	144.20	0.08	0.1

⁽¹⁾ Concentrations in streamtubes 5, 6, and 7 are identical to concentrations in streamtubes 3, 2, and 1, respectively.

Table B-3

Comparison of Cleary and Adrian Solution to Numerical Model Using 11 Streamtubes

$\frac{(\Delta y)^2}{\Delta T \cdot \varepsilon_y}$	Concentrations At 12.25 Seconds After Injection ⁽¹⁾						Mean Deviation	Mean Deviation Percent
	Streamtube No.							
	1	2	3	4	5	6		
(Cleary and Adrian Solution)	(78.43)	(82.38)	(89.05)	(96.31)	(101.86)	(103.93)		
0.25	78.31	82.29	89.02	96.36	101.98	104.09	0.09	0.1
0.50	77.95	82.06	88.98	96.52	102.27	104.42	0.32	0.4
0.75	78.01	82.10	88.99	96.49	102.22	104.36	0.28	0.3
1.00	79.09	82.84	89.15	96.03	101.28	103.23	0.44	0.5
1.25	78.46	82.41	89.06	96.30	101.83	103.89	0.02	0.0
1.50	79.42	83.06	89.20	95.88	100.99	102.89	0.66	0.7
2.00	80.46	83.77	89.36	95.43	100.07	101.81	1.36	1.5
4.00	82.48	85.16	89.66	94.56	98.30	99.69	2.70	3.0
8.00	84.23	86.35	89.92	93.79	96.77	97.88	3.87	4.3
	Concentrations At 24.50 Seconds After Injection ⁽¹⁾							
(Cleary and Adrian Solution)	(89.99)	(90.28)	(90.77)	(91.31)	(91.71)	(91.87)		
0.75	89.95	90.26	90.77	91.32	91.75	91.90	0.02	0.0
1.00	90.11	90.36	90.79	91.26	91.61	91.74	0.08	0.1
1.25	90.02	90.30	90.78	91.29	91.69	91.84	0.02	0.0

(1) Concentrations in streamtubes 7, 8, 9, 10, and 11 are identical to concentrations in streamtubes 5, 4, 3, 2, and 1, respectively.

Table B-4

Comparison of Cleary and Adrian Solution to Numerical Model using 19 Streamtubes

$\frac{(\Delta y)^2}{\Delta T \cdot \varepsilon y}$	Concentrations At 12.25 Seconds After Injection ⁽¹⁾										Mean Deviation	Mean Deviation Percent
	Streamtube No.											
	1	2	3	4	5	6	7	8	9	10		
(Cleary and Adrian Solution)	(45.07)	(45.89)	(47.44)	(49.55)	(52.00)	(54.51)	(56.82)	(58.68)	(59.89)	(60.30)		
0.50	44.57	45.44	47.09	49.35	51.95	54.64	57.10	59.08	60.37	60.81	0.33	0.6
0.84	45.08	45.90	47.44	49.55	52.00	54.51	56.82	58.68	59.88	60.29	0.00	0.0
1.01	45.53	46.30	47.75	49.74	52.03	54.40	56.57	58.32	59.45	59.84	0.29	0.6
1.26	45.09	45.91	47.45	49.56	52.00	54.51	56.81	58.67	59.87	60.28	0.01	0.0
1.51	45.73	46.48	47.89	49.82	52.05	54.35	56.46	58.15	59.25	59.63	0.43	0.8
2.10	46.48	47.15	48.41	50.13	52.12	54.16	56.04	57.55	58.53	58.87	0.91	1.7
4.19	47.73	48.26	49.26	50.63	52.22	53.85	55.35	56.55	57.33	57.60	1.72	3.3
	Concentrations At 24.5 Seconds After Injection ⁽¹⁾											
(Cleary and Adrian Solution)	(52.07)	(52.14)	(52.25)	(52.40)	(52.59)	(52.77)	(52.94)	(53.08)	(53.16)	(53.19)		
0.84	52.08	52.14	52.25	52.41	52.59	52.77	52.94	53.07	53.16	53.19	0.00	0.0
1.01	52.15	52.20	52.30	52.43	52.59	52.75	52.90	53.02	53.10	53.12	0.05	0.1
1.26	52.08	52.14	52.26	52.41	52.59	52.77	52.94	53.07	53.16	53.19	0.00	0.0

⁽¹⁾ Concentrations in streamtubes 11, 12, 13, 14, 15, 16, 17, 18, and 19 are identical to concentrations in streamtubes 9, 8, 7, 6, 5, 4, 3, 2, and 1, respectively.

ATTACHMENT B-1

```

PROGRAM CLEARY(INPUT,OUTPUT,TAPE5=INPUT,TAPE6=OUTPUT)
DIMENSION C(10,100),CONC(10,100),CONCEN(15),TERM(100)
REAL MASS
INTEGER POINTS,TUBES
READ(5,10) MASS,X1,Y1,VEL,DX,DY,DEPTH,TIME,TUBES
10  FORMAT(F13.10,2F10.8/F10.5,2F15.10,F10.8/F10.5,I10)
WRITE(6,20) MASS,X1,Y1,VEL,DX,DY,DEPTH,TIME,TUBES
20  FORMAT(/////20X,'****DATA INPUT***'///5X,'MASS(MG)=' ,
1    F13.10/5X,'X(FT)=' ,F10.8/5X,'Y(FT)=' ,F10.8/5X,
1    'VEL(FT/SEC)=' ,F10.5/5X,'DX(SQ FT/SEC)=' ,F15.10/
1    5X,'DY(SQ FT/SEC)=' ,F15.10/5X,'DEPTH(FT)=' ,F10.8/
1    5X,'TIME(SEC)=' ,F10.5/5X,'TUBES=' ,I5///20X,
1    '****PROGRAM OUTPUT****'///)
PI = 3.1415927
POINTS = TUBES*6

DO 200 J=1,POINTS
  DO 100 I=1,9
    X = 3.985698 + (.0001130*REAL(I-1))
    Y = .0073985 - (.0001130*REAL(J-1))
    ARGMT = ((X-X1-(VEL*TIME))**2)/(4.*DX*TIME)
    IF(ARGMT.GT.100.) THEN
      C(I,J) = 0.
      GO TO 45
    ENDIF
    EXP1 = EXP(-ARGMT)
    DEMON = DEPTH*((4.*PI*DX*TIME)**.5)
    TOTAL = 0.
    K = 0
30   K = K+1
    ARGMT = DY*((REAL(K)*PI/DEPTH)**2)*TIME
    IF(ARGMT.GT.100.) THEN
      TERM(K) = 0.
      GO TO 40
    ENDIF
    TERM(K) = EXP(-ARGMT)*COS((REAL(K)*PI*Y)/
1    DEPTH)*COS((REAL(K)*PI*Y1)/DEPTH)
    TOTAL = TOTAL+TERM(K)
    GO TO 30
40   C(I,J) = (MASS*EXP1/DENOM)*(1.+
1    (2.*TOTAL))/ .02832
45   WRITE(6,50) X,Y,I,J,C(I,J)
50   FORMAT(5X,'X=' ,F11.7,5X,'Y=' ,F11.7,5X,
1    'C(' ,I2,',',',',I2,',')=' ,F11.5)
100  CONTINUE
200  CONTINUE

```

```
K=0
DO 300 J=1,POINTS
  CONC(1,J)=C(1,J)+C(2,J)+C(3,J)+C(4,J)+C(5,J)
  CONC(2,J)=C(1,J)+C(2,J)+C(3,J)+C(4,J)+C(5,J)+C(6,J)
  CONC(3,J)=C(2,J)+C(3,J)+C(4,J)+C(5,J)+C(6,J)+C(7,J)
  CONC(4,J)=C(3,J)+C(4,J)+C(5,J)+C(6,J)+C(7,J)+C(8,J)
  CONC(5,J)=C(4,J)+C(5,J)+C(6,J)+C(7,J)+C(8,J)+C(9,J)
  CONC(6,J)=C(5,J)+C(6,J)+C(7,J)+C(8,J)+C(9,J)
  WRITE(6,250) (CONC(I,J),I=1,6)
250  FORMAT(1X,6F12.4)
300  CONTINUE

DO 400 K=1,TUBES
  ISTART=(6*(K-1))+1
  IEND=ISTART+5
  CONCEN(K)=0.
  DO 350 J=ISTART,IEND
    DO 340 I=1,6
      CONCEN(K)=CONCEN(K)+CONC(I,J)
340  CONTINUE
350  CONTINUE
  CONCEN(K)=CONCEN(K)/36
400  CONTINUE

DO 500 K=1,TUBES
  WRITE(6,450) K,CONCEN(K)
450  FORMAT(5X,'CONCEN(',I2,')=',F10.4)
500  CONTINUE

STOP
END
```

APPENDIX C

COMPARISON OF NUMERICAL MODEL
TO YEH AND TSAI MODEL

Appendix C

COMPARISON OF NUMERICAL MODEL TO YEH AND TSAI SOLUTION

Yeh and Tsai (1976) presented an analytical solution to the two-dimensional, steady-state, convective-diffusive, partial differential equation,

$$u \frac{\partial C}{\partial x} = \frac{\partial}{\partial y} \left(D_y \frac{\partial C}{\partial y} \right) + S(x,y) \quad (C-1)$$

for a continuously-released line source (equivalent to a point source in two dimensions) in shear flow subject to no-flux boundary conditions at the streambed and water surface. The velocity profile and diffusion coefficient are expressed as power functions,

$$u = a y^m \quad (C-2)$$

and

$$D_y = b y^n \quad (C-3)$$

The solution is

$$C(x,y) = M \left[\frac{1+m}{aH^{(1+m)}} + \sum_{i=1}^{\infty} \left\{ \alpha_i^2 y^{\left(\frac{1-n}{2}\right)} J_{-v} \left(2 v \lambda_i y^{\left(\frac{1-n}{2v}\right)} \right) \cdot y_1^{\left(\frac{1-n}{2}\right)} J_{-v} \left(2 v \lambda_i y_1^{\left(\frac{1-n}{2v}\right)} \right) \exp \left[- \frac{b(1-n)}{a} \lambda_i^2 (x-x_1) \right] \right\} \right] \quad (C-4)$$

where

$$v = \frac{1-n}{2+m-n} \quad (C-5)$$

and λ_i and α_i are defined by

$$J_{-v+1} \left(2 v \lambda_i H^{\left(\frac{1-n}{2v}\right)} \right) = 0 \quad (C-6)$$

and

$$\alpha_i^2 = \frac{2+m-n}{aH^{(2+m-n)} J_{-v}^2 \left(2 v \lambda_i H^{\left(\frac{1-n}{2v}\right)} \right)} \quad (C-7)$$

The symbols in the above equations are defined in Table C-1.

The Yeh and Tsai solution was applied using multiple point sources spaced uniformly over the equivalent area of a grid cell, as explained previously for the Cleary and Adrian solution. In the present case, the longitudinal dimension of all grid cells was set to 0.35 feet, the value used in the model runs described in Chapter 5. Thirty point sources were used to simulate a uniform injection over the area of a grid cell--three horizontal rows of ten point sources. The injection location was in the streamtube located at middepth. A continuous injection concentration of 1000 was introduced into this streamtube's grid cell at the injection location. An equivalent mass rate was used for the point sources as explained in Chapter 3. Thirteen streamtubes were used in this test.

Values of the coefficients in Eqs. C-2 and C-3 were

$$a = 0.7488$$

$$m = 1/7$$

$$b = 30 \times 10^{-8}$$

$$n = 0$$

Additional data used in the test are contained in Table 3-7.

The Yeh and Tsai solution for multiple point sources was coded into a FORTRAN V computer program listed in Attachment C-1. The

program includes a subroutine to compute the value of the Bessel function of the first kind of order $-v$ defined as (when v is not an integer)

$$J_{-v}(t) = \sum_{m=0}^{\infty} \frac{(-1)^m t^{-v+2m}}{2^{-v+2m} m! \Gamma(-v+m+1)} \quad (\text{C-8})$$

where $\Gamma(\) =$ Gamma function. The summation in Eq. C-8 was terminated when the absolute value of the last term computed in the summation was either less than 0.001 or less than 0.1 percent of the summation of the previously computed terms.

Oliver (1960) presented tables of Bessel function arguments which satisfy

$$J_{\beta}(\) = 0 \quad (\text{C-9})$$

These tables were used to solve for λ_i in Eq. C-6. In the present study, Eq. C-5 gives

$$v = 0.4667$$

Therefore,

$$-v+1 = 0.5333$$

Tables published in Oliver (1960) list the first 15 Bessel function arguments satisfying Eq. C-9 for $\beta = 0.5$ and $\beta = 1.0$. Arguments were estimated for $\beta = 0.5333$ by linear interpolation and are listed in Table C-2.

The summation of terms in Eq. C-4 was terminated when the absolute value of the last computed term was less than 0.01, given that at least four terms had been computed.

Results are presented in Chapter 3.

Table C-1

List of Symbols Used in Equations C-1 through C-7

C	= concentration
x	= distance along flow direction
y	= vertical distance above streambed
u	= point velocity
D_y	= vertical diffusion coefficient
S	= source function
a,b,m,n	= constants
M	= rate of mass injection per unit width
H	= depth of flow
$J_{-v}(\), J_{-v+1}(\)$	= Bessel function of the first kind of order $-v$ or of order $-v+1$
x_1	= longitudinal location of point source
y_1	= vertical location of point source

Table C-2

Bessel Function Arguments Satisfying Eq. C-9 Obtained by
Linear Interpolation of Data Presented by Oliver (1960)

Number	Argument
1	3.187600
2	6.332012
3	9.474691
4	12.616859
5	15.758807
6	18.900643
7	22.042411
8	25.184136
9	28.325834
10	31.467510
11	34.609172
12	37.750822
13	40.892464
14	44.034098
15	47.175728

ATTACHMENT C-1

```

PROGRAM YEH(INPUT,OUTPUT,TAPE5=INPUT,TAPE6=OUTPUT)
DIMENSION CONC(40,20),BETA(20),C(40,20)
INTEGER BETAS,START,END,TRACE
REAL MASS,M,N,ORDER,JV,LAMDA,JVZ,JVZS,NU
READ(5,20) MASS,A,M,B,N,DEPTH,XS,ZS,BETAS,TRACE
20  FORMAT(F14.11,F10.6,F10.6/F12.9,F10.6,F12.8/2F15.12/
1    2I10)
READ(5,30) (BETA(J),J=1,BETAS)
30  FORMAT((5F10.6))
WRITE(6,42) MASS,A,M,B,N,DEPTH,XS,ZS,BETAS,TRACE
42  FORMAT(/////20X,'*****DATA INPUT*****'//5X,'MASS(MG=',
1    F12.8/5X,'A=',F10.6/5X,'M=',F10.6/5X,'B=',F12.9/5X,
1    'N=',F10.6/5X,'DEPTH=',F12.8/5X,'XS=',F12.8/5X,
1    'ZS=',F12.8/5X,
1    'BETAS=',I10/5X,'TRACE=',I10)
WRITE(6,44) (I,BETA(I),I=1,BETAS)
44  FORMAT((5X,'BETA(',I2,')=',F10.6))
WRITE(6,46)
46  FORMAT(/////20X,'*****PROGRAM OUTPUT*****'/////),
1    ' CONCENTRATIONS DUE TO A POINT SOURCE: '//)

JV=0.
NU=(1.-N)/(2.+M-N)
ORDER=-NU
CONST=(1.+M)/(A*(DEPTH**(1.+M)))
ZSEXP=ZS**((1.-N)/(2.*NU))
WRITE(6,50) NU,ORDER,CONST,ZSEXP
50  FORMAT(/5X,'NU=',F10.7/5X,'ORDER=',F10.7/5X,
1    'CONST=',F14.8/5X,'ZSEXP=',F10.8)

DO 200 J=1,39
DO 150 I=1,19
X=7.685+(.035*REAL(I-1))
Z=.0073594230769-(.0001911538462*REAL(J-1))
SUM=0.
ZEXP=Z**((1.-N)/(2.*NU))
DO 100 K=1,BETAS
1    LAMDA=BETA(K)/(2.*NU*(DEPTH**((1.-N)/
(2.*NU))))
ARG=BETA(K)
CALL BESSEL(ORDER,ARG,JV,TRACE)
AI2=(2.+M-N)/(A*(DEPTH**(2.+M-N))*(JV**2.))
ARG=2.*NU*LAMDA*ZEXP
CALL BESSEL(ORDER,ARG,JV,TRACE)
JVZ=JV
ARG=2.*NU*LAMDA*ZSEXP
CALL BESSEL(ORDER,ARG,JV,TRACE)

```

```

        JVZS=JV
        STEP=AI2*(Z**((1.-N)/2.))*JVZ*(ZS**((1.-N)/
1          2.))*JVZS*EXP(-(B*(1.-N)/A)*(LAMDA**2.))*(X-XS)
        SUM=SUM+STEP
        IF(TRACE.EQ.1) THEN
            WRITE(6,60) X,Z,ZEXP,BETA(K),LAMDA,AI2,
1              JV,JVZ,ARG,JVZS,STEP,SUM
60          FORMAT(/5X,'X=',F10.6,5X,'Z=',F10.8,
1              5X,'ZEXP=',F10.8,5X,'BETA(K)=',F14.9,5X,
1              'LAMDA=',F14.6/5X,'AI2=',E16.6,5X,
1              'JV=',F30.8,5X,'JVZ=',F30.8/5X,
1              'ARG=',F14.8,5X,'JVZS=',F30.8,5X,
1              'STEP=',F14.8,5X,'SUM=',F14.8)
            ENDIF
            IF(ABS(STEP).LT..01.AND.I.GT.4) GO TO 110
100         CONTINUE
110         CONC(J,I)=(MASS*(CONST+SUM))/0.02832
            IF(REAL(J/5).NE.(REAL(J)/5.)) GO TO 150
            WRITE(6,120)X,Z,J,I,CONC(J,I)
120         FORMAT(5X,'X=',F12.8,5X,'Z=',F12.8,
1              5X,'CONC(',I3,',',I3,')=',F12.5)
150         CONTINUE
200         CONTINUE

        DO 420 K=1,39
            DO 410 L=1,10
                START=11-L
                END=START+9
                C(K,L)=0.
                DO 400 J=START,END
                    C(K,L)=CONC(K,J)+C(K,L)
400             CONTINUE
410             CONTINUE
420             CONTINUE
                WRITE(6,450)
450             FORMAT(///5X,'CONCENTRATIONS DUE TO AREA SOURCE, WHERE'
1              ', ' THE AREA SOURCE IS SIMULATED BY A GRID OF POINT'/
1              ' SOURCES COVERING A DEPTH EQUAL TO ONE STREAMTUBE'
1              ', ' AND A LENGTH EQUAL TO DELTA X: '//)
                DO 500 I=1,39
                    WRITE(6,480) (C(I,L),L=1,10)
480                 FORMAT(10F10.3)
500                 CONTINUE

                WRITE(6,510)
510             FORMAT(/////5X,'AVERAGE CONCETRATIONS IN VERTICAL CELL: '//)

                START=-2
                END=0
                DO 580 J=1,13
                    START=START+3
                    END=END+3

```

```

SUM=0.
DO 560 I=START,END
  DO 550 L=1,10
    SUM=C(I,L)+SUM
550    CONTINUE
560    CONTINUE
    AVGCON=SUM/30.
    WRITE(6,570) AVGCON
570    FORMAT(5X,F10.4)
580    CONTINUE

STOP
END

SUBROUTINE BESSEL(ORDER,ARG,JV,TRACE)
C
C   ***THIS SUBROUTINE COMPUTES VALUE FOR BESSEL FUNCTION
C   ***OF FIRST KIND OF ORDER 'ORDER'.
C
INTEGER TRACE
REAL NUMER, ORDER, MFACT, JV

JV = 0.
M = -1
40  M = M+1
    MFACT = 1.
    IF(M.EQ.0) THEN
      GO TO 65
    ELSE
      DO 60 I=1,M
        MFACT = MFACT*I
60    CONTINUE
      ENDIF
65    NUMER = ((-1.)**M)*(ARG**(ORDER+(2.*M)))
      GAM = GAMMA(ORDER+M+1.)
      DENOM = (2.**((ORDER+(2.*M))))*MFACT*GAM
      CHECK = NUMER/DENOM
      IF(TRACE.EQ.1) THEN
        WRITE(6,70) M, JV, MFACT, NUMER, GAM, DENOM, CHECK
70      FORMAT(5X, 'M=', I5, 5X, 'JV=', F30.8, 5X, 'MFACT=',
1         E16.6/5X, 'NUMER=', E16.6, 5X, 'GAM=', E16.6,
1         5X, 'DENOM=', E16.6, 5X, 'CHECK=', E16.6)
      ENDIF
      TEST=.001*ABS(JV)
      IF((ABS(CHECK).LT..0001.OR.ABS(CHECK).LT.TEST).AND.
1      M.GT.4) GO TO 80
      JV = JV+CHECK
      GO TO 40
80    RETURN
      END

```

APPENDIX D

DERIVATION OF LONGITUDINAL DISPERSION COEFFICIENT
USING A CONSTANT VERTICAL DIFFUSION COEFFICIENT
IN INFINITELY-WIDE, STEADY, UNIFORM, TURBULENT FLOW

Appendix D

DERIVATION OF LONGITUDINAL DISPERSION COEFFICIENT USING A CONSTANT
VERTICAL DIFFUSION COEFFICIENT IN INFINITELY-WIDE, STEADY,
UNIFORM, TURBULENT FLOW

Substituting Eq. 3-34,

$$u = \bar{u} + \frac{u_s}{\kappa} \left(1 + \ln \frac{y}{y_s}\right) \quad (3-34)$$

and Eq. 3-37,

$$\varepsilon_y = 0.067 y_s u_s \quad (3-37)$$

into Eq. 2-6,

$$D = - \frac{1}{y_s} \int_0^{y_s} u' \int_0^y \frac{1}{\varepsilon_y} \int_0^y u' dy dy dy \quad (2-6)$$

where

$$u' = u - \bar{u}$$

results in

$$\begin{aligned} D &= - \frac{u_s}{0.067 y_s^2 \kappa^2} \int_0^{y_s} \left(1 + \ln \frac{y}{y_s}\right) \int_0^y \int_0^y \left(1 + \ln \frac{y}{y_s}\right) dy dy dy \\ &= - \frac{u_s}{0.067 y_s^2 \kappa^2} \int_0^{y_s} \left(1 + \ln \frac{y}{y_s}\right) \int_0^y y \ln \frac{y}{y_s} dy dy \\ &= - \frac{u_s}{0.067 y_s^2 \kappa^2} \int_0^{y_s} \left(1 + \ln \frac{y}{y_s}\right) \left(\frac{1}{2} y^2 \ln \frac{y}{y_s} - \frac{1}{4} y^2\right) dy \end{aligned}$$

$$\begin{aligned}
&= - \frac{u_s}{0.067 y_s^2 \kappa^2} \int_0^{y_s} \left[\frac{1}{4} y^2 \ln \frac{y}{y_s} - \frac{1}{4} y^2 + \frac{1}{2} y^2 (\ln \frac{y}{y_s})^2 \right] dy \\
&= - \frac{u_s}{0.067 y_s^2 \kappa^2} \left[\frac{1}{4} \left(\frac{1}{3} y^3 \ln \frac{y}{y_s} - \frac{1}{9} y^3 \right) - \frac{1}{4} \left(\frac{1}{3} y^3 \right) \right. \\
&\quad \left. + \frac{1}{6} y^3 (\ln y)^2 - \frac{1}{3} \left(\frac{1}{3} y^3 \ln y - \frac{1}{9} y^3 \right) - \ln y \left(\frac{1}{3} y^3 \ln y - \frac{1}{9} y^3 \right) \right. \\
&\quad \left. + \frac{1}{2} (\ln y)^2 \left(\frac{1}{3} y^3 \right) \right]_0^{y_s} \\
&= - \frac{u_s}{0.067 y_s^2 \kappa^2} \left(- \frac{2}{27} y_s^3 \right) \\
&= \frac{1.1056 u_s y_s}{\kappa^2}
\end{aligned}$$

If von Karman's constant, κ , is taken to be 0.410 as assumed by Elder (1959),

$$D = 6.58 u_s y_s$$

If von Karman's constant is taken to be 0.4 as assumed by Schlichting (1979),

$$D = 6.91 u_s y_s$$

Symbols used in the above derivation are as follows:

D = longitudinal dispersion coefficient

u = point velocity

\bar{u} = vertically-averaged velocity

$u' = u - \bar{u}$

u_s = shear velocity = $\sqrt{y_s g S_o}$

y = vertical distance from streambed

y_s = vertical distance from streambed to water surface

κ = von Karman's constant

ε_y = vertical mixing coefficient

APPENDIX E

SERIES OF COMPUTED CONCENTRATION-TIME CURVES
GENERATED BY NUMERICAL MODEL FOR EACH EXPERIMENT

Injection location from top of plane = 27.7 ft
 Measurement location from top of plane = 40.8 ft
 Total mass per foot width = 0.169 mg

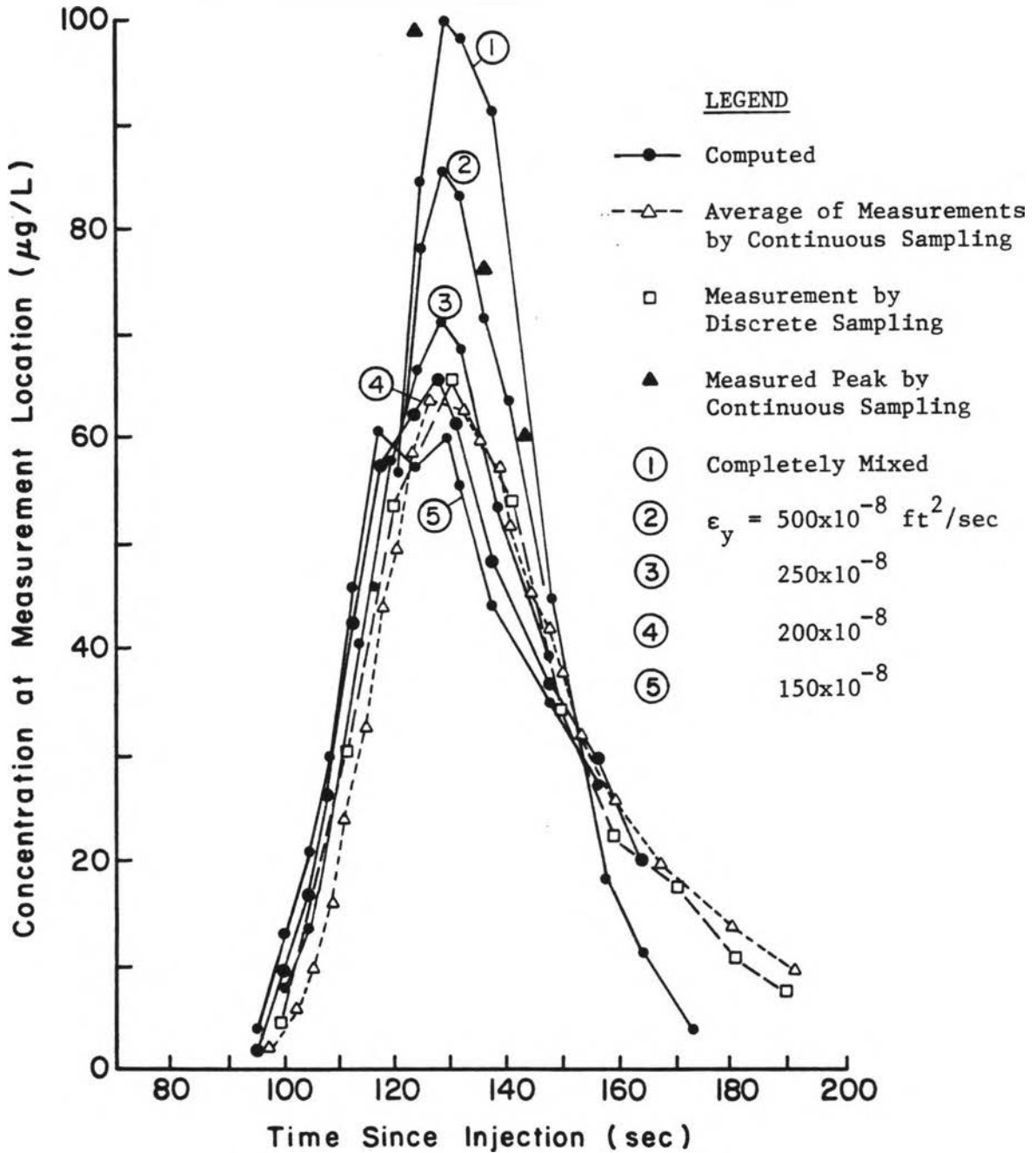


Figure E-1. Comparison of Measured and Computed Concentration Curves for $S_o = 0.001$ and $i = 2$ (Experiment No. 1a)

Injection location from top of plane = 32.8 ft
 Measurement location from top of plane = 40.8 ft
 Total mass per foot width = 0.181 mg

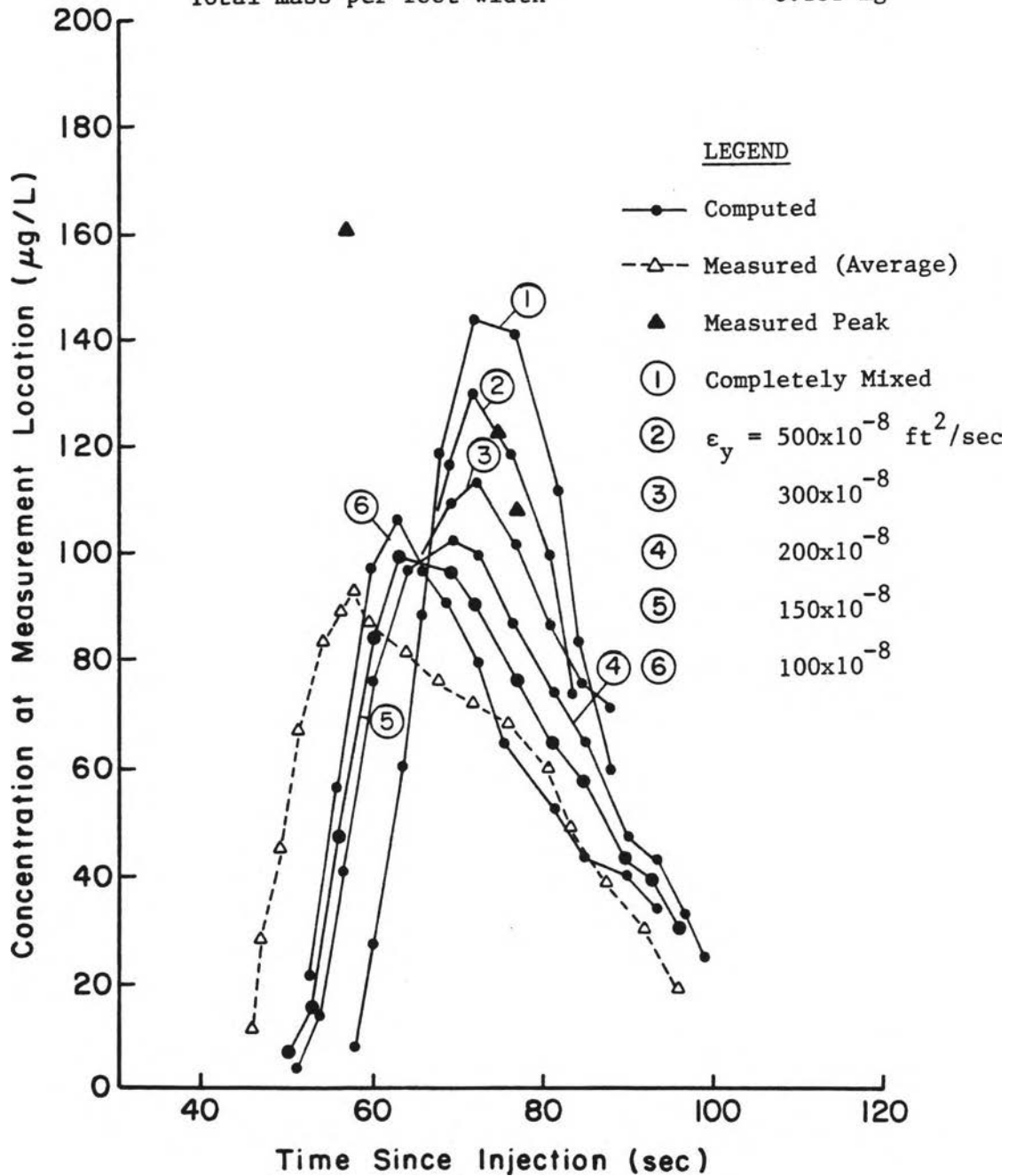


Figure E-2. Comparison of Measured and Computed Concentration Curves for $S_0 = 0.001$ and $i = 2$ (Experiment No 1b)

Injection location from top of plane = 27.7 ft
 Measurement location from top of plane = 40.8 ft
 Total mass per foot width = 0.212 mg

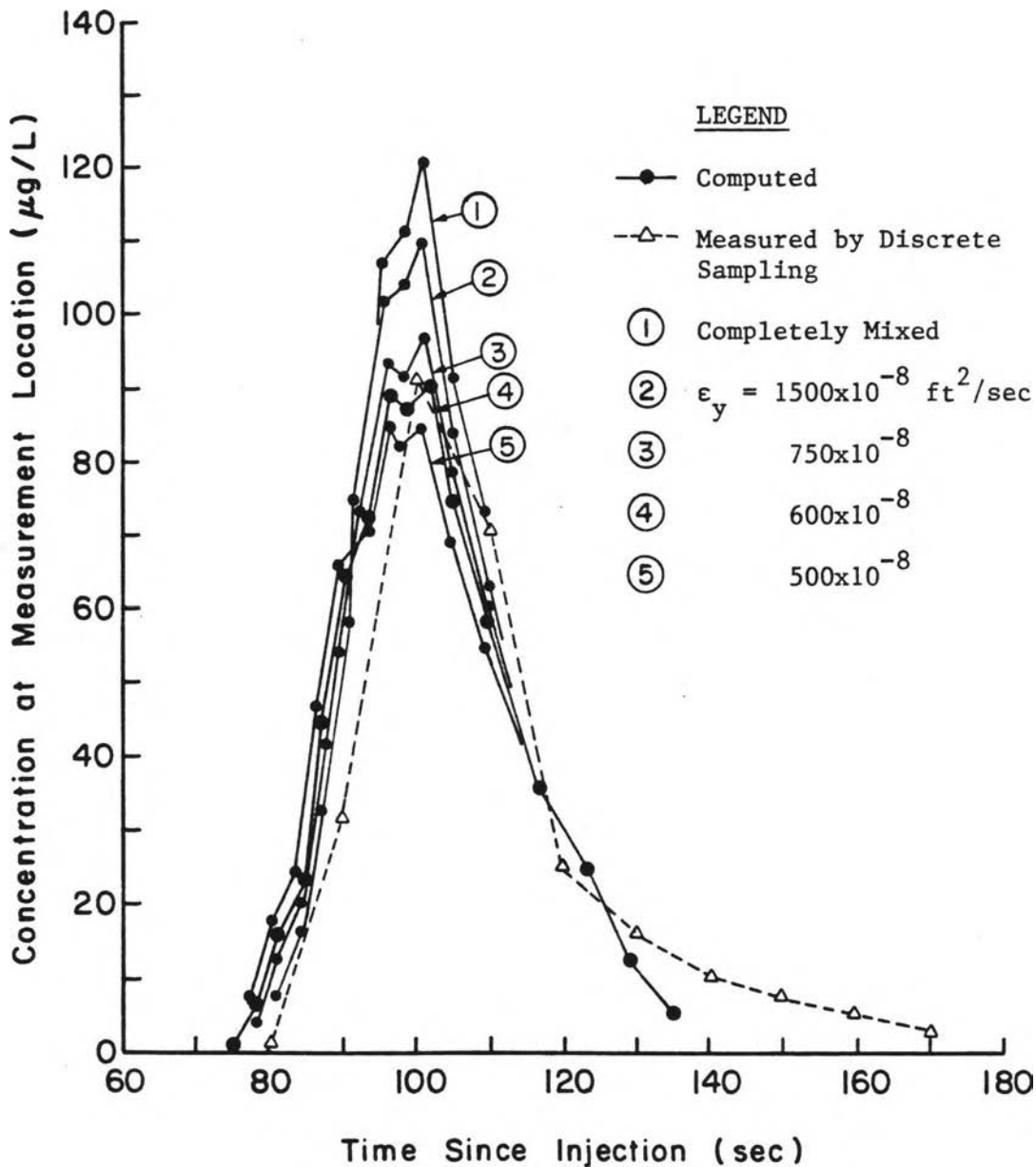


Figure E-3. Comparison of Measured and Computed Concentration Curves for $S_0 = 0.001$ and $i = 3$ (Experiment No. 2a)

Injection location from top of plane = 32.8 ft
 Measurement location from top of plane = 40.8 ft
 Total mass per foot width = 0.224 mg

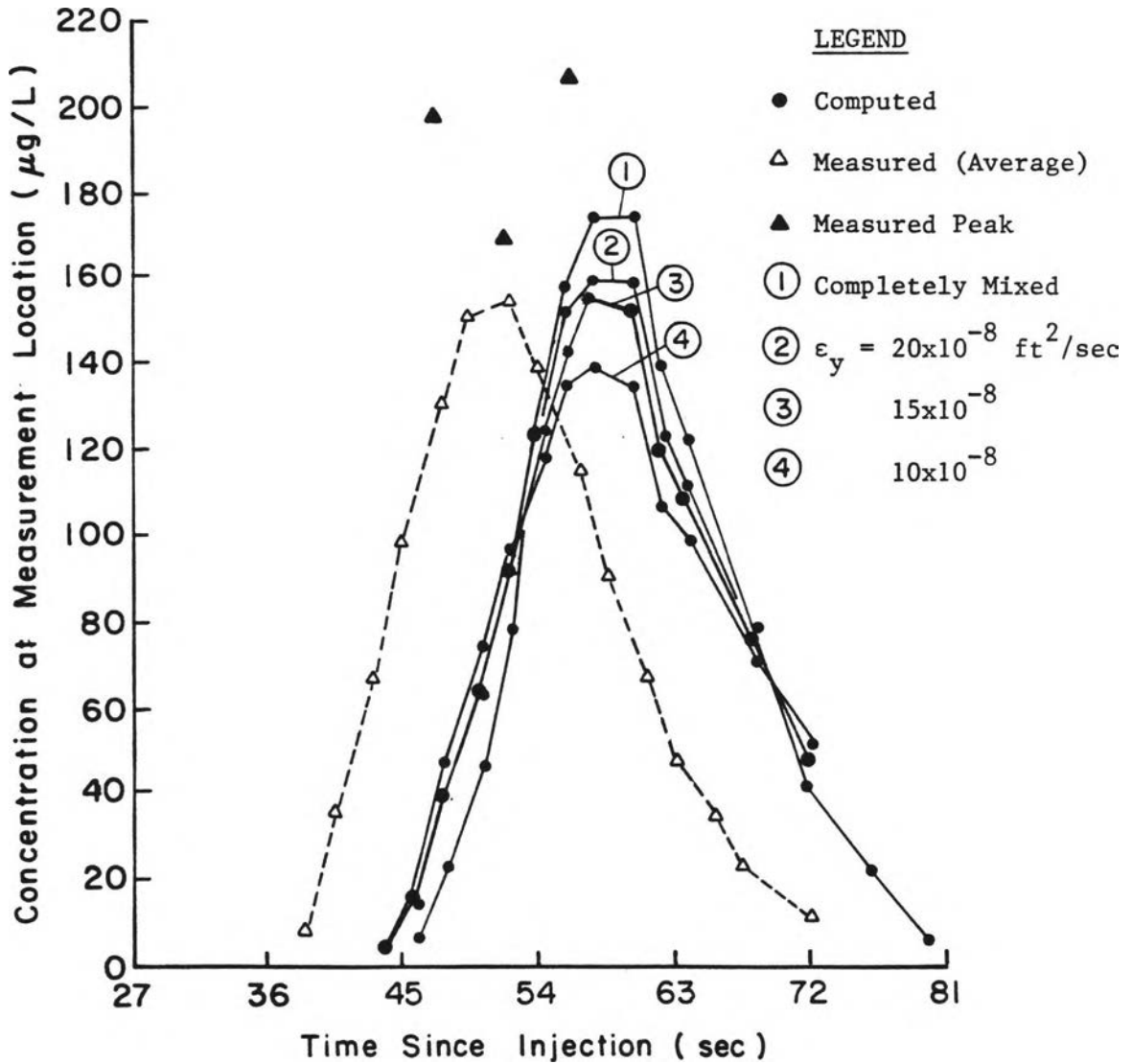


Figure E-4. Comparison of Measured and Computed Concentration Curves for $S_o = 0.001$ and $i = 3$ (Experiment No. 2b)

Injection location from top of plane = 32.8 ft
 Measurement location from top of plane = 40.8 ft
 Total mass per foot width = 0.262 mg

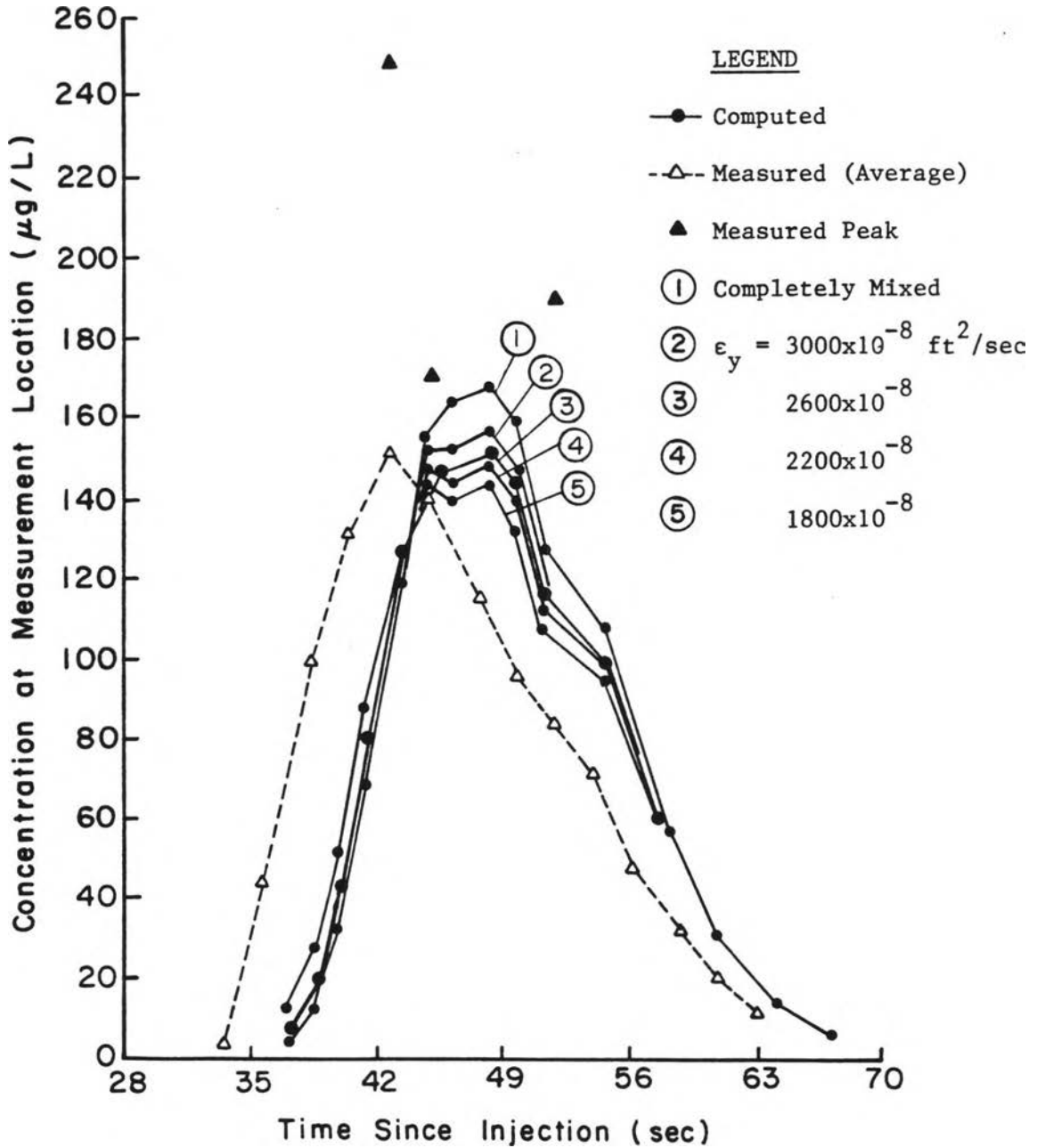


Figure E-5. Comparison of Measured and Computed Concentration Curves for $S_0 = 0.001$ and $i = 4$ (Experiment No. 3)

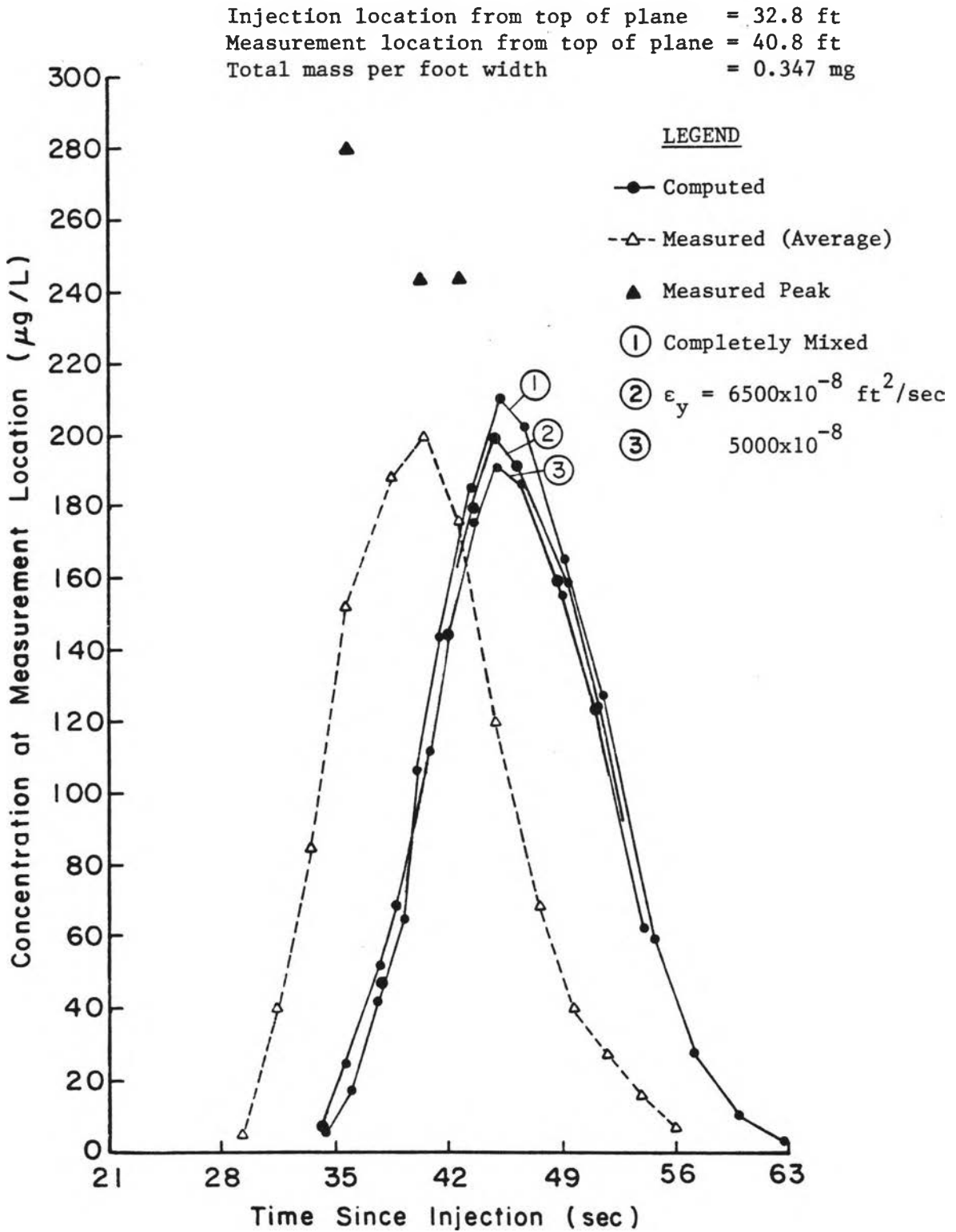


Figure E-6. Comparison of Measured and Computed Concentration Curves for $S_o = 0.001$ and $i = 5$ (Experiment No. 4)

Injection location from top of plane = 32.8 ft
 Measurement location from top of plane = 40.8 ft
 Total mass per foot width = 0.065 mg

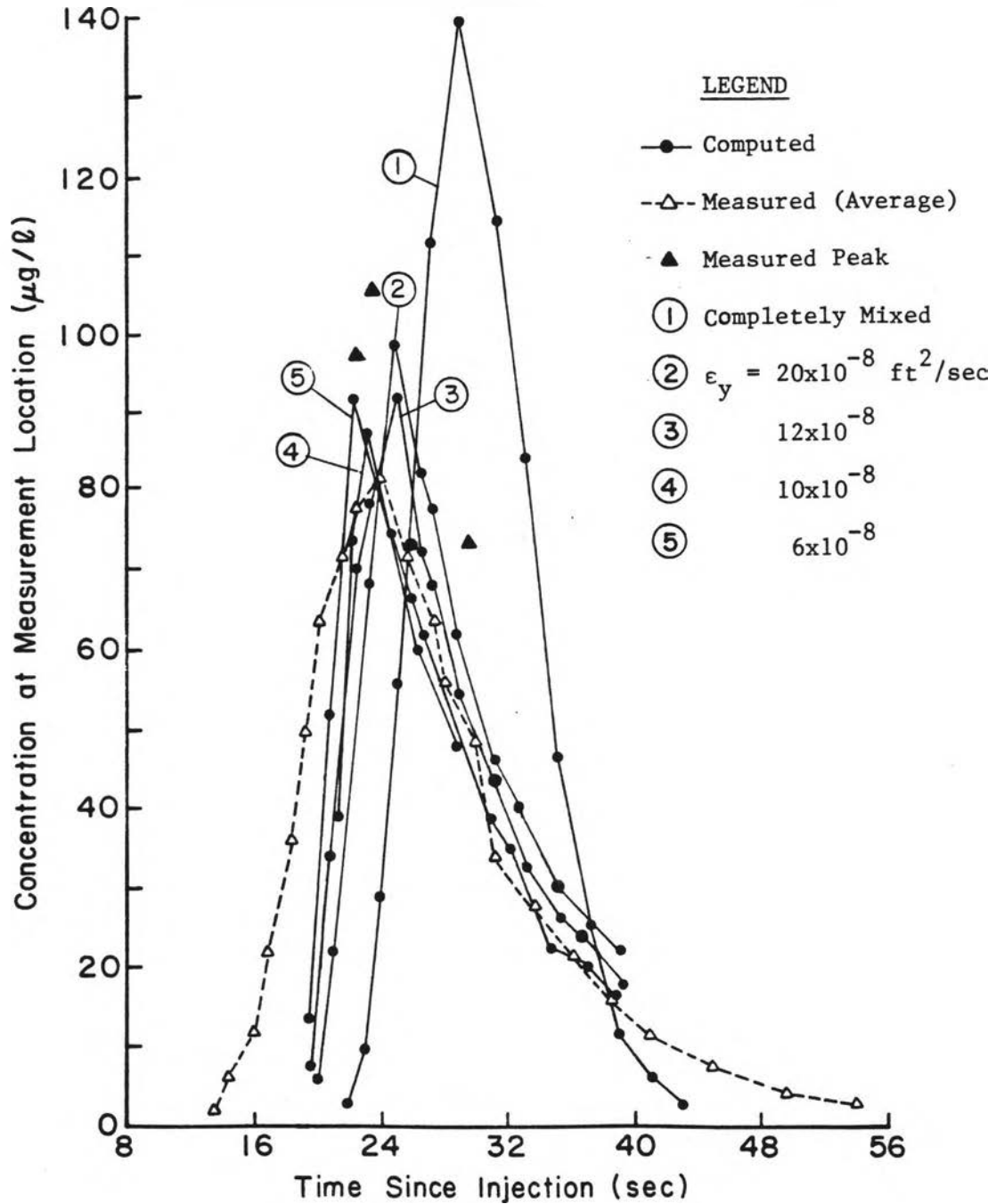


Figure E-7. Comparison of Measured and Computed Concentration Curves for $S_0 = 0.015$ and $i = 2$ (Experiment No. 5)

Injection location from top of plane = 32.8 ft
 Measurement location from top of plane = 40.8 ft
 Total mass per foot width = 0.060 mg

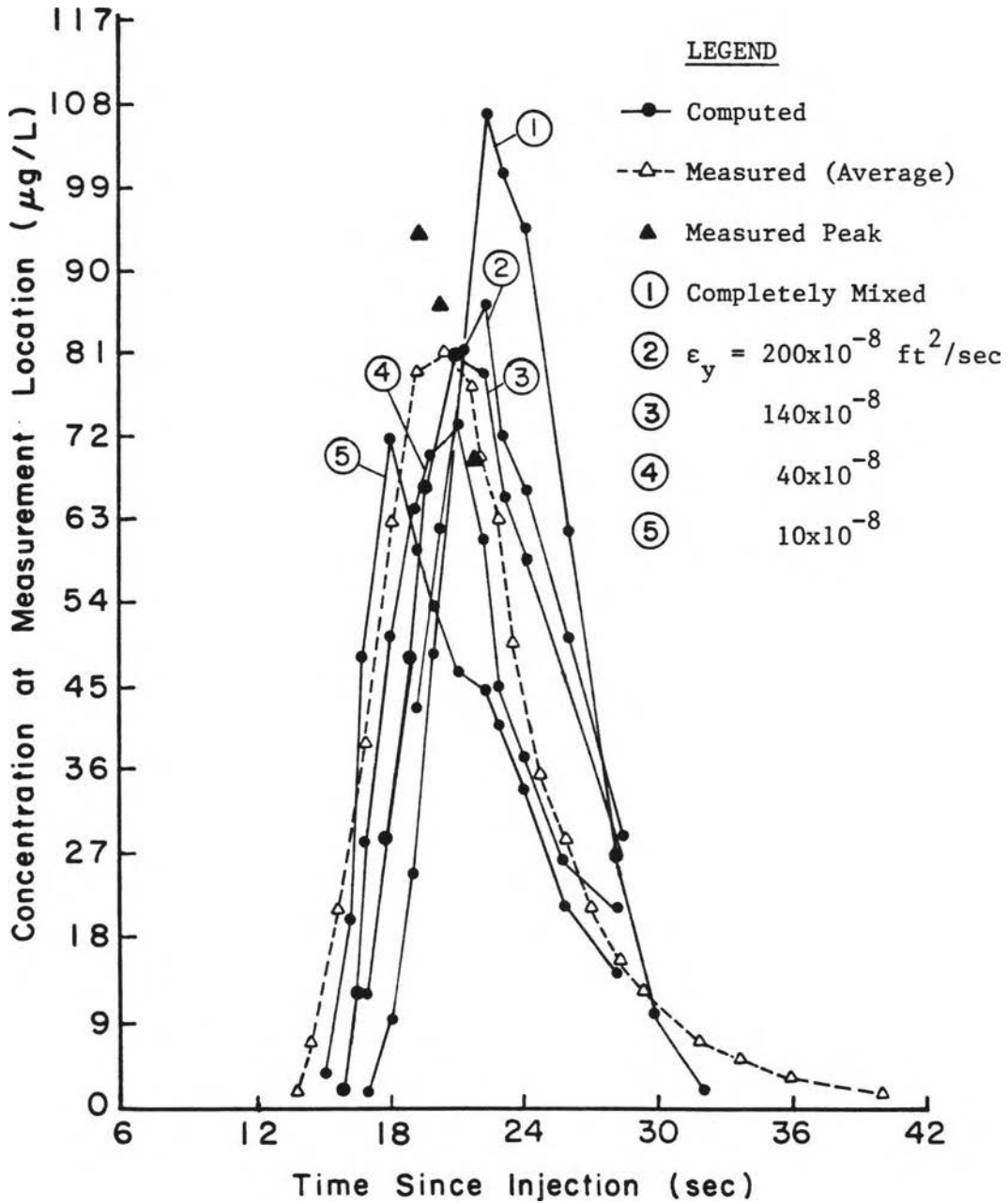


Figure E-8. Comparison of Measured and Computed Concentration Curves for $S_0 = 0.015$ and $i = 3$ (Experiment No. 6)

Injection location from top of plane = 32.8 ft
 Measurement location from top of plane = 40.8 ft
 Total mass per foot width = 0.060 mg

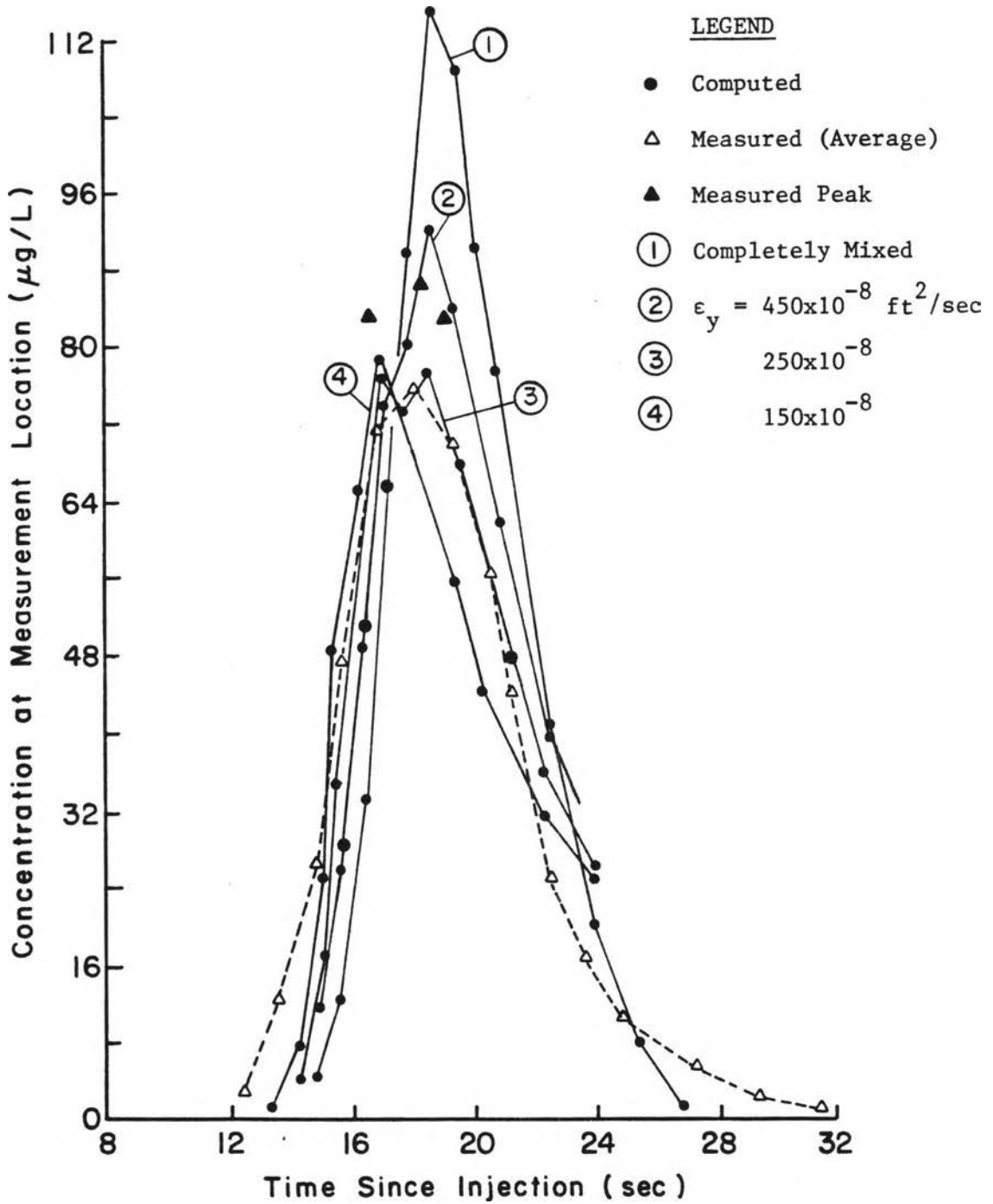


Figure E-9. Comparison of Measured and Computed Concentration Curves for $S_o = 0.015$ and $i = 4$ (Experiment No. 7)

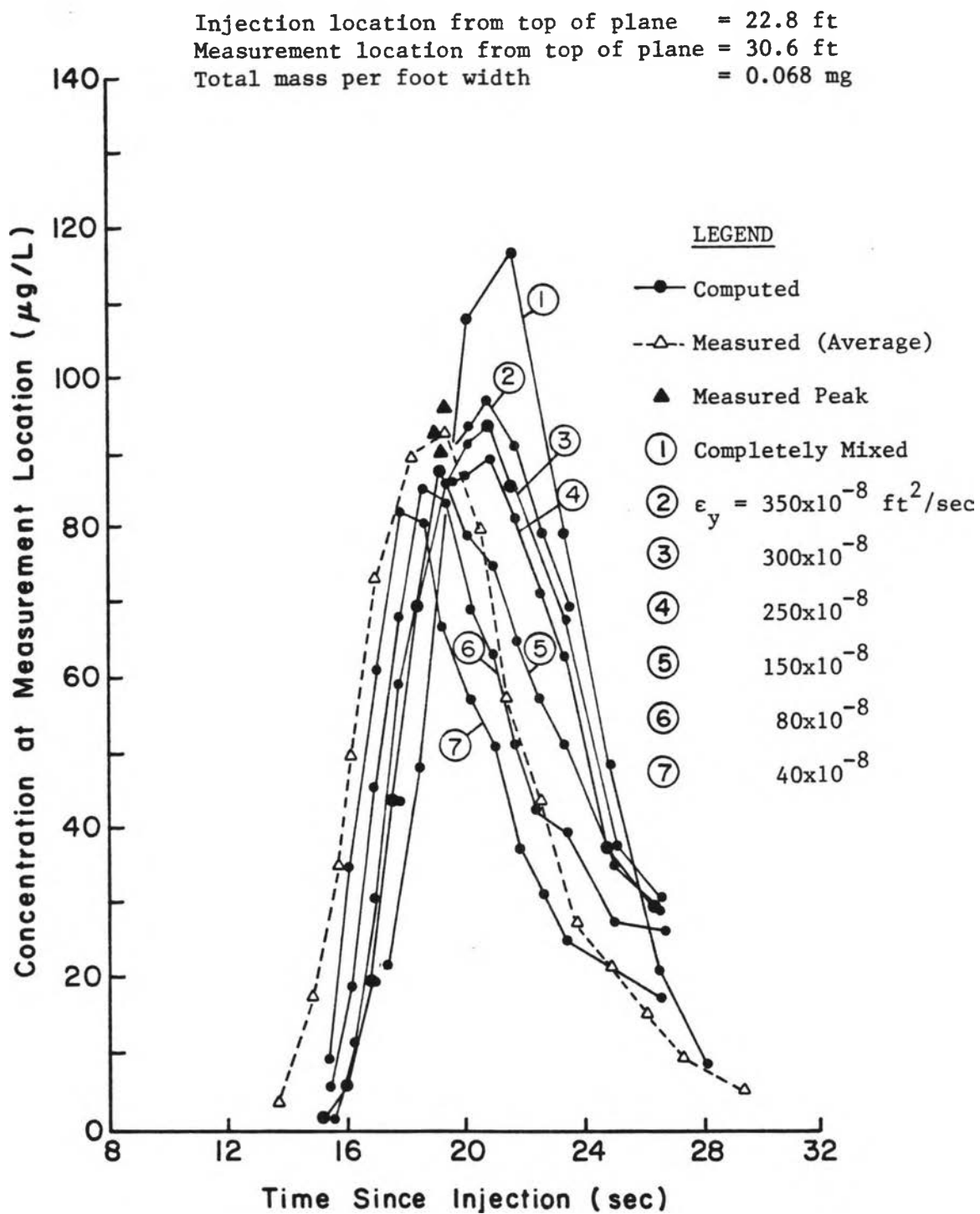


Figure E-10. Comparison of Measured and Computed Concentration Curves for $S_0 = 0.015$ and $i = 5$ (Experiment No. 8)

Injection location from top of plane = 27.7 ft
 Measurement location from top of plane = 40.8 ft
 Total mass per foot width = 0.139 mg

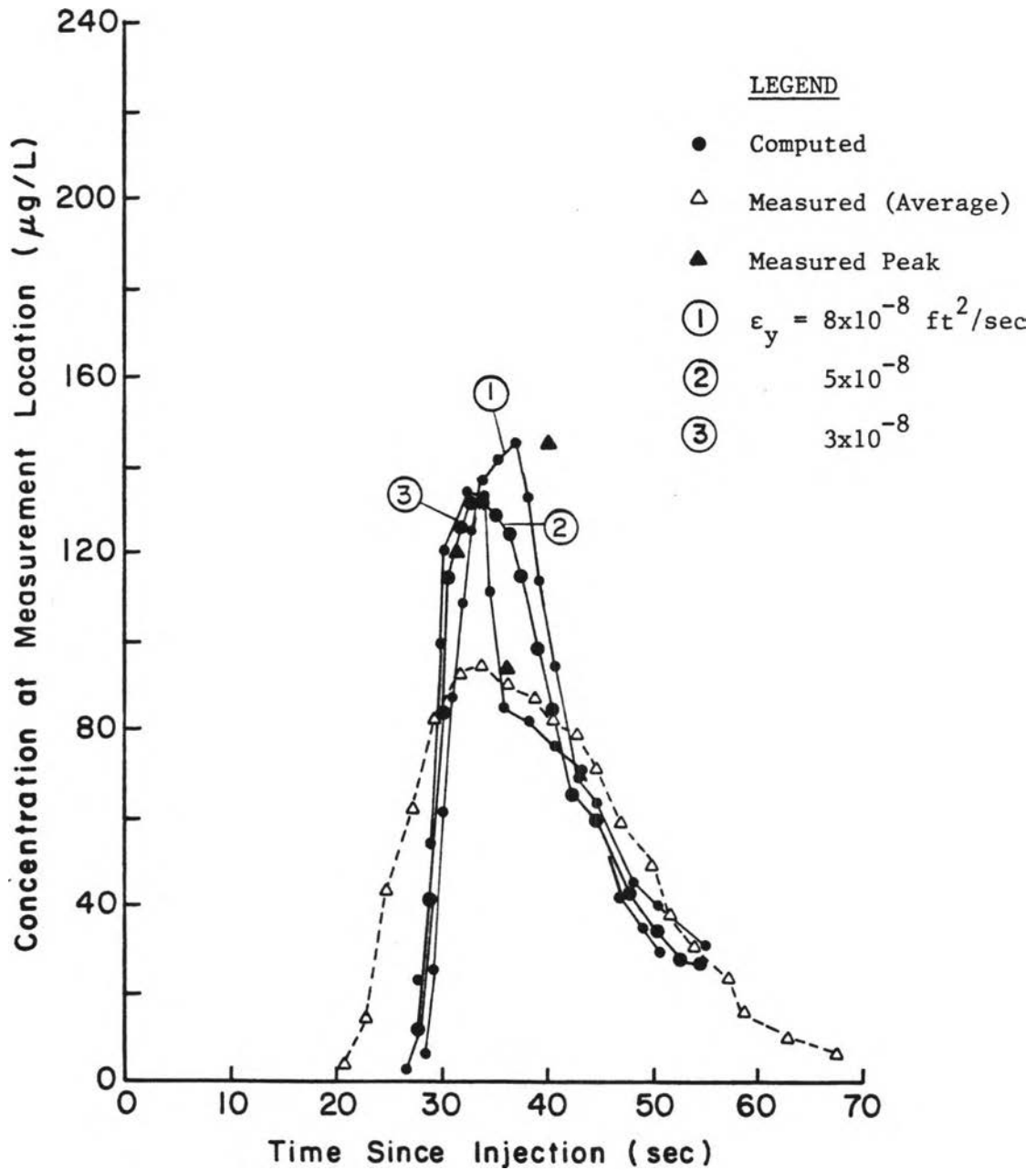


Figure E-11. Comparison of Measured and Computed Concentration Curves for $S_0 = 0.030$ and $i = 2$ (Experiment No. 9a)

Injection location from top of plane = 32.8 ft
 Measurement location from top of plane = 40.8 ft
 Total mass per foot width = 0.142 mg

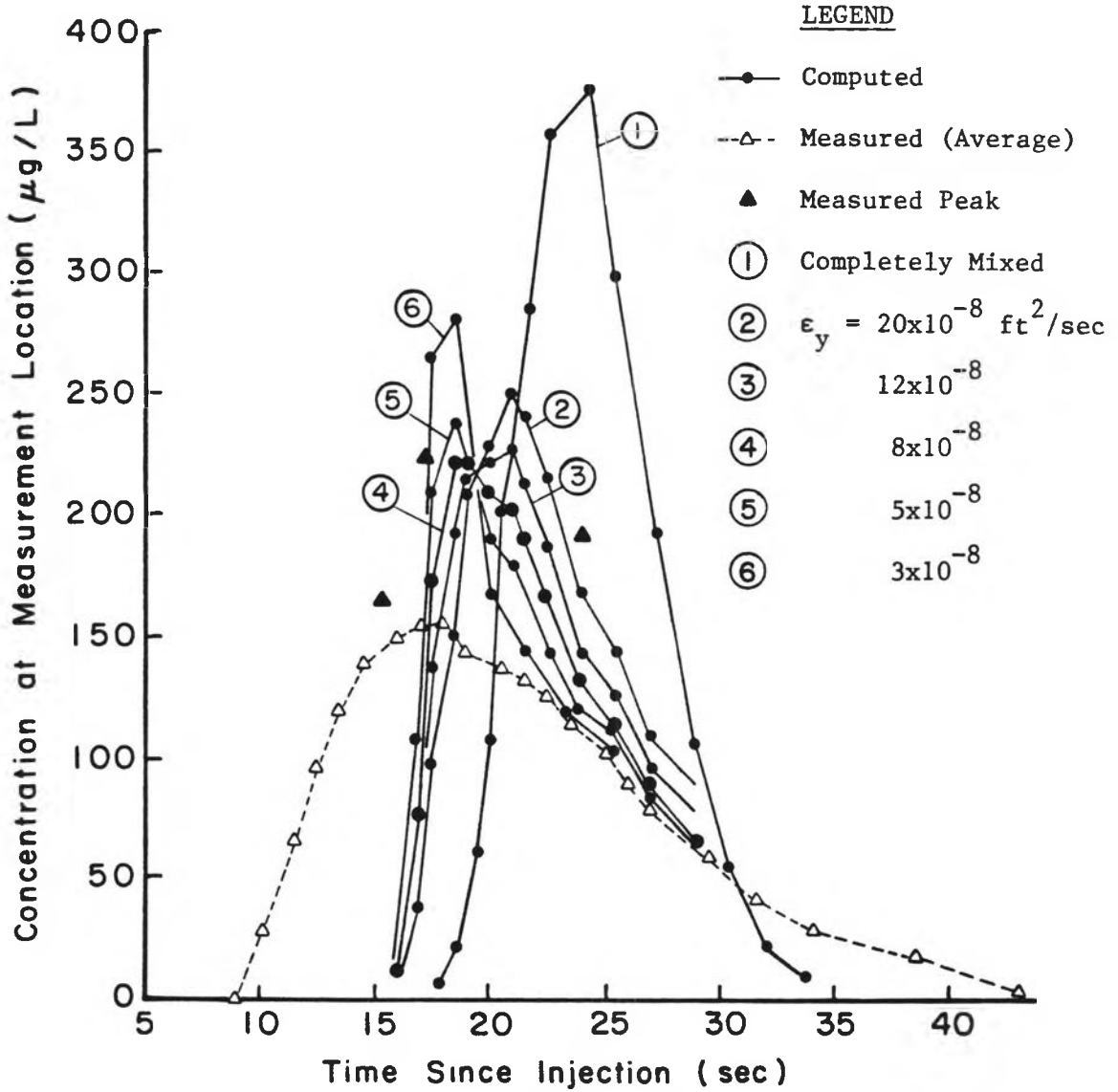


Figure E-12. Comparison of Measured and Computed Concentration Curves for $S_o = 0.030$ and $i = 2$ (Experiment No. 9b)

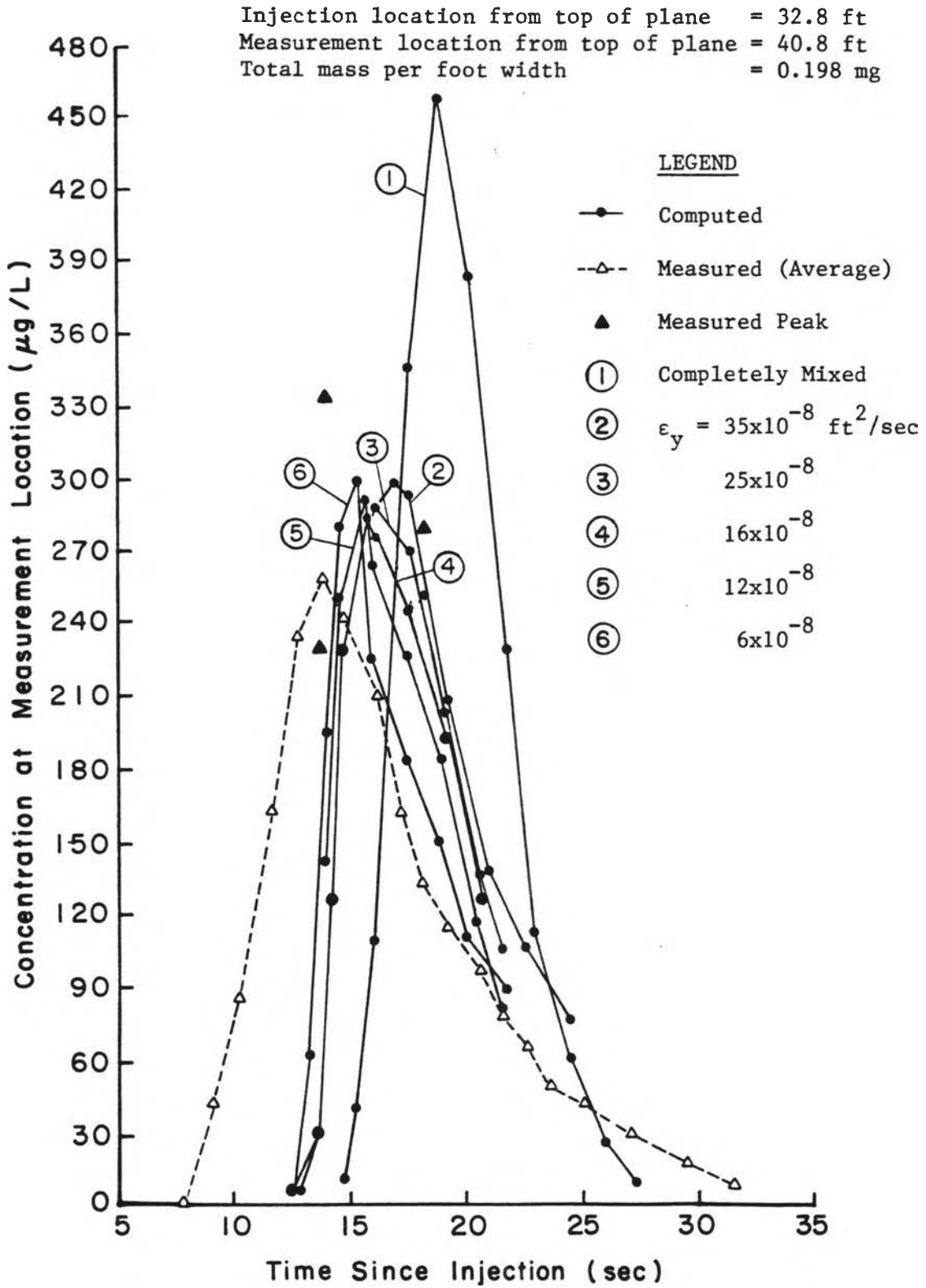


Figure E-13. Comparison of Measured and Computed Concentration Curves for $S_o = 0.030$ and $i = 3$ (Experiment No. 10)

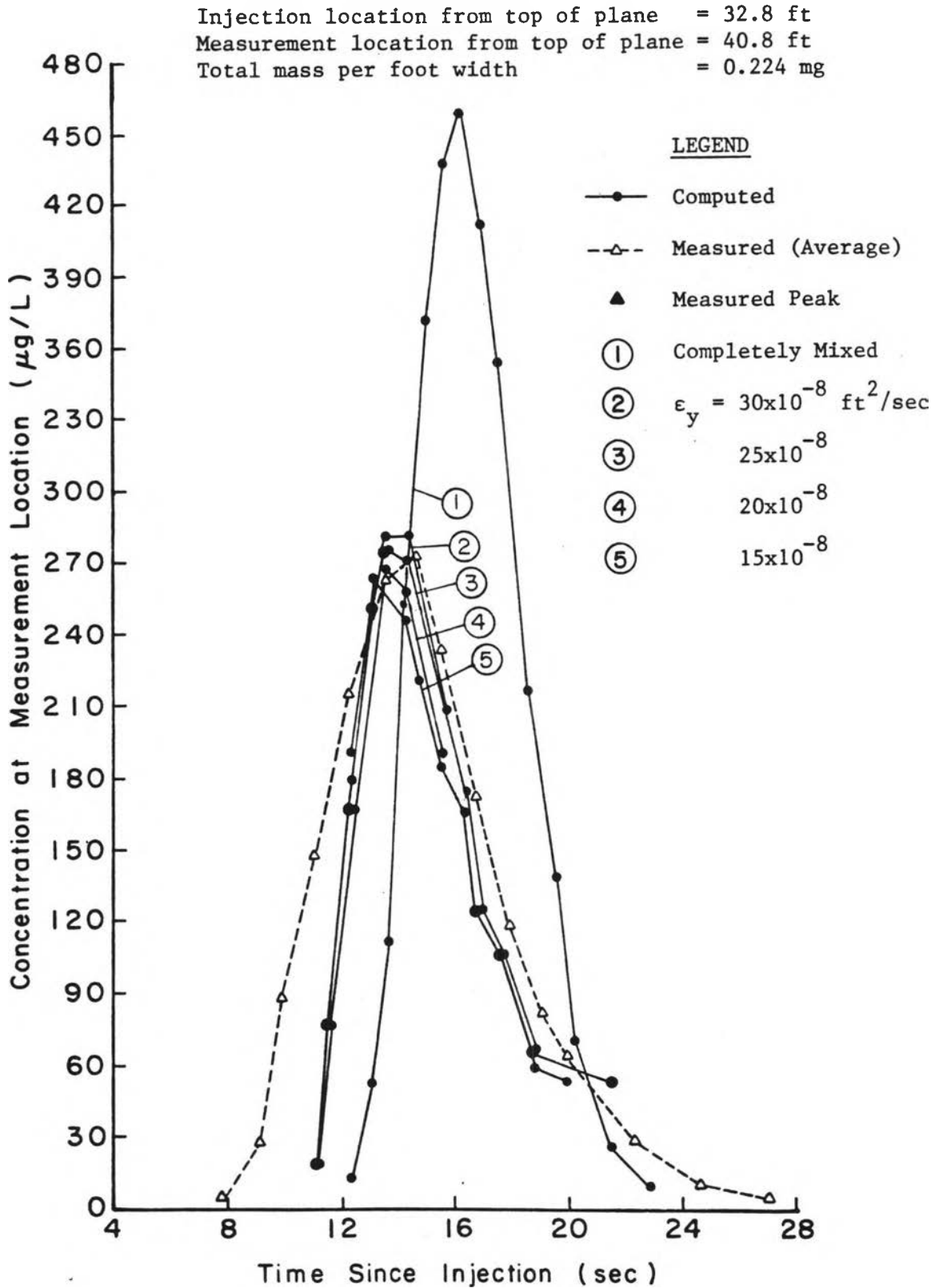


Figure E-14. Comparison of Measured and Computed Concentration Curves for $S_0 = 0.030$ and $i = 4$ (Experiment No. 11)

Injection location from top of plane = 27.7 ft
 Measurement location from top of plane = 40.8 ft
 Total mass per foot width = 0.241 mg

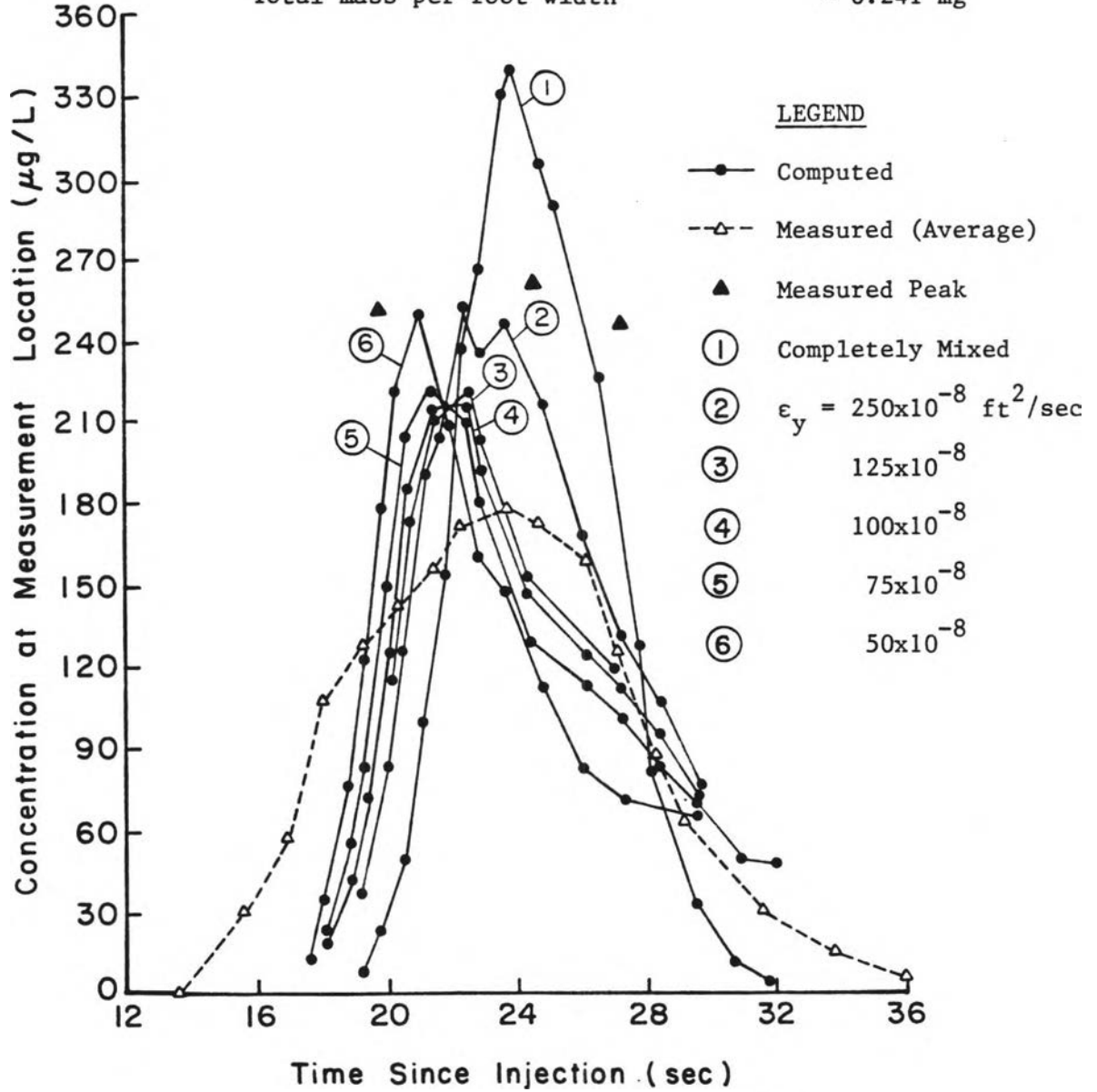


Figure E-15. Comparison of Measured and Computed Concentration Curves for $S_o = 0.030$ and $i = 5$ (Experiment No. 12)

APPENDIX F
DATA USED IN NUMERICAL
MODEL CALIBRATIONS

Appendix F

DATA USED IN NUMERICAL MODEL CALIBRATIONS

The input data used in the numerical model to calibrate ε_y values for each laboratory experiment are tabulated in this appendix. The following footnote explanations apply to the last set of data entries on each of the following pages:

- (1) Streamtube number, beginning at water surface.
- (2) Vertical height of streamtube, in percent of total depth.
- (3) Velocity of streamtube at injection location, in feet per second.

Parameter	Experiment No.								
	1a			1b			2a		
Bed Slope, S_o	0.001			0.001			0.001		
Intensity, i (in/hr)	2			2			3		
Injection Location from Top of Plane (ft)	27.7			32.8			27.7		
$f \cdot R_e$	60			60			66		
Viscosity, ν (ft ² /sec)	1.15×10^{-5}			1.15×10^{-5}			1.08×10^{-5}		
Δx (ft)	0.35			0.35			0.35		
ΔT (sec)	4.0			3.0			3.0		
Initial Conc. ($\mu\text{g/L}$)	1130			1144			1225		
Depth at Injection Location (ft)	0.01509			0.01583			0.01733		
Mean Velocity at Injection Location (ft/sec)	0.085			0.096			0.111		
Discharge per Unit Width at Injection Location (ft ² /sec)	0.00128			0.00152			0.00192		
	<u>(1)</u>	<u>(2)</u>	<u>(3)</u>	<u>(1)</u>	<u>(2)</u>	<u>(3)</u>	<u>(1)</u>	<u>(2)</u>	<u>(3)</u>
	1	4	0.007	1	4	0.007	1	4	0.009
	2	7	0.024	2	7	0.027	2	7	0.031
	3	10	0.048	3	10	0.054	3	10	0.062
	4	10	0.072	4	10	0.080	4	10	0.093
	5	10	0.092	5	10	0.102	5	10	0.118
	6	10	0.106	6	10	0.118	6	10	0.137
	7	10	0.116	7	10	0.129	7	10	0.149
	8	10	0.121	8	10	0.135	8	10	0.155
	9	4	0.121	9	4	0.136	9	4	0.153
	10	10	0.109	10	10	0.123	10	10	0.141
	11	9	0.090	11	9	0.101	11	9	0.119
	12	6	0.070	12	6	0.079	12	6	0.098

Parameter	Experiment No.								
	2a			3			4		
Bed Slope, S_o	0.001			0.001			0.001		
Intensity, i (in/hr)	3			4			5		
Injection Location from Top of Plane (ft)	32.8			32.8			32.8		
$f \cdot R_e$	66			72			78		
Viscosity, ν (ft ² /sec)	1.15×10^{-5}			1.02×10^{-5}			1.10×10^{-5}		
Δx (ft)	0.35			0.35			0.35		
ΔT (sec)	2.0			1.6			1.5		
Initial Conc. ($\mu\text{g/L}$)	1202			1287			1497		
Depth at Injection Location (ft)	0.0189			0.0205			0.0234		
Mean Velocity at Injection Location (ft/sec)	0.121			0.148			0.162		
Discharge per Unit Width at Injection Location (ft ² /sec)	0.00228			0.00304			0.00380		
	(1)	(2)	(3)	(1)	(2)	(3)	(1)	(2)	(3)
	1	6	0.107	1	6	0.137	1	7	0.154
	2	10	0.133	2	10	0.165	2	10	0.185
	3	10	0.158	3	10	0.192	3	10	0.213
	4	4	0.171	4	4	0.206	4	4	0.227
	5	7	0.170	5	14	0.204	5	12	0.224
	6	10	0.164	6	12	0.189	6	11	0.210
	7	10	0.152	7	11	0.163	7	11	0.185
	8	10	0.133	8	11	0.129	8	11	0.149
	9	10	0.107	9	10	0.087	9	11	0.103
	10	10	0.075	10	7	0.047	10	8	0.054
	11	8	0.040	11	5	0.014	11	5	0.016
	12	5	0.011						

Parameter	Experiment No.								
	5			6			7		
	(1)	(2)	(3)	(1)	(2)	(3)	(1)	(2)	(3)
Bed Slope, S_o	0.015			0.015			0.015		
Intensity, i (in/hr)	2			3			4		
Injection Location from Top of Plane (ft)	32.8			32.8			32.8		
$f \cdot R_e$	60			66			72		
Viscosity, ν (ft ² /sec)	1.07×10^{-5}			1.08×10^{-5}			1.07×10^{-5}		
Δx (ft)	0.35			0.35			0.35		
ΔT (sec)	1.0			1.0			0.75		
Initial Conc. ($\mu\text{g/L}$)	1029			806			714		
Depth at Injection Location (ft)	0.00630			0.00747			0.00844		
Mean Velocity at Injection Location (ft/sec)	0.241			0.305			0.360		
Discharge per Unit Width at Injection Location (ft ² /sec)	0.00152			0.00228			0.00304		
	1	4	0.185	1	6	0.259	1	4	0.315
	2	4	0.209	2	10	0.310	2	7	0.353
	3	4	0.231	3	10	0.363	3	8	0.399
	4	4	0.252	4	8	0.401	4	8	0.441
	5	4	0.271	5	4	0.421	5	8	0.474
	6	4	0.289	6	10	0.419	6	4	0.494
	7	4	0.305	7	10	0.396	7	8	0.490
	8	4	0.320	8	10	0.351	8	8	0.470
	9	4	0.333	9	10	0.285	9	8	0.435
	10	4	0.339	10	8	0.207	10	8	0.383
	11	4	0.337	11	8	0.123	11	8	0.315
	12	4	0.332	12	6	0.039	12	8	0.231
	13	4	0.324				13	8	0.131
	14	4	0.313				14	5	0.039
	15	4	0.300						
	16	4	0.284						
	17	4	0.266						
	18	4	0.244						
	19	4	0.220						
	20	4	0.194						
	21	4	0.165						
	22	4	0.133						
	23	4	0.098						
	24	4	0.061						
	25	4	0.021						

Parameter	Experiment No.								
	8			9a			9b		
Bed Slope, S_o	0.015			0.030			0.030		
Intensity, i (in/hr)	5			2			2		
Injection Location from Top of Plane (ft)	22.8			27.7			32.8		
$f \cdot R_e$	78			60			60		
Viscosity, ν (ft ² /sec)	1.05×10^{-5}			1.04×10^{-5}			1.05×10^{-5}		
Δx (ft)	0.35			0.35			0.35		
ΔT (sec)	0.8			1.0			0.8		
Initial Conc. ($\mu\text{g/L}$)	826			2986			2854		
Depth at Injection Location (ft)	0.00825			0.00468			0.00500		
Mean Velocity at Injection Location (ft/sec)	0.320			0.274			0.304		
Discharge per Unit Width at Injection Location (ft ² /sec)	0.00264			0.00128			0.00152		
	<u>(1)</u>	<u>(2)</u>	<u>(3)</u>	<u>(1)</u>	<u>(2)</u>	<u>(3)</u>	<u>(1)</u>	<u>(2)</u>	<u>(3)</u>
	1	7	0.291	1	5	0.031	1	4	0.232
	2	10	0.337	2	5	0.089	2	4	0.260
	3	10	0.383	3	5	0.141	3	4	0.287
	4	10	0.420	4	5	0.189	4	4	0.312
	5	4	0.438	5	5	0.231	5	4	0.335
	6	10	0.432	6	5	0.268	6	4	0.357
	7	10	0.403	7	5	0.300	7	4	0.377
	8	10	0.351	8	5	0.327	8	4	0.395
	9	10	0.275	9	5	0.349	9	4	0.411
	10	10	0.177	10	5	0.366	10	4	0.426
	11	9	0.062	11	5	0.377	11	4	0.426
				12	5	0.384	12	4	0.421
				13	5	0.381	13	5	0.412
				14	5	0.364	14	4	0.400
				15	5	0.344	15	4	0.384
				16	5	0.323	16	4	0.365
				17	5	0.298	17	4	0.341
				18	5	0.272	18	4	0.315
				19	5	0.243	19	4	0.284
				20	5	0.212	20	4	0.250
							21	4	0.213
							22	4	0.172
							23	4	0.127
							24	4	0.079
							25	4	0.027

Parameter	Experiment No.								
	10			11			12		
Bed Slope, S_o	0.030			0.030			0.030		
Intensity, i (in/hr)	3			4			5		
Injection Location from Top of Plane (ft)	32.8			32.8			27.7		
$f \cdot R_e$	66			72			78		
Viscosity, ν (ft ² /sec)	1.15×10^{-5}			1.17×10^{-5}			1.04×10^{-5}		
Δx (ft)	0.35			0.35			0.35		
ΔT (sec)	0.7			0.65			0.60		
Initial Conc. ($\mu\text{g/L}$)	3265			3245			3588		
Depth at Injection Location (ft)	0.00608			0.00694			0.00696		
Mean Velocity at Injection Location (ft/sec)	0.375			0.438			0.461		
Discharge per Unit Width at Injection Location (ft ² /sec)	0.00228			0.00304			0.00321		
	<u>(1)</u>	<u>(2)</u>	<u>(3)</u>	<u>(1)</u>	<u>(2)</u>	<u>(3)</u>	<u>(1)</u>	<u>(2)</u>	<u>(3)</u>
	1	5	0.312	1	4	0.381	1	4	0.378
	2	5	0.350	2	4	0.414	2	6	0.416
	3	5	0.386	3	4	0.444	3	7	0.461
	4	5	0.418	4	4	0.473	4	7	0.503
	5	5	0.447	5	4	0.499	5	7	0.539
	6	5	0.472	6	4	0.523	6	7	0.570
	7	5	0.495	7	4	0.544	7	4	0.587
	8	5	0.515	8	4	0.564	8	7	0.581
	9	5	0.516	9	4	0.581	9	7	0.560
	10	5	0.508	10	4	0.596	10	7	0.523
	11	5	0.492	11	4	0.598	11	7	0.470
	12	5	0.469	12	4	0.592	12	7	0.401
	13	5	0.440	13	4	0.580	13	7	0.317
	14	5	0.404	14	4	0.563	14	6	0.225
	15	5	0.361	15	4	0.541	15	6	0.128
	16	5	0.310	16	4	0.514	16	4	0.038
	17	5	0.254	17	4	0.482			
	18	5	0.190	18	4	0.444			
	19	5	0.119	19	4	0.402			
	20	5	0.041	20	4	0.354			
				21	4	0.301			
				22	4	0.243			
				23	4	0.180			
				24	5	0.112			
				25	4	0.039			

APPENDIX G

STEPWISE MULTIPLE LINEAR REGRESSIONS OF ε_y

Table G-1

Results of Stepwise Multiple Linear Regression Assuming $\varepsilon_y = f(i, \bar{u}, y_s, R_e)$

Step No.	r^2	Regression Coefficient ⁽¹⁾	Variables in Equation ⁽¹⁾		Variables Not in Equation ⁽¹⁾		
			Variable	Exponent	Variable	Partial Correlation ⁽²⁾	F to Enter ⁽³⁾
0					log \bar{i}	0.55	5.8
					log \bar{u}	-0.52	4.9
					log y_s	0.90	56.4
					log R_e	0.55	5.6
1	0.81	15.053	log y_s	3.56	log \bar{i}	0.84	29.00
					log \bar{u}	0.81	22.44
					log R_e	0.84	28.19
2	0.95	0.278	log y_s	3.23	log \bar{u}	-0.08	0.07
			log \bar{i}	2.23	log R_e	0.16	0.28

The addition of log \bar{u} or log R_e in the equation during Step 3 will not increase the explained variation sufficiently to warrant the inclusion of either in the final equation, based on an F test at $\alpha = 0.01$, where $F_{0.01}(2,12) = 6.93$.

Final Equation: $\varepsilon_y = 0.278 y_s^{3.23} \bar{i}^{2.23}$

- (1) Regression equation of the form $\varepsilon_y = \beta_0 \alpha_1^{\beta_1} \alpha_2^{\beta_2} \dots$, where β_0 = regression coefficient; $\alpha_1, \alpha_2, \dots$ = independent variables; and β_1, β_2, \dots = constants.
- (2) The correlation of each independent variable with the dependent variable, removing the effect of variables already in the equation.
- (3) A statistical test to determine the significance of adding each variable to the equation as if it were entered separately at the next step.

Table G-2

Results of Stepwise Multiple Linear Regression Assuming $\varepsilon_y = f(i, \bar{u}, y_s, R_e)$
Using Only Data with Depth-to-Drop Diameter Ratios Greater than 1.0

Step No.	r^2	Regression Coefficient ⁽¹⁾	Variables in Equation ⁽¹⁾		Variables Not in Equation ⁽¹⁾		
			Variable	Exponent	Variable	Partial Correlation ⁽²⁾	F to Enter ⁽³⁾
0					log $\frac{i}{\bar{u}}$	0.978	87.7
					log \bar{u}	0.973	72.1
					log y_s	0.984	122.2
					log R_e^s	0.968	60.2
1	0.97	2.472×10^{11}	log y_s	9.59	log $\frac{i}{\bar{u}}$	0.132	0.1
					log \bar{u}	0.049	0.0
					log R_e	0.038	0.0

The addition of log i , log \bar{u} , log R_e in the equation during Step 2 will not increase the explained variation sufficiently to warrant the inclusion of either in the final equation, based on an F test at $\alpha = 0.01$, where $F_{0.01}(1,4) = 21.2$

Final Equation: $\varepsilon_y = 2.472 \times 10^{11} y_s^{9.59}$

(1) Regression equation of the form $\varepsilon_y = \beta_0 \alpha_1^{\beta_1} \alpha_2^{\beta_2} \dots$, where β_0 = regression coefficient; $\alpha_1, \alpha_2 \dots$ = independent variables; and $\beta_1, \beta_2 \dots$ = constants.

(2) The correlation of each independent variable with the dependent variable, removing the effect of variables already in the equation.

(3) A statistical test to determine the significance of adding each variable to the equation as if it were entered separately at the next step.

Table G-3

Results of Stepwise Multiple Linear Regression Assuming $\epsilon_y = f(i, \bar{u}, R_e)$

Step No.	r^2	Regression Coefficient ⁽¹⁾	Variables in Equation ⁽¹⁾		Variables Not in Equation ⁽¹⁾		
			Variable	Exponent	Variable	Partial Correlation ⁽²⁾	F to Enter ⁽³⁾
0					log \bar{i}	0.55	5.8
					log \bar{u}	-0.52	4.9
					log R_e	0.55	5.6
1	0.30	3.223×10^{-8}	log \bar{i}	3.32	log \bar{u}	-0.95	116.6
					log R_e	0.05	0.1
2	0.94	3.663×10^{-11}	log \bar{i}	5.25	log R_e	0.54	4.7
			log \bar{u}	-3.25			

The addition of log R_e in the equation during Step 3 will not increase the explained variation sufficiently to warrant its inclusion in the final equation, based on an F test at $\alpha = 0.01$, where $F_{0.01}(2,12) = 6.93$.

Final Equation: $\epsilon_y = 3.663 \times 10^{-11} \bar{i}^{5.25} \bar{u}^{-3.25}$

(1) Regression equation of the form $\epsilon_y = \beta_0 \alpha_1^{\beta_1} \alpha_2^{\beta_2} \dots$, where β_0 = regression coefficient; $\alpha_1, \alpha_2 \dots$ = independent variables; and $\beta_1, \beta_2 \dots$ = constants.

(2) The correlation of each independent variable with the dependent variable, removing the effect of variables already in the equation.

(3) A statistical test to determine the significance of adding each variable to the equation as if it were entered separately at the next step.

APPENDIX H

EVALUATION OF TERMS 1 AND 2 IN EQ. 5-22

Evaluation of Term 1

Term 1 (Eq. 5-23) is evaluated in this section. The term is written as

$$\text{Term 1} = \int_0^{y_m} (u_L - \bar{u}) \int_0^y \int_0^y (u_L - \bar{u}) \, dy \, dy \, dy$$

Substituting Eq. 5-19 into the above equation and integrating,

$$\begin{aligned} \text{Term 1} &= \int_0^{y_m} (u_L - \bar{u}) \int_0^y \int_0^y \left[\frac{\bar{u}}{\bar{u}_p} u_m \left(\frac{2}{y_m} y - \frac{1}{y_m^2} y^2 \right) - \bar{u} \right] \, dy \, dy \, dy \\ &= \frac{\bar{u}}{\bar{u}_p} \int_0^{y_m} (u_L - \bar{u}) \int_0^y \int_0^y \left(\frac{2 u_m}{y_m} y - \frac{u_m}{y_m^2} y^2 - \bar{u}_p \right) \, dy \, dy \, dy \\ &= \frac{\bar{u}}{\bar{u}_p} \int_0^{y_m} (u_L - \bar{u}) \int_0^y \left(\frac{u_m}{y_m} y^2 - \frac{1}{3} \frac{u_m}{y_m^2} y^3 - \bar{u}_p y \right) \, dy \, dy \\ &= \left(\frac{\bar{u}}{\bar{u}_p} \right)^2 \int_0^{y_m} \left(\frac{2 u_m}{y_m} y - \frac{u_m}{y_m^2} y^2 - \bar{u}_p \right) \left(\frac{1}{3} \frac{u_m}{y_m} y^3 - \frac{1}{12} \frac{u_m}{y_m^2} y^4 - \frac{1}{2} \bar{u}_p y^2 \right) \, dy \\ &= \left(\frac{\bar{u}}{\bar{u}_p} \right)^2 \int_0^{y_m} \left[\frac{1}{2} \frac{u_m^2}{\bar{u}_p} y^2 - \frac{4}{3} \frac{u_m}{y_m} \bar{u}_p y^3 + \left(\frac{2}{3} \frac{u_m^2}{y_m^2} + \frac{7}{12} \frac{u_m}{y_m^2} \bar{u}_p \right) y^4 \right. \\ &\quad \left. - \frac{1}{2} \frac{u_m^2}{y_m} y^5 + \frac{1}{12} \frac{u_m^2}{y_m^4} y^6 \right] \, dy \end{aligned}$$

$$\begin{aligned}
&= \left(\frac{\bar{u}}{u_p}\right)^2 \left[\frac{1}{6} \bar{u}_p^2 y^3 - \frac{1}{3} \frac{u_m}{y_m} \bar{u}_p y^4 + \frac{1}{5} \left(\frac{2}{3} \frac{u_m^2}{y_m^2} + \frac{7}{12} \frac{u_m}{y_m} \bar{u}_p \right) y^5 \right. \\
&\quad \left. - \frac{1}{12} \frac{u_m^2}{y_m^2} y^6 + \frac{1}{84} \frac{u_m^2}{y_m^4} y^7 \right] \\
&= \left(\frac{\bar{u}}{u_p}\right)^2 y_m^3 \left(\frac{13}{210} \frac{u_m^2}{y_m^2} - \frac{13}{60} \frac{u_m \bar{u}_p}{y_m} + \frac{1}{6} \bar{u}_p^2 \right)
\end{aligned}$$

Evaluation of Term 2

Term 2 (Eq. 5-24) is evaluated in this section. The term is written as

$$\text{Term 2} = \int_{y_m}^{y_s} (u_U - \bar{u}) \int_0^y \int_0^y (u_U - \bar{u}) dy dy dy$$

Substituting Eq. 5-20 into the above equation and integrating,

$$\begin{aligned} \text{Term 2} &= \int_{y_s}^{y_m} (u_U - \bar{u}) \int_0^y \int_0^y \left\{ \frac{\bar{u}}{\bar{u}_p} u_m \left[1.0 + \frac{B_u}{y_s - y_m} (y - y_m) \right. \right. \\ &\quad \left. \left. + \frac{C_u}{(y_s - y_m)^2} (y - y_m)^2 \right] - \bar{u} \right\} dy dy dy \\ &= \frac{\bar{u}}{\bar{u}_p} \int_{y_m}^{y_s} (u_U - \bar{u}) \int_0^y \int_0^y \left[\left(u_m - \frac{u_m B_u y_m}{y_s - y_m} + \frac{u_m C_u y_m^2}{(y_s - y_m)^2} \right. \right. \\ &\quad \left. \left. - \bar{u}_p \right) + \left(\frac{u_m B_u}{y_s - y_m} - \frac{2 y_m u_m C_u}{(y_s - y_m)^2} \right) y + \frac{u_m C_u}{(y_s - y_m)^2} y^2 \right] dy dy dy \end{aligned}$$

Let

$$k_1 = u_m - \frac{u_m B_u y_m}{y_s - y_m} + \frac{u_m C_u y_m^2}{(y_s - y_m)^2} - \bar{u}_p$$

$$k_2 = \frac{u_m B_u}{y_s - y_m} - \frac{2 y_m u_m C_u}{(y_s - y_m)^2}$$

$$k_3 = \frac{u_m C_u}{(y_s - y_m)^2}$$

so that

$$\begin{aligned}
\text{Term 2} &= \frac{\bar{u}}{\bar{u}_p} \int_{y_m}^{y_s} (u_U - \bar{u}) \int_0^y \int_0^y (k_1 + k_2 y + k_3 y^2) dy dy dy \\
&= \frac{\bar{u}}{\bar{u}_p} \int_{y_m}^{y_s} (u_U - \bar{u}) \int_0^y (k_1 y + \frac{1}{2} k_2 y^2 + \frac{1}{3} k_3 y^3) dy dy \\
&= \left(\frac{\bar{u}}{\bar{u}_p}\right)^2 \int_{y_m}^{y_s} (k_1 + k_2 y + k_3 y^2) \left(\frac{1}{2} k_1 y^2 + \frac{1}{6} k_2 y^3 + \frac{1}{12} k_3 y^4\right) dy \\
&= \left(\frac{\bar{u}}{\bar{u}_p}\right)^2 \int_{y_m}^{y_s} \left(\frac{1}{2} k_1^2 y^2 + \frac{2}{3} k_1 k_2 y^3 + \left(\frac{7}{12} k_1 k_3 + \frac{1}{6} k_2^2\right) y^4 \right. \\
&\quad \left. + \frac{1}{4} k_2 k_3 y^5 + \frac{1}{12} k_3^2 y^6\right) dy \\
&= \left(\frac{\bar{u}}{\bar{u}_p}\right)^2 \left[\frac{1}{6} k_1^2 (y_s^3 - y_m^3) + \frac{1}{6} k_1 k_2 (y_s^4 - y_m^4) \right. \\
&\quad \left. + \left(\frac{7}{60} k_1 k_3 + \frac{1}{30} k_2^2\right) (y_s^5 - y_m^5) + \frac{1}{24} k_2 k_3 (y_s^6 - y_m^6) \right. \\
&\quad \left. + \frac{1}{84} k_3^2 (y_s^7 - y_m^7)\right]
\end{aligned} \tag{G-12}$$

APPENDIX I
LIST OF SYMBOLS

A	= cross-sectional area of flow (transverse to flow direction)
A_{ℓ}	= polynomial coefficient for lower velocity profile
A_u	= polynomial coefficient for upper velocity profile
B_{ℓ}	= polynomial coefficient for lower velocity profile
B_u	= polynomial coefficient for upper velocity profile
C_{ℓ}	= polynomial coefficient for lower velocity profile
C_u	= polynomial coefficient for upper velocity profile
c	= point concentration
\bar{c}	= vertically-averaged concentration
c_i	= initial concentration prior to diffusion
\bar{c}_p	= peak vertically-averaged concentration
d	= size of raindrop
D	= longitudinal dispersion coefficient
D_h	= hydraulic depth
F	= mass flux
f	= Darcy-Weisbach friction coefficient
g	= acceleration of gravity
i	= rainfall intensity
K_{y_s}	= constant related to y_s
K_u	= constant related to \bar{u}
K_{ε_y}	= constant related to ε_y
M	= mass
q	= discharge per unit width
R_c	= maximum cavity radius of raindrop splash
R_e	= Reynolds number
S_f	= friction slope
S_o	= bed slope

t	= time
T_E	= Eulerian time scale
T_L	= Lagrangian time scale
ΔT	= time step in numerical model
u	= time-averaged point velocity
\bar{u}	= vertically-averaged velocity
u'	= $u - \bar{u}$
u^*	= u/u_m
u_m	= maximum point velocity
u_o	= maximum velocity at water surface in laminar flow without rainfall
\bar{u}_p	= mean velocity of flow computed from the velocity profile
u_L	= lower velocity profile
u_U	= upper velocity profile
v	= impact velocity of raindrop
w	= pollutant mass per unit area
x	= distance along the flow direction measured from the top of the plane
x_{T_E}	= travel distance corresponding to T_E
x_{inj}	= distance from top of plane to injection location
x_{col}	= distance from top of plane to collection location
y	= vertical distance above streambed
y_m	= distance from streambed to u_m
y_s	= vertical distance above streambed to water surface
y^*	= y/y_m
ε	= characteristic mixing coefficient
ε_y	= vertical mixing coefficient
ε_m	= molecular diffusion coefficient

θ	= angle between channel bed and the horizontal
κ	= von Karman's constant
μ	= dynamic viscosity
ν	= kinematic viscosity
ρ	= density of water
σ_x^2	= variance of the distribution of the vertically-averaged concentration along the x axis
τ	= time
τ_o	= boundary shear stress